

GOING OUT OF EQUILIBRIUM IN ADS/CFT

By
Souvik Banerjee

PHYS07200804002

INSTITUTE OF PHYSICS

BHUBANESWAR

**A thesis submitted to the
Board of Studies in Physical Sciences**

In partial fulfillment of the requirements

For the Degree of

DOCTOR OF PHILOSOPHY

of

HOMI BHABHA NATIONAL INSTITUTE



July, 2014

Homi Bhabha National Institute

Recommendations of the Viva Voce Board

As members of the Viva Voce Board, we recommend that the dissertation prepared by **Souvik Banerjee** entitled “Going out of Equilibrium in AdS/CFT” may be accepted as fulfilling the dissertation requirement for the Degree of Doctor of Philosophy.

----- **Date :**
Chairman : Chairman of committee

----- **Date :**
Convener : Convener of Committee

----- **Date :**
Member : Member 1 of committee

----- **Date :**
Member : Member 2 of committee

----- **Date :**
Member : Member 3 of committee

Final approval and acceptance of this dissertation is contingent upon the candidate's submission of the final copies of the dissertation to HBNI.

I hereby certify that I have read this dissertation prepared under my direction and recommend that it may be accepted as fulfilling the dissertation requirement.

----- **Date :**
Guide : Dr. Sudipta Mukherji

STATEMENT BY AUTHOR

This dissertation has been submitted in partial fulfillment of requirements for an advanced degree at Homi Bhabha Institute (HBNI) and is deposited in the Library to be made available to borrowers under rules of the HBNI.

Brief quotations from this dissertation are allowable without special permission, provided that accurate acknowledgement of source is made. Requests for permission for extended quotation from or reproduction of this manuscript in whole or in part may be granted by the Competent Authority of HBNI when in his or her judgment the proposed use of the material is in the interests of scholarship. In all other instances, however, permission must be obtained from the author.

Souvik Banerjee

DECLARATION

I, hereby declare that the investigation presented in the thesis has been carried out by me. The work is original and the work has not been submitted earlier as a whole or in part for a degree/diploma at this or any other Institution or University.

Souvik Banerjee

To my beloved mother
who had eagerly longed for this day,
but could not witness....

ACKNOWLEDGEMENTS

I take this opportunity to express my sincere-most gratitude to my supervisor, Sudipta Mukherji. For the last five years I had been trying to copy his way of “enjoying” Physics, his unique way to probe a problem physically. I enjoyed to the highest extent the privilege I had to bang on his door anytime in the day and write on the green-board in his office, sometimes even without his permission. Moreover, I could not have learnt whatever little I have, if our path to the omfed tea-shop were shorter. In the next few years, I am definitely going to miss that green-board, the tea-shop and mostly, his attention to my most stupid questions. Whatever little Physics I can think independently at the end of this five-year period, owes its endless indebtedness to those indulgences.

At this point I should also thank Ayan Mukhopadhyay and Chethan Gowdigere for lending me a helping hand at the time when I required them the most. They helped me go through the hardest patch in my life so far, through intriguing discussions.

I am indebted to all my collaborators, in particular Ayan Mukhopadhyay, Samrat Bhowmick and George Siopsis from whom I have learnt a lot.

I sincerely thank all the past and present members of the high energy physics group in our Institute. I am hugely benefited by several discussion sessions with Jnanadeva Maharana, Ajit Srivastava, Anirban Basu, Amitabh Virmani.

The ultra high-energetic student-post-doc-faculty group never made me feel that I am that much away from home. The long association with Sayan da, Indranil da, Anirban da, Srikumar da, Nabyendu da, Poulomi di made every single day eventful.

This is also an opportunity to pay respect to my teachers in undergrads in Jadavpur. I would not have been where I am now if I were not motivated, inspired and guided by Dhiranjan Roy, Ranjan Bhattacharya, Narayan Banerjee and Soumitra Sengupta.

Finally I would say “I love you” to my family for an unconditional support, for being with me, all the time, each and every moment - that is beyond any expression. So I better stop here.

Contents

1	Introduction	1
1.1	Overview	1
1.2	Solitonic Solutions in Supergravity	3
1.3	The AdS/CFT Conjecture	6
1.4	Setting up the Dictionary	8
1.5	Finite Temperature : Thermal Retarded Correlators in AdS/CFT	12
1.6	Plan for the Rest of the Thesis	15
2	The Bragg-Williams Method	19
2.1	Bragg-Williams construction: a brief review	20
2.1.1	Paramagnetic to ferromagnetic transition	20
2.1.2	Hawking-Page transition: AdS-Schwarzschild black hole	21
2.2	Charged black holes	23
2.2.1	Born-Infeld black holes in AdS space	25
2.2.2	Action Calculation	29
2.2.2.1	Fixed Potential	29
2.2.2.2	Fixed Charge	31
2.2.3	Thermodynamical quantities	33
2.2.3.1	Fixed Potential	33
2.2.3.2	Fixed Charge	34
2.2.4	Construction of Bragg-Williams free energy & study of phase structure	34
2.2.4.1	Reissner-Nordström	35
2.2.4.2	Born-Infeld	38
2.2.5	R -charged black hole with spherical horizon: Instabilities	42
2.2.6	Proposal for effective potentials in the boundary theory	50
2.2.6.1	Reissner-Nordström	51
2.2.6.2	Born-Infeld	53
2.3	Towards Dynamics : Hairy to Reissner-Nodström Black Holes	55
2.4	Summary and future directions	64

3	The Holographic Spectral Function in Non-Equilibrium States	69
3.1	On non-equilibrium states, their holographic duals and quasi-normal modes	77
3.1.1	Conservative states in the kinetic approximation	77
3.1.2	Holographic duals of non-equilibrium states and typicality at strong-coupling	81
3.1.3	Quasinormal modes	86
3.1.4	Explicit examples of backgrounds	91
3.2	The holographic prescription for the non-equilibrium spectral function . . .	96
3.2.1	Scalar field equation and the non-equilibrium spectral function . . .	100
3.2.2	Fermionic field equations and the non-equilibrium spectral function	106
3.2.3	Generalization to backgrounds with other quasinormal modes . . .	117
3.3	Non-equilibrium Fermi surface and dispersion relations	121
3.3.1	Comparison with field-theoretic approach	121
3.3.2	Non-equilibrium dynamics at the Fermi-surface	123
3.3.3	Non-equilibrium shifts in energy and spin of quasi-particles	129
3.4	Taking into account non-linearities in the dynamics of the non-equilibrium variables	131
3.5	Summary and future directions	133
4	Cosmological Applications	147
4.1	The Bulk	149
4.2	Boundary Conditions	151
4.3	AdS Reissner-Nordström black hole	155
4.4	Cosmological Evolution	157
4.5	Summary and future directions : Part I	163
4.6	D3 brane with anisotropic time-dependent world volume	164
4.7	Probing with a D3 brane	168
4.8	The dynamic M5 Brane	172
4.9	Probing with a M5 brane	173
4.10	Summary and future directions : Part II	176
5	In Lieu of a Conclusion	181

List of Figures

- 2.1 BW free energy for five dimensional AdS-Schwarzschild black holes plotted against horizon radius \bar{r} for different temperatures \bar{T} . The solid line has two degenerate minima - representing co-existence of black hole phase (minimum at $\bar{r} = 1$) and the thermal AdS phase (with $\bar{r} = 0$). This happens at a critical temperature $\bar{T}_c = 3/(2\pi)$. While above this temperature black hole is stable (dotted line), AdS is a preferred phase below \bar{T}_c (dashed line). 23
- 2.2 This is a plot of W_{BW}^{RN} as a function of r_+ for fixed ϕ . The phase structure shown here is for $n = 4$ and for $\phi=0.0003$. The dashed line is for the critical temperature, $T = T_c$, the orange one is the transition involving a metastable phase, another feature of a generic first order phase transition. The red, green, blue and black lines are for $T > T_c$ in an increasing order. . 36
- 2.3 The phase structure of Reissner-Nordström in fixed potential ensembles. $T = 0$ line corresponds to extremal black holes. The extremal black holes are unstable. This plot is for $n = 4$ and we have set $l = 1$ here. 37
- 2.4 This is a plot of W_{BW}^{RN} as a function of r_+ for fixed T . The phase structure shown here is for $n = 4$ and for $T = 0.47$. The dashed line is for the critical value of potential, $\phi = \phi_c$, the blue one is for $\phi < \phi_c$. The black, orange, red and green lines are for $\phi > \phi_c$ in an increasing order. 38
- 2.5 W_{BW}^{GC} is plotted against r_+ using x as a parameter for $n = 4$. We have fixed $\phi = 0.2$ and have plotted for different values of temperature. The red line is for $T = T_c$. The blue and green lines are for $T > T_c$ in an increasing order, whereas the orange line is for $T < T_c$ 39
- 2.6 Phase diagram for the R -charged black hole with single charge shown in temperature, chemical potential plane. Line separating thermal AdS and black hole represents the first order phase transition line given by equation (2.105). On the other hand, the line between black hole and the unknown phase is a second order line - the equation of which is given in (2.106). The dashed line is for $\bar{T} = 1/\pi$ below which we can not extend various phases. . 43
- 2.7 $\bar{\mathcal{F}}$ is plotted as a function of the order parameter \bar{r} for $\bar{\mu} = 1$. The solid, dotted and dashed curves are for $\bar{T} = 1/\pi, 1.01/\pi, 1.015/\pi$ 48
- 2.8 $\bar{\mathcal{F}}$ is plotted as a function of the order parameter \bar{r} for $\bar{\mu} = .5$. The solid, dot-dashed, dotted and dashed lines are for $\bar{T} = 1/\pi, 1.3/\pi, 1.433/\pi, 1.45/\pi$. 48

2.9	$\bar{\mathcal{F}}$ for $\bar{\mu} = 2$. Solid, dashed and dotted lines are for $\bar{T} = 0.86, 0.93, 0.95$ respectively. Solid line represents \mathcal{F} at critical temperature. Below this temperature, black hole becomes unstable. The minima in the rest two curves show the stable black hole phase.	48
2.11	Parametric plot of q against r_+ for different values of the parameter, ϕ . . .	54
2.12	W_{BT}^{BI} is plotted against Q using x as a parameter for $n = 4$. We have fixed $\phi = 0.2$ and have plotted for different values of temperature. The red line is for $T = T_c$. The blue and green lines are for $T > T_c$ in an increasing order, whereas the orange line is for $T < T_c$	55
2.13	This figure is a plot of (2.136) and (2.139) for $a = 25$ and for different temperatures. The solid lines and the dashed lines represent the hairy and the RN black holes respectively. Green, magenta and black curves are for $\bar{T} = 0.11, 1/(2\pi), 0.2$ respectively. We see that while at low temperature free energy is minimized by the hairy black hole, RN black holes dominate at high temperature. At $\bar{T} = 1/(2\pi)$, free energies are equal at the minimum.	60
2.14	This figure is the behaviour of the free energy function close to $\bar{T} = \bar{T}_c = 1/(2\pi)$ for $a = 30$. Blue and red are for $\bar{T} \leq T_c$ and $\bar{T} \geq \bar{T}_c$ representing hairy and RN black holes respectively. At $\bar{T} = \bar{T}_c$, the minima for both are degenerate. Clearly, the order parameter \bar{r} , at which the minima occur, changes continuously around critical temperature leading to a continuous phase transition.	61
2.15	This figure shows behaviour of $\phi_h(t)$ after quenched to different temperatures below $\bar{T}_c = 1/(2\pi)$. The vertical axis is ϕ_h and the horizontal one is t . The plots are for $a = 90$. While the lower one (blue) curve is for temperature quenched to $\bar{T} = .13$, the upper one (red) is for $\bar{T} = .14$. We see $\phi_h(t)$ starts with zero value at $t = 0$ and at a later time reaches a non-zero negative stable point determined by the equation (2.145)	63
3.1	Contour for integration over $\omega_{(h)}$, with pole at negative imaginary axis . . .	99
4.1	Cosmological evolution scenarios for various values of parameters. Solid and dashed lines are plots of \dot{a}^2 and \ddot{a} , respectively. Dotted lines denote the black hole potential with its zeros indicating the positions of the inner and outer horizons.	161

4.2	Solid lines are plots of \dot{a}^2 whereas dotted lines are plots of the black hole potential for $\beta = 0$ and (a) $\Lambda_4 = 0$, (b) $\Lambda_4 = 0.05$. The inner fixed points and the position of the inner horizon are shown.	162
4.3	Plot of a vs τ for $\beta = 0$, $\Lambda_4 = 0$	162
4.4	Plots of a vs τ for $\beta = 0$, $\Lambda_4 = 0.05$. In (a) we have a bounce. Initial conditions are chosen as $a(0) = 0.356$. At $\tau = 3.642$, a reaches the second fixed point, $a = 3.059$. In (b) we have an accelerating solution, with initial condition chosen as $a(0) = 7.090$	162
4.5	Plot of a vs τ for $\beta = 6$, $\Lambda_4 = 0.05$. The initial condition is chosen as $a(0) = 7.705$	163
4.6	Plot of r as a function of time, t	170
4.7	Plot of t as a function of η	171
4.8	The functions, $f_1 = t^\alpha(\eta) f(r)$, $f_2 = t^\beta(\eta) f(r)$, $f_3 = t^\gamma(\eta) f(r)$, with $f(r)$ given in (4.77) are plotted as functions of η . α , β and γ are 0.7, .632, -0.332 respectively The plot of f_1 is in red, and that of f_2 and f_3 are in green and black respectively.	171
4.9	The functions, $t^{\alpha_i}(\eta) f(r)$, for $i = 1, 2, \dots, 5$ are plotted as functions of η for $p = 0.52$. This corresponding values for α_i 's are : $\alpha_1 = \alpha_2 = \alpha_3 = 0.52$, $\alpha_4 = -0.15$ and $\alpha_5 = -0.41$. The isotropic expansion corresponding to $\alpha_1, \alpha_2, \alpha_3$ is plotted in red. The contraction corresponding to α_4, α_5 are plotted in green and black respectively.	176

Synopsis

As of now, string theory is believed to be the most successful quantum theory of gravity and a strong contender to be the fundamental microscopic theory of “everything”. It starts with the idea that the world at its microscopic-most level is made up of some tiny stringy objects, which vibrate, do all kinds of funny acts and finally come up with the macroscopic world we see everyday. The different vibrational modes give rise to different elementary particles which we had so far been thinking of as the fundamental constituents of the universe. In other words, the long term goal of string theory is to provide a complete and universal microscopic foundation to more macroscopic theories and phenomenologies, such as the standard model of particle physics and Einstein’s theory of gravitation, to name a few. However, string theory is a framework that operates in such an ultra-high energy regime that this is far beyond the reach of even the most modern particle accelerators like RHIC and LHC. But this is not really a matter to worry as such. Asking whether string theory can explain the real world is probably as irrelevant as to ask whether one can solve the problem of the oscillation of a simple pendulum in quantum field theory. We need to remember, just like quantum field theory, the theory of strings is also a framework, the justification whereof would probably be found from the theories derived from it.

With this aim in view string theory has expanded its horizon to other branches of theoretical physics where the possibility of having a derived theory with greater testability increases with a decrement in energy scale. AdS/CFT correspondence is one such hypothesis derived in the string framework that nurtures this possibility. AdS/CFT, as we would discuss in gory detail in due course, is an illustrative realization of the old holographic principle which states that the degrees of freedom of quantum gravity reside on the boundary space-time. This in turn gives rise to a duality principle that maps the states in gauge theory to solutions in string theory living in one higher dimension. Particular significance and predictability of such a miraculous hypothesis can be put to test when the t’Hooft coupling and the rank of the gauge group of the gauge theory in question becomes so high that it becomes intractable by traditional methods in quantum field theory. Even in this case, the hypothesis ensures the “dual” theory to be a simple classical theory of gravity with minimally coupled matter fields, namely the supergravity theory that is also realized as some consistent truncation of string theory at low energy. The advantage of working in supergravity limit of string theory is that unlike the full string theory which is a theory with infinite degrees of freedom, here one has to deal with only finite degrees of freedom.

From the perspective of the full supersymmetric string theory this amounts to integrating out massive string excitations by taking the limit $\alpha' \rightarrow 0$ where $\sqrt{\alpha'}$ is a characteristic small length scale $\sim 10^{-33}$ cm and is related to the string tension as $T \equiv \frac{1}{2\pi\alpha'} \equiv \frac{1}{l_s^2}$, l_s being the string length scale.

In this thesis, we will use AdS/CFT, or more broadly the principles of gauge/ gravity duality to understand some features of physics out of equilibrium. We will discuss various non-equilibrium states and their gravity duals. We will categorize the constructions according to the phenomena we would like to address through them. In general, non-equilibrium phenomena occur in many branches of physics. Most celebrated among these, are relativistic heavy ion collision and cosmology. Many features of relativistic heavy ion collision were revealed in recent experiments like RHIC, though a little progress has been made to understand the very essential quantum kinetic theory governing their dynamics. Cosmological data are abundant, most of them, of course begging a proper explanatory theory. Not only this, even some recent condensed matter experiments, like tARPES where one can see the non-equilibrium evolution of Fermi-surface, still lack a proper theoretical justification. All these are excellent set ups to test the applicability of gauge/ gravity duality in non-equilibrium. In this thesis we would proceed towards addressing some of those issues in these directions by building up problem specific machinery.

In its weak form (i.e. in the limit when the rank of the gauge group, $N \rightarrow \infty$ with a large 't Hooft coupling, $\lambda = g_{YM}^2 N$ very large as well) AdS/CFT relates supergravity theory in $AdS_5 \times S^5$ background to a strongly coupled $\mathcal{N} = 4$ $SU(N)$ SYM theory living on the boundary of AdS_5 . For incorporating finite temperature, holographically, one introduces black hole in this AdS space-time in a way that the AdS nature of the space-time is preserved asymptotically. The intuition follows from the fact that stationary black holes behave like thermodynamical objects in all respect. The surface gravity at the black hole horizon can be identified with temperature while the mass, with the total energy. Furthermore, in all dynamical processes known, the area of the black hole event horizon can only increase monotonically, justifying its identification with entropy. Also, for any dynamical process the black hole horizon possesses uniform surface gravity mimicing the thermodynamical equilibration.

With this basic understanding of the holographic meaning of equilibrium the tools of holography enable us to develop methodologies to deal with different non-equilibrium scenarios in holographic set-up. We will develop tools and prescriptions contemplating on applications towards physically interesting problems like quantum quench, Fermi liquid

theory in non-equilibrium and cosmological evolution of the universe. We will argue some of the methods developed might as well be very much useful in understanding and improving upon existing tools to study ultra relativistic heavy ion collisions. As mentioned before, the methods we would use will be problem specific, but we will broadly categorize them in two parts. Following our understanding of holographic meaning of equilibrium, these are,

(A) *Going to a temperature other than the Hawking temperature of the black hole*

As mentioned before, in any dynamical gravitational process involving black holes, attaining Hawking temperature at the horizon signals the equilibration. Hence, at the level of free-energy, if we somehow make the temperature off-shell it would enable us to study the dynamics of equilibration. Motivated by *Bragg-Williams method* in condensed matter physics [1] and its adoption in black hole physics and holography [2], we use this idea to analyse, holographically, the phenomenon of temperature quench in specific black hole set-up [3]. Apart from the dynamics, we see, even the analysis of phase transition particularly of the first order, which otherwise is difficult to capture in the framework of Landau theory, becomes easier in this framework. We also show that this method works even when we take stringy α' corrections to gauge theory sector [4]. This method also proves handy in analysing the system out of chemical equilibrium. We also propose an effective off-shell potential in the gauge theory sector using out holographic knowledge of bulk gravity.

(B) *Obtaining time-dependent backgrounds suitable to study non-equilibrium phenomena*

There are different ways to construct time-dependent backgrounds. The first method among them is to obtain time-dependent bulk space-time dual to specific non-equilibrium states starting from the observables of the boundary theory. This analysis is based on the Fefferman-Graham construction of $AAAdS$ spaces. We considered non-equilibrium fluctuations on the top of equilibrium states which holographically mapped into incorporating quasi normal mode fluctuations on the AdS black hole in equilibrium. Upon constructing the background, we use this to find the spectral function in specific non-equilibrium states [5]. We further show the usefulness of the mechanism developed in understanding Fermi liquid theory for non-equilibrium strongly coupled systems.

The other methods of constructing time-dependent geometries are aimed at cosmological applications. The first of them [6] is based on Verlinde's idea [7] that the time in the AdS bulk and that of the boundary conformal field theory are different and a dynamic boundary space-time can in principle be obtained starting from a static bulk. This idea was further extended with charged black holes in [8]. Motivated by these two, we used the

techniques of holographic renormalization [9] with modified boundary conditions to come up with cosmological evolution on the boundary.

The second one in this line starts with a dynamical bulk itself. The time-dependent cosmological solution in supergravity is scarce in general. We, however, manage to find explicitly time-dependent brane solutions in 10 and 11 dimensional supergravity which takes Kasner-like scaling in world-volume directions on the brane [10]. Such solutions in near horizon limit reduces to $AdS_5 \times S^5$ and $AdS_7 \times S^4$ with Kasner scaling in transverse directions for Kasner $D3$ and $M5$ brane solutions respectively. The AdS_5 solutions with Kasner scaling as solutions to 5-dimensional Einstein's equation with a negative cosmological constant was however studied in the literature either in the context of understanding gauge theory near cosmological singularity [11] or in the context of anisotropic expansion of strongly coupled quark gluon plasma [12]. We, however, concentrate on cosmology, namely realizing cosmological evolution on probe dynamic branes in these time-dependent backgrounds and find interesting consequences like dynamical compactification of extra dimensions.

Bibliography

- [1] Chaikin and Lubensky “Principles of Condensed Matter Physics”
- [2] S. Jain, S. Mukherji and S. Mukhopadhyay, “Notes on R-charged black holes near criticality and gauge theory,” JHEP **0911**, 051 (2009) [arXiv:0906.5134 [hep-th]].
- [3] S. Banerjee, S. K. Chakrabarti, S. Mukherji and B. Panda, “Black hole phase transitions via Bragg-Williams,” Int. J. Mod. Phys. A **26**, 3469 (2011) [arXiv:1012.3256 [hep-th]].
- [4] S. Banerjee, “A Note on Charged Black Holes in AdS space and the Dual Gauge Theories,” Phys. Rev. D **82**, 106008 (2010) [arXiv:1009.1780 [hep-th]].
- [5] S. Banerjee, R. Iyer and A. Mukhopadhyay, “The holographic spectral function in non-equilibrium states,” Phys. Rev. D **85**, 106009 (2012) [arXiv:1202.1521 [hep-th]].
- [6] S. Banerjee, S. Bhowmick, A. Sahay and G. Siopsis, “Generalized Holographic Cosmology,” Class. Quant. Grav. **30**, 075022 (2013) [arXiv:1207.2983 [hep-th]].
- [7] I. Savonije and E. P. Verlinde, “CFT and entropy on the brane,” Phys. Lett. B **507**, 305 (2001) [hep-th/0102042].
- [8] S. Mukherji and M. Peloso, “Bouncing and cyclic universes from brane models,” Phys. Lett. B **547**, 297 (2002) [hep-th/0205180].
- [9] S. de Haro, S. N. Solodukhin and K. Skenderis, “Holographic reconstruction of space-time and renormalization in the AdS / CFT correspondence,” Commun. Math. Phys. **217**, 595 (2001) [hep-th/0002230].
- [10] S. Banerjee, S. Bhowmick and S. Mukherji, “Anisotropic branes,” arXiv:1301.7194 [hep-th].
- [11] S. R. Das, J. Michelson, K. Narayan and S. P. Trivedi, “Time dependent cosmologies and their duals,” Phys. Rev. D **74**, 026002 (2006) [hep-th/0602107].
- [12] S. -J. Sin, S. Nakamura and S. P. Kim, “Elliptic Flow, Kasner Universe and Holographic Dual of RHIC Fireball,” JHEP **0612**, 075 (2006) [hep-th/0610113].

List of Publications/Preprints

- *[1] “*Anisotropic branes*”,
Souvik Banerjee, Samrat Bhowmick, Sudipta Mukherji
 Phys. Lett. B **726**, 461 (2013) arXiv:1301.7194 [hep-th].
- *[2] “*Generalized Holographic Cosmology*”,
Souvik Banerjee, Samrat Bhowmick, Anurag Sahay, George Siopsis
 Class. Quant. Grav. **30**, 075022 (2013) arXiv:1207.2983 [hep-th].
- *[3] “*The holographic spectral function in non-equilibrium states*”,
Souvik Banerjee, Ramkrishnan Iyer, Ayan Mukhopadhyay
 Phys. Rev. D **85**, 106009 (2012) arXiv:1202.1521 [hep-th].
- *[4] “*Black hole phase transitions via Bragg-Williams*”,
Souvik Banerjee, Sayan K. Chakrabarti, Binata Panda, Sudipta Mukherji
 Int. J. Mod. Phys. A **26**, 3469 (2011) arXiv:1012.3256 [hep-th].
- *[5] “*A Note on Charged Black Holes in AdS space and the Dual Gauge Theories* ”,
Souvik Banerjee,
 Phys. Rev. D **82**, 106008 (2010) arXiv:1009.1780 [hep-th].

A (*) indicates papers on which this thesis is based.

1

Introduction

1.1 Overview

As of now, string theory [1–6] is believed to be the most successful quantum theory of gravity and a strong contender to be the fundamental microscopic theory of “everything”. It starts with the idea that the world at its microscopic-most level is made up of some tiny stringy objects, which vibrate, do all kinds of funny acts and finally come up with the macroscopic world we see everyday. The different vibrational modes give rise to different elementary particles which we had so far been thinking of as the fundamental constituents of the universe. In other words, the long term goal of string theory is to provide a complete and universal microscopic foundation to more macroscopic theories and phenomenologies, such as the standard model of particle physics and Einstein’s theory of gravitation, to name a few. However, string theory is a framework that operates in such an ultra-high energy regime that this is far beyond the reach of even the most modern particle accelerators like RHIC and LHC. But this is not really a matter to worry as such. Asking whether string theory can explain the real world is probably as irrelevant as to ask whether one can solve the problem of the oscillation of a simple pendulum in quantum field theory. We need to remember, just like quantum field theory, the theory of strings is also a framework, the justification whereof would probably be found from the theories derived from it.

With this aim in view string theory has expanded its horizon to other branches of theoretical physics where the possibility of having a derived theory with greater testability increases with a decrement in energy scale. AdS/CFT correspondence [7–10] is one such hypothesis derived in the string framework that nurtures this possibility. AdS/CFT, as we would discuss in gory detail in due course, is an illustrative realization of the old holo-

graphic principle which states that the degrees of freedom of quantum gravity reside on the boundary space-time. This in turn gives rise to a duality principle that maps the states in gauge theory to solutions in string theory living in one higher dimension. Particular significance and predictability of such a miraculous hypothesis can be put to test when the t'Hooft coupling and the rank of the gauge group of the gauge theory in question becomes so high that it becomes intractable by traditional methods in quantum field theory. Even in this case, the hypothesis ensures the “dual” theory to be a simple classical theory of gravity with minimally coupled matter fields, namely the supergravity theory that is also realized as some consistent truncation of string theory at low energy. The advantage of working in supergravity limit of string theory is that unlike the full string theory which is a theory with infinite degrees of freedom, here one has to deal with only finite degrees of freedom. From the perspective of the full supersymmetric string theory this amounts to integrating out massive string excitations by taking the limit $\alpha' \rightarrow 0$ where $\sqrt{\alpha'}$ is a characteristic small length scale $\sim 10^{-33}$ cm and is related to the string tension as $T \equiv \frac{1}{2\pi\alpha'} \equiv \frac{1}{l_s^2}$, l_s being the string length scale.

In this thesis, we will use AdS/CFT, or more broadly the principles of gauge/ gravity duality to understand some features of physics out of equilibrium. We will discuss various non-equilibrium states and their gravity duals. We will categorize the constructions according to the phenomena we would like to address through them. In general, non-equilibrium phenomena occur in many branches of physics. Most celebrated among these, are relativistic heavy ion collision and cosmology. Many features of relativistic heavy ion collision were revealed in recent experiments like RHIC, though a little progress has been made to understand the very essential quantum kinetic theory governing their dynamics. Cosmological data are abundant, most of them, of course begging a proper explanatory theory. Not only this, even some recent condensed matter experiments, like tARPES where one can see the non-equilibrium evolution of Fermi-surface, still lack a proper theoretical justification. All these are excellent set ups to test the applicability of gauge/ gravity duality in non-equilibrium. We would proceed slowly towards addressing some of those issues in these directions by building up problem specific machinery. In the rest of this chapter we will cover some basics that will be proven handy in course of our journey out of equilibrium.

1.2 Solitonic Solutions in Supergravity

In this thesis we will be mostly interested in type II supergravity solutions. This is a low energy effective theory of type II (A or B) superstring theory with following field contents:

- graviton $g_{\mu\nu}$, antisymmetric tensor $B_{\mu\nu}$ and dilaton ϕ coming from $(NS-NS)$ sector of the theory.
- $p + 1$ form fields A_{p+1} originating from the massless spectrum of $(R-R)$ sector. Depending on p is even or odd, the theory is type IIA or type IIB respectively.
- space-time Fermions that belong to $(R-NS)$ and $(NS-R)$ sectors.

In Einstein frame, the action for the type II supergravity can be written as [11–14],

$$I_E = \frac{1}{16\pi G_{10}} \int d^{10}x \sqrt{|g|} \left(R - \frac{1}{2} \partial_\mu \phi \partial^\mu \phi - \frac{1}{2} \sum_p \frac{1}{(p+2)!} e^{a_p \phi} F_{p+2}^2 + \dots \right), \quad (1.1)$$

with $a_p = -\frac{1}{2}(p-3)$. The dots denote the $(NS-NS)$ 3 form field strength and the fermionic terms. G_{10} is the Newton's constant in 10 dimensions.

The equations of motion for graviton, dilaton and the $p+2$ form field strengths are, respectively,

$$\begin{aligned} R_\nu^\mu &= \frac{1}{2} \partial^\mu \phi \partial_\nu \phi + \frac{1}{2(p+2)!} e^{a_p \phi} \left((p+2) F^{\mu\xi_2 \dots \xi_{p+2}} F_{\nu\xi_2 \dots \xi_{p+2}} - \frac{p+1}{8} \delta_\nu^\mu F_{p+2}^2 \right), \\ \nabla^2 \phi &= \frac{1}{\sqrt{g}} \partial_\mu (\sqrt{g} \partial^\mu \phi) = \frac{a_p}{2(p+2)!} F_{p+2}^2, \\ \partial_\mu (\sqrt{g} e^{a_p \phi} F^{\mu\nu_2 \dots \nu_{p+2}}) &= 0. \end{aligned} \quad (1.2)$$

The field strength, F_{p+2} in the action is termed as electric. One can also define its magnetic dual

$$\tilde{F}_{10-p-2} = e^{a_p \phi} * F_{p+2} \quad (1.3)$$

and show that under the duality transformations,

$$a_p \phi \rightarrow -a_p \phi, (p+2) \rightarrow (10-p-2), F_{p+2} \rightarrow \tilde{F}_{10-p-2}, \quad (1.4)$$

the equations of motion (1.2) remain invariant [14].

With a view to motivating our way towards AdS/ CFT correspondence, we will contemplate on a particular solitonic solution of type II B supergravity, namely the $D3$ brane solution. From the perspective of string theory this can as well be thought of as a 3 dimensional hypersurface on which an open string can end. The letter “D” stands for Dirichlet - the string end points attached to the hypersurface can move freely on the brane and hence satisfy Neumann boundary condition along 3 brane directions + 1 time direction. In the remaining 6 spatial directions, Dirichlet boundary condition is obeyed.

In Einstein frame the $D3$ brane solution is given by

$$\begin{aligned} ds^2 &= H^{-1/2}(-f dt^2 + \sum_{i=1}^3 (dx^i)^2) + H^{1/2}(f^{-1} dr^2 + r^2(d\Omega_5^2)), \\ H &= 1 + \left(\frac{h}{r}\right)^4, f = 1 - \left(\frac{r_0}{r}\right)^4, \\ h^8 + r_0^4 h^4 &= \frac{Q^2}{16}, \quad \phi = \text{Constant}, \end{aligned} \tag{1.5}$$

where we have imposed the self duality condition, namely, $F_5 = *F_5$.

Solution for five form field strength is,

$$F_{ti_1 i_2 i_3 r} = \epsilon_{i_1 i_2 i_3} H^{-2} \frac{Q}{r^5}. \tag{1.6}$$

Here r is the radial coordinate in transverse directions of the brane. Q is an integration constant which is related to the $D3$ brane charge, μ_3 given by

$$\mu_3 = \frac{\Omega_5 Q}{(2\pi)^{\frac{7}{2}} l_s^4 g_s}, \tag{1.7}$$

where g_s is the string coupling constant given by $g_s = e^\phi$ and Ω_5 , the volume of the 5-sphere. ϕ being a constant, can be set to zero. The metric, (1.5) has a singularity at $r = 0$ and a horizon at $r = r_0$ where the metric function, f vanishes. In the extremal limit, $r \rightarrow 0$, the horizon sits on the singularity and this configuration preserves half of the space-time supersymmetries. Configurations with arbitrary r_0 , however, break all supersymmetries.

Near Horizon limit of Extremal Brane

In the extremal limit, $r \rightarrow 0$, the metric, (1.5) takes the simple form

$$ds^2 = H^{-1/2}(-dt^2 + \sum_{i=1}^3 (dx^i)^2) + H^{1/2}(dr^2 + r^2(d\Omega_5^2)),$$

$$h^4 = \frac{Q}{4}, \quad f(r) = 1, \quad H = 1 + \frac{Q}{4r^4}. \quad (1.8)$$

We now consider N -coincident $D3$ branes. For a single $D3$ brane the normalized flux is given by

$$\mu_3 = T_3(2\pi)^{\frac{7}{2}} l_s^4 g_s. \quad (1.9)$$

For coincident N number of branes it changes in a multiplicative way with N :

$$\mu_3^{(N)} = NT_3(2\pi)^{\frac{7}{2}} l_s^4 g_s. \quad (1.10)$$

Using (1.7), this in turn fixes the integration constant, Q as

$$Q = 16N\pi g_s l_s^4. \quad (1.11)$$

With all these considerations taken into account, the metric for N coincident $D3$ branes takes the form

$$ds^2 = H^{-1/2}(-dt^2 + \sum_{i=1}^3 (dx^i)^2) + H^{1/2}(dr^2 + r^2(d\Omega_5^2))$$

$$H = 1 + \frac{4\pi N g_s l_s^4}{r^4} = 1 + \frac{l^4}{r^4}, \quad (1.12)$$

where $\frac{l^4}{l_s^4} = 4N\pi g_s$.

l is the characteristic length scale proportional to the gravitational field strength. In the asymptotic limit, $r \gg l$, the metric takes the form of a flat Minkowski metric. In the near horizon limit, $r \ll l$ the metric becomes 5-dimensional Anti de Sitter (AdS_5) $\times S^5$.

$$ds^2_{AdS_5 \times S^5} = \underbrace{\frac{r^2}{l^2}(-dt^2 + \sum_{i=1}^3 (dx^i)^2)}_{AdS_5} + \frac{l^2}{r^2}dr^2 + \underbrace{l^2(d\Omega_5^2)}_{S^5}. \quad (1.13)$$

Hints Towards a Duality :

- The isometry group of AdS_5 is $SO(2, 4)$. Additionally, the S^5 part has an isometry group $SO(6) \sim SU(4)_R$. This is, surprisingly, the same as the Bosonic subgroup of the superconformal group of $\mathcal{N} = 4$ supersymmetric Yang-Mills(SYM) gauge theory $PSU(2, 2|4)$.

$$PSU(2, 2|4) \subset SO(2, 4) \times SU(4)_R, \quad (1.14)$$

corresponding to the conformal group and the R symmetry group respectively.

- Looking at the supergravity spectrum, one can note a mapping of the supergravity tower of states to the single trace operators and their descendants in the conformal field theory living on the flat asymptotic boundary of the AdS_5 space-time. The matching also extends at the level of correlators of those operators.

Motivated by the holographic principles, the afore-mentioned hints guide towards a possible duality principle that connects two apparently distinct sectors, namely a supergravity theory in AdS_5 space and $\mathcal{N} = 4$ SYM theory in $D = 4$. This indeed is the AdS/CFT correspondence which we will jot down in more precise manner next.

1.3 The AdS/CFT Conjecture

The AdS/CFT correspondence, in its *strongest form* is based on the open string-closed string duality which states that the dynamics of open strings contains that of closed strings. As we know, closed string contains gravity whereas the open string spectrum does not contain graviton. This correspondence, in its simplest setting implies a duality between type IIB string theory on asymptotically $AdS_5 \times S^5$ with constant 5-form RR field strength (generated by massless closed string modes) and $\mathcal{N} = 4$ $SU(N)$ SYM theory in $3 + 1$ dimensions (generated by massless open string modes), the parameters of the two theories being related as :

$$\begin{aligned} g_s &= g_{YM}^2, \\ g_{YM}^2 N &= \lambda = \frac{l^4}{4\pi l_s^4} \end{aligned} \quad (1.15)$$

λ has a name -it is called 't Hooft coupling.

The 't Hooft Limit

This very *strong form* of the conjecture is physically intractable particularly since we do not quite understand quantization of string theory in RR background itself. The 't Hooft limit, namely, $N \rightarrow \infty$ with $\lambda = g_{YM}^2 N$ fixed provides with the following simplifications :

- In the $\mathcal{N} = 4$ $SU(N)$ SYM theory we can safely neglect non-planar diagrams as they are suppressed by orders of $\frac{1}{N^{2g}}$, g being the genus of the surface.
- In the string theory side, it also becomes simple and in fact it suffices to work with classical string theory in $AdS_5 \times S^5$ background which is much more well understood. The justification lies in the fact that the perturbative expansion in string theory is basically a genus expansion of surfaces. Correlation function on a genus g surface usually scales as g_s^{2g-2} . But in the 't Hooft limit, $g_s = \frac{\lambda}{N}$ itself goes to zero resulting in vanishing contributions from higher genus surfaces.

Simplifying further : the Large λ Limit

AdS/CFT conjecture probably finds its maximum usefulness when we further send the 't Hooft coupling λ to infinity. Two things happen :

- $\mathcal{N} = 4$ $SU(N)$ SYM theory enters into a strongly coupled regime. Available perturbative techniques therefore becomes invalid.
- However, the dual string theory simply reduces to supergravity. This can be visualized on noting that perturbative expansion of the Lagrangian in curvature in this background is basically an expansion in $\lambda^{-\frac{1}{2}}$, since the Ricci scalar scales as : $R \sim \frac{1}{l^2} = \frac{\lambda^{-\frac{1}{2}}}{\alpha'}$. In large λ limit, we can therefore safely drop out higher order curvature terms and end up in achieving a supergravity limit of the full superstring theory. This supergravity theory is classical type IIB supergravity in $AdS_5 \times S^5$ space-time.
- This is the weak form of AdS/CFT correspondence but the most tractable one from the gravity side of the story. Since it relates the weakly coupled supergravity to a strongly coupled quantum field theory, this form is *believed to be* the most useful version of all the three forms in taming otherwise quite intractable strongly coupled phases of the boundary gauge theories. In this thesis, we will be dealing with this weak form of gauge/ gravity duality principle only.

1.4 Setting up the Dictionary

In the supergravity limit, the 10-dimensional type IIB action, (1.1) reduces to

$$I_{SUGRA} = \frac{1}{16\pi G_{10}} \int d^{10}x \sqrt{|g|} \left(R - \frac{1}{2} \frac{1}{5!} F_5^2 \right). \quad (1.16)$$

We are focusing on non-dilatonic solutions. For $D3$ brane solution, as we have seen before, the dilaton profile is constant and hence this can as well be set to zero. To get to a form suitable for reduction over S^5 we write the metric breaking it explicitly as :

$$ds^2 = g_{\mu\nu}^5 dx^\mu dx^\nu + l^2 d\Omega_5^2. \quad (1.17)$$

Here $d\Omega_5$ is the metric on S^5 . Taking $g_{\mu\nu}^5$ as the metric of AdS_5 , we end up in getting the following 5-dimensional reduced action :

$$ds_5^2 = \frac{1}{16\pi G_5} \int d^5x \sqrt{|g^{(5)}|} (R^{(5)} - 2\Lambda). \quad (1.18)$$

Here G_5 is the 5-dimensional Newton's constant related to its 10-dimensional counterpart as $G_5 = \frac{G_{10}}{\pi^3 l^5}$. Λ is the cosmological constant and is given by $\Lambda = -\frac{6}{l^2}$. The steps towards obtaining this 5-dimensional reduced action with a negative cosmological constant, Λ are the following :

- The metric being diagonal, the full 10-dimensional Ricci scalar completely decouples into two parts - the Ricci scalar on AdS_5 which we denote as $R^{(5)}$ and that on S^5 which is a constant.
- The full 10-dimensional 5-form field strength, F_5 has non-vanishing contributions in form of constant 0-forms on AdS_5 .
- The constant contributions coming from the Ricci scalar on S^5 and that from the constant 0-forms add up and give the negative cosmological constant appearing in (1.18).

A more detailed discussion on this can be found in [15, 16].

From the 5-dimensional point of view the AdS_5 space-time can therefore be thought of as a maximally symmetric solution of Einstein's equation in presence of a negative

cosmological constant :

$$R_{AB} - \frac{1}{2}RG_{AB} = \Lambda G_{AB}. \quad (1.19)$$

This is a solution with constant negative curvature such that :

$$R_{ABCD} = \frac{1}{l^2} (G_{AC}G_{BD} - G_{AD}G_{BC}). \quad (1.20)$$

For future use, we will, at this point, introduce new coordinates known as the Fefferman-Graham coordinates. The metric for the AdS_5 space-time in this coordinates takes the form:

$$ds^2 = \frac{l^2}{\rho^2} (d\rho^2 + \eta_{\mu\nu} dz^\mu dz^\nu). \quad (1.21)$$

ρ is the radial coordinate here and satisfies $\rho \geq 0$, $\rho = 0$ being the boundary. But it is worth noting that the metric having a second order pole at $\rho = 0$, does not yield an induced metric on the boundary. However, one is allowed to define a conformal structure at the boundary through a *defining function*, $r(\rho, z)$ which has a first order zero at the boundary. In the interior, however, $r(\rho, z)$ is positive definite everywhere. With this, one can define boundary metric, $g^{(0)}$ as

$$g^{(0)} = r^2 G|_{\rho=0} \quad (1.22)$$

$r(\rho, z)$ is otherwise arbitrary. We can therefore as well choose $r = \rho$. With this choice the boundary metric becomes flat Minkowski, namely, $g_{\mu\nu}^{(0)} = \eta_{\mu\nu}$.

Now we define asymptotically AdS_5 ($AAdS_5$) space-time as a spacetime having the following form of the metric in Fefferman-Graham coordinates:

$$ds^2 = \frac{l^2}{\rho^2} (d\rho^2 + g_{\mu\nu}(\rho, z) dz^\mu dz^\nu), \quad (1.23)$$

where we have replaced the flat Minkowski part, $\eta_{\mu\nu}$ in (1.21) by $g_{\mu\nu}(\rho, z)$. This metric is free of coordinate and curvature singularities upto a finite radial distance from the boundary. Furthermore, $\rho \rightarrow 0$ limit of the metric, $g_{\mu\nu}(\rho, z)$ is smooth and takes the following expansion near the boundary:

$$g_{\mu\nu}(\rho, z) = g_{\mu\nu}^{(0)}(z) + g_{\mu\nu}^{(2)}(z)\rho^2 + g_{\mu\nu}^{(4)}(z)\rho^4 + \bar{g}_{\mu\nu}^{(4)}(z)\log(\rho^2) + \dots \quad (1.24)$$

It can be shown the above form indeed yields a solution of Einstein's equation in the presence of a negative cosmological constant.

Justification

The above form of asymptotically AdS metric gets its justification from the fact that one can precisely draw a one-to-one map connecting the bulk diffeomorphisms preserving the form of the metric given by (1.23) and boundary conformal transformations.

Under such bulk diffeomorphism the $g_{\mu\nu}$ of (1.23) transform infinitesimally as:

$$\delta g_{\mu\nu}(\rho, z) = 2\sigma(z)(1 - \rho\partial_\rho)g_{\mu\nu}(\rho, z) + \nabla_\mu a_\nu(\rho, z) + \nabla_\nu a_\mu(\rho, z). \quad (1.25)$$

Here ∇ is the covariant derivative in terms of the metric, $g_{\mu\nu}$ and $a_\mu = \alpha^\nu g_{\mu\nu}$ is defined as:

$$a^\mu(\rho, z) = \frac{1}{2} \int_0^\rho d\rho' g^{\mu\nu}(\rho', z) \partial_\nu \sigma(\rho', z). \quad (1.26)$$

It can be easily checked that under this bulk diffeomorphisms, the boundary metric, $g_{\mu\nu}^{(0)}(z)$ is transformed as

$$\delta g_{\mu\nu}^{(0)}(z) = 2\sigma(z)g_{\mu\nu}^{(0)}(z), \quad (1.27)$$

which is nothing but a Weyl transformation.

Therefore, in asymptotically AdS_5 space-time $SO(4, 2)$ conformal symmetry of the boundary theory can be realized as the asymptotic symmetry group. The lifting of symmetry from boundary to bulk can be easily understood in terms of simple scale transformation. A uniform scale transformation of the boundary coordinates, $z \rightarrow \lambda z$, λ being constant gets lifted to $z \rightarrow \lambda z$, $\rho \rightarrow \lambda\rho$ in the bulk.

Fields in $AAAdS_5$

Just like the metric itself, any field $\Phi(\rho, z)$ in $AAAdS_5$ space-time also assumes an asymptotic expansion near the boundary:

$$\Phi(\rho, z) = \rho^\alpha \left(\Phi^{(0)}(z) + \Phi^{(2)}(z)\rho^2 + \dots + \Phi^{(2n)}(z)\rho^{2n} + \bar{\Phi}^{(2n)}(z)\log(\rho^2) + \dots \right). \quad (1.28)$$

The job is now to impose the equations of motion of $\Phi(\rho, z)$ which includes $g_{\mu\nu}(\rho, z)$ as well. No matter whether the equations of motion are linearized perturbations around the AdS_5 or the full non-linear equations of gravity, the field equations of motion will be second order differential equations in ρ and hence will have two independent series solutions. Asymptotically these two solutions will go as ρ^α and $\rho^{\alpha+2n}$ in the leading order.

Now we jot down the main features of the series solutions:

- Expect the coefficient, $\Phi^{(2n)}(z)$, all other coefficients, $\Phi^{(2k)}(z)$ for $0 < k < n$ are algebraically determined in terms of $\Phi^{(0)}(z)$ and their derivatives up to order $2k$. $\Phi^{(2n)}(z)$ remains undetermined by equations of motion.
- The coefficient, $\bar{\Phi}^{(2n)}(z)$ is also determined by $\Phi^{(0)}(z)$ and their derivatives in a similar spirit.
- We call $\Phi^{(0)}(z)$ the *non-normalizable mode*, $\Phi^{(2n)}(z)$, the *normalizable mode* and $\bar{\Phi}^{(2n)}(z)$, the *anomaly coefficient*. In other words, though a bit misnomer (strictly speaking, these are only coefficients of expansions, not a solution or mode!), the *non-normalizable* and the *normalizable* modes refer to the leading term in the asymptotic expansion of the two linearly independent solutions of the field equations of motion.
- Once we invoke regularity in the interior of the *AdS* space-time, the normalizable mode corresponding to any linearized perturbation around the *AdS* space-time gets fixed in terms of the corresponding non-normalizable mode, though the normalizable mode is *not* a local functional of the non-normalizable mode. This is a generic observation and it goes through even when we consider perturbation around more non-trivial backgrounds like *AdS* black holes. We will use these ideas later on in this thesis.

The Dictionary

With the basic set up ready, we are now in a position to state the dictionary of gauge/gravity duality.

- Corresponding to every field, Φ in the bulk gravity, there exists a gauge-invariant operator which we will denote as O_Φ . For instance, the bulk metric corresponds to the stress-energy tensor at the boundary whereas the gauge fields in the bulk are mapped to boundary symmetry currents.
- The non-normalizable mode, $\Phi^{(0)}$ in the asymptotic expansion, (1.28) is identified with the source that couples to the operator, O_Φ in the boundary gauge theory. As an example, the boundary metric, $g_{\mu\nu}^{(0)}$ is identified as the metric on the flat Minkowski space on which the gauge theory lives. It couples to the stress energy tensor operator of the boundary gauge theory.

- The partition function on the bulk side with $\Phi^{(0)}$ specified as boundary condition, gives the generating functional on the field theory side.

$$\begin{aligned}
 Z_{String} \left[\underbrace{\Phi|_{\rho=0} = \Phi^{(0)}}_{\text{Dirichlet Boundary condition}} \right] &= \int_{\Phi \approx \Phi^{(0)}} \mathcal{D}\Phi \exp(-S[\Phi]) \\
 &= \left\langle \exp \left(- \int \Phi^{(0)} O_{\Phi} \right) \right\rangle_{QFT}. \quad (1.29)
 \end{aligned}$$

In the limit when 't Hooft coupling is large and so is the rank of the gauge group, as discussed earlier, the left hand side of (1.29) can be approximated by supergravity partition function with the action, S replaced by the supergravity action, S_{Sugra} .

- This, however, is not the end of the story. In order to end up in getting finite correlation functions for the local gauge-invariant operators in the boundary theory, one needs to get rid of the divergent parts of the supergravity action. The methodology to making the observables in gauge theory sector finite by adding appropriate counter-terms to supergravity action is well known in the literature and goes by the name, “holographic renormalization” technique.
- Finally, functional differentiations of the renormalized action with respect to the source, $\Phi^{(0)}$ give correlators of all the local gauge-invariant operators.
- For AdS_5 space-time, it is always possible to find a suitable renormalization scheme in which the normalizable mode of graviton, $g_{\mu\nu}^{(4)}(z)$ can be identified with boundary stress energy tensor.

1.5 Finite Temperature : Thermal Retarded Correlators in AdS/CFT

In the thesis, we will mostly deal with finite temperature systems. The dictionary we just gave is typically for zero temperature. In the bulk gravity sector the most natural way of introducing temperature is to consider black holes in the AdS geometry. The intuition follows from the fact that stationary black holes behave like thermodynamical objects in all respect. The surface gravity at the black hole horizon can be identified with temperature while the mass, with the total energy. Furthermore, in all dynamical processes known, the

area of the black hole event horizon can only increase monotonically, justifying its identification with entropy. Also, for any dynamical process the black hole horizon possesses uniform surface gravity mimicking the thermodynamical equilibration. Since we are interested to study strongly coupled gauge theory on Minkowski space-time, we will fix the boundary metric to $\eta_{\mu\nu}$ by imposing Dirichlet boundary condition. We will focus on the cases where the topology of the horizon is the same as that of the boundary. Considering all these, a 5-dimensional black hole metric which asymptotes to AdS_5 takes the form:

$$ds^2 = -r^2 f(r) dt^2 + \frac{dr^2}{r^2 f(r)} + r^2(dx^2 + dy^2 + dz^2), \quad (1.30)$$

with $f(r) = 1 - \frac{r_0^4}{r^4}$, r_0 being the position of the horizon.

With proper coordinate redefinition, this metric can as well be re-written in Fefferman-Graham form, (1.23). In the asymptotic region, $r \rightarrow \infty$, $f(r)$ goes to 1, reducing the form of the metric to that of AdS_5 space-time.

In the thesis, we will also deal with a larger class of black hole solutions obtained by boosting the boundary coordinates, (t, x, y, z) . The class of solution is obtained by replacing $dt \rightarrow u_\mu dx^\mu$, u_μ being a time-like vector in Minkowski space, satisfying $u_\mu u_\nu \eta^{\mu\nu} = -1$. We further construct the projection vector $P_{\mu\nu} = u_\mu u_\nu + \eta_{\mu\nu}$ that projects on the spatial slice orthogonal to u_μ . With all these ingredients, the metric for the class of boosted solutions, known as the *boosted black branes* is given by

$$ds^2 = -r^2 f(r) u_\mu u_\nu dx^\mu dx^\nu + \frac{dr^2}{r^2 f(r)} + r^2 P_{\mu\nu} dx^\mu dx^\nu. \quad (1.31)$$

The boosted black brane metric can also be cast in the Fefferman-Graham form (1.23). In this form, the metric shows no coordinate singularity all the way to the horizon. From the Fefferman-Graham form of the above metric one can easily read off the boundary stress-energy tensor. When $u^\mu = (1, 0, 0, 0)$ we retrieve back (1.30). With this choice of u^μ , the energy density, ϵ and the pressure density, P are given by $\epsilon = 3\pi^4 T^4$ and $P = \pi^4 T^4$. These are exactly of the same form as that of black body radiation and hence establishes the fact that (1.31) is indeed the holographic dual for CFT states in thermal equilibrium.

Thermal Retarded Correlators

We will end this discussion with a prescription to thermal retarded correlators that we will use later on. In quantum field theories, retarded correlators measure the causal response to a source. It was argued in [17] that one way to ensure causal response in a theory of gravity is to replace the regularity condition of the solution in the interior of AdS with the incoming wave boundary condition at the horizon. This is causal in the sense that classically probe waves can only fall into the horizon but never come out. Once we invoke this condition, the two point function turns out to be the ratio of the normalizable and the non-normalizable modes.

Let us write the general solution of the bulk field as :

$$\begin{aligned}\Phi(r, t, x, y) = & \mathcal{A}(\omega, \mathbf{k}) \exp(-i\omega t + i\mathbf{k} \cdot \mathbf{x}) r^{-\Delta_-} (1 + \dots) \\ & + \mathcal{B}(\omega, \mathbf{k}) \exp(-i\omega t + i\mathbf{k} \cdot \mathbf{x}) r^{-\Delta_+} (1 + \dots),\end{aligned}\quad (1.32)$$

where $\Delta_- < \Delta_+$ and $\Delta_+ > 0$. Since in the leading order the Fefferman-Graham coordinate, ρ is related to the Schwarzschild coordinate, r as $\rho \sim \frac{1}{r}$ this leads to identifying \mathcal{A} with the non-normalizable mode or the source and \mathcal{B} with the normalizable mode or the response.

The two point thermal retarded correlator then takes the form [18, 19]:

$$\langle O_\Phi O_\Phi \rangle = \mathcal{C} \frac{\mathcal{B}(\omega, \mathbf{k})}{\mathcal{A}(\omega, \mathbf{k})} + \text{Contact terms}, \quad (1.33)$$

\mathcal{C} is a scheme independent constant.

It can be shown that the retarded correlator has a pole only when the non-normalizable mode, $\mathcal{A}(\omega, \mathbf{k})$ vanishes. This vanishing of non-normalizable mode + infalling wave boundary condition at the horizon gives a very special solution for $\Phi(r, t, x, y)$. These are called quasi-normal modes of the linearized perturbation around the black brane space-time. Going by our earlier logic this means, the poles of the retarded propagator of the boundary gauge theory can occur *iff* the dispersion relations corresponding to quasi-normal modes are satisfied.

1.6 Plan for the Rest of the Thesis

Upon understanding the basic notion and the tools of holography, we will proceed further, in subsequent chapters of this thesis, to develop methodologies to deal with different non-equilibrium scenarios in holographic set-up. We will develop tools and prescriptions contemplating on applications towards physically interesting problems like quantum quench, Fermi liquid theory in non-equilibrium and cosmological evolution of the universe. We will argue some of the methods developed might as well be very much useful in understanding and improving upon existing tools to study ultra relativistic heavy ion collisions. As mentioned in the overview, the methods we would use will be problem specific, but we will broadly categorize them in two parts. Following our understanding of holographic meaning of equilibrium, these are,

(A) *Going to a temperature other than the Hawking temperature of the black hole*

As we mentioned in previous subsection, in any dynamical gravitational process involving black holes, attaining Hawking temperature at the horizon signals the equilibration. Hence, at the level of free-energy, if we somehow make the temperature off-shell it would enable us to study the dynamics of equilibration. Motivated by *Bragg-Williams method* in condensed matter physics [20] and its adoption in black hole physics and holography [21], we will use this idea to analyze, holographically, the phenomenon of temperature quench in specific black hole set-up. Apart from the dynamics, we will see, even the analysis of phase transition particularly of the first order, which otherwise is difficult to capture in the framework of Landau theory, becomes easier in this framework. This *Bragg-Williams method* and applications thereof involving different black hole geometries will be discussed in detail in chapter 1 of this thesis.

(B) *Obtaining time-dependent backgrounds suitable to study non-equilibrium phenomena*

There are different ways to construct time-dependent backgrounds. In chapter 2 of this thesis we will discuss how to obtain time-dependent bulk space-time dual to specific non-equilibrium states starting from the observables of the boundary theory. This analysis is based on the Fefferman-Graham construction of AdS spaces which we have already developed in section 1.4. We will consider non-equilibrium fluctuations on the top of equilibrium states which holographically maps into incorporating quasi normal mode fluctuations on the AdS black hole in equilibrium. Upon constructing the background, we will use this to find the spectral function in specific non-equilibrium states. We will show the useful-

ness of the mechanism developed in understanding Fermi liquid theory for non-equilibrium strongly coupled systems.

The other methods of constructing time-dependent geometries are aimed at cosmological applications. The first of them is based on Verlinde's idea [22] that the time in the AdS bulk and that of the boundary conformal field theory are different and a dynamic boundary space-time can in principle be obtained starting from a static bulk. This idea was further extended with charged black holes in [23]. Motivated by these two, we will use the techniques of holographic renormalization with modified boundary conditions to come up with cosmological evolution on the boundary.

The second one in this line starts with a dynamical bulk itself. The time-dependent cosmological solution in supergravity is scarce in general. We, however, manage to find explicitly time-dependent brane solutions in 10 and 11 dimensional supergravity which takes Kasner-like scaling in world-volume directions on the brane. Such solutions in near horizon limit reduces to $AdS_5 \times S^5$ and $AdS_7 \times S^4$ with Kasner scaling in transverse directions for Kasner $D3$ and $M5$ brane solutions respectively. The AdS_5 solutions with Kasner scaling as solutions to 5-dimensional Einstein's equation with a negative cosmological constant was however studied in the literature either in the context of understanding gauge theory near cosmological singularity [25] or in the context of anisotropic expansion of strongly coupled quark gluon plasma [26]. We will, however, concentrate on cosmological implications, namely realizing cosmological evolution on probe dynamic branes in these time-dependent backgrounds and find interesting consequences like dynamical compactification of extra dimensions.

The third chapter in this thesis is fully devoted to such cosmological applications.

Bibliography

- [1] B. Zwiebach, “A first course in string theory,” Cambridge, UK: Univ. Pr. (2004) 558 p.
- [2] J. Polchinski, “String theory. Vol. 1: An introduction to the bosonic string,” Cambridge, UK: Univ. Pr. (1998) 402 p.
- [3] J. Polchinski, “String theory. Vol. 2: Superstring theory and beyond,” Cambridge, UK: Univ. Pr. (1998) 531 p.
- [4] K. Becker, M. Becker, J. H. Schwarz, “String theory and M-theory: A modern introduction,” Cambridge, UK: Cambridge Univ. Pr. (2007) 739 p.
- [5] M. B. Green, J. H. Schwarz, E. Witten, “Superstring Theory. Vol. 1: Introduction,” Cambridge, UK: Univ. Pr. (1987) 469 P. (Cambridge Monographs On Mathematical Physics).
- [6] M. B. Green, J. H. Schwarz, E. Witten, “Superstring Theory. Vol. 2: Loop Amplitudes, Anomalies And Phenomenology,” Cambridge, UK: Univ. Pr. (1987) 596 P. (Cambridge Monographs On Mathematical Physics).
- [7] J. M. Maldacena, “ The large N limit of superconformal field theories and supergravity,” Adv. Theor. Math. Phys. **2** (1998) 231–252, [arXiv:hep-th/9711200] .
- [8] S. S. Gubser, I. R. Klebanov, and A. M. Polyakov, “ Gauge theory correlators from non-critical string theory,” Phys. Lett. B **428**, 105 (1998) 105–114, [arXiv:hep-th/9802109].
- [9] E. Witten, “ Anti-de sitter space and holography,” Adv. Theor. Math. Phys **2** (1998) 253–291 [arXiv:hep-th/9802150] .
- [10] O. Aharony, S. S. Gubser, J. M. Maldacena, H. Ooguri and Y. Oz, “Large N field theories, string theory and gravity,” Phys. Rept. **323**, 183 (2000) [hep-th/9905111].
- [11] M. J. Duff, R. R. Khuri and J. X. Lu, “String solitons,” Phys. Rept. **259**, 213 (1995) [hep-th/9412184].
- [12] K. S. Stelle, “BPS branes in supergravity,” In *Trieste 1997, High energy physics and cosmology* 29-127 [hep-th/9803116].

- [13] R. Argurio, “Brane physics in M theory,” hep-th/9807171.
- [14] J. L. Petersen, “Introduction to the Maldacena conjecture on AdS / CFT,” Int. J. Mod. Phys. A **14**, 3597 (1999) [hep-th/9902131].
- [15] H. J. Kim, L. J. Romans and P. van Nieuwenhuizen, “The Mass Spectrum of Chiral N=2 D=10 Supergravity on S^5 ,” Phys. Rev. D **32**, 389 (1985).
- [16] Y. Kiem and D. Park, “A Nonperturbative evidence toward the positive energy conjecture for asymptotically locally AdS(5) IIB supergravity on S^5 ,” Phys. Rev. D **59**, 044010 (1999) [hep-th/9809174].
- [17] G. T. Horowitz and V. E. Hubeny, “Quasinormal modes of AdS black holes and the approach to thermal equilibrium,” Phys. Rev. D **62**, 024027 (2000) [hep-th/9909056].
- [18] D. T. Son and A. O. Starinets, “Minkowski space correlators in AdS / CFT correspondence: Recipe and applications,” JHEP **0209**, 042 (2002) [hep-th/0205051].
- [19] N. Iqbal and H. Liu, “Real-time response in AdS/CFT with application to spinors,” Fortsch. Phys. **57**, 367 (2009) [arXiv:0903.2596 [hep-th]].
- [20] Chaikin and Lubensky “Principles of Condensed Matter Physics”
- [21] S. Jain, S. Mukherji and S. Mukhopadhyay, “Notes on R-charged black holes near criticality and gauge theory,” JHEP **0911**, 051 (2009) [arXiv:0906.5134 [hep-th]].
- [22] I. Savonije and E. P. Verlinde, “CFT and entropy on the brane,” Phys. Lett. B **507**, 305 (2001) [hep-th/0102042].
- [23] S. Mukherji and M. Peloso, “Bouncing and cyclic universes from brane models,” Phys. Lett. B **547**, 297 (2002) [hep-th/0205180].
- [24] S. de Haro, S. N. Solodukhin and K. Skenderis, “Holographic reconstruction of space-time and renormalization in the AdS / CFT correspondence,” Commun. Math. Phys. **217**, 595 (2001) [hep-th/0002230].
- [25] S. R. Das, J. Michelson, K. Narayan and S. P. Trivedi, “Time dependent cosmologies and their duals,” Phys. Rev. D **74**, 026002 (2006) [hep-th/0602107].
- [26] S. -J. Sin, S. Nakamura and S. P. Kim, “Elliptic Flow, Kasner Universe and Holographic Dual of RHIC Fireball,” JHEP **0612**, 075 (2006) [hep-th/0610113].

2

The Bragg-Williams Method

Prelude

Going by the plan chalked out in the introduction, we start with our first scheme to go out of equilibrium through a construction of an effective free-energy which is off-shell in temperature. This construction which goes by the name “Bragg-Williams Method” was, however, originally proposed as an efficient mean field technique to study phase transition phenomena in condensed matter physics. As we know, within the mean field approximation, phase transition is primarily described via Landau theory. Under the assumptions that the order parameter is small and uniform near the transition, this theory provides us with a wealth of information about the nature of the phase transition. It is based upon a power series expansion of free energy in terms of the order parameter. The terms in this expansion are normally determined by symmetry considerations of the phases. Furthermore, owing to the smallness of the order parameter, only a few leading terms are kept. The usefulness of the Landau theory lies in its simplicity as most of its predictions can be achieved by solving simple algebraic equations [1]. While this theory is most suitable in describing a second order phase transition, one needs to be somewhat careful to treat first order phase transition within this framework. This is because, in a first order transition, order parameter suffers a discontinuous jump across the critical temperature. If this change is large, a power series expansion of free energy may acquire ambiguities. One then requires a more complete mean field theory. This is where the Bragg-Williams (BW) method [2, 3] comes in handy. Originally used to describe order - disorder transition of alloys, it has a wide range of applications [1, 4]. In this approach, one constructs an approximate expression for the free energy in terms of the order parameter and uses the condition that its equilibrium

value minimizes the free energy. In the following sections we will extend this novel idea to study phase transitions involving *AdS* black holes. We will start with Schwarzschild *AdS* black hole and later generalize it for charged black holes in *AdS*. Going off-shell to study black hole phase transition within the BW framework gets support from a previous work of Fursaev and Solodukhin [5]. We will discuss their approach later in this chapter. In the process we will propose one possible construction for an effective off-shell free energy of the boundary gauge theory. Finally we will show, through a specific example, how this method can be immensely helpful in understanding the phenomenon of quantum quench. But even before going into its applications, we need to know this construction in a set up where it was born. This chapter is primarily based on our work, [6, 7].

2.1 Bragg-Williams construction: a brief review

This section is a review of BW theory and is pedagogical in nature. It has two subsections. In the first subsection, we discuss Ising model and use BW theory to capture second order paramagnetic to ferromagnetic transition. In the next subsection we describe how to generalize this concept for Schwarzschild black hole in AdS space and reproduce the qualitative features of the first order Hawking-Page transitions.

2.1.1 Paramagnetic to ferromagnetic transition

Bragg-Williams construction is perhaps best described via Ising model [1]. Let us consider Ising model on a lattice where, on each site, the classical spin variable σ_l takes values ± 1 . These spins interact via a nearest neighbour coupling $J > 0$. The Hamiltonian is given by

$$H = -J \sum_{\langle ll' \rangle} \sigma_l \sigma_{l'}. \quad (2.1)$$

Here the sum is over the nearest neighbour l and l' . The order parameter is $m = \langle \sigma \rangle$, the average of the spin. For spatially uniform m , the entropy can be computed exactly. The total magnetic moment is

$$m = \frac{N_{+1} - N_{-1}}{N}, \quad (2.2)$$

where N_{+1} and N_{-1} are the total number of $+1$ and -1 spins respectively. The total number of lattice sites is denoted by N . The entropy is the logarithm of the number of states and is

Chapter 2. The Bragg-Williams Method

given by

$$S = \ln({}^N C_{N+1}) = \ln({}^N C_{N(1+m)/2}) \quad (2.3)$$

which, for entropy per unit spin, gives

$$s(m) = \frac{S}{N} = \ln 2 - \frac{1}{2}(1+m)\ln(1+m) - \frac{1}{2}(1-m)\ln(1-m). \quad (2.4)$$

In BW theory, the energy $\langle H \rangle$ is approximated via replacing σ by its position independent average m . Thus

$$E = -J \sum_{\langle ll' \rangle} m^2 = -\frac{1}{2} J N z m^2, \quad (2.5)$$

where z is the number of nearest neighbours in the lattice. One then constructs the BW free energy per spin as

$$\begin{aligned} f(T, m) &= \frac{E - TS}{N} \\ &= -\frac{1}{2} J z m^2 - T \ln 2 + \frac{T}{2}(1+m)\ln(1+m) + \frac{T}{2}(1-m)\ln(1-m) \end{aligned} \quad (2.6)$$

The BW free energy $f(T, m)$ can be plotted as a function of m for various temperatures. It can be checked that, for $T > Jz$, it has a single minimum at $m = 0$. However, for $T < Jz$, two minima occurs for non-zero values of m leading to paramagnetic to ferromagnetic transition. Critical temperature (T_c) for this second order transition can be found by setting first and second derivative of f to zero with the result $T_c = Jz$. More details about Bragg-Williams mean field construction in the context of statistical mechanics and condensed matter can be found in [1, 4].

2.1.2 Hawking-Page transition: AdS-Schwarzschild black hole

We can implement similar construction for AdS black holes as well. Let us consider a Schwarzschild black hole in $(n+2)$ dimensional AdS space. The metric is given by

$$ds^2 = -V(r)dt^2 + V(r)^{-1}dr^2 + r^2 d\Omega_n^2, \quad (2.7)$$

with

$$V(r) = \left(1 - \frac{M}{r^{n-1}} + \frac{r^2}{l^2}\right). \quad (2.8)$$

Chapter 2. The Bragg-Williams Method

Here M is a parameter related to the mass or internal energy of the hole and l is the inverse radius of AdS space. We have set $(n + 2)$ dimensional gravitational constant G_{n+2} to one. The black hole has a single horizon where g_{tt} vanishes. We will identify the horizon radius as r_+ . The dimensionless temperature, energy and entropy densities are give by

$$\begin{aligned}\bar{T} = lT &= \frac{(n+1)\bar{r}^2 + (n-1)}{4\pi\bar{r}}, \\ \bar{E} = lE &= \frac{n(\bar{r}^{n+1} + \bar{r}^{n-1})}{16\pi}, \\ \bar{S} &= \frac{\bar{r}^n}{4}.\end{aligned}\tag{2.9}$$

Here $l\bar{r} = r_+$. Before constructing the BW free energy, we will have to decide on an order parameter. Noticing the form of the entropy and the energy, it is only natural to consider \bar{r} as the order parameter. We will see later that this order parameter has right behaviour expected from the instability associated with this hole. We are now in a position to construct the BW free energy $\bar{\mathcal{F}}(\bar{r}, \bar{T})$ as

$$\bar{\mathcal{F}}(\bar{r}, \bar{T}) = \bar{E} - \bar{T}\bar{S} = \frac{n(\bar{r}^{n+1} + \bar{r}^{n-1})}{16\pi} - \bar{T}\frac{\bar{r}^n}{4}.\tag{2.10}$$

A plot of the free energy in five dimensions as a function of \bar{r} for various temperatures is shown in figure (2.1). Note that in (2.10), the temperature is a parameter. Its dependence on \bar{r} as given in (2.9) appears after minimizing $\bar{\mathcal{F}}$ with respect to \bar{r} . At this minimum $\bar{\mathcal{F}}$ reduces to the on-shell free energy of the black hole. It is given by

$$\bar{F} = \bar{\mathcal{F}}|_{\min} = -\frac{\bar{r}^{n-1}(\bar{r}^2 - 1)}{16\pi}.\tag{2.11}$$

We identify the AdS free energy with \bar{r} equals to zero. The first order transition appears when

$$\bar{\mathcal{F}} = 0, \text{ and } \frac{\partial \bar{\mathcal{F}}}{\partial \bar{r}} = 0,\tag{2.12}$$

are satisfied simultaneously. This happens for

$$\bar{r} = 1, \text{ and } \bar{T}_c = \frac{3}{2\pi}.\tag{2.13}$$

Below this temperature, black hole phase becomes unstable. As can be seen from the dashed line of figure (2.1), the $\bar{r} = 0$ phase is preferred. This is identified as the AdS

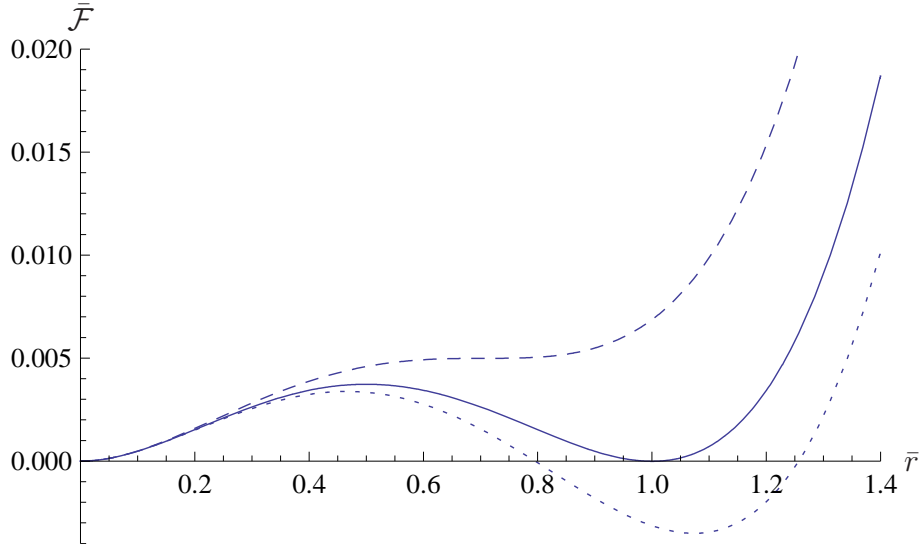


Figure 2.1: BW free energy for five dimensional AdS-Schwarzschild black holes plotted against horizon radius \bar{r} for different temperatures \bar{T} . The solid line has two degenerate minima - representing co-existence of black hole phase (minimum at $\bar{r} = 1$) and the thermal AdS phase (with $\bar{r} = 0$). This happens at a critical temperature $\bar{T}_c = 3/(2\pi)$. While above this temperature black hole is stable (dotted line), AdS is a preferred phase below \bar{T}_c (dashed line).

phase. This is a first order transition causing a discontinuous change in the order parameter \bar{r} . This instability is well known in the literature as *the Hawking-Page (HP) instability* [8], where below a critical temperature, a AdS-Schwarzschild black hole becomes unstable and crosses over to the thermal AdS space via a first order phase transition.

Upon constructing the BW free energy for Schwarzschild AdS black holes, we now move onto incorporating charged black holes in AdS space in this frame-work.

2.2 Charged black holes

As discussed in the introduction, for a $(n+1+q)$ dimensional theory of gravity compactified on $AdS_{n+1} \times X^q$, the dual field theory lives on a space whose topology is same as that of the boundary of AdS_{n+1} . The isometries of X^q becomes global symmetries of the field theory. Now when X^q is a five-sphere, the $SO(6)$ isometry allows one to introduce three independent R-charges through rotation in S^5 direction. These three R-charges correspond to the three Cartans of $SO(6)$. Consequently, one can turn on three independent chemical

potentials in $\mathcal{N} = 4$ SYM. At finite temperature, the gravity dual of this theory is the Reissner-Nordström black holes of $\mathcal{N} = 2$ gauged supergravity [9–11]. For the special case, when the charges are equal, these black holes reduce to the Reissner-Nordström black holes in AdS space. Many features of these black holes and their gauge theory duals were studied in [12, 13].

Furthermore, it is also clear from the previous discussions that working at the supergravity level corresponds to analyzing gauge theories, at infinite coupling, with large number of colours. To see any finite coupling/finite colour effect in gauge theory, one requires studying string theory on AdS. However, since this is as yet a poorly understood area, many authors have looked into the effects of adding α' corrections to supergravity. See [14–17] for an incomplete list of references. In general, it is also expected that string theory will introduce higher order gauge field corrections to supergravity actions. These corrections, in turn, would modify various equilibrium and non-equilibrium properties of the gauge theory. The reader can look at [18] for work in this direction. At finite temperature, the gravity duals of these are the black holes in the presence of higher derivative corrections. Construction of such black holes becomes progressively difficult as one introduces more and more higher derivative terms in the action. In fact, in many cases, one relies on perturbative construction of the black holes. However, there exists a rare example of exact black hole solution which takes into account a specific set of gauge field higher derivative corrections to all orders. These are the black holes in the Born-Infeld (BI) theories in the presence of a negative cosmological constant. BI black holes were constructed in [19, 20]. *Assuming* that there exists a dual gauge theory, equilibrium and non-equilibrium properties of the finite temperature gauge theory were studied by many authors by exploiting the black hole solution [21, 22]. We have discussed previously that adding a gauge field in the bulk is equivalent to turning of a chemical potential in the gauge theory. Since BI black holes accommodate all order gauge field corrections, they incorporate large chemical potential contributions into the gauge theory. In this section we will address some issues along these directions.

This section is structured as follows. In the next subsection we review the Born-Infeld black hole solutions in AdS space in $(n + 1)$ -dimensions. In subsection 2 we compute the Born-Infeld actions in two different thermodynamical ensembles - namely the fixed potential and the fixed charge ensembles. In the following subsection we compute different thermodynamic quantities in the two ensembles directly from the action. In subsection 4, we go into the study of phase structure of those black holes in grand canonical (fixed

potential) ensemble. Although those have already been well studied [19, 23, 24], we use Bragg-Williams technique to find an off-shell potential. We start with an easier system, namely the Reissner-Nordström, which is the zeroth order expansion of Born-Infeld solution and study its phase structure using Bragg-Williams construction. This again shows a first order phase transition corresponding to the Hawking-Page phase transition from black hole phase to AdS phase. We then repeat the same exercise for Born-Infeld case. In the next subsection, we continue this study, but this time with R-charge black holes whose phase structure exhibit both the first and the second order phase transitions. With this we move on to proposing some possible gauge theoretic free energy construction in the last subsection. We successfully construct off-shell boundary potentials dual to Reissner-Nordström and Born-Infeld black holes.

2.2.1 Born-Infeld black holes in AdS space

We start by reviewing some essential features of Born-Infeld action and its black hole solution. Let us consider the $(n + 1)$ dimensional Einstein-Born-Infeld action with a negative cosmological constant Λ of the form

$$S = \frac{1}{16\pi G} \int d^{n+1}x \sqrt{-g} \left[(\mathcal{R} - 2\Lambda) + L(F) \right], \quad (2.14)$$

where $L(F)$ is given by

$$L(F) = 4\beta^2 \left(1 - \sqrt{1 + \frac{F^{\mu\nu} F_{\mu\nu}}{2\beta^2}} \right). \quad (2.15)$$

The constant β is called the Born-Infeld parameter and has the dimension of mass. In the limit $\beta \rightarrow \infty$, higher order gauge field fluctuations can be neglected and, therefore, $L(F)$ reduces to the standard Maxwell form

$$L(F) = -F^{\mu\nu} F_{\mu\nu} + \mathcal{O}(F^4). \quad (2.16)$$

Thus the action, S , reduces to the standard form for which the Reissner-Nordström in AdS is the black hole solution. Thermodynamics and phase structure of such black holes were studied in detail in [12, 13].¹

¹In what follows, for simplicity, we will work in a unit in which $16\pi G = 1$, G being the Newton's constant in $(n + 1)$ dimensions.

Chapter 2. The Bragg-Williams Method

Equations of motions can be obtained by varying the action with respect to the gauge field A_μ and the metric $g_{\mu\nu}$. For A_μ and for $g_{\mu\nu}$ those are respectively given by

$$\nabla_\mu \left(\frac{F^{\mu\nu}}{\sqrt{1 + \frac{F^2}{2\beta^2}}} \right) = 0, \quad (2.17)$$

and

$$\mathcal{R}_{\mu\nu} - \frac{1}{2}\mathcal{R}g_{\mu\nu} + \Lambda g_{\mu\nu} = \frac{1}{2}g_{\mu\nu}L(F) + \frac{2F_{\mu\alpha}F_\nu{}^\alpha}{\sqrt{1 + \frac{F^{\mu\nu}F_{\mu\nu}}{2\beta^2}}}, \quad (2.18)$$

where $\mathcal{R}_{\mu\nu}$ is the Ricci tensor and \mathcal{R} , the Ricci scalar. In order to solve the equations of motion, we use the metric ansatz

$$ds^2 = -V(r)dt^2 + \frac{dr^2}{V(r)} + f^2(r)g_{ij}dx^i dx^j, \quad (2.19)$$

The metric on the foliating submanifold, g_{ij} , is a function of coordinates x^i and spans an $(n - 1)$ -dimensional hypersurface with scalar curvature $(n - 1)(n - 2)k$, k being a constant which characterizes the afore-mentioned hypersurface. Depending on whether the black hole horizon is elliptical, flat or hyperbolic, k can be taken as ± 1 and 0 respectively without any loss of generality. For the metric (2.19), we have non-vanishing components of Ricci tensor

$$\mathcal{R}_t^t = -\frac{V''}{2} - (n - 1)\frac{V'R'}{2R}, \quad (2.20)$$

$$\mathcal{R}_r^r = -\frac{V''}{2} - (n - 1)\frac{V'R'}{2R} - (n - 1)\frac{VR''}{R}, \quad (2.21)$$

$$\mathcal{R}_j^i = \left(\frac{n - 2}{R^2}k - \frac{1}{(n - 1)R^{n-1}}[V(R^{n-1})]' \right) \delta_j^i, \quad (2.22)$$

where the primed quantities denote the derivatives with respect to r .

Let us consider the case where all the components of $F^{\mu\nu}$ are zero except F^{rt} . In that case (2.17) can be immediately solved to yield

$$F^{rt} = \frac{\sqrt{(n - 1)(n - 2)}\beta q}{\sqrt{2\beta^2 r^{2n-2} + (n - 1)(n - 2)q^2}}. \quad (2.23)$$

Here q is an integration constant and is related to the electromagnetic charge. From (2.23)

we can also find the electric gauge potential as

$$A_t = \frac{1}{c} \frac{q}{r^{n-2}} {}_2F_1 \left[\frac{n-2}{2n-2}, \frac{1}{2}, \frac{3n-4}{2n-2}, -\frac{(n-1)(n-2)q^2}{2\beta^2 r^{2n-2}} \right] - \phi, \quad (2.24)$$

where ϕ is a constant and can be interpreted as the electrostatic potential difference between the black hole horizon and infinity and c is a constant given by $c = \sqrt{\frac{2(n-2)}{n-1}}$. ${}_2F_1$ is a hypergeometric function. Furthermore, we choose ϕ in a way that makes A_t vanish at the horizon ².

$$\phi = \frac{1}{c} \frac{q}{r_+^{n-2}} {}_2F_1 \left[\frac{n-2}{2(n-1)}, \frac{1}{2}, \frac{3n-4}{2(n-1)}, -\frac{(n-1)(n-2)q^2}{2\beta^2 r_+^{2n-2}} \right]. \quad (2.25)$$

Now if F^{rt} is the only non-zero component of all the $F^{\mu\nu}$'s, one can easily check from equation (2.18) that $\mathcal{R}_r^r = \mathcal{R}_t^t$ and hence, from (2.20) and (2.21) it follows $R''(r) = 0$ which has two solutions, $f(r) = r$ and $f(r) = \text{Constant}$. We will consider the case of $f(r) = r$ here. With this, and setting $\Lambda = -n(n-1)/2l^2$, we get the solution for $V(r)$ as [20, 24]

$$\begin{aligned} V(r) = & k - \frac{m}{r^{n-2}} + \left(\frac{4\beta^2}{n(n-1)} + \frac{1}{l^2} \right) r^2 \\ & - \frac{2\sqrt{2}\beta}{(n-1)r^{n-2}} \int \sqrt{2\beta^2 r^{2n-2} + (n-1)(n-2)q^2} dr. \end{aligned} \quad (2.26)$$

m here is an integration constant. Later we will see that this is related to the ADM mass of the black hole. The integral can also be expressed in terms of hypergeometric functions:

$$\begin{aligned} V(r) = & k - \frac{m}{r^{n-2}} + \left(\frac{4\beta^2}{n(n-1)} + \frac{1}{l^2} \right) r^2 - \frac{2\sqrt{2}\beta \sqrt{2\beta^2 r^{2n-2} + (n-1)(n-2)q^2}}{n(n-1)r^{n-3}} \\ & + \frac{2(n-1)q^2}{nr^{2n-4}} {}_2F_1 \left[\frac{n-2}{2(n-1)}, \frac{1}{2}, \frac{3n-4}{2(n-1)}, -\frac{(n-1)(n-2)q^2}{2\beta^2 r^{2n-2}} \right]. \end{aligned} \quad (2.27)$$

It is worth mentioning here that there is an ambiguity in the lower limit of the integral in the RHS of eqn.(2.26). In order to fix this up, one has to invoke again the fact that $V(r)$ should reduce to that of Reissner-Nordström [12] once $\beta \rightarrow \infty$ limit is taken. This

²Actually A_t at the horizon $r = r_+$ cannot be chosen arbitrarily. The event horizon of the afore-mentioned background is a killing horizon of killing vector ∂_t and therefore contains a bifurcation surface at $r = r_+$ where the killing vector vanishes. This in turn demands the vanishing of A_t at $r = r_+$ if the one form A is to be well-defined [25, 26]. A more detailed discussion regarding this can be found in [27].

Chapter 2. The Bragg-Williams Method

tells that the lower limit of the integral should be such that the integral vanishes at that limit.

Black hole horizon satisfies $V(r) = 0$. Denoting the solution as $r = r_+$, one can express m in terms of r_+ as

$$m = r_+^{n-2} + \left[\frac{4\beta^2}{n(n-1)} + \frac{1}{l^2} \right] r_+^n - \frac{2\sqrt{2}\beta r_+}{n(n-1)} \sqrt{2\beta^2 r_+^{2n-2} + (n-1)(n-2)q^2} \\ + \frac{2(n-1)q^2}{nr_+^{n-2}} {}_2F_1 \left[\frac{n-2}{2n-2}, \frac{1}{2}, \frac{3n-4}{2n-2}, -\frac{(n-1)(n-2)q^2}{2\beta^2 r_+^{2n-2}} \right]. \quad (2.28)$$

Next, to find the temperature of the black hole, we follow the standard prescription and expand $V(r)$ in Taylor expansion around $r = r_+$ so that

$$V(r) \simeq \frac{\partial V}{\partial r} \Big|_{r=r_+} (r - r_+)$$

Using this and a redefinition of the variable r , the radial and temporal part of the metric reduces to the form

$$ds^2 = d\rho^2 + \rho^2 d \left(\frac{\partial V}{\partial r} \Big|_{r=r_+} \frac{\tau}{2} \right)^2 \quad (2.29)$$

τ being the Euclidean time. Now, to avoid conical singularity $\left(\frac{\partial V}{\partial r} \Big|_{r=r_+} \frac{\tau}{2} \right)$ should have a periodicity of 2π and the periodicity in τ is therefore given by

$$\beta_{bh} = \frac{4\pi}{\frac{\partial V}{\partial r} \Big|_{r=r_+}}$$

This period is identified with the inverse of black hole temperature, $T_{bh} = \frac{1}{\beta_{bh}}$.

For our case $\frac{\partial V}{\partial r} \Big|_{r=r_+}$ can be easily found from eqn. (2.26). Once again, one has to fix the lower limit of the integral and regarding this, the discussion at the end of eqn. (2.27) still holds. Finally the temperature of the black hole comes out to be

$$T_{bh} = \frac{1}{4\pi} \left[\frac{n-2}{r_+} k + \left\{ \frac{4\beta^2}{n-1} + \frac{n}{l^2} \right\} r_+ - \frac{2\sqrt{2}\beta}{(n-1)r_+^{n-2}} \sqrt{2\beta^2 r_+^{2n-2} + (n-1)(n-2)q^2} \right], \quad (2.30)$$

which matches exactly with the expression of temperature obtained in [20, 24]. From now

on we will take $k = 1$ for all our computations.

There are normally two ways to calculate thermodynamic quantities. First, one assumes that the black hole satisfies laws of thermodynamics and uses that to find thermodynamic quantities. Second is to compute the action for a black hole and use it to derive various state variables following standard prescription. Here we will follow the second path.

2.2.2 Action Calculation

We will now calculate the black hole action in two different ensembles. First, we will focus on the grand canonical ensemble which is defined as a fixed potential ensemble. In the language of thermodynamics, this can be thought of as connecting the system to a heat reservoir full of quanta at a temperature, T_{bh} , the reservoir being identified as a pure AdS background with charged and uncharged quanta which are free to fluctuate in presence of a constant potential ϕ . The scenario is quite different in case of a fixed charge, namely the canonical ensemble. Since AdS with localized charge is not a solution of BIAdS equation, pure AdS background cannot serve the purpose of a heat reservoir. It turns out that extremal black hole background is a good candidate in this regard.³ In order to keep charge, Q fixed, we, in this case, retain only neutral quanta in the heat reservoir.⁴

2.2.2.1 Fixed Potential

The action for this is the one given in (2.14) analytically continued to Euclidean space by taking $t \rightarrow i\tau$. We then use the equation of motion given in (2.18) for the metric to eliminate \mathcal{R} to obtain the on-shell action as:

$$S = \int d^{n+1}x \sqrt{-g} \left[\frac{4\Lambda}{n-1} - \frac{2L(F)}{n-1} - \frac{4F^2}{(n-1)} \frac{1}{\sqrt{1 + \frac{F^2}{2\beta^2}}} \right], \quad (2.31)$$

It is worth mentioning in this regard that since the space is asymptotically AdS, there is no contribution from the Gibbons-Hawking-York boundary term. Also the surface term that arises from the variation of the action with respect to the gauge field vanishes in this case, since, for this particular ensemble, the potential is kept fixed at ∞ . Furthermore, since we

³This follows from an argument of [12] where the extremal black hole solution was used as a background on which the free energy was computed for canonical ensemble. We expect this to hold good for our finite β case as well.

⁴In grand canonical ensemble, an action calculation in four dimensions was performed earlier in [23]. We generalize the computation for arbitrary dimensions.

Chapter 2. The Bragg-Williams Method

contemplate on purely electrical solutions only (only non-zero component of $F^{\mu\nu}$ being $F^{r\tau}$), the possibility of having a Chern-Simons term does not arise as well.

Now we use the equation of motion for the gauge field given in (2.17) and get the full on-shell action as

$$I_{bh} = \omega_{n-1} \int_0^{\beta_{bh}} d\tau \int_{r_+}^{\infty} dr \left[\frac{2n}{l^2} r^{n-1} + \frac{8\beta^2}{n-1} r^{n-1} - \frac{8\beta}{n-1} \sqrt{\beta^2 r^{2n-2} + q^2 \frac{(n-1)(n-2)}{2}} \right], \quad (2.32)$$

ω_{n-1} being the volume of a unit $(n-1)$ sphere. This integral is clearly divergent. This is because of the infinite volume of the black hole spacetime. This is where the idea of introducing a heat reservoir in form of background pure AdS spacetime, as discussed in the beginning of this section exactly fits in. What we would do is to subtract from (2.32) the pure AdS action,

$$I_{AdS} = \omega_{n-1} \int_0^{\beta_{AdS}} d\tau \int_0^{\infty} dr \left[\frac{2n}{l^2} r^{n-1} \right], \quad (2.33)$$

which is also evidently infinity.

In order to implement this regularization scheme [28] properly, we put an upper cut-off R on the radial integration, which we would eventually take to infinity. For the black hole space-time to be smooth, β_{bh} is given by the inverse of Hawking temperature, T_{bh} , given in eqn.(2.30). β_{AdS} can, in general, be anything. But there is one constraint. β_{AdS} should have the value which makes the geometries of the AdS and the black hole spacetimes the same on the asymptotic hypersurface defined by $r = R$. This is done by setting

$$\begin{aligned} \beta_{AdS} \sqrt{1 + \frac{R^2}{l^2}} &= \beta_{bh} \left[1 - \frac{m}{R^{n-2}} + \frac{4\beta^2}{n(n-1)} R^2 + \frac{R^2}{l^2} \right. \\ &\quad - \frac{2\sqrt{2}\beta}{n(n-1)R^{n-3}} \sqrt{2\beta^2 R^{2n-2} + (n-1)(n-2)q^2} \\ &\quad \left. + \frac{2(n-1)q^2}{nR^{2n-4}} {}_2F_1 \left[\frac{n-2}{2(n-1)}, \frac{1}{2}, \frac{3n-4}{2(n-1)}, -\frac{(n-1)(n-2)q^2}{2\beta^2 R^{2n-2}} \right] \right]^{\frac{1}{2}}. \end{aligned} \quad (2.34)$$

After some algebraic manipulation, this becomes,

$$\begin{aligned}\beta_{AdS} = & \beta_{bh} \left[1 - \frac{ml^2}{2R^n} + \frac{2\beta^2 l^2}{n(n-1)} \left\{ 1 - \sqrt{1 + \frac{(n-1)(n-2)q^2}{2\beta^2 R^{2n-2}}} \right\} \right. \\ & \left. + \frac{(n-1)q^2 l^2}{nR^{2n-2}} {}_2F_1 \left[\frac{n-2}{2(n-1)}, \frac{1}{2}, \frac{3n-4}{2(n-1)}, -\frac{(n-1)(n-2)q^2}{2\beta^2 R^{2n-2}} \right] \right]. \quad (2.35)\end{aligned}$$

Using this relation along with eqn (2.28) and then taking the limit $R \rightarrow \infty$ we finally get the Born-Infeld action in the grand canonical ensemble as

$$\begin{aligned}I_{GC} = & \omega_{n-1} \beta_{bh} \left[r_+^{n-2} - \frac{r_+^n}{l^2} - \frac{4\beta^2 r_+^n}{n(n-1)} \left\{ 1 - \sqrt{1 + \frac{(n-1)(n-2)q^2}{2\beta^2 r_+^{2n-2}}} \right\} \right. \\ & \left. - \frac{2(n-1)}{n} q^2 \frac{1}{r_+^{n-2}} {}_2F_1 \left[\frac{n-2}{2(n-1)}, \frac{1}{2}, \frac{3n-4}{2(n-1)}, -\frac{(n-1)(n-2)q^2}{2\beta^2 r_+^{2n-2}} \right] \right]. \quad (2.36)\end{aligned}$$

As a consistency check of our result, we see that with $\beta \rightarrow \infty$ limit,

$$I_{GC} \Big|_{\beta \rightarrow \infty} = \omega_{n-1} \beta_{bh} \left[r_+^{n-2} - \frac{r_+^n}{l^2} - \frac{q^2}{r_+^{n-2}} \right]. \quad (2.37)$$

which is exactly the same as the Reissner-Nordström action for the grand canonical ensemble as obtained in [12].

2.2.2.2 Fixed Charge

In this ensemble, we, instead of fixing the potential at infinity, fix the charge of the black hole. Then the action given in (2.31) is no longer the appropriate one. Since the potential is not fixed at infinity, the boundary term as obtained by the variation of the gauge field, unlike in the case of fixed potential ensemble, has a non-vanishing contribution given by

$$I_s = -4 \int d^n x \sqrt{-h} \frac{F_{\mu\nu}}{\sqrt{1 + \frac{F^2}{2\beta^2}}} n_\mu A_\nu, \quad (2.38)$$

which after some straightforward computation becomes

$$I_s = 2(n-1) \omega_{n-1} \beta_{bh} \frac{q}{r_+^{n-2}} {}_2F_1 \left[\frac{n-2}{2(n-1)}, \frac{1}{2}, \frac{3n-4}{2(n-1)}, -\frac{(n-1)(n-2)q^2}{2\beta^2 r_+^{2n-2}} \right], \quad (2.39)$$

Chapter 2. The Bragg-Williams Method

h being the determinant of the induced metric at the boundary and n_μ , the radial unit vector pointing outward. Not only that, we also have to subtract the pure AdS background as before to ensure the convergence of the integral, the difference with the previous case of fixed potential ensemble being only that in the present case AdS background cannot be interpreted as the metric background or heat reservoir as argued before.

$$I_{bh} + I_s - I_{AdS} = \omega_{n-1}\beta_{bh} \left[r_+^{n-2} - \left\{ \frac{r_+^n}{l^2} + 4\beta^2 r_+^n \right\} + \frac{2\sqrt{2}\beta r_+}{n(n-1)} \sqrt{2\beta^2 r_+^{2n-2} + (n-1)(n-2)q^2} \right. \\ \left. + \frac{2(n-1)^2 q^2}{nr_+^{n-2}} {}_2F_1 \left[\frac{n-2}{2(n-1)}, \frac{1}{2}, \frac{3n-4}{2(n-1)}, -\frac{(n-1)(n-2)q^2}{2\beta^2 r_+^{2n-2}} \right] \right]. \quad (2.40)$$

The metric background in this case is the extremal black hole. The action for the extremal black hole can be found by substituting in (2.40), the condition for extremality with $r_+ = r_{ex}$, r_{ex} being the horizon of the extremal black hole.

The condition for extremality can be obtained by setting $T_{bh} = 0$ as

$$(n-2)r_{ex}^{n-3} + \left[\frac{n}{l^2} + \frac{4\beta^2}{n-1} \right] r_{ex}^{n-1} - \frac{2\sqrt{2}\beta}{n-1} \sqrt{2\beta^2 r_{ex}^{2n-2} + (n-1)(n-2)q^2} = 0. \quad (2.41)$$

And with this the action for the extremal black hole becomes

$$I_{ex} = 2(n-1)\omega_{n-1}\beta_{bh} \left[\frac{r_{ex}^{n-2}}{n} + \frac{(n-1)q^2}{nr_{ex}^{n-2}} {}_2F_1 \left[\frac{n-2}{2(n-1)}, \frac{1}{2}, \frac{3n-4}{2(n-1)}, -\frac{(n-1)(n-2)q^2}{2\beta^2 r_{ex}^{2n-2}} \right] \right]. \quad (2.42)$$

Subtracting the extremal background, finally, the full Born-Infeld action for canonical ensemble becomes:

$$I_C = \omega_{n-1}\beta_{bh} \left[r_+^{n-2} - \left\{ \frac{r_+^n}{l^2} + \frac{4\beta^2 r_+^n}{n(n-1)} \right\} + \frac{2\sqrt{2}\beta r_+}{n(n-1)} \sqrt{2\beta^2 r_+^{2n-2} + (n-1)(n-2)q^2} \right. \\ + \frac{2(n-1)^2 q^2}{nr_+^{n-2}} {}_2F_1 \left[\frac{n-2}{2(n-1)}, \frac{1}{2}, \frac{3n-4}{2(n-1)}, -\frac{(n-1)(n-2)q^2}{2\beta^2 r_+^{2n-2}} \right] \\ - 2(n-1)\omega_{n-1}\beta_{bh} \left\{ \frac{r_{ex}^{n-2}}{n} \right. \\ \left. + \frac{(n-1)q^2}{nr_{ex}^{n-2}} {}_2F_1 \left[\frac{n-2}{2(n-1)}, \frac{1}{2}, \frac{3n-4}{2(n-1)}, -\frac{(n-1)(n-2)q^2}{2\beta^2 r_{ex}^{2n-2}} \right] \right\} \right]. \quad (2.43)$$

As a check of our computation, if we take $\beta \rightarrow \infty$ limit of (2.43) we get,

$$I_C \Big|_{\beta \rightarrow \infty} = \omega_{n-1} \beta_{bh} \left[r_+^{n-2} - \frac{r_+^n}{l^2} - \frac{(2n-3)q^2}{r_+^{n-2}} - \frac{2(n-1)}{n} r_{ex} - \frac{2(n-1)^2}{n} \frac{q^2}{r_{ex}^{n-2}} \right], \quad (2.44)$$

which is exactly the same as the Reissner-Nordström action as obtained for the fixed charge ensemble in [12]. Next, we calculate thermodynamic quantities directly from those actions.

2.2.3 Thermodynamical quantities

The state variables for the system can be computed from the actions, I_{GC} and I_C given in (2.36) and (2.43) respectively.

2.2.3.1 Fixed Potential

The grand canonical free energy is given by $F_{GC} = E - TS - Q\phi$. Now F is also equal to $\frac{I_{GC}}{\beta_{bh}}$. Combining these two definitions we can find the state variables for the system as follows:

$$E = \left(\frac{\partial I_{GC}}{\partial \beta_{bh}} \right)_{\phi} - \frac{\phi}{\beta_{bh}} \left(\frac{\partial I_{GC}}{\partial \phi} \right)_{\beta_{bh}}, \quad (2.45)$$

$$S = \beta_{bh} \left(\frac{\partial I_{GC}}{\partial \beta_{bh}} \right)_{\phi} - I_{GC}, \quad (2.46)$$

$$Q = -\frac{1}{\beta_{bh}} \left(\frac{\partial I_{GC}}{\partial \phi} \right)_{\beta_{bh}}. \quad (2.47)$$

Now for this ensemble, ϕ is a constant. Thus to find the partial derivatives keeping ϕ constant, one has to substitute the condition $\frac{\partial \phi}{\partial r_+} = 0$, which we obtain from (2.24) keeping in mind that in this case q is no longer a constant, but a function of r_+ .

With all these, we get the state variables as:

$$\begin{aligned} E = & \omega_{n-1}(n-1) \left[r_+^{n-2} + \left\{ \frac{r_+^n}{l^2} + \frac{4\beta^2 r_+^n}{n(n-1)} \right\} - \frac{2\sqrt{2}\beta r_+}{n(n-1)} \sqrt{2\beta^2 r_+^{2n-2} + (n-1)(n-2)q^2} \right. \\ & \left. + \frac{2(n-1)q^2}{nr_+^{n-2}} {}_2F_1 \left[\frac{n-2}{2(n-1)}, \frac{1}{2}, \frac{3n-4}{2(n-1)}, -\frac{(n-1)(n-2)q^2}{2\beta^2 r_+^{2n-2}} \right] \right], \end{aligned} \quad (2.48)$$

using (2.28), which can also write this as

$$E = \omega_{n-1}(n-1)m, \quad (2.49)$$

and

$$S = 4\pi\omega_{n-1}r_+^{n-1}, \quad (2.50)$$

$$Q = 2\sqrt{2(n-1)(n-2)}\omega_{n-1}q. \quad (2.51)$$

2.2.3.2 Fixed Charge

In the canonical ensemble, the free energy is given by $F_C = E - TS$, which is again equal to $\frac{I_C}{\beta_{bh}}$. Then in a similar way as done before, one can find the corresponding state variables as:

$$E = \left(\frac{\partial I_C}{\partial \beta_{bh}} \right)_q = (n-1)m - (n-1)m_{ex}, \quad (2.52)$$

$$S = \beta_{bh} \left(\frac{\partial I_C}{\partial \beta_{bh}} \right)_q - I_C = 4\pi\omega_{n-1}r_+^{n-1}, \quad (2.53)$$

where m_{ex} is given by

$$m_{ex} = 2 \left[\frac{r_{ex}^{n-2}}{n} + \frac{(n-1)q^2}{nr_{ex}^{n-2}} {}_2F_1 \left[\frac{n-2}{2(n-1)}, \frac{1}{2}, \frac{3n-4}{2(n-1)}, -\frac{(n-1)(n-2)q^2}{2\beta^2 r_{ex}^{2n-2}} \right] \right] \quad (2.54)$$

This expression for m_{ex} can also be obtained by plugging in (2.28) the condition for extremality, (2.41).

Having obtained the thermodynamical quantities, we would like to study various stable, unstable and metastable phases associated with the black hole. For that, we construct an “off-shell” free energy, the saddle points of which dictates the (in)stability of the black hole. The details of this construction is discussed in the next subsection.

2.2.4 Construction of Bragg-Williams free energy & study of phase structure

In the case of $\beta \rightarrow \infty$, i.e. for Reissner-Nordström black hole, we know from [12] that there is a first order Hawking-Page (HP) transition. At a critical temperature, the black hole becomes unstable. The system prefers the AdS phase. This transition is of first order in nature, marked by a discontinuous change in the gravitational entropy. Our primary motivation would be to study the fate of this transition when β is finite. So we would be interested in constructing Bragg-Williams potential for Born-Infeld black hole. In order

to do so, we have to first decide on an order parameter. To this end, we note that a first order phase transition is characterized by a discrete jump of the order parameter. Like in the case of Schwarzschild AdS , in charged case also this jump shows up in the horizon radius of the black hole. Indeed, at the Hawking-Page (HP) point, AdS phase (identified with $r_+ = 0$) crosses over to the black hole phase (with non-zero r_+). So again, we find it suitable to use r_+ as the order parameter. Before we go on to discuss the phase structure in the Born-Infeld theory, we find it instructive to first analyze the Reissner-Nordström case. In a later sub-section, we generalize this for Born-Infeld black holes. We, further, stick to the grand canonical ensemble for the rest of our discussions.

2.2.4.1 Reissner-Nordström

The Bragg-Williams free energy for a Reissner-Nordström black hole in a grand canonical ensemble is given by $W_{GC} = E - TS - Q\phi$ with T and ϕ treated as external parameters. E can be found by taking $\beta \rightarrow \infty$ limit of (2.48) with the understanding that since we are working in a fixed potential ensemble we have to write q in terms of ϕ . In order to achieve this we use the relation between charge and potential of Reissner-Nordström black hole,

$$\phi = \frac{1}{c} \frac{q}{r_+^{n-2}}, \quad (2.55)$$

which can be directly obtained by taking $\beta \rightarrow \infty$ limit of eqn.(2.25).

With this, the Bragg-Williams free energy for the Reissner-Nordström black hole is given by

$$\begin{aligned} W_{BW}^{RN} &= E - TS - Q\phi \\ &= \omega_{n-1} \left[(n-1)r_+^{n-2}(1 - c^2\phi^2) - 4\pi r_+^{n-1}T + \frac{r_+^n}{l^2}(n-1) \right]. \end{aligned} \quad (2.56)$$

The on-shell temperature can be computed by differentiating W_{BW}^{RN} with respect to r_+ and then setting it to zero. The temperature comes out to be ⁵

$$T_{RN} = \frac{(n-2)l^2(1 - c^2\phi^2) + nr_+^2}{4\pi l^2 r_+}, \quad (2.57)$$

which is the same as the $\beta \rightarrow \infty$ limit of (2.30) and also matches with the expression

⁵In eqn.(2.56), r_+ should be treated as an unconstrained variable. Only on shell, r_+ is related to ϕ and T . This can be found by inverting eqn.(2.57) for r_+ .

for the temperature of Reissner-Nordström black holes obtained in [12]. The behaviour of W_{BW}^{RN} as a function of the order parameter for a fixed ϕ and for different temperatures is shown in the figure 2.2.

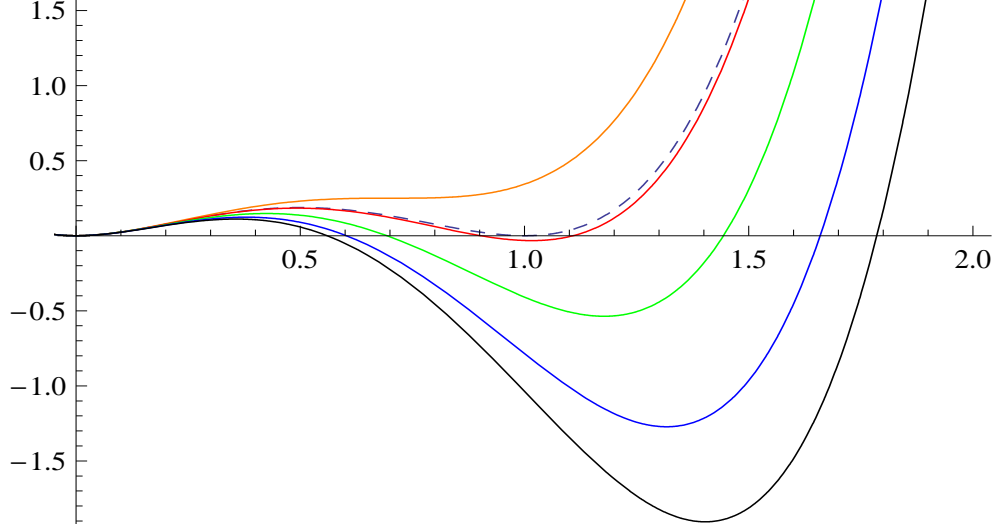


Figure 2.2: This is a plot of W_{BW}^{RN} as a function of r_+ for fixed ϕ . The phase structure shown here is for $n = 4$ and for $\phi=0.0003$. The dashed line is for the critical temperature, $T = T_c$, the orange one is the transition involving a metastable phase, another feature of a generic first order phase transition. The red, green, blue and black lines are for $T > T_c$ in an increasing order.

We see from the phase diagram that the r_+^3 term present in the free energy expression for $n = 4$ brings in an asymmetry in W_{BW}^{RN} as a function of r_+ and results in an emergence of a secondary minimum at finite value of r_+ . The value of W_{BW}^{RN} at this secondary minimum is greater than zero when $T < T_c$, but becomes zero at the critical temperature $T = T_c$. For all $T > T_c$, W_{BW}^{RN} is negative at the secondary minimum. Thus there is a phase transition from black hole to AdS as we tune the temperature below T_c , with a discontinuous change in r_+ at $T = T_c$. This is, clearly, the signature of a first order phase transition occurring at $T = T_c$.

An analytic expression for T_c can be obtained on requiring that W_{BW}^{RN} is an extremum with respect to r_+ in equilibrium, i.e., $\left(\frac{\partial W_{BW}^{RN}}{\partial r_+}\right) = 0$ along with the condition that the free energies of the ordered and the disordered phases match exactly at the transition, which, in turn, implies, $W_{BW}^{RN} = 0$. From these two conditions, we obtain the critical value of the order parameter, r_+ .

Chapter 2. The Bragg-Williams Method

For Reissner-Nordström case, in $(n + 1)$ dimensions, the requirement, $W_{BW}^{RN} = 0$ gives

$$r_+ = \frac{4\pi l^2 T + \sqrt{16l^4 T^2 \pi^2 - 4l^2(n-1)^2(1 - c^2 \phi^2)}}{2(n-1)}. \quad (2.58)$$

The other one, namely $\left(\frac{\partial W_{BW}^{RN}}{\partial r_+}\right) = 0$ gives

$$r_+ = \frac{4\pi l^2 T + \sqrt{16l^4 T^2 \pi^2 - 4l^2(n-2)(1 - c^2 \phi^2)}}{2n}. \quad (2.59)$$

Equations (2.58) and (2.59) can be solved to yield the transition temperature, T_c in terms of the corresponding critical value of ϕ

$$T_c = \frac{(n-1)}{2\pi l} \sqrt{1 - c^2 \phi_c^2}. \quad (2.60)$$

This is precisely the same critical temperature, T_c as obtained from the W_{BW}^{RN} vs r_+ diagram, as expected.

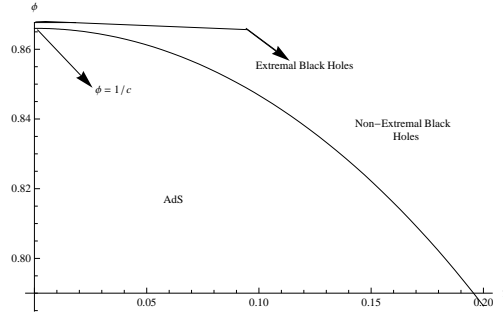


Figure 2.3: The phase structure of Reissner-Nordström in fixed potential ensembles. $T = 0$ line corresponds to extremal black holes. The extremal black holes are unstable. This plot is for $n = 4$ and we have set $l = 1$ here.

A similar exercise can also be done keeping T fixed and studying the phase structure varying the parameter, ϕ . The resulting phase structure is shown in figure 2.4.

The behaviour shows, as expected, the features of first order phase transition at $\phi = \phi_c$.

The analytic expression for $\phi = \phi_c$ can be obtained from eqn.(2.60) as

$$\phi_c = \frac{1}{c} \sqrt{1 - \frac{4\pi^2 l^2 T_c^2}{(n-1)^2}}. \quad (2.61)$$

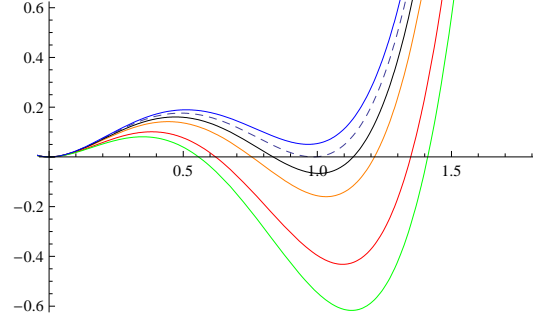


Figure 2.4: This is a plot of W_{BW}^{RN} as a function of r_+ for fixed T . The phase structure shown here is for $n = 4$ and for $T = 0.47$. The dashed line is for the critical value of potential, $\phi = \phi_c$, the blue one is for $\phi < \phi_c$. The black, orange, red and green lines are for $\phi > \phi_c$ in an increasing order.

The full phase structure in $\phi - T$ plane is shown in fig.2.3. Having discussed the $\beta \rightarrow \infty$ case, in the next sub-section we turn our attention to finite β .

2.2.4.2 Born-Infeld

It turns out, owing to the non-linear relation between ϕ and q as in eqn.(2.25), a complete analytical treatment is difficult in this case. One way to circumvent this problem is to make large β expansion and introduce $\frac{1}{\beta}$ correction order by order over the Reissner-Nordström construction. However, this would not allow us to study the Bragg-Williams potential at finite β . So we restrict ourselves to a semi-analytic approach to construct the free energy. This is done as follows. First we define a new variable, x as

$$x = \frac{q}{r_+^{n-1}}. \quad (2.62)$$

The horizon radius, r_+ can now be rewritten as

$$r_+(x, \phi) = \frac{\phi c}{x {}_2F_1\left[\frac{n-2}{2(n-1)}, \frac{1}{2}, \frac{3n-4}{2(n-1)}, -\frac{(n-1)(n-2)x^2}{2\beta^2}\right]}. \quad (2.63)$$

We can write down the grand canonical Bragg-Williams free energy for a Born-Infeld black hole as

$$W_{BW}^{GC} = E - TS - \phi Q, \quad (2.64)$$

where E , S and Q are given by (2.48) with the substitution (2.63) being taken care of. To see how W_{BW}^{GC} behaves with change in the order parameter, we, therefore, do a parametric plot. The behaviour is shown in fig.2.5⁶, which again shows a first order phase transition at a critical temperature, T_c .

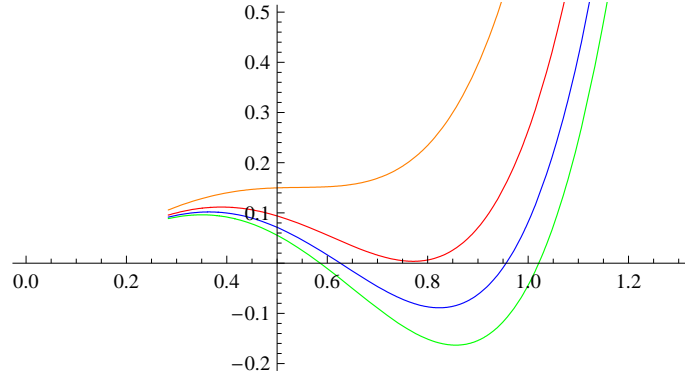


Figure 2.5: W_{BW}^{GC} is plotted against r_+ using x as a parameter for $n = 4$. We have fixed $\phi = 0.2$ and have plotted for different values of temperature. The red line is for $T = T_c$. The blue and green lines are for $T > T_c$ in an increasing order, whereas the orange line is for $T < T_c$.

We would like to mention one point in this regard. For the Reissner-Nordström, in grand canonical ensemble, we would observe this phase structure only when $\phi c < 1$ [12]. For Born-Infeld case also there is a similar critical value for ϕc which can be determined by plotting the on-shell free energy against T for different values of ϕ [23].

Interlude I : From elliptical to planar horizon

Our notion here is to consider the limit where the boundary (and the horizon) of AdS_{n+1} is R^n (flat) instead of $R \times S^3$ (elliptical). For Reissner-Nordström in an asymptotically AdS space in $(n + 1)$ dimensions, the metric ansatz is similar to the Born-Infeld case, (2.19)

⁶Those plots go down smoothly to $r_+ = 0$ as in the case of Reissner-Nordström. But unfortunately, that feature is not clearly visible in this phase diagram because of the fact that, the parameter, x , we have chosen for plotting goes as $\frac{1}{r}$. However, this feature can be easily checked from the expression for free energy directly.

Chapter 2. The Bragg-Williams Method

and the solution thereof is

$$V(r) = k - \frac{m}{r^{n-2}} + \frac{q^2}{r^{2n-4}} + \frac{r^2}{l^2}, \quad (2.65)$$

[12] where k is related to scalar curvature. For elliptical horizon $k = 1$, whereas for $k = 0$, the horizon geometry will be flat. This solution can, in fact, be obtained by taking $\beta \rightarrow \infty$ limit of (2.26). Thus for $k = 0$,

$$ds^2 = -V(r)dt^2 + \frac{dr^2}{V(r)} + \frac{r^2}{l^2} \sum_{i=1}^{n-1} (dx_i)^2, \quad (2.66)$$

with

$$V(r) = \frac{r^2}{l^2} - \frac{m}{r^{n-2}} + \frac{q^2}{r^{2n-4}}. \quad (2.67)$$

The limit in which one can go from the elliptic geometry of the horizon to a flat horizon is termed as “ infinite volume limit ”, since the area of a flat horizon is infinite. This limit can be obtained by introducing a dimensionless parameter, λ with which we scale different relevant quantities as [12]

$$r \rightarrow \lambda^{\frac{1}{n}} r, t \rightarrow \lambda^{-\frac{1}{n}} t, m \rightarrow \lambda m, q \rightarrow \lambda^{\frac{n-1}{n}} q, \quad (2.68)$$

and finally then taking $\lambda \rightarrow \infty$. In fact, one can check, this is precisely the limit in which $V(r)$ for $k = 1$ reduces to that for $k = 0$. Furthermore, the $(n - 1)$ volume has also to be scaled as

$$l^2 d\Omega_{n-1}^2 \rightarrow \lambda^{-\frac{2}{n}} \sum_{i=1}^{n-1} (dx_i)^2. \quad (2.69)$$

From (2.55), one can find the scaling for ϕ ,

$$\phi \rightarrow \lambda^{\frac{1}{n}} \phi. \quad (2.70)$$

In the same spirit, one can scale thermodynamic quantities too. Temperature, entropy, Energy and thermodynamic potential scale as [9]

$$T \rightarrow \lambda^{\frac{1}{n}} T, S \rightarrow S, E \rightarrow \lambda^{\frac{1}{n}} E, W \rightarrow \lambda^{\frac{1}{n}} W. \quad (2.71)$$

Chapter 2. The Bragg-Williams Method

The on-shell temperature, (2.57), on rescaling and then taking $\lambda \rightarrow \infty$ limit, becomes

$$T_{RN} |_{\lambda \rightarrow \infty} = \frac{nr_+^2 - (n-2)c^2 l^2 \phi^2}{4\pi l^2 r_+}, \quad (2.72)$$

which is the same temperature as obtained directly by differentiating (2.67) with respect to r_+ and dividing by 4π (The Hawking temperature of a black hole, $T_H = \frac{\kappa}{2\pi}$ where κ is the surface gravity given by $\kappa = -\frac{1}{2} \frac{\partial g_{tt}}{\partial r} |_{r=r_+}$. The physical reasoning behind this was discussed before in the context of Born-Infeld black holes. One can repeat the same with the $V(r)$ defined in (2.67) and come across the same expression for temperature.)

For Reissner-Nordström black holes in grand canonical ensemble, Energy, entropy and the Bragg-Williams free energy are given by

$$E = \frac{\omega_{n-1}}{16\pi G} (n-1) \left[r_+^{n-2} (1 + \phi^2 c^2) + \frac{r_+^n}{l^2} \right], \quad (2.73)$$

$$S = \frac{\omega_{n-1} r_+^{n-1}}{4G}, \quad (2.74)$$

$$Q\phi = \frac{\omega_{n-1}}{8\pi G} \phi^2 c^2 (n-1) r_+^{n-2}, \quad (2.75)$$

$$W_{BW}^{RN} = \frac{\omega_{n-1}}{16\pi G} \left[(n-1) r_+^{n-2} (1 - c^2 \phi^2) - 4\pi r_+^{n-1} T + \frac{r_+^n}{l^2} (n-1) \right]. \quad (2.76)$$

With the scaling defined above and taking the limit $\lambda \rightarrow \infty$ thereafter, those become

$$E = \lambda^{\frac{n-1}{n}} \frac{\omega_{n-1}}{16\pi G} (n-1) \left[r_+^{n-2} \phi^2 c^2 + \frac{r_+^n}{l^2} \right], \quad (2.77)$$

$$S = \lambda^{\frac{n-1}{n}} \frac{\omega_{n-1} r_+^{n-1}}{4G}, \quad (2.78)$$

$$Q\phi = \lambda^{\frac{n-1}{n}} \frac{\omega_{n-1}}{8\pi G} \phi^2 c^2 (n-1) r_+^{n-2}, \quad (2.79)$$

$$W_{BW}^{RN} = \lambda^{\frac{n-1}{n}} \frac{\omega_{n-1}}{16\pi G} \left[(n-1) \frac{r_+^n}{l^2} - (n-1) r_+^{n-2} c^2 \phi^2 - 4\pi r_+^{n-1} T \right]. \quad (2.80)$$

Thus on taking $\lambda \rightarrow \infty$ limit, all those quantities diverge. This is quite expected a result because, for a flat horizon geometry, the horizon area is infinity. So, instead of total energy, entropy and charge, one has to consider the corresponding densities. From (2.69), the $(n-1)$ volume ω_{n-1} should also scale as $\omega_{n-1} \rightarrow \lambda^{-\frac{n-1}{n}} \omega_{n-1}$. Then the energy density,

entropy density and off-shell free energy density are given by

$$\varepsilon = \frac{E}{\omega_{n-1}} = \frac{1}{16\pi G}(n-1)\left[r_+^{n-2}\phi^2c^2 + \frac{r_+^n}{l^2}\right], \quad (2.81)$$

$$s = \frac{S}{\omega_{n-1}} = \frac{r_+^{n-1}}{4G}, \quad (2.82)$$

$$\rho\phi = \frac{Q\phi}{\omega_{n-1}} = \frac{1}{8\pi G}\phi^2c^2(n-1)r_+^{n-2}, \quad (2.83)$$

$$\Omega_{BW}^{RN} = \frac{W_{BW}^{RN}}{\omega_{n-1}} = \frac{1}{16\pi G}\left[(n-1)\frac{r_+^n}{l^2} - (n-1)r_+^{n-2}c^2\phi^2 - 4\pi r_+^{n-1}T\right]. \quad (2.84)$$

$\frac{\partial \Omega_{BW}^{RN}}{\partial r_+} = 0$ gives the correct on-shell temperature, (2.72).

Now following the discussion leading to eqn.(2.60), one can check that there is no real solution for T_c in this case. This is consistent with the infinite volume limit taken, because as we arrive at the flat horizon geometry, there will be only black hole phase and hence the possibility of Hawking-Page phase transition from black hole to AdS does not arise at all.

2.2.5 R -charged black hole with spherical horizon: Instabilities

As mentioned in the beginning of this section, R -charged black holes are asymptotically AdS solutions to five dimensional $\mathcal{N} = 2$ gauged supergravity [10]. These black holes can carry three independent gauge charges and the stability of these black holes were studied, for example, in [29–31]. Here we will only focus on singly charged black hole with spherical horizon. The reason to study those black holes are that they exhibit even richer phase structure consisting of both the first and the second order transitions.

For single R -charged holes, the phase structure is shown in figure (2.6). It is plotted in the $T - \mu$ plane where μ is the chemical potential conjugate to the charge. There are three distinct phases, namely, the thermal AdS, black hole and a yet unknown phase. At a low temperature and small chemical potential, the system is always in thermal AdS phase. The cross-over from AdS to the black hole phase is shown by the dotted line in the plot. This is the usual first order HP transition. The black hole phase at fixed temperature also becomes unstable once the chemical potential is increased beyond a critical value. The corresponding stable phase is unknown as yet⁷. However, if a stable phase exists, this transition would be a continuous phase transition marked by divergences of specific heat and susceptibility.

⁷It may also be possible that there is no stable phase at all.

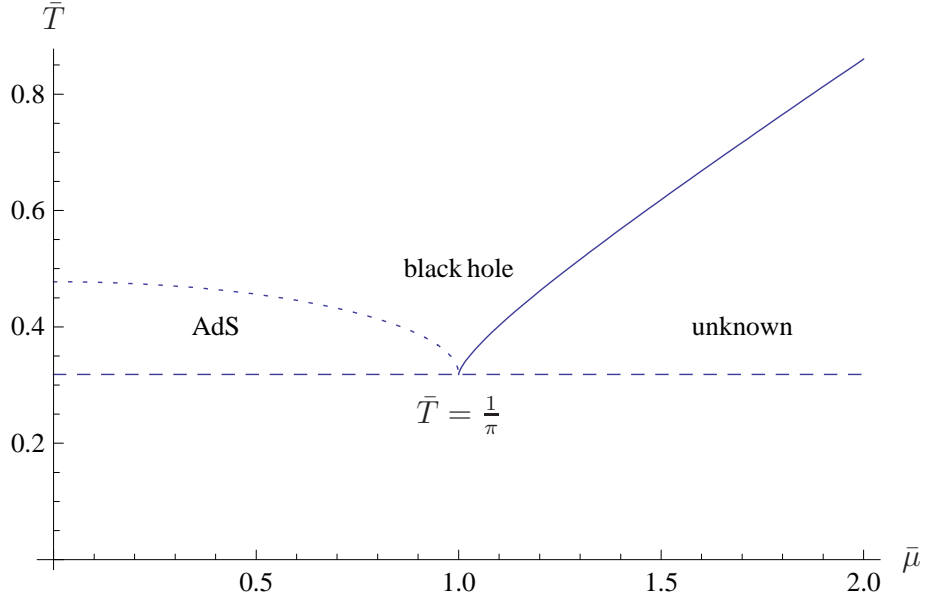


Figure 2.6: Phase diagram for the R -charged black hole with single charge shown in temperature, chemical potential plane. Line separating thermal AdS and black hole represents the first order phase transition line given by equation (2.105). On the other hand, the line between black hole and the unknown phase is a second order line - the equation of which is given in (2.106). The dashed line is for $\bar{T} = 1/\pi$ below which we can not extend various phases.

The solid line in figure (2.6) represents this critical line. Upon understanding, schematically, the rich phase structure of R -charged black holes with spherical horizon, we give below the details of the phase structure.

The black hole metric with a single $U(1)$ charge is given by

$$ds^2 = -H^{-\frac{2}{3}} f dt^2 + H^{\frac{1}{3}} \left(f^{-1} dr^2 + r^2 d\Omega_3^2 \right), \quad (2.85)$$

where

$$f = 1 - \frac{m}{r^2} + \frac{r^2}{l^2} H, \quad H = 1 + \frac{q}{r^2}. \quad (2.86)$$

In the above equation, $d\Omega_3^2$ is the metric on unit three sphere, l and m are related to the cosmological constant and the ADM mass of the black hole. In particular, l has a dimension of length. The zero of f gives the location of the horizon and in the above parametrization,

the horizon appears at $r = r_+$ where

$$r_+ = \left(\frac{-l^2 - q + \sqrt{(l^2 + q)^2 + 4ml^2}}{2} \right)^{\frac{1}{2}}. \quad (2.87)$$

There is a non-trivial gauge field potential associated with this geometry and is given by

$$A_t^i = \frac{\sqrt{q(r_+^2 + q)(1 + r_+^2)}}{r_+^2 + q}. \quad (2.88)$$

From the above we see that q is related to the physical charge. More explicitly, the physical charge

$$Q = \sqrt{q(r_+^2 + q)(1 + r_+^2)}. \quad (2.89)$$

The chemical potential is defined as the value of A_t^i at the horizon and is given by

$$\mu = \sqrt{\frac{q(1 + r_+^2)}{r_+^2 + q}}. \quad (2.90)$$

It will be convenient for us to scale all the dimensionful quantities with appropriate powers of l and make them dimensionless. We write all these parameters with a bar on the top. For example, the dimensionless horizon radius and Hawking temperature of the black hole are given by,

$$\bar{r} = \frac{r_+}{l}, \quad \bar{q} = \frac{q}{l^2}, \quad \bar{T} = lT = \frac{2\bar{r}^2 + \bar{q} + 1}{2\pi\sqrt{\bar{r}^2 + \bar{q}}}. \quad (2.91)$$

Furthermore, we define the dimensionless Newton's constant \bar{G} as $\bar{G} = l^3 G$ and set $\bar{G} = \pi/4$. With this convention, energy and entropy are given by

$$\bar{E} = \frac{3}{2}\bar{m} + \bar{q}, \quad \bar{S} = 2\pi\bar{r}^2\sqrt{\bar{r}^2 + \bar{q}}. \quad (2.92)$$

We would like to study the system in the grand canonical ensemble where we treat \bar{T} and $\bar{\mu}$ as external parameters. The free energy is given by

$$\bar{F} = \bar{E} - \bar{T}\bar{S} - \bar{\mu}\bar{Q} = -\frac{\bar{r}^2(\bar{r}^4 + \bar{\mu}^2 - 1)}{2(\bar{r}^2 - \bar{\mu}^2 + 1)} = -\bar{P}. \quad (2.93)$$

Here \bar{P} is the pressure. Let us note that \bar{F} changes sign when $\bar{r}^4 + \bar{\mu}^2 - 1$ changes sign. This is a first order transition and it leads to a crossover from AdS phase to the black hole

phase. For the gauge theory this represents the deconfining transition. Given all these thermodynamic quantities, it is straightforward to compute the specific heat and susceptibility. These are given respectively by

$$\begin{aligned}\bar{C} &= \left(\bar{T} \frac{\partial \bar{S}}{\partial \bar{T}} \right)_{\bar{\mu}} = \frac{2\pi\bar{r}^2(1 + 2\bar{r}^2 + \bar{q})(3 + 3\bar{r}^2 - \bar{q})\sqrt{\bar{r}^2 + \bar{q}}}{2\bar{r}^4 + \bar{r}^2 + \bar{q}\bar{r}^2 - \bar{q}^2 + 2\bar{q} - 1}, \\ \bar{\chi} &= \left(\frac{\partial \bar{Q}}{\partial \bar{\mu}} \right)_{\bar{T}} = \frac{(\bar{r}^2 + \bar{q})(2\bar{r}^4 + \bar{r}^2 + 5\bar{r}^2\bar{q} + 6\bar{q} - \bar{q}^2 - 1)}{2\bar{r}^4 + \bar{r}^2 + \bar{q}\bar{r}^2 - \bar{q}^2 + 2\bar{q} - 1}.\end{aligned}\quad (2.94)$$

We note that specific heat and susceptibility diverge at

$$2\bar{r}^4 + \bar{r}^2 + \bar{q}\bar{r}^2 - \bar{q}^2 + 2\bar{q} - 1 = 0. \quad (2.95)$$

This represents the line of continuous phase transition. As one approaches this critical line, correlation length diverges. This shows up, as above, in the divergences of some thermodynamic quantities. Near this critical line, the black holes are expected to exhibit some universal features. These are encoded in a set of critical exponents normally called α, β, γ and δ . Going close to this line with $\bar{\mu}$ fixed, we define exponents α, β, γ as

$$\bar{C} \sim (\bar{T} - \bar{T}_c)^{-\alpha}, \quad \bar{Q} - \bar{Q}_c \sim (\bar{T} - \bar{T}_c)^\beta, \quad \bar{\chi} \sim (\bar{T} - \bar{T}_c)^{-\gamma}. \quad (2.96)$$

Here \bar{T}_c is the value of the critical temperature for the chosen $\bar{\mu}$ (The critical line can be expressed in terms of \bar{T} and $\bar{\mu}$ and is given later, see (2.106)). Similarly, one defines \bar{Q}_c . The other static exponent δ is defined as

$$\bar{Q} - \bar{Q}_c \sim (\bar{\mu} - \bar{\mu}_c)^{\frac{1}{\delta}}. \quad (2.97)$$

Here one approaches the critical line with a trajectory on which \bar{T} is constant. For the black holes in consideration, these quantities are easily calculable and are given by

$$(\alpha, \beta, \gamma, \delta) = \left(\frac{1}{2}, \frac{1}{2}, \frac{1}{2}, 2 \right). \quad (2.98)$$

Firstly note that these exponents are same as the one computed for black holes with planar horizon [33, 34]. Secondly, they satisfy the scaling relations

$$\alpha + 2\beta + \gamma = 2, \quad \gamma = \beta(\delta - 1). \quad (2.99)$$

Our main task is now to construct an effective potential that captures all the phases that we have just discussed. We will use the BW approach for this purpose. This approach requires us to identify an order parameter. Noting the fact that, for a first order transition, the change in order parameter is discontinuous and for second order, it changes continuously, we continue to use the horizon radius \bar{r} of the black hole as the order parameter. Once a suitable order parameter is identified, one constructs the BW potential which depends on the order parameter, the temperature and the chemical potential. This is given by

$$\bar{\mathcal{F}}(\bar{r}, \bar{T}, \bar{\mu}) = \bar{E} - \bar{T}\bar{S} - \bar{\mu}\bar{Q}. \quad (2.100)$$

In our case, using (2.89) and (2.92), we immediately get⁸

$$\bar{\mathcal{F}}(\bar{r}, \bar{T}, \bar{\mu}) = \frac{1}{2}\bar{r}^2 \left[3 - 4\pi\bar{T} \frac{\bar{r}\sqrt{1+\bar{r}^2}}{\sqrt{1+\bar{r}^2}-\bar{\mu}^2} + \bar{r}^2 \left(3 + \frac{\bar{\mu}^2}{1+\bar{r}^2-\bar{\mu}^2} \right) \right]. \quad (2.101)$$

The saddle point of $\bar{\mathcal{F}}$, namely

$$\frac{\partial \bar{\mathcal{F}}}{\partial \bar{r}} = 0 \quad (2.102)$$

gives the equilibrium temperature. Using (2.101), from (2.102) we get

$$\bar{T} = \frac{\sqrt{1+\bar{r}^2}(1+2\bar{r}^2-\bar{\mu}^2)}{2\pi\bar{r}\sqrt{1+\bar{r}^2-\bar{\mu}^2}}. \quad (2.103)$$

Upon using (2.90), the above expression reduces to the one in (2.91). Furthermore, substituting (2.103) in (2.101), we get the on-shell free energy expression as in (2.93). We now proceed to study $\bar{\mathcal{F}}$ as we change \bar{T} and $\bar{\mu}$. From the expression of temperature, it is easy to note that it has a minimum $\bar{T}_0 = 1/\pi$ when $\bar{r} = 0$ and $\bar{\mu} = 1$. In what follows, we will focus ourselves in the region $\bar{T} \geq \bar{T}_0$ and $\bar{\mu} \geq 0$. As noted before, the first order transition line is given by the equation

$$\bar{r}^4 + \bar{\mu}^2 - 1 = 0. \quad (2.104)$$

Expressed in terms of \bar{T} and $\bar{\mu}$, this equation reduces to

$$\bar{T} = \frac{2 + \sqrt{1 - \bar{\mu}^2}}{2\pi}, \quad (2.105)$$

⁸For a black hole with flat horizon a similar construction was provided in [32].

represented by the dotted line in figure (2.6). On the other hand, the second order instability line (2.95) reads as

$$\bar{T} = \frac{(-\Delta\bar{\mu}^2 + \Gamma + \Delta)}{\sqrt{2\pi}\Gamma} \sqrt{\frac{\Gamma(\Gamma + 2\Delta)}{\Delta(\Gamma - 2\Delta(\bar{\mu}^2 - 1))}} \quad (2.106)$$

where

$$\Delta = (\bar{\mu}^2 - 1)^{\frac{2}{3}}(\bar{\mu} + 1)^{\frac{2}{3}}, \quad \Gamma = \bar{\mu}^4 + (\Delta - 2)\bar{\mu}^2 + \Delta^2 - \Delta + 1. \quad (2.107)$$

This is denoted by the solid line in figure (2.6).

To see that $\bar{\mathcal{F}}(\bar{r}, \bar{T}, \bar{\mu})$ captures the whole phase diagram, we first fix $\bar{\mu}$ and plot $\bar{\mathcal{F}}$ for various temperatures starting with $\bar{T} = \bar{T}_0 = 1/\pi$. We start with $\bar{\mu} = 1$. The behaviour is shown in figure (2.7). We note that at $\bar{T} = \bar{T}_0 = 1/\pi$, $\bar{\mathcal{F}}$ has a minimum at $\bar{r} = 0$. Its first and second derivatives with respect to \bar{r} also vanish at that point. In this sense, it is a point of inflection for $\bar{\mathcal{F}}$. If we increase \bar{T} further, we get minima for increasing values of \bar{r} – representing stable black hole phases with increasing size. This is in complete agreement with the phase diagram in figure (2.6). Next, we analyze the system for $0 \leq \bar{\mu} < 1$. From figure (2.6), we expect that $\bar{\mathcal{F}}$ should show a HP transition as we increase the temperature beyond a critical value. We precisely see this in figure (2.8), where we have plotted $\bar{\mathcal{F}}$ for $\bar{\mu} = .5$. While the point $\bar{r} = 0$ is identified with the AdS phase, any finite value of \bar{r} represents a black hole with \bar{r} being the horizon. As we increase the temperature, we note a crossover from AdS to the black hole phase at $\bar{T} = \bar{T}_{HP} = 1.433/\pi$. This is shown by the dotted line in the figure. At this temperature the order parameter \bar{r} changes discontinuously from zero to a finite value - clearly a signature of a first-order transition. Now as we decrease $\bar{\mu}$, HP transition temperature increases. In particular, for $\bar{\mu} = 0$, $\bar{T}_{HP} = 3/(2\pi)$ as expected for AdS-Schwarzschild black hole. Finally, we increase $\bar{\mu}$ beyond 1. For $\bar{\mu} = 2$, $\bar{\mathcal{F}}$ is shown in figure (2.9). Plot is shown for different temperature, starting with the critical one (solid curve). Below this temperature, we reach the yet unknown phase and the black hole is unstable. At higher temperatures (dashed and dotted curve), minima of the curves represent the stable black hole phases.

We can continue the same exercise for \bar{T} fixed at any value above $1/\pi$ and change $\bar{\mu}$. For $\bar{T}_{HP} \leq 3/(2\pi)$ and $\bar{\mu} \leq 1$, we first cross the HP line. Close to this point, $\bar{\mathcal{F}}$ behaves similar to figure that of (2.8). Further increasing $\bar{\mu}$ but keeping \bar{T} fixed, we hit the continuous phase transition line leading to figure (2.9). For $\bar{T} \geq 3/(2\pi)$, the first order

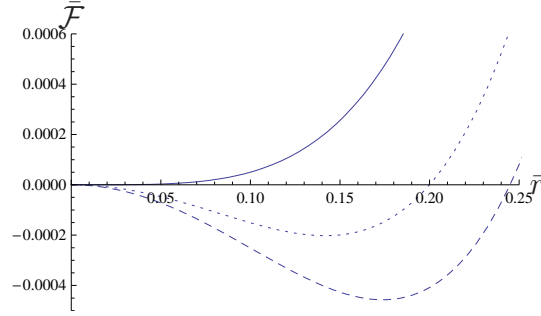


Figure 2.7: $\bar{\mathcal{F}}$ is plotted as a function of the order parameter \bar{r} for $\bar{\mu} = 1$. The solid, dotted and dashed curves are for $\bar{T} = 1/\pi, 1.01/\pi, 1.015/\pi$.

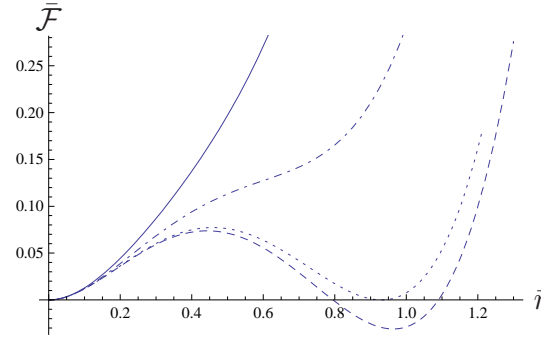


Figure 2.8: $\bar{\mathcal{F}}$ is plotted as a function of the order parameter \bar{r} for $\bar{\mu} = .5$. The solid, dot-dashed, dotted and dashed lines are for $\bar{T} = 1/\pi, 1.3/\pi, 1.433/\pi, 1.45/\pi$.

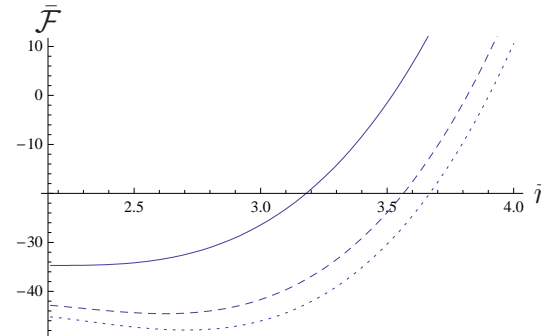


Figure 2.9: $\bar{\mathcal{F}}$ for $\bar{\mu} = 2$. Solid, dashed and dotted lines are for $\bar{T} = 0.86, 0.93, 0.95$ respectively. Solid line represents $\bar{\mathcal{F}}$ at critical temperature. Below this temperature, black hole becomes unstable. The minima in the rest two curves show the stable black hole phase.

transition is lost. Black hole is always a stable phase for low $\bar{\mu}$. However, as we take $\bar{\mu}$ to a critical value, black hole ceases to be stable and we reach the second order line getting a figure similar to figure (2.9).

Finally, let us now discuss about the procedure for obtaining the critical exponents from the mean field potential $\bar{\mathcal{F}}$ which has already been written in (2.98). We note that the specific heat at fixed chemical potential can be obtained from (2.101).

$$\bar{C}_{\bar{\mu}} = -\bar{T} \frac{\partial^2 \bar{\mathcal{F}}}{\partial \bar{T}^2} \bigg|_{\bar{\mu}} \sim (\bar{T} - \bar{T}_c)^{-\frac{1}{2}}, \quad (2.108)$$

which gives $\alpha = \frac{1}{2}$. If we approach the critical line along constant $\bar{\mu} = \bar{\mu}_c$, then we see that

$$\bar{Q} - \bar{Q}_c \sim (\bar{T} - \bar{T}_c)^{\frac{1}{2}}, \quad (2.109)$$

where \bar{Q}_c is the critical value of the charge at fixed $\bar{\mu}_c$. This shows that the critical exponent β has the value $\frac{1}{2}$. Similarly, the susceptibility behaves near the critical temperature as

$$\chi = \frac{\partial \bar{Q}}{\partial \bar{\mu}} \bigg|_{\bar{T}} \sim (\bar{T} - \bar{T}_c)^{-\frac{1}{2}}. \quad (2.110)$$

This leads us to the critical exponent $\gamma = \frac{1}{2}$. Finally, on approaching the critical line with $\bar{T} = \bar{T}_c$ we get

$$\bar{Q} - \bar{Q}_c \sim (\bar{\mu} - \bar{\mu}_c)^{\frac{1}{2}}. \quad (2.111)$$

So, this gives us $\delta = 2$.

Interlude II : On geometric realization of Bragg-Williams constructions

The Bragg-Williams construction owes its justification to a previous work by Fursaev and Solodukhin [5]. In this work they studied space-time manifolds with conical singularities. We discussed before in the context of AdS Born-Infeld black holes that temperature of the black hole comes as a consequence of ensuring that the space-time near horizon is free from any conical singularity. Therefore the most natural geometric interpretation of the “off-shellness” must arise from the space-time with conical singularity at the horizon

hypersurface.

According to the construction in [5], the Ricci tensor and curvature scalar of a manifold $\tilde{\mathcal{M}}$ with conical singularity on the surface, Σ (horizon in our case) can be expressed in terms of the Ricci tensor and curvature scalar for singularity-free region, $\mathcal{M} \equiv \tilde{\mathcal{M}} / \Sigma$ respectively.

$$\tilde{R}_{\mu\nu} = R_{\mu\nu} + n_\mu n_\nu \Delta_\Sigma \delta_\Sigma. \quad (2.112)$$

Here $\tilde{R}_{\mu\nu}$ and $R_{\mu\nu}$ are Ricci tensors on $\tilde{\mathcal{M}}$ and \mathcal{M} respectively. δ_Σ is the delta function and is defined as $\int_{\tilde{\mathcal{M}}} f \delta_\Sigma = \int_\Sigma f$ for any function, f . n_μ 's are components of unit vectors orthogonal to Σ . Δ_Σ is the conical deficit angle given by $\Delta_\Sigma = 2\pi - \frac{\beta}{\beta_H}$, β_H being the periodicity of Euclidean time to get rid of conical singularity at the horizon and β , an arbitrary period.

One can then easily find the Ricci scalar for the full manifold $\tilde{\mathcal{M}}$ in terms of Ricci scalar of \mathcal{M} and plug back in the Hilbert-Einstein action. The first term of the action becomes:

$$\int_{\tilde{\mathcal{M}}} \sqrt{g} \tilde{R} = \int_{\mathcal{M}} \sqrt{g} R + I_{\text{Singular}}. \quad (2.113)$$

For all the static, stationary black holes we considered I_{Singular} is proportional to $\Delta_\Sigma A_\Sigma$, A_Σ being the area of the horizon, Σ for a fixed cone. The constant of proportionality depends on the number of unit vectors orthogonal to Σ .

One can evaluate these quantities for specific black holes and find the off-shell action. Multiplying the off-shell action by β^{-1} we get the off-shell version of free energy which turns out to be identical to our Bragg-Williams free energy.

Similar idea was nurtured in a recent work [35], though in the context of the BTZ black hole, a $2 + 1$ dimensional asymptotically AdS black hole. We have, however, checked that the arguments of [5] go through in favour of the BW construction of free energy, off-shell in temperature, for any asymptotically AdS black hole.

2.2.6 Proposal for effective potentials in the boundary theory

So far we constructed effective off-shell potential for different supergravity solutions and analyzed their rich phase structures. Let us now pause for a bit and ask the following question: Can we at least phenomenologically construct an effective potential in the boundary gauge theory which describe its equilibrium and non-equilibrium properties? In

particular if our bulk has electrical charges, gauge theory in question must also have associated R-charges and corresponding chemical potentials.

It is worth mentioning that direct computation of effective potential in terms of the order parameter in gauge theory is difficult. However, it is possible to use AdS/CFT conjecture and our computations in the previous subsections to propose an effective potential whose saddle points represent various phases of the gauge theory. However, we should emphasize that the potential constructed this way may not be unique, except perhaps close to the transition line.

In the following, we first deal with the simpler case of gauge theory dual of Reissner-Nordström black hole. Finally we generalize it to the Born-Infeld case.

2.2.6.1 Reissner-Nordström

While in the gravity theory the order parameter was r_+ , in the dual theory the corresponding order parameter would be the physical charge, $Q = \int^* F$, which turns out to be the same as the charge one derives from the action. In our case, $Q = \omega_{n-1} \frac{1}{8\pi G} \sqrt{(n-1)(n-2)} q$, where q is the “charge” that appears in the action and ω_{n-1} , the $n-1$ dimensional transverse volume.

The conjugate chemical potential μ is the same as the electric potential, ϕ at the horizon given eqn.(2.55). In $n+1$ dimensions,

$$\mu = \phi = \sqrt{\frac{n-1}{2(n-2)}} \frac{q}{r_+^{n-2}} = \frac{4\pi G Q}{(n-2)\omega_{n-1} r_+^{n-2}}. \quad (2.114)$$

We now use (2.114) to express W_{BW}^{RN} given in (2.56) in terms of Q and ϕ in the following form

$$\begin{aligned} W_{BT}^{RN} = & \frac{N_c^2}{8\pi^2} \omega_{n-1} \left[\frac{2\pi^2(n-1)(1-c^2\phi^2)}{(n-2)} \frac{Q}{\phi} - \frac{2^{\frac{3n-5}{n-2}} \pi^{\frac{3n-4}{n-2}} T}{(n-2)^{\frac{n-1}{n-2}}} \left(\frac{Q}{\phi} \right)^{\frac{n-1}{n-2}} \right. \\ & \left. + \frac{2^{\frac{n}{n-2}} \pi^{\frac{2n}{n-2}} (n-1)}{(n-2)^{\frac{n}{n-2}} l^2} \left(\frac{Q}{\phi} \right)^{\frac{n}{n-2}} \right], \end{aligned} \quad (2.115)$$

where Q is rescaled as $Q = \frac{Q}{N_c^2 \omega_{n-1}}$, N_c being the number of colours. The motivation behind doing this scaling is that in the deconfined phase, the free energy and the charge, both are of the order of N_c^2 . Therefore, the appropriate observable in large N_c limit, is,

Chapter 2. The Bragg-Williams Method

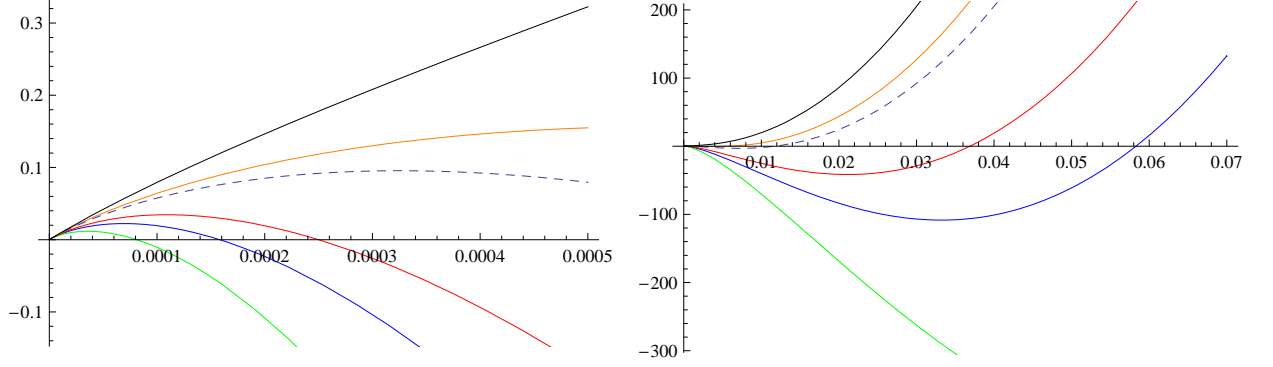


Figure 2.10: Plots of W_{BT}^{RN} vs order parameter, Q (the left one) for small Q values and (the right one) with relatively large range of values for Q for $n = 4$, show the signature of first order phase transition. The dashed line is for $T = T_c$. The orange and the black lines are for $T < T_c$ in decreasing order in temperature, and the red, the blue and the green lines are for $T > T_c$ in increasing order in temperature. For both the plots ϕ is kept fixed at the value 0.03. We have also taken $N_c = 1$, $\omega_3 = 1$ and $l = 1$ while plotting these.

instead of Q , $\lim_{N_c \rightarrow \infty} \frac{Q}{N_c^2}$. We have also used the relation $G = \frac{\pi l^{n-1}}{2N_c^2}$ and while using this in the expression for effective potential, we have made it dimensionless by redefining G as $\frac{G}{l^{n-1}}$. The plot of the boundary effective potential W_{BT}^{RN} given in (2.115) against the new order parameter Q again gives a first order phase transition as shown in fig.2.10. This phase transition corresponds to the confinement-deconfinement transition in the strongly coupled gauge theory as discussed in [28].

The temperature of the gauge theory can be found by extremizing W_{BW}^{RN} with respect to the order parameter, Q and this comes out to be

$$T = \frac{(n-2)^2 2^{-\frac{3n-5}{n-2}} \pi^{-\frac{3n-4}{n-2}}}{n-1} \left(\frac{Q}{(n-2)\phi} \right)^{-\frac{1}{n-2}} \phi \left[\frac{2(n-1)\pi^2}{(n-2)\phi} (1 - c^2 \phi^2) + \frac{n(n-1)}{l^2(n-2)^2 \phi} 2^{\frac{n}{n-2}} \pi^{\frac{2n}{n-2}} \left(\frac{Q}{(n-2)\phi} \right)^{\frac{2}{n-2}} \right], \quad (2.116)$$

which is exactly the same as the Reissner-Nordström temperature as in (2.57) once we substitute in it Q in terms of r_+ and ϕ through eqn.(2.114).

Following our previous discussion, we would now try to find the confinement-deconfinement

transition temperature, T_c . The condition $W_{BT}^{RN} = 0$ gives

$$T = 2\pi \left[2^{\frac{1}{n-2}} \pi^{\frac{2}{n-2}} \left(\frac{Q}{(n-2)\phi} \right)^{\frac{1}{n-2}} \right]^{1-n} \left[\frac{(n-1)(1-c^2\phi^2) \left(2^{\frac{1}{n-2}} \pi^{\frac{2}{n-2}} \left(\frac{Q}{(n-2)\phi} \right)^{\frac{1}{n-2}} \right)^{n-2}}{8\pi^2} \right. \\ \left. + \frac{(n-1) \left(2^{\frac{1}{n-2}} \pi^{\frac{2}{n-2}} \left(\frac{Q}{(n-2)\phi} \right)^{\frac{1}{n-2}} \right)^n}{8l^2\pi^2} \right], \quad (2.117)$$

whereas, the other requirement, $\left(\frac{\partial W_{BT}^{RN}}{\partial Q} \right) = 0$ gives (2.116). From (2.117) and (2.116), we can find an equation involving critical charge, Q_c as

$$2^{\frac{2}{n-2}} \pi^{\frac{4}{n-2}} \left(\frac{Q_c}{(n-2)\phi} \right)^{\frac{2}{n-2}} - l^2 + c^2 l^2 \phi_c^2 = 0. \quad (2.118)$$

Substituting this relation in (2.117) or (2.116) we can write down the critical temperature, T_c for the confinement-deconfinement transition as

$$T_c = \frac{(n-1)}{2\pi l} \sqrt{1 - c^2 \phi_c^2}, \quad (2.119)$$

which turns out to be exactly the same as that obtained in (2.60).

2.2.6.2 Born-Infeld

One can generalize the ideas mentioned in the previous sub-section to the case of Born-Infeld to find a gauge theory effective potential. But because of the non-linear non-invertible relationship between the electric potential at the horizon, ϕ and the charge, Q as in eqn.(2.25), it is not possible to write an exact expression for r_+ in terms of Q and ϕ . However, a parametric plot suggests that our construction leads us to a candidate effective potential for Born-Infeld dual. Following the case of Reissner-Nordström, we propose, in this case, the gauge theory effective potential, in $n = 4$ as

$$W_{BT}^{BI} = N_c^2 \omega_3 \left[-\frac{Tr_+^3}{2\pi} - Q\phi + \frac{3}{8\pi^2} \left(\frac{\beta^2 r_+^4}{3} + \frac{r_+^4}{l^2} + r_+^2 - \frac{\beta r_+ \sqrt{2\beta^2 r_+^6 + 8\pi^4 Q^2}}{3\sqrt{2}} \right. \right. \\ \left. \left. + \frac{2\pi^4 Q^2 {}_2F_1\left(\frac{1}{3}, \frac{1}{2}, \frac{4}{3}, -\frac{4\pi^4 Q^2}{\beta^2 r_+^6}\right)}{r_+^2} \right) \right], \quad (2.120)$$

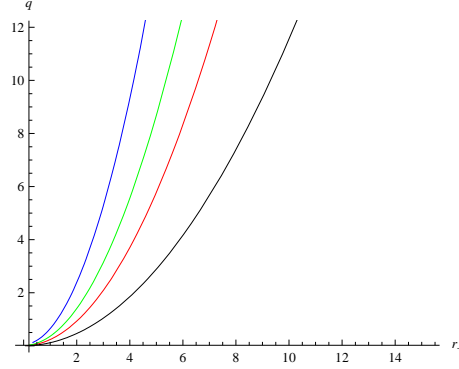


Figure 2.11: Parametric plot of q against r_+ for different values of the parameter, ϕ .

along with the relation among chemical potential, μ , charge, q and r_+ from which one has to express r_+ in terms of μ and q .

$$\mu = \phi = \frac{\sqrt{3}q}{2r_+^2} {}_2F_1\left[\frac{1}{3}, \frac{1}{2}, \frac{4}{3}, -\frac{3q^2}{\beta^2 r_+^6}\right], \quad (2.121)$$

where q is the “charge” appearing at the action which can be related to the physical charge, “ Q ” through the relation given in eqn. (2.51). One can solve this equation numerically to find a relation between r_+ and q for a fixed value of the parameter, ϕ .

Equation (2.120) is derived from (2.64) by first substituting in it the expressions for E , S and Q given in equations (2.48), (2.50) and (2.51) with reinstatement of the gravitational constant, G for $n = 4$. We then use the relation $G = \frac{\pi l^3}{2N_c^2}$. However, we make G dimensionless by dividing it by l^3 and scale Q as $\frac{Q}{N_c^2}$ for the same reason as given in the previous section in the context of Reissner-Nordström.

In order to study the phase structure, we use x , defined in eqn.(2.62), as a parameter and carry out a parametric plot of W_{BT}^{BI} against Q , the order parameter in the boundary theory. The resulting phase structure [fig.2.12]⁹ shows a first order phase transition at some critical temperature, $T = T_c$ which turns out to be exactly the same as that in fig. 2.5.

To conclude, for Reissner-Nordström black hole, we are able to construct a candidate off-shell potential in terms of R-charge, Q , which, on-shell, gives all the stable phases of $\mathcal{N} = 4$ super Yang-Mills theory on S^3 at finite temperatures and finite non-zero chemical

⁹Again one expects the plots to go smoothly towards $Q = 0$, which indeed is the case as can be checked from the free energy. But by the same argument given before, this is not visible because of the choice of the plotting parameter.

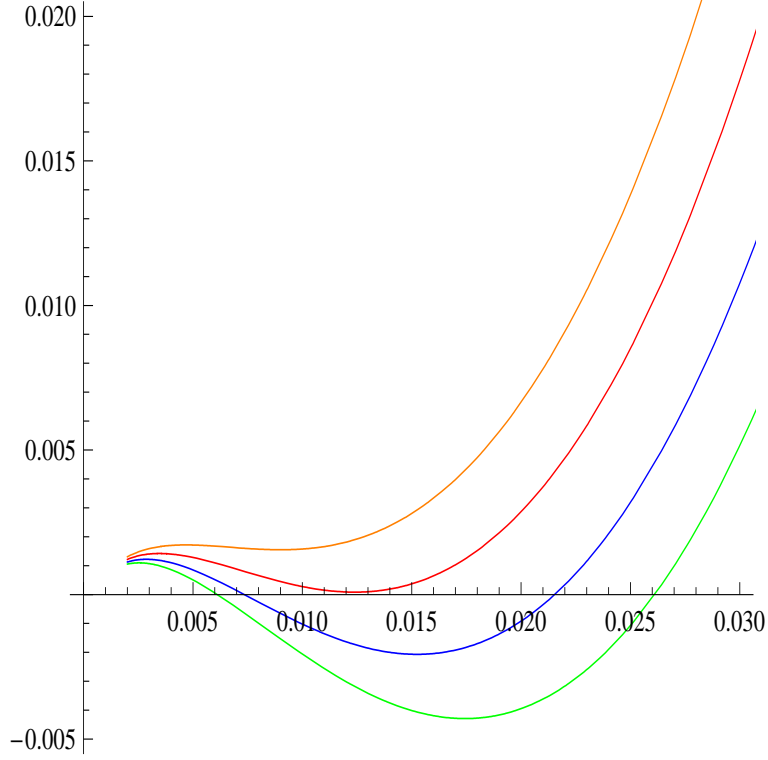


Figure 2.12: W_{BT}^{BI} is plotted against Q using x as a parameter for $n = 4$. We have fixed $\phi = 0.2$ and have plotted for different values of temperature. The red line is for $T = T_c$. The blue and green lines are for $T > T_c$ in an increasing order, whereas the orange line is for $T < T_c$.

potentials. As for Born-Infeld black holes, an analytic construction becomes difficult. Via a semi-analytic approach, we showed that our construction leads to an effective potential with expected behaviour.

Now that we have a gauge theory effective potential, we could perhaps explore the details of the transition from the deconfining phase to the confining phase as we reduce the temperature.

2.3 Towards Dynamics : Hairy to Reissner-Nodström Black Holes

We end this chapter with a section where we give an attempt to study quench phenomena in the BW frame-work. This study necessitates similar construction for certain hairy black

Chapter 2. The Bragg-Williams Method

holes. The one which we consider here was found in [36]. These are electrically charged black hole solutions in four dimensional AdS space with a conformally coupled scalar. Unlike previous examples, here, the horizon is a negatively curved two dimensional constant curvature manifold.

In this section, we first review the main features of the hairy black holes [36] and their instability [37]. We then characterize this instability via BW construction and argue that this black holes undergo a continuous transition at high temperature.

We consider four dimensional gravity action in the presence of a negative cosmological constant where the matter content is given by a conformally coupled real self interacting scalar field and a Maxwell gauge field.

$$S = \int d^4x \sqrt{-g} \left(\frac{1}{16\pi} \left(R + \frac{3}{l^2} \right) - \frac{F_{\mu\nu} F^{\mu\nu}}{16\pi} - \frac{1}{2} g^{\mu\nu} \partial_\mu \phi \partial_\nu \phi - \frac{1}{12} R \phi^2 - \alpha \phi^4 \right). \quad (2.122)$$

The black holes of this theory are described by the metric

$$ds^2 = -V(r)dt^2 + V(r)^{-1}dr^2 + r^2 d\sigma^2, \quad (2.123)$$

with

$$V(r) = \frac{r^2}{l^2} - \left(1 + \frac{M}{r} \right)^2. \quad (2.124)$$

In the expression of the metric, $d\sigma^2$ represents the line element of a constant negative curvature two dimensional manifold. The scalar and the non-zero component of the electromagnetic field are given by

$$\phi = \sqrt{\frac{1}{2\alpha l^2}} \left(\frac{M}{r + M} \right), \quad A_t(r) = -\frac{q}{r}. \quad (2.125)$$

It is important to note that the mass and charge are not independent but related via

$$q^2 = M^2 \left(\frac{2\pi}{3l^2\alpha} - 1 \right) = M^2(a - 1). \quad (2.126)$$

Here a is defined as

$$a = \frac{2\pi}{3l^2\alpha}. \quad (2.127)$$

In terms of appropriately scaled variables, the temperature, chemical potential, internal

energy, charge, and entropy densities are given by [36]

$$\begin{aligned}\bar{T} &= \frac{1}{2\pi}(2\bar{r} - 1), \quad \bar{\mu} = \frac{\bar{q}}{\bar{r}}, \\ \bar{E} &= \frac{1}{4\pi}\bar{r}(\bar{r} - 1), \quad \bar{Q} = \frac{\bar{q}}{4\pi}, \\ \bar{S} &= \frac{\bar{r}^2}{4}\left(1 - \frac{a(\bar{r} - 1)^2}{\bar{r}^2}\right).\end{aligned}\tag{2.128}$$

Note that due to the conformal coupling of the scalar to the curvature, the entropy density gets modified from standard form by an“effective” gravitational constant [37]. We also note that entropy remains positive only in the temperature range

$$\frac{1}{2\pi}\left(\frac{\sqrt{a}-1}{\sqrt{a}+1}\right) \leq \bar{T} \leq \frac{1}{2\pi}\left(\frac{\sqrt{a}+1}{\sqrt{a}-1}\right).\tag{2.129}$$

We call the limiting values to be $\bar{T}_{\min}, \bar{T}_{\max}$ respectively.

There is an additional black hole solution to the action (2.122). We will call this the Reissner-Nordström solution. The metric has the form [36]

$$ds^2 = -V(\rho)dt^2 + V(\rho)^{-1}d\rho^2 + \rho^2 d\sigma^2,\tag{2.130}$$

with

$$V(\rho) = \frac{\rho^2}{l^2} - \left(1 + \frac{2M_0}{\rho} - \frac{q_0^2}{\rho^2}\right).\tag{2.131}$$

with

$$\phi = 0, \text{ and } A_t = -\frac{q_0}{\rho}.\tag{2.132}$$

The event horizon is located at $V(\rho) = 0$, the solution of which we will call $\bar{\rho}$. Thermodynamic quantities associated with this black holes are

$$\begin{aligned}\bar{T} &= \frac{1}{2\pi}\left(\frac{3}{2}\bar{\rho} - \frac{1}{2\bar{\rho}} - \frac{\bar{q}_0^2}{2\bar{\rho}^3}\right), \\ \bar{E} &= \frac{1}{8\pi}\left(\bar{\rho}^3 - \bar{\rho} - \frac{q_0^2}{\bar{\rho}}\right), \\ \bar{Q} &= \frac{\bar{q}_0}{4\pi}, \quad \bar{S} = \frac{\bar{\rho}^2}{4}, \quad \bar{\mu} = \frac{\bar{q}_0}{\bar{\rho}}.\end{aligned}\tag{2.133}$$

Chapter 2. The Bragg-Williams Method

In the following, we will argue that the hairy black holes, in the grand canonical ensemble, are unstable and crosses over to the RN black holes at high temperature. We will also characterize this instability via BW analysis. First of all, in order to compare two different black holes, namely the RN and the hairy one, we will have to make sure that they have the same temperature and chemical potential. That means

$$\begin{aligned} \frac{1}{2\pi} \left(\frac{3}{2} \bar{\rho} - \frac{1}{2\bar{\rho}} - \frac{\bar{q}_0^2}{2\bar{\rho}^3} \right) &= \frac{1}{2\pi} (2\bar{r} - 1), \\ \frac{\bar{q}_0}{\bar{\rho}} &= \frac{\bar{q}}{\bar{r}}. \end{aligned} \quad (2.134)$$

These two equations allow us to express \bar{q}_0 and $\bar{\rho}$ in terms of \bar{q} and \bar{r} . In particular, for $\bar{\rho}$, we get

$$\bar{\rho} = \frac{1}{3\bar{r}} \left(-\bar{r} + 2\bar{r}^2 + \sqrt{3\bar{q}^2 + 4\bar{r}^2 - 4\bar{r}^3 + 4\bar{r}^4} \right). \quad (2.135)$$

The BW free energy density for both the black holes can now be easily computed as was done in the previous sections. For the hairy one it reads

$$\begin{aligned} 4\pi \bar{\mathcal{F}}_{\text{hair}} &= 4\pi (\bar{E} - \bar{T} \bar{S} - \bar{Q} \bar{\mu}) \\ &= \bar{r}(\bar{r} - 1) - \pi \bar{r}^2 \left(1 - a \frac{(\bar{r} - 1)^2}{\bar{r}^2} \right) \bar{T} - \bar{r}(\bar{r} - 1) \sqrt{a - 1} \bar{\mu} \\ &= \bar{r}(\bar{r} - 1) - \pi \bar{r}^2 \left(1 - a \frac{(\bar{r} - 1)^2}{\bar{r}^2} \right) \bar{T} - \frac{(a - 1)}{2} \bar{r}(\bar{r} - 1) (2\pi \bar{T} - 1). \end{aligned} \quad (2.136)$$

In going from the first line to the second, we use the fact that for hairy black holes, \bar{q} is not independent, but related to $\bar{\mu}$ and hence \bar{r} through (2.126). Similarly, the conjugates $\bar{\mu}$ is related to \bar{T} via

$$\bar{\mu} = \frac{1}{2} \sqrt{a - 1} (2\pi \bar{T} - 1). \quad (2.137)$$

We used this equation to get to the last line of (2.136). As for RN black holes, we can

proceed similarly to get

$$\begin{aligned}
 4\pi\bar{\mathcal{F}}_{\text{RN}} &= 4\pi(\bar{E} - \bar{T}\bar{S} - \bar{Q}\bar{\mu}) \\
 &= \frac{\bar{\rho}^3}{2} - \frac{\bar{\rho}}{2} + \frac{q_0^2}{2\bar{\rho}} - \pi\bar{\rho}^2\bar{T} - \bar{q}_0\bar{\mu} \\
 &= \frac{\bar{\rho}^3}{2} - \frac{\bar{\rho}}{2} + \frac{\bar{\rho}}{2}(a-1)(\bar{r}-1)^2 - \pi\bar{\rho}^2\bar{T} - \frac{\bar{\rho}}{2}(a-1)(\bar{r}-1)(2\pi\bar{T}-1),
 \end{aligned} \tag{2.138}$$

where we need to substitute $\bar{\rho}$ using (2.135) and further \bar{q} by \bar{m} and hence by \bar{r} . In order to write (2.138), we have also made use of the second identification given in (2.134). Further, using (2.135) and (2.136), after some simplification, we can re-write $\bar{\mathcal{F}}_{\text{RN}}$ as

$$\begin{aligned}
 \bar{\mathcal{F}}_{\text{RN}}(\bar{r}, \bar{T}, \bar{a}) &= \frac{1}{54} \left[(1+\bar{r})(-1-\bar{r}+\delta)(-5+4\bar{r}-6\pi\bar{T}) + 3a(\bar{r}-1)\{3+12\bar{r}^2-\delta \right. \\
 &\quad \left. + 30\pi\bar{T} - 6\pi\delta\bar{T} + \bar{r}(-21+4\delta-18\pi\bar{T})\} \right] + \bar{r}(\bar{r}-1) \\
 &\quad - \pi\bar{r}^2 \left(1 - a \frac{(\bar{r}-1)^2}{\bar{r}^2} \right) \bar{T} - \frac{(a-1)}{2} \bar{r}(\bar{r}-1)(2\pi\bar{T}-1).
 \end{aligned} \tag{2.139}$$

with

$$\delta = \sqrt{3a(\bar{r}-1)^2 + (\bar{r}+1)^2}. \tag{2.140}$$

The saddle point of (2.136) and (2.139) occurs at

$$\bar{r} = \frac{1}{2}(1+2\pi\bar{T}), \tag{2.141}$$

and at the minima,

$$\begin{aligned}
 \bar{\mathcal{F}}_{\text{hair}} &= -\frac{1}{8\pi} \left(\bar{r}^2 + a(\bar{r}-1)^2 \right), \\
 \bar{\mathcal{F}}_{\text{RN}} &= \frac{1}{216\pi} \left(2 + 6\bar{r} - 21\bar{r}^2 + 2\bar{r}^3 - 2\delta(1+\bar{r})^2 - 3a(-1+\bar{r})^2(-3+2\delta+6\bar{r}) \right).
 \end{aligned} \tag{2.142}$$

While for $\bar{T} \leq \bar{T}_c = 1/(2\pi)$, $\bar{\mathcal{F}}_{\text{hair}}$ minimizes the free energy, for $\bar{T} \geq \bar{T}_c$, RN represents the stable black holes. From (2.141), it follows that at the critical temperature \bar{T}_c , $\bar{r} = \bar{r}_c = 1$. Near \bar{T}_c it follows that

$$\bar{r} - \bar{r}_c \sim \bar{T} - \bar{T}_c, \quad \bar{\mathcal{F}} - \bar{\mathcal{F}}_c \sim (\bar{T} - \bar{T}_c)^3, \tag{2.143}$$

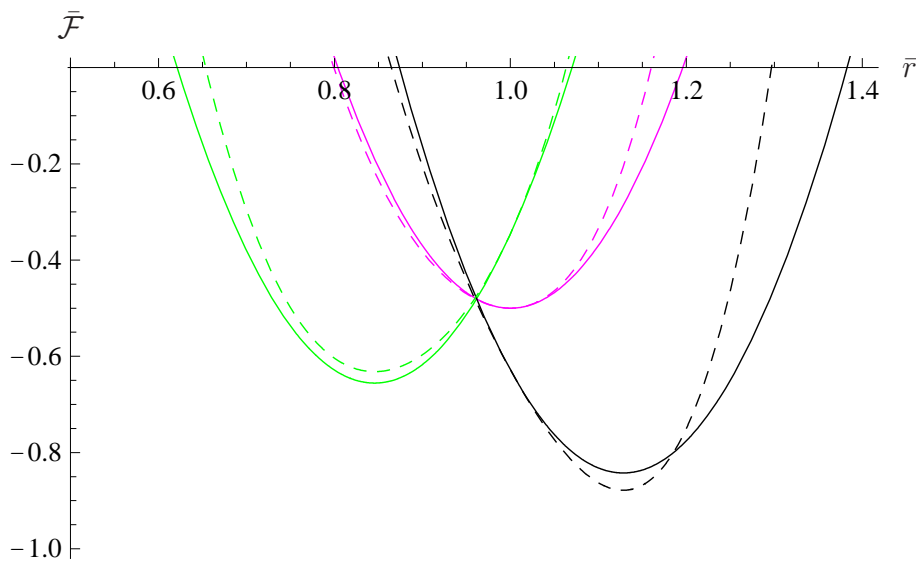


Figure 2.13: This figure is a plot of (2.136) and (2.139) for $a = 25$ and for different temperatures. The solid lines and the dashed lines represent the hairy and the RN black holes respectively. Green, magenta and black curves are for $\bar{T} = 0.11, 1/(2\pi), 0.2$ respectively. We see that while at low temperature free energy is minimized by the hairy black hole, RN black holes dominate at high temperature. At $\bar{T} = 1/(2\pi)$, free energies are equal at the minimum.

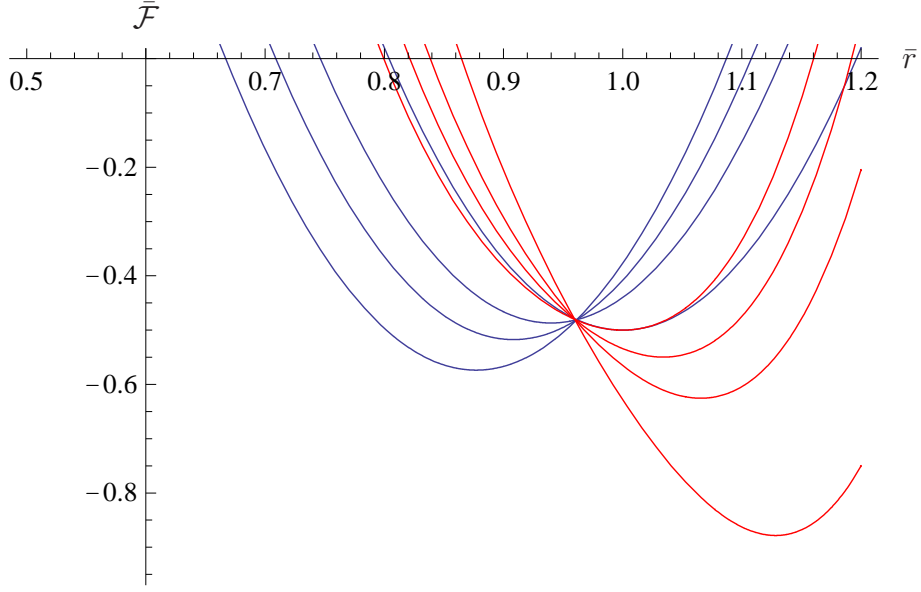


Figure 2.14: This figure is the behaviour of the free energy function close to $\bar{T} = \bar{T}_c = 1/(2\pi)$ for $a = 30$. Blue and red are for $\bar{T} \leq \bar{T}_c$ and $\bar{T} \geq \bar{T}_c$ representing hairy and RN black holes respectively. At $\bar{T} = \bar{T}_c$, the minima for both are degenerate. Clearly, the order parameter \bar{r} , at which the minima occur, changes continuously around critical temperature leading to a continuous phase transition.

where $\bar{\mathcal{F}}_c$ is the value of $\bar{\mathcal{F}}$ at $\bar{r} = \bar{r}_c$. The derivative of specific heat with respect to temperature has a discontinuity around \bar{r}_c of $(2 + a)\pi^2$. This is thus a continuous phase transition from hairy to RN black holes. The critical exponent following from (2.143) is $\alpha = -1, \beta = 1$. In figure 2.13, we have plotted $\bar{\mathcal{F}}$ for different black holes at different temperatures and scalar couplings. The behaviour of $\bar{\mathcal{F}}$ close \bar{T}_c is shown in figure 2.14.

We note that the BW free energy constructed in (2.136) can also be expressed using the value of the scalar ϕ at the horizon as order parameter. Inverting (2.125), we can express $\bar{\mathcal{F}}_{\text{hair}}$ as,

$$4\pi\bar{\mathcal{F}}_{\text{hair}} = \frac{\sqrt{a}}{(\sqrt{\frac{3a}{\pi}} - 2\phi_h)^2} \left(4\sqrt{a}\pi\bar{T}\phi_h^2 + \sqrt{\frac{3}{\pi}}(1 + a - 2(a-1)\pi\bar{T})\phi_h - 3\sqrt{a}\bar{T} \right). \quad (2.144)$$

Here ϕ_h is the value of the scalar at the horizon. The expression on the right has a minimum at

$$\phi_h = \sqrt{\frac{3a}{4\pi}} \left(\frac{2\pi\bar{T} - 1}{2\pi\bar{T} + 1} \right), \quad (2.145)$$

Chapter 2. The Bragg-Williams Method

such that, for $\bar{T} = \bar{T}_c$, $\phi = 0$.

Having reached this far, we now like to address some dynamical issues associated with this system. In particular, we ask as to how the order parameter ϕ_h behaves in time as we temperature quench the system from $\bar{T} > \bar{T}_c$ to $\bar{T} < \bar{T}_c$. We assume that, during the quench, the temperature changes so fast that ϕ_h , immediately after the change, is identical to its value before. However, at a later time ϕ_h must roll down to its stable position given by (2.145). In the following, we will be interested in finding out the interpolating solution $\phi_h(t)$ which connects the unstable to the stable point.

The equation that we need to solve is

$$\partial_t^2 \phi_h(t) + \frac{\partial \bar{\mathcal{F}}_{\text{hair}}}{\partial \phi_h(t)} = 0, \quad (2.146)$$

where $\bar{\mathcal{F}}_{\text{hair}}$ is given by (2.144). This equation can be immediately integrated once to get

$$\frac{1}{2}(\partial_t \phi_h)^2 + \bar{\mathcal{F}}_{\text{hair}}(\phi_h) = C. \quad (2.147)$$

The integration constant C can be fixed by the boundary condition $\partial_t \phi_h = 0$ for $\phi_h = 0$. This gives

$$\frac{1}{2}(\partial_t \phi_h)^2 + \bar{\mathcal{F}}_{\text{hair}}(\phi_h) = \bar{\mathcal{F}}_{\text{hair}}(0) \quad (2.148)$$

It turns out that this equation can be integrated exactly with the boundary condition $\phi_h(t) = 0$ at $t = 0$. The result can be expressed in a form

$$f(\phi_h, a, \bar{T}) = t, \quad (2.149)$$

where f is a known function of ϕ_h . Furthermore, it has parametric dependences on \bar{T} and a . This function is too non-illuminating and hence we do not display it here. It however turns out that the equation above can not be analytically inverted to get $\phi_h(t)$ as an explicit function of t . Nevertheless, numerically it can be solved and the result is shown in the figure 2.15. In the plot, we have shown two cases where temperature \bar{T} is quenched down to .14 (red) and .13 (blue). The value of a that we have chosen is 90. Starting from $\phi_h(t) = 0$ at $t = 0$, $\phi_h(t)$ rolls down to respective stable points dictated by the equation (2.145).

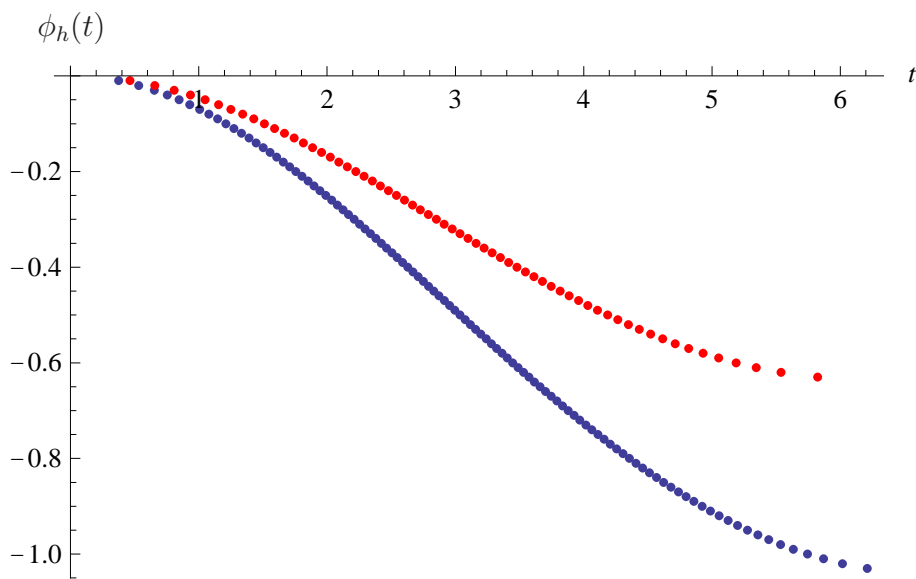


Figure 2.15: This figure shows behaviour of $\phi_h(t)$ after quenched to different temperatures below $\bar{T}_c = 1/(2\pi)$. The vertical axis is ϕ_h and the horizontal one is t . The plots are for $a = 90$. While the lower one (blue) curve is for temperature quenched to $\bar{T} = .13$, the upper one (red) is for $\bar{T} = .14$. We see $\phi_h(t)$ starts with zero value at $t = 0$ and at a later time reaches a non-zero negative stable point determined by the equation (2.145)

2.4 Summary and future directions

In this chapter our aim was to study black hole instabilities within the framework of BW theory of phase transition. After providing a pedagogical review to this subject, we employed BW method in two cases. One involved charged black holes in five dimensional AdS space. This included Reissner-Nordström and Born-Infeld black holes and also general R -charged black holes with spherical horizon. In the presence of non-zero chemical potential, the R -charged black hole undergoes both first and second order transitions whereas in the case of Reissner-Nordström and Born-Infeld black holes only first order transitions take place. We found that BW theory, with horizon radius as order parameter, captures all these instabilities. We hope that, via AdS/CFT correspondence, the constructed BW free energy will be useful to study the phases of strongly coupled $\mathcal{N} = 4$ SYM theory on R^3 at finite temperature and chemical potential.

The other example that we studied is the fate of four dimensional hairy black holes with hyperbolic horizon. Again, via a BW analysis we argued that with the increase in temperature, this black hole becomes unstable, loses its “hair” and turns into a stable RN black hole. This transition is analogous to a third order phase transition with a singularity in the derivative of the specific heat. The BW free energy is constructed in (2.136). Using value of the scalar on the horizon as order parameter, we studied its behaviour under temperature quench. The corresponding rolling down solutions were semi-analytically constructed.

Within the AdS/CFT correspondence, in [38, 39], second order instabilities associated with hairy black holes with flat horizon were used to understand holographic superconductors at the boundary. We note that superconductors with possible higher order transition (similar to the one we discussed) has been reported earlier, see for example [40]. We hope a construction like (2.144) will be useful to analyse such holographic superconductors, however in hyperbolic space.

Bibliography

- [1] P.M. Chaikin and T.C. Lubensky, *Principles of condensed matter physics*, Cambridge University Press, Chapter 4, (2009).
- [2] W.L. Bragg and E.J. Williams, *The effect of thermal agitation on atomic arrangement in alloys*, Proc. Roy. Soc. London, 145A, 699, (1934).
- [3] W.L. Bragg and E.J. Williams, *The effect of thermal agitation on atomic arrangement in alloys II*, Proc. Roy. Soc. London, 151A, 540, (1935).
- [4] R. Kubo, *Satistical Mechanics*, North-Holland Publication, Chapetr 5, (1965).
- [5] D. V. Fursaev and S. N. Solodukhin, “On the description of the Riemannian geometry in the presence of conical defects,” Phys. Rev. D **52**, 2133 (1995) [hep-th/9501127].
- [6] S. Banerjee, “A Note on Charged Black Holes in AdS space and the Dual Gauge Theories,” Phys. Rev. D **82**, 106008 (2010) [arXiv:1009.1780 [hep-th]].
- [7] S. Banerjee, S. K. Chakrabarti, S. Mukherji and B. Panda, “Black hole phase transitions via Bragg-Williams,” Int. J. Mod. Phys. A **26**, 3469 (2011) [arXiv:1012.3256 [hep-th]].
- [8] S. W. Hawking and D. N. Page, “Thermodynamics Of Black Holes In Anti-De Sitter Space,” Commun. Math. Phys. **87**, 577 (1983).
- [9] D. T. Son and A. O. Starinets, “Hydrodynamics of R-charged black holes,” JHEP **0603**, 052 (2006) [arXiv:hep-th/0601157].
- [10] K. Behrndt, M. Cvetič and W. A. Sabra, “Non-extreme black holes of five dimensional $N = 2$ AdS supergravity,” Nucl. Phys. B **553**, 317 (1999) [arXiv:hep-th/9810227].
- [11] M. Cvetič, M. J. Duff, P. Hoxha, J. T. Liu, H. Lu, J. X. Lu, R. Martinez-Acosta and C. N. Pope *et al.*, “Embedding AdS black holes in ten-dimensions and eleven-dimensions,” Nucl. Phys. B **558**, 96 (1999) [hep-th/9903214].
- [12] A. Chamblin, R. Emparan, C. V. Johnson and R. C. Myers, “Charged AdS black holes and catastrophic holography,” Phys. Rev. D **60**, 064018 (1999) [hep-th/9902170].

- [13] A. Chamblin, R. Emparan, C. V. Johnson and R. C. Myers, “Holography, thermodynamics and fluctuations of charged AdS black holes,” *Phys. Rev. D* **60**, 104026 (1999) [hep-th/9904197].
- [14] M. Cvetič, S. Nojiri and S. D. Odintsov, “Black hole thermodynamics and negative entropy in deSitter and *Nucl. Phys. B* **628**, 295 (2002) [arXiv:hep-th/0112045].
- [15] S. Nojiri and S. D. Odintsov, “(Anti-) de Sitter black holes in higher derivative gravity and dual *Phys. Rev. D* **66**, 044012 (2002) [arXiv:hep-th/0204112].
- [16] M. Brigante, H. Liu, R. C. Myers, S. Shenker and S. Yaida, “Viscosity Bound Violation in Higher Derivative Gravity,” *Phys. Rev. D* **77**, 126006 (2008) [arXiv:0712.0805 [hep-th]].
- [17] A. Buchel, R. C. Myers and A. Sinha, “Beyond $\eta/s = 1/4\pi$,” *JHEP* **0903**, 084 (2009) [arXiv:0812.2521 [hep-th]].
- [18] R. C. Myers, M. F. Paulos and A. Sinha, “Holographic Hydrodynamics with a Chemical Potential,” *JHEP* **0906**, 006 (2009) [arXiv:0903.2834 [hep-th]].
- [19] S. Fernando and D. Krug, “Charged Black Hole Solutions in Einstein-Born-Infeld gravity with a Cosmological constant,” *Gen. Rel. Grav.* **35**, 129 (2003) [arXiv:hep-th/0306120].
- [20] T. K. Dey, “Born-Infeld black holes in the presence of a cosmological constant,” *Phys. Lett. B* **595**, 484 (2004) [arXiv:hep-th/0406169].
- [21] R. G. Cai and Y. W. Sun, “Shear Viscosity from AdS Born-Infeld Black Holes,” *JHEP* **0809**, 115 (2008) [arXiv:0807.2377 [hep-th]].
- [22] H. S. Tan, “Born-Infeld Hydrodynamics via Gauge/Gravity Duality,” *JHEP* **0904**, 131 (2009) [arXiv:0903.3424 [hep-th]].
- [23] S. Fernando, “Thermodynamics of Born-Infeld-anti-de Sitter black holes in the grand canonical ensemble,” *Phys. Rev. D* **74**, 104032 (2006) [hep-th/0608040].
- [24] R. -G. Cai, D. -W. Pang and A. Wang, “Born-Infeld black holes in (A)dS spaces,” *Phys. Rev. D* **70**, 124034 (2004) [hep-th/0410158].

- [25] S. A. Hartnoll, “Lectures on holographic methods for condensed matter physics,” *Class. Quant. Grav.* **26**, 224002 (2009) [arXiv:0903.3246 [hep-th]].
- [26] S. Kobayashi, D. Mateos, S. Matsuura, R. C. Myers and R. M. Thomson, “Holographic phase transitions at finite baryon density,” *JHEP* **0702**, 016 (2007) [hep-th/0611099].
- [27] I. Racz and R. M. Wald, “Extension of space-times with Killing horizon,” *Class. Quant. Grav.* **9**, 2643 (1992).
- [28] E. Witten, “Anti-de Sitter space, thermal phase transition, and confinement in gauge theories,” *Adv. Theor. Math. Phys.* **2**, 505 (1998) [hep-th/9803131].
- [29] S. S. Gubser, “Thermodynamics of spinning D3-branes,” *Nucl. Phys. B* **551**, 667 (1999) [arXiv:hep-th/9810225].
- [30] M. Cvetič and S. S. Gubser, “Phases of R-charged black holes, spinning branes and strongly coupled gauge theories,” *JHEP* **9904**, 024 (1999) [arXiv:hep-th/9902195].
- [31] D. Yamada, “Metastability of R-charged black holes,” *Class. Quant. Grav.* **24**, 3347 (2007) [arXiv:hep-th/0701254].
- [32] S. Jain, S. Mukherji and S. Mukhopadhyay, “Notes on R-charged black holes near criticality and gauge theory,” *JHEP* **0911**, 051 (2009) [arXiv:0906.5134 [hep-th]].
- [33] R. G. Cai and K. S. Soh, “Critical behavior in the rotating D-branes,” *Mod. Phys. Lett. A* **14**, 1895 (1999) [arXiv:hep-th/9812121].
- [34] K. Maeda, M. Natsuume and T. Okamura, “Dynamic critical phenomena in the AdS/CFT duality,” *Phys. Rev. D* **78**, 106007 (2008) [arXiv:0809.4074 [hep-th]].
- [35] M. Eune, W. Kim and S. -H. Yi, “Hawking-Page phase transition in BTZ black hole revisited,” *JHEP* **1303**, 020 (2013) [arXiv:1301.0395 [gr-qc]].
- [36] C. Martinez, J. P. Staforelli and R. Troncoso, “Charged topological black hole with a conformally coupled scalar field,” *Phys. Rev. D* **74**, 044028 (2006) [arXiv:hep-th/0512022].
- [37] C. Martinez and A. Montecinos, “Phase transitions in charged topological black holes dressed with a scalar hair,” arXiv:1009.5681 [hep-th].

- [38] S. S. Gubser, “Breaking an Abelian gauge symmetry near a black hole horizon,” *Phys. Rev. D* **78**, 065034 (2008) [arXiv:0801.2977 [hep-th]].
- [39] S. A. Hartnoll, C. P. Herzog and G. T. Horowitz, “Building a Holographic Superconductor,” *Phys. Rev. Lett.* **101**, 031601 (2008) [arXiv:0803.3295 [hep-th]].
- [40] M.F. Hundley, J.D. Thompson and G.M. Kwei, *Solid State Com.* **70**, 1155 (1989).

The Holographic Spectral Function in Non-Equilibrium States

Prelude

As discussed in the introduction, holography has given us a new paradigm to deal with strongly coupled systems [1]. One of the many attractive features of this paradigm is that we can deal with phenomena at strong coupling in real time.

Though there has been substantial progress in using holography to study hydrodynamics [2–5] and relaxation of strongly coupled systems [6–8], we still lack a systematic method for studying non-equilibrium Green’s functions in holography. The latter turn out to be extremely useful in many applications such as understanding thermalization¹ and obtaining strongly coupled generalizations of quantum kinetic theories, to name a few. The importance of pursuing this direction can be readily illustrated by two examples.

Modeling the space-time evolution of matter formed by ultra-relativistic collisions of heavy ions at RHIC and ALICE is a great theoretical challenge. It is equally challenging to develop reliable methods of inference for deducing this space-time evolution [10]. Ultimately, it is important to not only understand how the matter thermalizes incredibly fast in time ≤ 1 fm at temperature about 175 MeV (at RHIC) and subsequently undergoes hydrodynamic expansion, but also how hadrons and resonances are produced and transported in this so-called fireball before finally getting frozen chemically and thermally. Ultimately, we do infer the expansion of the fireball from the emitted hadrons. If the expansion of the RHIC

¹Holographic non-equilibrium Green’s functions as an aid for understanding thermalization have been studied earlier in [9] using geodesic approximation, etc.

fireball is indeed governed by strongly coupled physics, then we can expect that holography will not only help us in modeling the space-time evolution of the fireball, but also help us improve upon existing techniques like Hanbury-Brown-Twiss pion-interferometry used to deduce the expansion of the fireball.

Quantum kinetic theories are already being employed to understand the dynamics of the hadron gas after the chemical and thermal freeze-out in the hydrodynamically expanding fireball [11]. However, in order to understand the details of how the hadron gas comes to existence in the first place and its subsequent freeze-out, as also correlations in the emissions of hadrons, one needs quantum kinetic theories constructed using non-equilibrium Green's functions. Therefore, to understand such questions at strong coupling using holography, we need to develop formalism to systematically obtain non-equilibrium Green's functions. The second example pertains to holographic models of non-Fermi liquids [12–16]². Holography has been successful in reproducing some of the features of ARPES experiments in cuprates and other strongly correlated electron systems - the spectral function has a pole on a momentum shell at zero frequency and also shows non-trivial scaling for low energy excitations. These results may be interpreted as holographic reproduction of Fermi surfaces different from that in Landau's Fermi liquid theory. In absence of a better way of dealing with strongly interacting fermions at finite density, holographic methods could provide us with useful qualitative insights.

Nevertheless, to test such holographic models, we need to see if we can also reproduce qualitative aspects of non-equilibrium dynamics in strongly interacting fermionic systems. Ultimately, when the electrons are weakly interacting, Landau's Fermi liquid theory gives a unified way of dealing with both equilibrium and non-equilibrium phenomena. It is reasonable to expect that holography can do a similar job at strong coupling. Once again, we need to understand how to obtain quantum kinetic theory from holography, and therefore a systematic method of obtaining non-equilibrium Green's functions.

There are two important issues associated with obtaining non-equilibrium Green's functions in field theory [18].

1. There is no partition function which plays the role of generating functional of non-equilibrium Green's functions. As we will review briefly later, these are obtained from a generalized effective action. The effective action technique guarantees the full hierarchy is consistently solved and Ward identities are preserved.

²For interesting holographic models of Fermi liquids see [17]. Our comments are applicable to such models as well.

Chapter 3. The Holographic Spectral Function in Non-Equilibrium States

2. We cannot use conventional perturbation theory to obtain the behavior in time, like for instance, dependence of observables on hydrodynamic and relaxation modes. This is because usual time-dependent perturbation theory gives us the behavior in time in the form of a Taylor series, which fails to capture late time behavior like exponential decay.

Therefore, even at weak coupling non-equilibrium field theory is hard and typically we need to make educated guesses, depending on the understanding of a specific system. It will be remarkable if, on the strong coupling side, holography can provide us with a good perturbation theory for the non-equilibrium observables we will deal with here. The lack of a generating functional for non-equilibrium correlation functions on the field theory side, nevertheless, makes it hard to use the holographic dictionary to translate such observables to the field theory side.

The observables of primary importance are two-point correlation functions. In the vacuum, once the Euclidean Green's function is specified, we can analytically continue to obtain the Feynman propagator, the retarded and advanced Green's function etc. at equilibrium. At finite temperature too, it thus suffices to know the retarded Green's function, from which we can obtain other propagators like the Feynman propagator. At non-equilibrium the situation is different - we cannot deduce from the retarded Green's function, for instance, the Feynman propagator which will have independent dynamics. Nevertheless, all Green's functions can be expressed in terms of two independent, real observables - the *spectral function* and the *statistical function*, which we briefly review now.

The spectral component (or spectral function) of bosonic Green's functions (in d spatial dimensions) can be defined as the Wigner transform (i.e. the Fourier transform in the relative coordinate \mathbf{r} and time difference t_r) of the commutator

$$\mathcal{A}(\omega, \mathbf{k}, \mathbf{x}, t) = \int d^d r dt_r e^{i(\omega t_r - \mathbf{k} \cdot \mathbf{r})} \left\langle \left[\Phi\left(\mathbf{x} + \frac{\mathbf{r}}{2}, t + \frac{t_r}{2}\right), \Phi\left(\mathbf{x} - \frac{\mathbf{r}}{2}, t - \frac{t_r}{2}\right) \right] \right\rangle. \quad (3.1)$$

Similarly in case of fermionic fields, we can define the spectral component as the Wigner transform of the anti-commutator

$$\mathcal{A}(\omega, \mathbf{k}, \mathbf{x}, t) = \int d^d r dt_r e^{i(\omega t_r - \mathbf{k} \cdot \mathbf{r})} \left\langle \left\{ \Psi\left(\mathbf{x} + \frac{\mathbf{r}}{2}, t + \frac{t_r}{2}\right), \bar{\Psi}\left(\mathbf{x} - \frac{\mathbf{r}}{2}, t - \frac{t_r}{2}\right) \right\} \right\rangle. \quad (3.2)$$

In both the equations above $\langle \dots \rangle$ denotes expectation value in a non-equilibrium state. The

Chapter 3. The Holographic Spectral Function in Non-Equilibrium States

fermionic spectral function is :

$$A(\omega, \mathbf{k}, \mathbf{x}, t) = \text{Tr}(\gamma^t \mathcal{A}(\omega, \mathbf{k}, \mathbf{x}, t)). \quad (3.3)$$

The statistical function (also known as the Keldysh propagator) is defined as the Wigner transform of the anti-commutator of two bosonic fields

$$G_K(\omega, \mathbf{k}, \mathbf{x}, t) = -\frac{i}{2} \int d^d r dt_r e^{i(\omega t_r - \mathbf{k} \cdot \mathbf{r})} \left\langle \left\{ \Phi\left(\mathbf{x} + \frac{\mathbf{r}}{2}, t + \frac{t_r}{2}\right), \Phi\left(\mathbf{x} - \frac{\mathbf{r}}{2}, t - \frac{t_r}{2}\right) \right\} \right\rangle. \quad (3.4)$$

or as the same of the commutator of two fermionic fields

$$G_K(\omega, \mathbf{k}, \mathbf{x}, t) = -\frac{i}{2} \int d^d r dt_r e^{i(\omega t_r - \mathbf{k} \cdot \mathbf{r})} \left\langle \left[\Psi\left(\mathbf{x} + \frac{\mathbf{r}}{2}, t + \frac{t_r}{2}\right), \bar{\Psi}\left(\mathbf{x} - \frac{\mathbf{r}}{2}, t - \frac{t_r}{2}\right) \right] \right\rangle. \quad (3.5)$$

All propagators can be expressed as appropriate linear combinations of the spectral and statistical functions. We will be interested in the retarded correlation function in particular. It is actually more convenient to define the Wigner transform of the retarded correlator. In case of bosonic fields, this is defined as

$$G_R(\omega, \mathbf{k}, \mathbf{x}, t) = -i \int d^d r dt_r e^{i(\omega t_r - \mathbf{k} \cdot \mathbf{r})} \theta(t_r) \left\langle \left[\Phi\left(\mathbf{x} + \frac{\mathbf{r}}{2}, t + \frac{t_r}{2}\right), \Phi\left(\mathbf{x} - \frac{\mathbf{r}}{2}, t - \frac{t_r}{2}\right) \right] \right\rangle. \quad (3.6)$$

Similarly for fermionic fields, the anti-commutator is used above.

It is clear from the definitions of the spectral functions (3.1) and (3.3) respectively that the bosonic spectral function is related to the retarded correlator via $\mathcal{A}(\omega, \mathbf{k}, \mathbf{x}, t) = -2\text{Im}G_R(\omega, \mathbf{k}, \mathbf{x}, t)$, while for the fermionic spectral function, the relation is $A(\omega, \mathbf{k}, \mathbf{x}, t) = -2\text{Im}(\text{Tr}(\gamma^t G_R(\omega, \mathbf{k}, \mathbf{x}, t)))$. The retarded correlation function does not contain any more information than the spectral function, since it is analytic in ω for a given \mathbf{k} for every \mathbf{x} and t . Therefore,

$$G_R(\omega, \mathbf{k}, \mathbf{x}, t) = \int \frac{d\omega'}{2\pi} \frac{\mathcal{A}(\omega', \mathbf{k}, \mathbf{x}, t)}{\omega - \omega' + i\epsilon} \quad (3.7)$$

in both the bosonic and fermionic cases.

On the other hand the Feynman propagator G_F is a linear combination of both the spectral and statistical components. For both bosonic and fermionic fields, prior to Wigner transform :

$$G_F(\mathbf{x}, t, \mathbf{y}, t') = G_K(\mathbf{x}, t, \mathbf{y}, t') - \frac{i}{2} \mathcal{A}(\mathbf{x}, t, \mathbf{y}, t') \text{sign}(t - t'). \quad (3.8)$$

Chapter 3. The Holographic Spectral Function in Non-Equilibrium States

Since the Feynman propagator involves the statistical function which is unrelated to the spectral function algebraically out of equilibrium, we cannot deduce this propagator from the retarded function in non-equilibrium states.

At equilibrium, both the spectral and statistical functions depend only on ω and \mathbf{k} , i.e. they are homogeneous in \mathbf{x} and t , owing to translational invariance. Furthermore, they are related by fluctuation-dissipation relations :

$$G_{\mathcal{K}}(\omega, \mathbf{k}) = -i \left(\frac{1}{2} + n_{\text{BE}}(\omega) \right) \mathcal{A}(\omega, \mathbf{k}) \quad (3.9)$$

for the bosonic case and

$$G_{\mathcal{K}}(\omega, \mathbf{k}) = -i \left(\frac{1}{2} - n_{\text{FD}}(\omega) \right) \mathcal{A}(\omega, \mathbf{k}) \quad (3.10)$$

for the fermionic case, with $n_{\text{BE}}(\omega) = (e^{\beta\omega} - 1)^{-1}$ being the Bose-Einstein distribution and $n_{\text{FD}}(\omega) = (e^{\beta\omega} + 1)^{-1}$ being the Fermi-Dirac distribution.

Away from equilibrium, the statistical and spectral functions follow a coupled set of equations which were first found by Kadanoff and Baym [18]. These equations are not so easily tractable in field theory even at weak-coupling, however educated guesses lead us to standard kinetic equations like the Boltzmann equation with quantum corrections. We will skip issues involving renormalization etc. and simply mention here that they can be dealt with efficiently at the level of the effective action.

The spectral function, especially for fermions, is directly measurable by ARPES like experiments. Usually it is the equilibrium spectral functions that are measured experimentally, so that we need be concerned with their dependence on frequency and momentum only. Recently however, there have been time-resolved ARPES experiments in which non-equilibrium time-dependent spectral functions have been measured in approximately spatially homogeneous situations and their dependence on frequency, momentum as well as time have been obtained (see, for example, time-resolved ARPES across the metal-insulator transition in [19]). Conceptually, when integrated over frequency at a given momentum and at a given point in space-time, the spectral function gives the space-time dependent density of states. The spectral function thus reveals the non-equilibrium structure of the effective phase-space of quasi-particles (provided we do have well defined quasi-particles).

The statistical function, on the other hand, carries complementary information about how quasi-particles (whenever they can be defined) are distributed in phase-space and time and can be indirectly measured. For instance, in the case of a single species of fermions,

Chapter 3. The Holographic Spectral Function in Non-Equilibrium States

the conserved current is

$$j^\mu(\mathbf{x}, t) = iq \int d\omega d^d k \text{Tr}(\gamma^\mu G_K(\omega, \mathbf{k}, \mathbf{x}, t)) + \text{constant}, \quad (3.11)$$

where q is the conserved charge of the fermionic field, and the constant is independent of the state and required to provide an infinite subtraction which produces a finite result. In the so called quasi-particle approximation, we can assume that the statistical function is peaked only when ω is on-shell, so that it reduces to the standard phase-space distribution which follows the semi-classical Boltzmann equation in certain limits.

This completes our very brief review of the spectral and statistical functions respectively. In this chapter, we would like to describe the methodology to obtain the non-equilibrium retarded function holographically. Our focus will be on the retarded function because we can compute it using linear response theory even in a non-equilibrium state. The holographic dictionary enables defining the source and expectation value of an operator in *any arbitrary state*. Therefore, we can avoid issues associated with the lack of a generating functional for non-equilibrium correlation functions.

To be specific, we would like to achieve the following :

1. to evaluate the retarded correlation function and the spectral function in non-equilibrium states,
2. to find space-time dependent shifts in the energy and spins of quasi-particles in the non-equilibrium medium, and
3. to obtain the space-time dependent shifts in energy per particle and spin orientation at the holographic Fermi surface.

With respect to the last point, we will reproduce a strongly coupled version of what is expected from Landau's Fermi liquid theory, as reviewed later. The second objective is justified on the grounds that it is known that in non-equilibrium states, the effective masses of quasi-particles become space-time dependent (via an inhomogeneous temperature distribution for instance, or an inhomogeneous distribution of the velocity field as discussed later). We will succeed in all these objectives for scalar and fermionic operators.

We only consider spectral function here and do not address the information contained in the statistical function and how to obtain it holographically. Partial work in the latter direction appeared in [20] and more work is in progress. These issues will be complicated

Chapter 3. The Holographic Spectral Function in Non-Equilibrium States

by the fact that we are dealing with composite operators in holography and we leave this for future study. We note here that there has been previous work where the equilibrium statistical function has been defined holographically in a consistent manner [21], based on the correspondence between the generating functional of field-theoretic correlation functions and a suitable partition function of quantum gravity. However, these cannot be readily generalized to non-equilibrium states because of the lack of a generating functional for non-equilibrium correlation functions as observed before.

The key result we present in this chapter is the development of perturbation theory of scalar and fermionic fields in holographic duals of non-equilibrium backgrounds. At equilibrium, the incoming boundary condition mimics causal response in field theory and suffices to define a well-defined linear response theory holographically [22, 23]. However, the incoming wave boundary condition does not suffice to give well defined linear response theory in non-equilibrium states. This can be briefly demonstrated as follows.

Suppose we have a non-equilibrium background in which a hydrodynamic mode with momentum $\mathbf{k}_{(h)}$ has been excited. Let the source of the operator at equilibrium be $J^{(0)}(\mathbf{x}, t)$ and the expectation value be $O^{(0)}(\mathbf{x}, t)$ which can be read-off from the profile of the field $\Phi^{(0)}(r, \mathbf{x}, t)$ in the bulk. The non-equilibrium bulk contribution can be denoted as $\Phi^{(1)}(\mathbf{k}_{(h)}, r, \mathbf{x}, t)$ and this gives contribution to both the source $J^{(1)}$ and expectation value $O^{(1)}$ of the operator. The full retarded function can be obtained from :

$$G_R(\mathbf{x}, t; \mathbf{y}, t') = \mathcal{C} \frac{O^{(0)}(\mathbf{x}, t) + O^{(1)}(\mathbf{k}_{(h)}, r, \mathbf{x}, t)}{J^{(0)}(\mathbf{y}, t') + J^{(1)}(\mathbf{k}_{(h)}, r, \mathbf{y}, t')}, \quad (3.12)$$

where \mathcal{C} is a constant which depends on the action and has been set to unity here. However, the general solution for $\Phi^{(1)}$ will have :

- i) two homogeneous solutions which are incoming and outgoing at the horizon respectively and,
- ii) a particular solution which will be completely determined by the hydrodynamic background perturbation and the equilibrium solution $\Phi^{(0)}$.

This particular solution will contribute to both $O^{(1)}$ and $J^{(1)}$, as will the homogeneous solutions. The incoming boundary condition will set the coefficient of the outgoing homogeneous solution to zero. The coefficient of the homogeneous incoming wave solution is left arbitrary. At equilibrium, this arbitrary coefficient cancels between the numerator and denominator, but at non-equilibrium we have an extra coefficient from $\Phi^{(1)}$ and therefore (3.12) is ill-defined.

Chapter 3. The Holographic Spectral Function in Non-Equilibrium States

Later in this chapter, we show that careful treatment of regularity of the solution at the horizon implies that the coefficient of the homogenous incoming solution should also be zero in presence of background quasinormal modes. This will allow us to put forth a well-defined prescription for obtaining the non-equilibrium retarded Green's function and spectral function holographically. In fact, the prescription can be precisely stated in a manner which is independent of the non-equilibrium state. Thus, holography gives a very well-defined perturbation expansion of non-equilibrium observables which can be understood in an universal manner.

This chapter is based on our work, [24]. The organization of the chapter is as follows. In section 3.1, we give a general review of holographic duals of non-equilibrium states. Though most of this section is a review, the explicit metrics for charged hydrodynamics and homogeneous relaxation in section 3.1.4 in AdS_4 are new as far as we are aware of the literature. The key point in the discussion in section 3.1.2 however, to the best of our knowledge, is novel. Here we argue that in a non-supersymmetric theory with a gravity dual, there may exist a window of temperature and chemical potential at large N , in which a generic non-equilibrium state can be characterized by just a finitely few operators with low scaling dimensions even far away from the hydrodynamic limit. We also point out that there are surprising similarities with solutions of the Boltzmann equation on the weak coupling side, which we review in section 3.2.1.

In section 3.2, we develop the formalism for obtaining non-equilibrium retarded Green's function and spectral function holographically in the approximation where the background fluctuation is linearized i.e. when the non-equilibrium state is studied in the linearized approximation. An interesting result is that we can read off the relaxation modes in the background by measuring the non-equilibrium spectral function.

In section 3.3, we compare our holographic approach with field theory. We also make a comparison with Landau's Fermi liquid theory regarding non-equilibrium dynamics of the Fermi surface. Furthermore, we obtain a holographic prescription to calculate space-time dependent non-equilibrium shifts in the energy and spin of the quasi-particles.

In section 3.4, we show that our prescription for the holographic retarded Green's function readily generalizes when we take non-linearities in the dynamics of the variables characterizing the non-equilibrium state into account.

Finally, in section 3.5, we conclude by pointing out interesting issues that could be addressed numerically.

3.1 On non-equilibrium states, their holographic duals and quasi-normal modes

An equilibrium state can always be characterized by a few macroscopic variables related by an equation of state. The distribution functions of particles, density of states, expectation values of operators, Green's functions, etc. depend on these macroscopic variables. We also know, in principle, how to calculate the equation of state relating the macroscopic variables of equilibrium states. Most importantly, we know in principle how to calculate the dependence of the observables in the underlying field theory on these variables characterizing equilibrium states.

The most pressing problem in dealing with non-equilibrium states is that, typically even at the coarse-grained level, we need an infinite number of macroscopic variables to characterize them. These variables also depend on space and time. Aside from taking recourse to a kinetic approximation, which is typically uncontrolled (but intuitively well-motivated) from the point of view of the exact field theory, we usually do not know how to obtain the equations of motion of these macroscopic variables (thereby generalizing the notion of equation of state applicable at equilibrium). It is also not clear how to relate observables in the field theory to the macroscopic coarse-grained non-equilibrium variables.

Here, we will address these issues from the point of view of holography. Firstly, we will identify a special sector of non-equilibrium states which can be described in terms of a finite number of operators of low scaling dimensions in kinetic theories. These states exist for any value of the coupling at least in the kinetic approximation. Then we will argue holographically that these states also exist in the exact field theory and are generic at strong coupling and large N after a microscopic time-scale, irrespective of the initial condition. We will further discuss how solutions in gravity describe such non-equilibrium states.

3.1.1 Conservative states in the kinetic approximation

Let us first look at the kinetic approximation in some details. In particular let us analyze the Boltzmann limit which is valid typically when, nl_{mfp}^d is small, where n is the typical number density, l_{mfp} is the mean free path and d is the number of spatial dimensions.

Boltzmann equation describes the dynamics of particle-distributions in phase space. It can be reduced to local dynamics of the infinite number of moments of the phase-space

Chapter 3. The Holographic Spectral Function in Non-Equilibrium States

distribution of particles $f^{(s)}(\mathbf{x}, \mathbf{p}, t)$ of a given species s . These moments are

$$f_{\mu_1 \mu_2 \dots \mu_n}^{(s)}(\mathbf{x}, t) = \int \frac{d^d p}{p^{(s)0}} p_{\mu_1} p_{\mu_2} \dots p_{\mu_n} f^{(s)}(\mathbf{x}, \mathbf{p}, t) \quad (3.13)$$

where p^μ is the $d + 1$ -momentum with p^0 being on-shell energy for each species s .

A conserved current (for instance the baryon number current) is given by :

$$j_\mu(\mathbf{x}, t) = \sum_s q_s \int \frac{d^d p}{p^{(s)0}} p_\mu f^{(s)}(\mathbf{x}, \mathbf{p}, t), \quad (3.14)$$

where q_s is the charge (for instance baryon charge) of the s -th species.

The energy-momentum tensor is given by

$$t_{\mu\nu}(\mathbf{x}, t) = \sum_s \int \frac{d^d p}{p^{(s)0}} p_\mu p_\nu f^{(s)}(\mathbf{x}, \mathbf{p}, t). \quad (3.15)$$

Thus we see that the energy-momentum tensor and conserved currents are parametrized by a weighted sum of first few moments of the quasi-particle distribution functions.

Three comments are in order here :

1. The Boltzmann equation has no dependence on temperature or non-equilibrium parameters. The latter parametrize the solutions. The thermal Bose-Einstein or Fermi-Dirac distributions are exact solutions of the Boltzmann equation. In absence of external fields, Boltzmann's H-theorem indicates all solutions finally equilibrate into thermal Bose-Einstein or Fermi-Dirac distribution.
2. The integrals involved in collision terms on the right hand side of the Boltzmann equation (see eq. (3.106) for weakly interacting electrons) have divergences coming from phase-space volume. To regulate these divergences one can put a IR-cutoff corresponding to the thermal mass of the quarks and gluons with temperature being the final equilibrium temperature [25]. The dispersion relations are also accordingly modified.
3. In the dilute limit the effect of the interactions is taken into account via an effective thermal mass. Thus the energy-momentum tensor takes a free particle form with an effective thermal mass.

It can be shown that the higher velocity moments parametrize the flow of the flow, the

Chapter 3. The Holographic Spectral Function in Non-Equilibrium States

flow of the flow of the flow, etc. of charge, energy and momentum. For example, if we define :

$$S_{\mu\nu\rho}(\mathbf{x}, t) = \sum_s \int \frac{d^d p}{p^{(s)0}} p_\mu p_\nu p_\rho f^{(s)}(\mathbf{x}, \mathbf{p}, t), \quad (3.16)$$

then the heat-current is $S_\mu = S_{\mu\nu\rho} \eta^{\nu\rho}$.

The Boltzmann equation can have solutions where the partial conserved currents are $j^{(s)\mu}$ are all proportional to each other. This happens precisely when chemical equilibrium is achieved, and in fact any arbitrary solution achieves chemical equilibrium after sufficiently long time. In that case, we can define a four-velocity field u^μ and charge density ρ such that :

$$j_\mu^{(s)} = \rho^{(s)} u_\mu, \quad \rho = \sum_s \rho^{(s)}, \quad j_\mu = \sum_s j_\mu^{(s)} = \rho u_\mu. \quad (3.17)$$

The energy-density ϵ is :

$$\epsilon = t_{\mu\nu} u^\mu u^\nu. \quad (3.18)$$

The hydrodynamic variables are ϵ , ρ and u^μ . We can define temperature T and chemical potential μ fields in terms of ϵ and ρ by using the equation of state of the full system at thermal and chemical equilibrium locally.

There are special solutions of the full non-linear Boltzmann equation, known as *normal solutions* in the literature, which are purely hydrodynamic [26]. These solutions are such that all the moments $f_{\mu_1 \dots \mu_n}^{(s)}$ of the phase-space quasi-particle distributions of various species are algebraic functions of just the hydrodynamic variables u_μ , T and μ , and their *spatial* derivatives in the local inertial frame co-moving with u^μ . The full phase-space distributions can thus be characterized uniquely by the hydrodynamic variables. Furthermore, any arbitrary solution of the Boltzmann equation can be approximated by an appropriate normal solution after a sufficiently long time.

The hydrodynamic equations can be derived from the Boltzmann equation; these are the Navier-Stokes equation, charge diffusion equation and Fourier's law of energy transport with systematic higher derivative corrections. The shear viscosity, charge diffusion constant, thermal conductivity and all the higher order transport coefficients can be obtained from the relevant Boltzmann equation specified by the dominant collision processes.

These solutions can be further generalized to what were named *conservative solutions* [6]. In such solutions, the various moments $f_{\mu_1 \dots \mu_n}^{(s)}$ are algebraic functionals of ρ , u_μ (or equivalently the conserved current j_μ) and the energy-momentum tensor $t_{\mu\nu}$, and their spatial derivatives in a local inertial frame co-moving with u^μ . Thus the full solu-

Chapter 3. The Holographic Spectral Function in Non-Equilibrium States

tion can be specified by $t_{\mu\nu}$ and j_μ . In such solutions the energy-momentum tensor is not necessarily hydrodynamic. Furthermore, any solution of the Boltzmann equation reduces to an appropriate *conservative solution* after sufficiently long time, and the latter reduces to an appropriate *normal solution* after the relaxational time scale. The first claim follows from the fact that the independent dynamical parts of higher moments of the quasi-particle distributions decay faster compared to the non-hydrodynamic relaxational mode of the energy-momentum tensor [27].

The energy-momentum tensor $t_{\mu\nu}$ and the conserved current j_μ (or equivalently the charge density ρ and the velocity u_μ) follow a closed system of equations in conservative solutions of the Boltzmann equation. This gives a systematic generalization of phenomenology beyond hydrodynamics to include processes like relaxation. These phenomenological equations have been obtained in [6, 7].

Obviously, the existence of normal and conservative solutions of the Boltzmann equation can be seen at the linearized level and provides a method to obtain good approximations to the transport coefficients and relaxation parameters.

Thus, *in the semi-classical kinetic limit captured by the Boltzmann equation, an arbitrary non-equilibrium state can be approximated by a conservative state whose dynamics is given by the conserved current and the energy-momentum tensor even away from the hydrodynamic limit.* This approximation is reliable after a microscopic time-scale which is shorter than the leading non-hydrodynamic relaxation mode, i.e. the time scale of local thermalization.

The quasi-particle distribution is said to have locally thermalized when it can be characterized well by space-time dependent parameters of equilibrium distribution. Afterwards, hydrodynamics takes over and the system equilibrates globally. In a generic solution of the Boltzmann equation, we thus have three time scales. The first time-scale is the time for chemical equilibration t_{chem} after which inelastic collisions effectively cease, the second time scale is t_{cons} after which an approximation by an appropriate conservative solution becomes valid, and the third time scale is after which the hydrodynamic approximation is valid and is also the time scale of thermalization t_{therm} . The hierarchy is

$$t_{chem} < t_{cons} < t_{therm}.$$

The conservative solutions of Boltzmann equation describe the dynamics of both thermalization and hydrodynamics in an unified framework in the Boltzmann limit.

We note that there is no scale which parametrically separates the dynamics of the non-hydrodynamic part of the energy-momentum tensor and conserved currents from that of other relaxation modes. Thus we may argue that even if conservative states exist beyond the Boltzmann limit, they may not be typical non-equilibrium states after microscopic times as in the Boltzmann equation. The typicality is just a special feature of the Boltzmann limit.

In fact, once we go away from the dilute limit necessary for the Boltzmann equation to be reliable or consider genuine quantum dynamics (not just quantum statistics), the typicality of conservative states will no longer be preserved. The conserved currents and energy-momentum tensor do not seem to capture generic dynamics beyond the hydrodynamic limit. Conservative solutions may exist beyond the Boltzmann approximation, but only in the purely hydrodynamic limit can they approximate a generic state.

We will argue that if a theory has a holographic dual, then in certain phases in the large N limit, the dynamics can indeed be captured by just the conserved current and energy-momentum tensor generically, after a microscopic time-scale which is much shorter than the time-scale for local thermalization. In such cases, the conservative state can indeed capture generic non-equilibrium dynamics even far away from the hydrodynamic limit.

3.1.2 Holographic duals of non-equilibrium states and typicality at strong-coupling

Holography maps a field theory to a quantum theory of gravity in one extra spatial dimension. It further states that in the large N and strongly coupled limit, the dual theory of gravity reduces to a classical theory. Therefore, in this limit states of the field theory are dual to solutions of the classical theory of gravity which are regular in an appropriate sense. Furthermore, every operator is dual to a field and the expectation value of an operator in a state can be obtained from the asymptotic behavior of the dual field in the corresponding gravity solution.

The question of which operators matter in characterizing states in the large N and strong coupling limit can be seen from the masses of the dual fields. The mass of the field is related to the scaling dimension of the dual operator.

The large N limit in the (D dimensional) field theory side is the limit when the scale l , corresponding to asymptotic curvature radius of the ($D+1$ dimensional) space-time, is large compared to the effective Planck scale l_P (in $D + 1$ dimensions) on the quantum gravity (string theory) side of the holographic correspondence. The strong coupling limit on the

field-theory side is the limit when the length of the fundamental string l_s is small compared to the asymptotic curvature radius l on the quantum gravity side. The first condition $l_P \ll l$ allows us to consider the classical limit of gravity. The second condition $l_s \ll l$ allows us to ignore the massive stringy fields corresponding to higher excitations of the fundamental string.

Nevertheless, string theory is a theory in 10 dimensions. So, there has to be a compact space of $9 - D$ dimensions on top of the $D + 1$ dimensional non-compact coordinates. The conditions $l_s \ll l$ and $l_P \ll l$, i.e. strong coupling and large N limit in the field theory side allows us to decouple the massive stringy modes whose masses scale like l_s^{-1} when l_s and l_P are small compared to l . Thus from the ten-dimensional viewpoint we are left with just the massless fields which include the graviton and gauge fields. However, the compactification over the compact $9 - D$ dimensions still creates a tower of Kaluza-Klein fields which are dual to operators with possibly small scaling dimensions if the typical size of the compact dimensions is of the same order as the asymptotic curvature radius l .

In a supersymmetric set-up [28], the typical radius of the $9 - D$ dimensional compact space is indeed of the same order as the $D + 1$ dimensional asymptotic curvature radius l . Therefore, in the strong coupling and large N field-theoretic limit, the Kaluza-Klein spectrum still plays a role in characterizing states. In fact, these Kaluza-Klein fields are dual to chiral primary operators and their descendants. Therefore, a prediction of the holographic correspondence is that at large N the scaling dimensions of the chiral primary operators do not deviate much from the weak coupling limit.

Despite the presence of the Kaluza-Klein spectrum, it is known that almost all known supergravity theories in 10 dimensions admit consistent truncation at the classical level to gauged supergravity in $D + 1$ dimensions when dimensionally reduced over the appropriate $9 - D$ dimensional compact space. The $D + 1$ dimensional graviton is dual to the energy-momentum operator on the field-theory side and the $D + 1$ dimensional gauge fields are dual to the conserved currents with the global symmetry groups being gauged in the gravity side.

One can also show that all solutions of $D + 1$ dimensional gauged supergravities which thermalize to black branes with regular future horizons can be characterized uniquely by the expectation values of the energy-momentum tensor and conserved currents of the dual states ³. These solutions thus correspond to special non-equilibrium states - namely the

³Despite these not being Cauchy data from the gravity point of view, this holds if the geometry corresponds to regular perturbations of a black brane at late time [29]. We also note that the consistent truncation

strongly coupled version of the conservative states which can be characterized by the energy-momentum tensor and conserved currents alone. The parameters of phenomenological equations for the energy-momentum tensor and conserved currents which generalize hydrodynamics should now be obtained from gravity and not from kinetic theories valid at weak coupling [6–8]. Evidence that the solutions of pure gravity in particular, which have regular future horizons, can be interpreted as conservative states has been presented in [7] for the special case of homogeneous relaxation. It has been proved that regularity at the horizon gives an equation of motion for the non-hydrodynamic energy-momentum tensor with precise coefficients for this case.

Furthermore, such conservative states should also exist holographically away from the strong coupling and large N limit, since the dual solutions in gravity can be constructed by perturbatively correcting the gauged supergravity solutions in l_s^2/l^2 and $1/N^2$. Nevertheless, in the known supersymmetric cases these solutions are always special and not typical even in the strong coupling and large N limit, because the intrinsic dynamics of Kaluza-Klein modes are absent in these solutions.

The situation can be expected to be very different in non-supersymmetric cases. There is no analogue of chiral primary operators and typically we do not expect that quantum corrections to scaling dimensions of operators will be small at strong coupling, unless these are suppressed because of symmetries.

In order to use our intuition obtained from well studied examples with the field theory being conformal and supersymmetric, we will need to focus only on a certain window of temperatures and chemical potentials, such that :

1. the effective coupling is strong,
2. the beta function is vanishing or approximately so, i.e. the system is close to a critical point, and
3. there are no new emergent symmetries at the critical point other than the (exact or approximate) full conformal symmetry.

Furthermore, we also require that the large N approximation is valid, or useful for qualitative understanding. Probably, all these requirements could be satisfied for the fireball at RHIC near temperatures of 175 MeV and small baryon charge densities as supported by

to pure gravity does not involve separation of scales. This simply reflects the fact that the conservative states are not typical states in these examples.

lattice data [30]. We can also hope that the strange metallic phase of strongly correlated electron systems will satisfy these requirements in a window of temperatures and chemical potentials.

We note that certain examples of non-supersymmetric holography have been proposed in the literature [31]. However, in these special examples, infinite number of gauge symmetries appear in the bulk at large N , implying infinite number of global symmetries in the dual field theory. Our observations below will not be necessarily true in such cases ⁴.

In case of a typical non-supersymmetric theory with a gravity dual, at temperatures and chemical potentials such that the system is close to a strongly coupled critical point, we expect there will be a few operators whose scaling dimensions will be small. We observe that the scaling dimensions depend on the scale through the coupling and hence also on the phase of the theory being considered which is parametrized by the temperature and chemical potential. The relevant operators with small scaling dimensions in the window of temperature and chemical potentials considered here can be expected to be

1. the energy-momentum tensor,
2. the conserved currents, and
3. order parameters of spontaneous symmetry breaking.

Therefore, the operators dual to the Kaluza-Klein modes of gravity are expected to have large scaling dimensions very similar to those dual to the stringy modes. If this expectation is true, the typical scale of the compact dimensions should be of the same order as l_s and not l .

For instance, in the case of QCD, the relevant operators with small scaling dimensions in the conditions of RHIC can be expected to be

1. energy-momentum tensor,
2. the baryon number current,
3. the approximately conserved $SU(3)_L \times SU(3)_R$ flavor symmetry of the light quarks, and

⁴The examples [31] are also not stringy and so far well defined only in the large N limit, i.e. only when the theory of gravity is classical.

Chapter 3. The Holographic Spectral Function in Non-Equilibrium States

4. the order parameter of chiral symmetry breaking having zero baryon number, transforming as $(3_L, 3_R)$ under the flavor symmetry group and with scaling dimension approximately 3.

The dual massless fields on the gravity side should be

1. the graviton,
2. a $U(1)$ abelian gauge field,
3. $SU(3)_L \times SU(3)_R$ non-Abelian gauge fields, and
4. a neutral scalar field transforming in the $(3_L, 3_R)$ representation of the non-Abelian gauge group and with mass approximately given by $m^2 = -3/l^2$ ⁵.

Such a holographic model for QCD has already been proposed in [32]. However, our arguments above show that such models can be considered more seriously in the conditions of RHIC. In fact, for RHIC conditions we also do not need the hardwall cut-off proposed in these models to achieve confinement, as the mass gap is expected to become very mild at temperatures close to 175 MeV and for small baryon number densities.

Furthermore, if the temperature is higher than 125 MeV, chiral symmetry is expected to be restored, so that the profile of the bulk scalar field dual to the chiral symmetry breaking order parameter will be stabilized by a potential. Therefore, only the conserved currents and energy-momentum tensor can characterize non-equilibrium dynamics at large N and large 't Hooft coupling λ for temperatures above 125 MeV. The other fields in the holographic dual should have masses which grow like $1/l_s$ i.e. $1/\lambda^{\frac{1}{4}}$, and thus are expected to be effectively decoupled from the classical theory.

The correlation functions of the non-Abelian gauge fields in the gravity backgrounds which thermalize to a black brane are all we need to construct quantum kinetic theories of production and freeze-out of axial and vector mesons (and resonances) in the expanding fireball holographically. The interpretation of poles of correlation functions of these gauge fields in terms of mesons has been given in [32]. Using the methods to be described later, we can obtain the non-equilibrium corrections to these mesonic poles systematically.

⁵As the chiral symmetry breaking order parameter is $\langle \bar{q}^i q^j \rangle$, it has approximate mass dimension of 3. Moreover, QCD being asymptotically free, the dual boundary condition will be approximately AdS_5 -like as well. Then we can use the standard relation for AdS_5 for mass of the field m and the scaling dimension of the dual operator Δ which gives $m^2 = -3/l^2$ when $\Delta = 3$.

Chapter 3. The Holographic Spectral Function in Non-Equilibrium States

Let us estimate the relevant time scale at strong coupling after which the conservative solutions become relevant. This in the dual gravity description is given by the mass of the lightest stringy field or Kaluza-Klein mode. According to the discussion above, the time scale should be $O(\lambda^{-\frac{1}{4}})$ in a non-susy conformal theory at strong coupling. After such a time-scale, we may expect that the massive fields in gravity will decay and the relevant dynamics will be described by the metric, gauge fields and the light fields dual to order parameters of symmetry breaking relevant at the critical point. Thus decay of a massive field in gravity can be interpreted as transition to a conservative state at strong coupling where the dynamics is governed by the energy-momentum tensor, conserved currents and order parameters alone.

We conclude *in a typical non-supersymmetric theory which has a holographic dual, in a window of temperature and chemical potentials such that the dynamics is strongly coupled and approximately conformal, all non-equilibrium states can be characterized by just the energy-momentum tensor and conserved currents (and order parameters of spontaneous symmetry breaking if any), irrespective of the initial conditions, after a microscopic time-scale which scales with the coupling λ like $1/\lambda^{\frac{1}{4}}$ in the large N limit.* In other words, conservative states are typical states irrespective of the initial conditions after a microscopic time-scale much smaller than the time-scale of thermalization in the strongly coupled and nearly conformal phase at large N .

If the above arguments are indeed relevant for QCD and strange metals in a window of temperature and chemical potentials, we have a unique opportunity to understand non-equilibrium dynamics with only a finitely few operators in this special phase of these theories. As conservative states will be typical non-equilibrium states, we can use general phenomenological equations for non-equilibrium dynamics as proposed in [6, 7], and also hope to construct a general theory of kinetics and fluctuations to connect to experiments as we want to do here and more completely in the future.

If the above arguments fail, the reasons should certainly be deep. In that case, we also need to know how to generalize non-equilibrium holography beyond the sector of conservative states sufficiently so that we can describe a typical non-equilibrium state.

3.1.3 Quasinormal modes

The thermal states in the field theory at large N and strong coupling are captured by black brane solutions of classical gravity holographically. In the linearized limit, the non-

equilibrium fluctuations are captured by the linearized equations of motion of gauge field and the metric fluctuations about the black brane background. These fluctuations are dual to perturbations of the energy-momentum tensor and conserved currents about thermal equilibrium. Furthermore, these fluctuations should satisfy the incoming boundary condition at the horizon and Dirichlet boundary condition asymptotically [22]. Thus they are quasinormal modes capturing intrinsic fluctuations in the dual field theory which can exist in absence of sources and provide good approximation to a typical non-equilibrium state close to equilibrium at strong coupling and large N .

There is, however, a significant difference between the linearized Boltzmann limit and the quasinormal mode approximation of solutions of gravity. Instead of a finitely few decay modes on top of the hydrodynamic mode, we have an infinite tower of quasi-normal modes. The reason that we do not have an infinite tower of modes for the energy-momentum tensor perturbations in the Boltzmann equation is that it has only one time derivative (which in a Lorentz-invariant language is the derivative along the local velocity field). Quantum corrections to the Boltzmann equation are known to result in an infinite number of time derivatives, and it is not hard to see this will produce an infinite number of decay modes as well.

We will now obtain the phenomenological form of the non-equilibrium energy-momentum tensor and conserved current. Instead of stating in a Lorentz-invariant way, we will state the form of the energy-momentum tensor in the frame where the dual thermal state is at rest, i.e. the laboratory frame. It is convenient to define the velocity perturbation $\delta \mathbf{u}(\mathbf{x}, t)$ such that the velocity field is co-moving with the energy-flow, instead of the charge-flow as done usually in the Boltzmann limit. Thus the non-equilibrium energy-momentum tensor thus takes the Landau-Lifshitz form in the global co-moving frame :

$$\begin{aligned} t_{00} &= \epsilon(T, \mu) + \frac{\partial \epsilon(T, \mu)}{\partial T} \delta T(\mathbf{x}, t) + \frac{\partial \epsilon(T, \mu)}{\partial \mu} \delta \mu(\mathbf{x}, t), \\ t_{0i} &= t_{i0} = \left(\epsilon(T, \mu) + p(T, \mu) \right) \delta u_i(\mathbf{x}, t), \\ t_{ij} &= p(T, \mu) \delta_{ij} + \left(\frac{\partial p(T, \mu)}{\partial T} \delta T(\mathbf{x}, t) + \frac{\partial p(T, \mu)}{\partial \mu} \delta \mu(\mathbf{x}, t) \right) \delta_{ij} + \pi_{ij}(\mathbf{x}, t). \end{aligned} \quad (3.19)$$

Above p is the pressure and π_{ij} is the shear-stress tensor. The shear-stress tensor can thus be defined as the dissipative part of the energy-momentum tensor or the spatial components of the energy-momentum tensor not in local equilibrium in the co-moving frame. The

Chapter 3. The Holographic Spectral Function in Non-Equilibrium States

conserved current takes the form :

$$\begin{aligned} j_0 &= \rho(T, \mu) + \frac{\partial \rho(T, \mu)}{\partial T} \delta T(\mathbf{x}, t) + \frac{\partial \rho(T, \mu)}{\partial \mu} \delta \mu(\mathbf{x}, t) + \nu_0(\mathbf{x}, t), \\ j_i &= \rho(T, \mu) \delta u_i(\mathbf{x}, t) + \nu_i(\mathbf{x}, t). \end{aligned} \quad (3.20)$$

Above ν_i is the dissipative part of the conserved current or the spatial components of the current away from local equilibrium in the co-moving frame. However, as the co-moving frame is aligned with the energy flow, the charge can have a non-equilibrium part by itself. This is ν_0 .

In order to have conformal invariance, we should further have

$$\epsilon(T, \mu) = d p(T, \mu), \quad \delta \epsilon = d \delta p, \quad \pi_{ij} \delta_{ij} = 0, \quad (3.21)$$

with d being the number of spatial dimensions in the field theory. Above $\delta \epsilon$ and δp denote change in energy density and pressure due to change in temperature and chemical potential. From now onwards, we will be interested in the specific case when the field theory is conformal, so that on the gravity side we will be using asymptotically *AdS* boundary conditions.

The shear-stress tensor and the dissipative part of the current can be split into hydrodynamic parts $\pi_{ij}^{(h)}$ and $\nu_i^{(h)}$ respectively which are functions of the hydrodynamic fields δT and $\delta \mathbf{u}$, and non-hydrodynamic parts $\pi_{ij}^{(nh)}$ and $\nu_i^{(nh)}$ respectively which cannot be parametrized by hydrodynamic variables alone. On the other hand, ν_0 does not have any purely hydrodynamic part.

Chapter 3. The Holographic Spectral Function in Non-Equilibrium States

In the case of a conformal field theory, at the linearized level,

$$\begin{aligned}
\pi_{ij} &= \pi_{ij}^{(h)} + \pi_{ij}^{(nh)}, \quad \nu_i = \nu_i^{(h)} + \nu_i^{(nh)}, \\
\pi_{ij}^{(h)} &= -\eta(T, \mu) \left(\partial_i \delta u_j + \partial_j \delta u_i - \frac{2}{d} (\partial \cdot \delta u) \delta_{ij} \right) + \dots, \\
\nu_i^{(h)} &= -\mathcal{D}(T, \mu) \left(\frac{\partial \rho(T, \mu)}{\partial T} \partial_i \delta T + \frac{\partial \rho(T, \mu)}{\partial \mu} \partial_i \delta \mu \right) + \dots, \\
\pi_{ij}^{(nh)} &= \sum_{n=1}^{\infty} a_{(n)ij} e^{i(\mathbf{k} \cdot \mathbf{x} - \omega_{(n)}(\mathbf{k})t)}, \quad \text{with } a_{(n)ij} \delta_{ij} = 0 \text{ for all } n, \\
\nu_i^{(nh)} &= \sum_{n=1}^{\infty} b_{(n)i} e^{i(\mathbf{k} \cdot \mathbf{x} - \tilde{\omega}_{(n)}(\mathbf{k})t)}, \\
\nu_0^{(nh)} &= \sum_{n=1}^{\infty} c_{(n)} e^{i(\mathbf{k} \cdot \mathbf{x} - \tilde{\omega}_{(n)}(\mathbf{k})t)}. \tag{3.22}
\end{aligned}$$

Above, $\pi_{ij}^{(h)}$ and $\nu_i^{(h)}$ have been expanded in the derivative expansion, which is an expansion in the scale of variation of hydrodynamic variables over the mean free path. We also require δu_i and δT to be small uniformly for the linearized approximation to be valid. Furthermore, η is the shear viscosity and \mathcal{D} is the charge diffusion constant. On the other hand $a_{(n)ij}$, $b_{(n)i}$ and $c_{(n)}$ parametrize the dissipative non-hydrodynamic modes of the energy-momentum tensor and conserved current. The n here represents the various non-hydrodynamic branches of quasinormal mode perturbations which dissipate because their dispersion relations $\omega_{(n)}(\mathbf{k})$, $\tilde{\omega}_{(n)}(\mathbf{k})$ and $\tilde{\omega}_{(n)}(\mathbf{k})$ have negative imaginary parts. We require $a_{(n)ij}/p$, $b_{(n)i}/\rho$ and $c_{(n)}/\rho$ to be small for the linearized approximation to be valid.

We note the separation of π_{ij} and ν_i into hydrodynamic and non-hydrodynamic parts can also be done at the non-linear level. This is so because even at the non-linear level the hydrodynamic parts $\pi_{ij}^{(h)}$ and $\nu_i^{(h)}$ are solutions by themselves - from the perspective of kinetic theories this follows from existence of *normal solutions* as discussed before and from the point of view of gravity they give regular metrics via fluid/gravity correspondence. For any π_{ij} and ν_i , the non-hydrodynamic parts $\pi_{ij}^{(nh)}$ and $\nu_i^{(nh)}$ are just whatever remains after subtracting out the purely hydrodynamic parts $\pi_{ij}^{(h)}$ and $\nu_i^{(h)}$ constructed algebraically from the profile of the hydrodynamic variables in the full solution of the energy-momentum tensor and conserved currents.

In order to obtain the hydrodynamic modes at the linearized level, we simply put all $a_{(n)ij}$ and $b_{(n)i}$ to zero in (3.22) and impose the conservation of energy, momentum and

Chapter 3. The Holographic Spectral Function in Non-Equilibrium States

charge :

$$\partial^\mu t_{\mu\nu} = 0, \quad \partial^\mu j_\mu = 0. \quad (3.23)$$

We then obtain three modes, the sound mode, the shear mode and the charge diffusion mode. In the sound mode,

$$\begin{aligned} \delta \mathbf{u}(\mathbf{k}) & \text{ is parallel to } \mathbf{k}, \\ \omega & = \pm \frac{1}{\sqrt{d}} |\mathbf{k}| - i \left(\frac{d-1}{d} \right) \frac{\eta(T, \mu)}{\epsilon(T, \mu) + p(T, \mu)} |\mathbf{k}|^2 + \dots, \\ \delta \epsilon(\mathbf{k}) & = d \delta p(\mathbf{k}) = \pm \sqrt{d} |\delta \mathbf{u}(\mathbf{k})| \left(\epsilon(T, \mu) + p(T, \mu) \right) + \dots, \\ \frac{\delta \rho(\mathbf{k})}{\rho} & = \frac{\delta \epsilon(\mathbf{k})}{\epsilon(T, \mu) + p(T, \mu)} + \dots. \end{aligned} \quad (3.24)$$

Above (...) refers to higher derivative corrections in powers of \mathbf{k} . Using thermodynamic relations locally, one can obtain $\delta T(\mathbf{k})$ and $\delta \mu(\mathbf{k})$ from $\delta \epsilon(\mathbf{k})$ and $\delta \rho(\mathbf{k})$.

In the shear mode,

$$\begin{aligned} \delta \mathbf{u}(\mathbf{k}) & \text{ is orthogonal to } \mathbf{k}, \\ \omega & = -i \frac{\eta(T)}{\epsilon(T) + p(T)} |\mathbf{k}|^2 + \dots, \\ \delta \epsilon(\mathbf{k}) & = \delta p(\mathbf{k}) = \delta \rho(\mathbf{k}) = 0. \end{aligned} \quad (3.25)$$

In the charge-diffusion mode

$$\begin{aligned} \delta \epsilon(\mathbf{k}) & = 0, \quad \delta p(\mathbf{k}) = 0, \quad \delta \mathbf{u}_i(\mathbf{k}) = 0, \\ \omega & = -i \mathcal{D}(T, \mu) |\mathbf{k}|^2. \end{aligned} \quad (3.26)$$

The quasinormal modes of the metric and gauge fields contains these hydrodynamic modes as the only branches in which ω and \mathbf{k} can go simultaneously to zero. We can also obtain the transport coefficients by using the incoming boundary condition at the horizon. We will be interested in the shear mode in particular. The shear-viscosity is given by [2]:

$$\frac{\eta(T, \mu)}{s(T, \mu)} = \frac{T \eta(T, \mu)}{\epsilon(T, \mu) + p(T, \mu)} = \frac{1}{4\pi}. \quad (3.27)$$

Above, s is the entropy density and we have used the thermodynamic identity $s = (\epsilon + p)/T$.

Chapter 3. The Holographic Spectral Function in Non-Equilibrium States

In order to obtain the simplest non-hydrodynamic modes we need to set the perturbations of the hydrodynamic variables δu_i , δT and $\delta\mu$ in (3.22) to zero. Also we look for spatially homogeneous perturbations so that the momentum \mathbf{k} is zero. Nevertheless, unlike the case of hydrodynamic modes, the frequency $\omega_{(n)}$ do not vanish when \mathbf{k} goes to zero. In such a configuration, for arbitrary $a_{(n)ij}$, it is easy to see that energy and momentum is conserved because $\partial^\mu t_{\mu\nu}$ vanishes identically. When the chemical potential is set to zero, the quasi-normal modes in five dimensional gravity in AdS_5 give [33] :

$$\omega_{(n)}(\mathbf{k} = 0) = \pi T \left[\pm 1.2139 - 0.7775 i \pm 2n(1 \mp i) \right], \text{ for large } n. \quad (3.28)$$

Clearly, the conservation equations are not enough to reproduce all the quasi-normal modes. We need extra phenomenological equations. Such phenomenological equations can be derived from kinetic theories like Boltzmann equation at weak coupling or gravity at strong coupling. However, we can also write them on general phenomenological grounds. At present, these will not be important for us, we merely mention these have been found in the most general form in [6, 7].

We will be interested in the spectral function in this class of non-equilibrium states, whose dynamics is determined by the non-equilibrium fluctuations of energy-momentum tensor and conserved currents only. If we want to obtain these spectral functions holographically, we need the explicit metric and gauge field corresponding to the non-equilibrium state. It will be important for us to write the metric and gauge field fluctuation about the equilibrium black-brane background explicitly in terms of δu_i , δT , $\delta\mu$, $\pi_{ij}^{(nh)}$, ν_0 and $\nu_i^{(nh)}$. As we will show in the next subsection, the spectral function in the dual states will depend explicitly just on these non-equilibrium variables.

Later in section 3.4, we will discuss what happens when we take into account nonlinearities in the dynamics of δu_i , δT , $\pi_{ij}^{(nh)}$, etc.

3.1.4 Explicit examples of backgrounds

We will be interested in strongly coupled conformal field theories in three space-time dimensions in the large N limit. Therefore, as discussed earlier, we will be concerned with solutions of Einstein-Maxwell equations which are asymptotically AdS_4 and are quasi-normal mode fluctuations about a Reissner-Nordstrom black brane with both mass and charge.

Chapter 3. The Holographic Spectral Function in Non-Equilibrium States

As discussed earlier, on the gravity side we will need the Einstein-Maxwell action :

$$S = \frac{1}{2\kappa^2} \int d^4x \left(R + \frac{6}{l^2} - \frac{l^2}{4} F_{MN} F^{MN} \right). \quad (3.29)$$

Above l sets the scale of asymptotic (negative) curvature via a (negative) cosmological constant. This is required so that the asymptotic isometry of the spacetime is the same as the conformal group in 3 dimensions. We will use κ to denote the effective Newton's constant in four-dimensional gravity in lieu of Planck length l_P .

The metric of the Reissner-Nordstrom black brane in AdS_4 is :

$$ds^2 = \frac{l^2}{r^2} \frac{dr^2}{f\left(\frac{rr_0}{l^2}\right)} + \frac{l^2}{r^2} \left(-f\left(\frac{rr_0}{l^2}\right) dt^2 + dx^2 + dy^2 \right), \quad (3.30)$$

where f is the so-called blackening function given by :

$$f(s) = 1 - \left(3 \frac{r_*^4}{r_0^4} + 1 \right) s^3 + 3 \frac{r_*^4}{r_0^4} s^4. \quad (3.31)$$

In case of the gauge field, it is convenient to use the gauge $A_r = 0$. The only non-zero component of the gauge field is A_t and is given by :

$$A_t = \frac{2\sqrt{3}r_*^2}{l^2 r_0} \left(1 - \frac{rr_0}{l^2} \right). \quad (3.32)$$

The boundary of AdS_4 in these coordinates is at $r = 0$ and the outer horizon is at $r = l^2/r_0$. The total mass M and charge Q of the black hole are given by :

$$Q = \sqrt{3}r_*^2, \quad M = r_0^3 + 3 \frac{r_*^4}{r_0}. \quad (3.33)$$

Using the standard holographic dictionary we can relate the two parameters r_* and r_0 of the geometry and the Newton's constant κ in to the energy density ϵ , charge density ρ and entropy density s as below :

$$\epsilon = 2p = \frac{r_0^3}{\kappa^2 l^4} \left(3 \frac{r_*^4}{r_0^4} + 1 \right), \quad \rho = \frac{\sqrt{3}}{\kappa^2} \left(\frac{r_*}{l} \right)^2, \quad s = \frac{2\pi r_0}{\kappa^2 l^2}. \quad (3.34)$$

Chapter 3. The Holographic Spectral Function in Non-Equilibrium States

The thermodynamic relation

$$d\epsilon = Tds + \mu d\rho \quad (3.35)$$

gives the temperature and chemical potential as below :

$$T = \frac{3r_0}{4\pi l^2} \left(1 - \left(\frac{r_*}{r_0}\right)^4\right), \quad \mu = \frac{2\sqrt{3}r_*^2}{l^2 r_0}. \quad (3.36)$$

The first example of a non-equilibrium background we will describe is that with a hydrodynamic shear-mode turned on. The velocity perturbation will be denoted as $\delta \mathbf{u}(k_{(h)})$ with $k_{(h)}$ being the three-momentum of the fluctuation. We recall that $\mathbf{k}_{(h)} \cdot \delta \mathbf{u}(\mathbf{k}_{(h)}) = 0$, as the shear wave perturbation is transverse.

It is a well-defined problem to find a given metric and gauge field perturbation in the bulk corresponding to a definite energy-momentum tensor and conserved current fluctuation about the equilibrium at the boundary, when the Dirichlet boundary condition is imposed for the bulk perturbations at the boundary. The latter is needed so that the dual field theory lives in flat space and is influenced by an externally fixed chemical potential. Regularity at the horizon fixes the transport coefficients appearing in the energy-momentum tensor and conserved currents.

This procedure can be readily implemented in Fefferman-Graham coordinates [29]. A similar procedure can be implemented in Schwarzschild-like coordinates as well because the Schwarzschild radial coordinate and the Fefferman-Graham radial coordinate are only functions of each other when the temperature remains unperturbed. Then it follows [29] that :

$$\begin{aligned} \delta g_{ij} & \text{ will be proportional to } (k_{(h)i} \delta u_j(\mathbf{k}_{(h)}) + k_{(h)j} \delta u_i(\mathbf{k}_{(h)})) e^{i(\mathbf{k}_{(h)} \cdot \mathbf{x} - \omega_{(h)} t)}, \text{ and,} \\ \delta g_{i0} & \text{ will be proportional to } \delta u_i(\mathbf{k}_{(h)}) e^{i(\mathbf{k}_{(h)} \cdot \mathbf{x} - \omega_{(h)} t)}. \end{aligned}$$

It can be also shown that in the radial gauge, $A_r = 0$, the fluctuation in the gauge field is also proportional to the fluctuation in the conserved current, i.e. proportional to :

$$\delta u_i(\mathbf{k}_{(h)}) e^{i(\mathbf{k}_{(h)} \cdot \mathbf{x} - \omega_{(h)} t)}.$$

Chapter 3. The Holographic Spectral Function in Non-Equilibrium States

The explicit metric is given by :

$$\begin{aligned}
 ds^2 = & \frac{l^2}{r^2} \frac{dr^2}{f\left(\frac{rr_0}{l^2}\right)} + \frac{l^2}{r^2} \left(-f\left(\frac{rr_0}{l^2}\right) dt^2 + dx^2 + dy^2 \right. \\
 & \left. - 2\left(1 - f\left(\frac{rr_0}{l^2}\right)\right) \delta u_i(\mathbf{k}_{(h)}) e^{i(\mathbf{k}_{(h)} \cdot \mathbf{x} - \omega_{(h)} t)} dt dx^i \right) \\
 & + \frac{2l^2}{r^2} \left(-i \frac{l^2}{3r_0} k_{(h)i} \delta u_j(\mathbf{k}_{(h)}) e^{i(\mathbf{k}_{(h)} \cdot \mathbf{x} - \omega_{(h)} t)} h\left(\frac{rr_0}{l^2}\right) dx^i dx^j \right) + O(\epsilon^2), \quad (3.37)
 \end{aligned}$$

where,

$$h(s) = 3 \int_0^s d\tilde{s} \frac{\tilde{s}^2}{(1 + \tilde{s} + \tilde{s}^2 - 3\frac{r_*^4}{r_0^4} \tilde{s}^4)(1 - \tilde{s})}, \quad (3.38)$$

and

$$\omega_{(h)} = -i \frac{\mathbf{k}_{(h)}^2}{4\pi T} + O(\epsilon^3), \quad \eta = \frac{r_0^2}{2\kappa^2 l^2} = 4\pi s. \quad (3.39)$$

In the radial gauge $A_r = 0$, the gauge field takes the form

$$\begin{aligned}
 A_t &= \frac{2\sqrt{3}r_*^2}{l^2 r_0} \left(1 - \frac{rr_0}{l^2}\right) + O(\epsilon^2), \\
 A_i &= -\frac{2\sqrt{3}r_*^2}{l^2 r_0} \left(1 - \frac{rr_0}{l^2}\right) \delta u_i(\mathbf{k}_{(h)}) e^{i(\mathbf{k}_{(h)} \cdot \mathbf{x} - \omega_{(h)} t)} + O(\epsilon^2). \quad (3.40)
 \end{aligned}$$

Above ϵ denotes the parameter of derivative expansion in hydrodynamics.

It is to be noted that we have written the full metric and gauge field in a global frame co-moving with the equilibrium part of the energy-momentum tensor and conserved currents, i.e. in the laboratory frame. We can readily make the metric and gauge field Lorentz-covariant by boosting such that the unperturbed velocity field is a four-velocity vector u^μ [5]. However, this will be unnecessary for the purposes of this paper as we will be interested in the results in the laboratory frame.

Also one can readily realize that the metric is singular at the outer horizon $r = l^2/r_0$. This is however only an artifact of the coordinate system. We can systematically change coordinates order by order in the derivative expansion so that the metric and gauge fields are manifestly regular at the horizon [29]. In our coordinates, the radius of convergence of the derivative expansion is of the order of the effective mean-free path or the inverse of the effective temperature at a given radius given by $T_{eff}(r) = T/\sqrt{f(rr_0/l^2)}$. Therefore, we have a finite radius of convergence of the derivative expansion a finite distance away from

Chapter 3. The Holographic Spectral Function in Non-Equilibrium States

the horizon. Furthermore, we will be interested in calculating boundary correlators which are independent of the choice of bulk coordinate system.

The metric (3.37) and gauge field (3.40) in manifestly regular coordinates are given in appendix A.

The second example which we will be concerned with will be a homogeneous non-hydrodynamic perturbation of the energy-momentum tensor, i.e. with one $a_{(n)ij}$ in (3.22) turned on. The momentum of this perturbation is zero on account of homogeneity, but its frequency is non-zero and complex like in (3.28). The metric can be obtained following [7] in the Fefferman-Graham coordinate and re-expressed in the Schwarzschild coordinate used here by simply changing the radial coordinate. Again, as the temperature remains unperturbed, up to linear order the change of coordinate involves transformation of one variable. It can be shown that the metric perturbation is proportional to

$$a_{(n)ij}e^{-i\omega_{(n)}t}.$$

Explicitly the perturbed metric is :

$$\begin{aligned} ds^2 = & \frac{l^2}{r^2} \frac{dr^2}{f\left(\frac{rr_0}{l^2}\right)} + \frac{l^2}{r^2} \left(-f\left(\frac{rr_0}{l^2}\right) dt^2 + dx^2 + dy^2 \right) \\ & + \frac{2l^2}{r^2} \left(a_{(n)ij} e^{-i\omega_{(n)}t} \tilde{h}\left(\frac{rr_0}{l^2}, \omega_{(n)}\right) dx^i dx^j \right) + O(\delta^2), \end{aligned} \quad (3.41)$$

with δ being the parameter of non-hydrodynamic amplitude expansion. Furthermore, $\tilde{h}(s, \omega_{(n)})$ follows the equation of motion :

$$\begin{aligned} \frac{d^2 \tilde{h}(s, \omega_{(n)})}{ds^2} - \frac{\left(2 + (1 + 3\frac{r_*^4}{r_0^4})s^3 - 6\frac{r_*^4}{r_0^4}s^4\right)}{sf(s)} \frac{d\tilde{h}(s, \omega_{(n)})}{ds} \\ + \frac{\omega_{(n)}^2 l^4}{r_0^2} \left(\frac{1}{f^2(s)} \right) \tilde{h}(s, \omega_{(n)}) = 0. \end{aligned} \quad (3.42)$$

We will also require that :

$$\tilde{h}(s, \omega_{(n)}) = s^3 + O(s^4) \text{ as } s \rightarrow 0. \quad (3.43)$$

This is the asymptotic boundary condition and determines \tilde{h} uniquely as it puts the coefficient of the non-normalizable to zero and the coefficient of the normalizable mode to

be unity so that the boundary energy-momentum tensor fluctuation is as given by (3.22). Though the equation for \tilde{h} cannot be analytically solved, the solution can be readily expanded in a power series in $\omega_{(n)}$.

Furthermore, the gauge field remains unperturbed from the black brane profile.

The metric above is also not manifestly regular at the horizon, but once again it is just an artifact of the choice of coordinates. One can again translate the metric systematically to Eddington-Finkelstein coordinates to see manifest regularity [7]. The regularity is manifest only when we sum over all orders in $\omega_{(n)}$. This is to be expected because, although the amplitude of the non-hydrodynamic perturbation $a_{(n)ij}$ is small, its rate of change in time is not small (unlike the hydrodynamic modes) since $\omega_{(n)}$ is of the same order as the temperature.

Though we will not discuss the details here, we can construct the explicit metrics in the case of both hydrodynamic and non-hydrodynamic perturbations even at the non-linear level [5, 7]. The metric is regular at each order in the derivative expansion for hydrodynamic perturbations and for each order in the amplitude expansion for non-hydrodynamic perturbations, provided all time-derivatives (or covariantly speaking convective derivatives) are summed over at each order in the latter case [7].

3.2 The holographic prescription for the non-equilibrium spectral function

As discussed in the Introduction, the spectral function is given by the imaginary part of the retarded propagator which can be obtained from causal response of an operator to its source. A convenient way to obtain the spectral function is to calculate the retarded propagator using linear response theory first and then isolate its imaginary part.

In this section, we will consider single trace scalar and fermionic operators in field theory whose back-reaction to the metric is suppressed by $O(1/N^2)$. As we have argued in subsection 3.1.2, the possibly interesting scalar operators in the strong coupling and large N limit are order parameters of symmetry breaking. If we are in a range of temperature and chemical potentials, where such symmetry breaking does not occur, the profile of the scalar fields dual to these operators vanishes in the background classically. Therefore, the backreaction is indeed $O(1/N^2)$ suppressed. This observation may be applied to study pion correlations in the quark-gluon plasma at RHIC.

Chapter 3. The Holographic Spectral Function in Non-Equilibrium States

In popular holographic models of strongly correlated systems, the electron is thought to couple to a composite operator made out of strongly interacting fractionalized degrees of freedom (for a clear exposition please see [34]). The holographic dual is thought to capture the dynamics of the fractionalized degrees of freedom. The strongly interacting fractionalized degrees of freedom are $O(N^2)$, but the coupling of the electron to the composite operator of the strongly coupled theory is $O(1)$. The spectral function obtained from photo-electron spectroscopy (ARPES) will receive corrections from the spectral function of the composite fermionic operator of the strongly coupled sector. As the coupling of the electron to this operator is $O(1)$, we can ignore the backreaction of the fermionic field dual to this operator on the geometry representing the dual state, at the leading order. If this picture is qualitatively viable, our set-up will be relevant for describing non-equilibrium features of non-Fermi liquids described by such models.

Holographically, causal response implies the incoming boundary condition at the horizon. The event horizon separates space-time into two causal parts, one that is inside and ends at a singularity, and the other that is outside and stretches all the way to the boundary. No light ray can come out of the inside region to the outside region, though light rays can propagate from the outside to the inside. Therefore, the perturbations which respect the causal structure of the space-time are those which are purely incoming at the horizon, having no component which propagates from the inside to the outside.

The event horizon is not only a feature of the eternal static black hole, but also of the perturbed black hole (for instance, the black hole with the quasi-normal mode fluctuations of the metric and gauge fields). The event horizons of these non-equilibrium geometries are also perturbed from their equilibrium location and their positions can be calculated in a perturbative expansion [35]. Equilibration in this context means that the event horizon will have uniform surface gravity (the gravitational analogue of temperature) everywhere and it happens only far in the future.

Though the incoming boundary condition is insufficient for a well defined perturbation theory in non-equilibrium geometries as noted in the Introduction, we expect regularity at the future horizon to be a sufficient condition. It turns out that it is sufficient to impose the regularity condition only far in the future, that is in the asymptotic static black brane geometry. This has been observed before in [5, 7] in another context - while constructing time-dependent non-linear solutions of gravity with regular future horizons perturbatively. In such solutions it indeed suffices to impose regularity of the perturbations at the final equilibrium location of the horizon. In fact, the incoming boundary condition is itself tied

Chapter 3. The Holographic Spectral Function in Non-Equilibrium States

up to regularity [36] ⁶. In this section we will find a precise non-equilibrium generalization of the incoming boundary condition for bosonic and fermionic field configurations in non-equilibrium geometries.

For purposes of illustration, let us consider the non-equilibrium state which is the simplest to analyze from the gravity point of view - it is the AdS black brane with a linearized hydrodynamic shear mode perturbation of spatial momentum $\mathbf{k}_{(h)}$. The advantage of this geometry is that it can be shown that the event horizon does not fluctuate up to first order in the derivative expansion (i.e. up to first order in $\mathbf{k}_{(h)}/T$) essentially because the temperature field does not fluctuate as discussed in section 3.1. We will first demonstrate how we can develop a prescription for obtaining the holographic spectral function in such a non-equilibrium state. Our aim will be to obtain the correction to the equilibrium spectral function up to first order in derivative expansion, i.e. up to first order in $\mathbf{k}_{(h)}/T$.

The explicit metric and gauge field of the black brane with the hydrodynamic shear mode perturbation is given in (3.37) and (3.40) respectively up to first order in the derivative expansion. We will work explicitly with four space-time dimensions in gravity, as we will be interested primarily in a three space-time dimensional dual strongly coupled field theory. This is because we are interested in applications to strongly correlated electron systems at finite density living in two spatial dimensions. As argued in subsection 3.1.2, our analysis may apply to the strange metallic phase in a qualitative manner.

An elegant way to solve the equations of motion of scalar and fermionic fields is by using the Fourier transform in all the field-theory (i.e. boundary) coordinates. Obviously, in order to express the equations of motion of the fields in Fourier space, it is necessary to do the Fourier transform of the background perturbation first, i.e. we need to do the Fourier transform of the velocity field fluctuation δu_i . The dispersion relation for this fluctuation is as given by eqs. (3.25) and (3.27). We see that the frequency given by the dispersion relation is strictly (negative) imaginary, while the frequency related to Fourier transform is strictly real. Furthermore, the negative imaginary frequency given by the dispersion relation makes δu_i decay in the future but grow in the past as a function of time. A Fourier transform of such a function needs to be defined with care. In order to distinguish from the frequency and momenta associated with the scalar/fermionic field, we will denote the frequency and momenta of δu_i as $\omega_{(h)}$ and $\mathbf{k}_{(h)}$ respectively. The correct Fourier transform

⁶See also [7] for an explicit proof in a non-hydrodynamic context.

which reproduces the hydrodynamic dispersion relation is :

$$\delta u_i(\omega_{(h)}, \mathbf{k}_{(h)}) = - \left(\frac{1}{2\pi i} \right) \frac{\delta u_i(\mathbf{k}_{(h)})}{\omega_{(h)} + i \frac{\mathbf{k}_{(h)}^2}{4\pi T}}. \quad (3.44)$$

To check the above, one can try to reproduce the time dependence by doing the inverse Fourier transform. This needs to be done with a specific contour prescription for integration over $\omega_{(h)}$ as shown in Fig.3.1. This contour is the usual contour associated with the retarded propagator in field theory - it runs from $-\infty$ to ∞ infinitesimally below the real axis and then closes itself through the circle at infinity. This contour picks up contribution only from the negative imaginary pole reproducing the correct time dependence of δu_i at given $\mathbf{k}_{(h)}$.

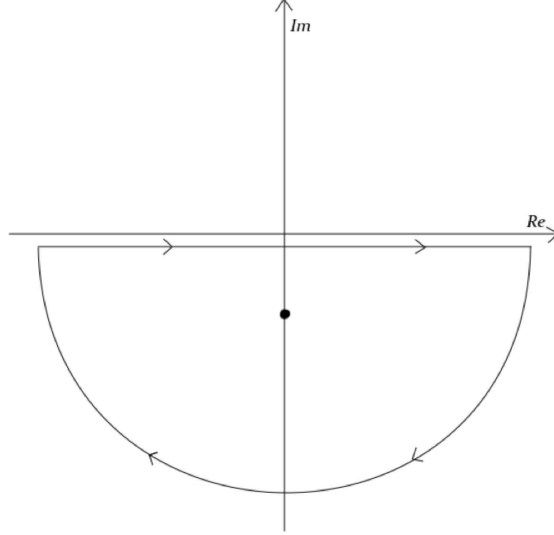


Figure 3.1: Contour for integration over $\omega_{(h)}$, with pole at negative imaginary axis

It will be easier to solve the scalar/fermionic field equations after doing the Fourier transform of δu_i , however we need to finally integrate over $\omega_{(h)}$ with the above contour prescription in order to obtain the observed behavior in real time.

For demonstrative purposes, we will analyze the scalar field equations first and then the fermionic field equations. Finally, we will see how we can apply our prescription for the non-equilibrium retarded Green's function when the background contains other quasinormal modes of the metric and gauge field.

3.2.1 Scalar field equation and the non-equilibrium spectral function

We will be interested in the non-equilibrium holographic spectral function for a scalar operator first. This requires us to solve the equation of motion of the dual scalar field in the non-equilibrium background; in particular we need to understand how the equilibrium part determines the non-equilibrium part completely. Without this, as we have mentioned before, the spectral function cannot be determined.

We will need to specify the equilibrium part of the solution first. We can assume, without loss of generality, that the equilibrium solution is in a specific (ω, \mathbf{k}) mode and obtain the non-equilibrium correction for each such mode. Using the fact that our field equation is linear, we can then linearly superimpose the solutions with the non-equilibrium correction for each equilibrium mode to obtain the most general solution.

The background in which the scalar field propagates is the AdS_4 Reissner-Nordstrom black hole with the hydrodynamic shear-mode perturbation. This hydrodynamic mode is given by the velocity perturbation δu_i in a specific momentum $\mathbf{k}_{(h)}$ but its dependence on $\omega_{(h)}$ is given by (3.44). We have to consider the background first in a definite $\omega_{(h)}$ perturbation and then integrate over $\omega_{(h)}$ finally with the contour prescription discussed before. The scalar field while propagating in the background will pick up a $(\omega + \omega_{(h)}, \mathbf{k} + \mathbf{k}_{(h)})$ mode. The profile of the scalar field, will therefore be of the following form :

$$\Phi(\mathbf{x}, t, r) = \Phi^{(0)}(\omega, \mathbf{k}, r)e^{-i(\omega t - \mathbf{k} \cdot \mathbf{x})} + \Phi^{(1)}(\omega, \mathbf{k}, \omega_{(h)}, \mathbf{k}_{(h)}, r)e^{-i((\omega + \omega_{(h)})t - (\mathbf{k} + \mathbf{k}_{(h)}) \cdot \mathbf{x})}. \quad (3.45)$$

The equilibrium part of the solution is $\Phi^{(0)}(\omega, \mathbf{k}, r)$ and the non-equilibrium part is $\Phi^{(1)}(\omega, \mathbf{k}, \omega_{(h)}, \mathbf{k}_{(h)}, r)$. The non-equilibrium part does not depend on the combination $\omega + \omega_{(h)}$ and $\mathbf{k} + \mathbf{k}_{(h)}$ as the space-time translational invariances of the equilibrium background are broken explicitly by the hydrodynamic quasinormal modes.

If the scalar field Φ is minimally coupled to gravity, and its mass and charge are m and q respectively, the equation of motion of the equilibrium part is simply

$$\square_{\omega', \mathbf{k}'}^{ARN} \delta(\omega' - \omega) \delta^2(\mathbf{k}' - \mathbf{k}) \Phi^{(0)}(\omega, \mathbf{k}, r) = 0, \quad (3.46)$$

where $\square_{\omega, \mathbf{k}}^{ARN}$ is the (gauge-invariant) Laplacian in the AdS Reissner-Nordstrom background

Chapter 3. The Holographic Spectral Function in Non-Equilibrium States

metric (3.30) and gauge field (3.32) as given by :

$$\begin{aligned}\square_{\omega, \mathbf{k}}^{ARN} &= r^2 f\left(\frac{rr_0}{l^2}\right) \partial_r^2 + r \left[-2f\left(\frac{rr_0}{l^2}\right) + \frac{rr_0}{l^2} f'\left(\frac{rr_0}{l^2}\right) \right] \partial_r \\ &+ r^2 l^2 \left[\frac{(\omega + q\mu(1 - \frac{rr_0}{l^2}))^2}{f\left(\frac{rr_0}{l^2}\right)} - \mathbf{k}^2 \right] + m^2 l^2.\end{aligned}\quad (3.47)$$

Again, f is the blackening function of the AdS Reissner-Nordstrom black brane which vanishes at the horizon located at $r = l^2/r_0$.

With the metric and gauge field in presence of hydrodynamic shear perturbation given by (3.37) and (3.40) respectively, the equation of motion for the non-equilibrium part up to first order in the hydrodynamic momenta $\mathbf{k}_{(h)}$ is :

$$\square_{\omega', \mathbf{k}'}^{ARN} \delta(\omega' - \omega - \omega_{(h)}) \delta^2(\mathbf{k}' - \mathbf{k} - \mathbf{k}_{(h)}) \Phi^{(1)}(\omega, \omega_{(h)}, \mathbf{k}, \mathbf{k}_{(h)}, r) = \begin{aligned} &V(\omega, \omega_{(h)}, \mathbf{k}, \mathbf{k}_{(h)}, r) \\ &\Phi^{(0)}(\omega, \mathbf{k}, r), \end{aligned}\quad (3.48)$$

with

$$\begin{aligned}V &= V_1 + V_2, \\ V_1 &= \frac{2r^2}{f\left(\frac{rr_0}{l^2}\right)} \left(\omega \left(1 - f\left(\frac{rr_0}{l^2}\right) \right) + q\mu \left(1 - \frac{rr_0}{l^2} \right) \right) \delta \mathbf{u}(\omega_{(h)}, \mathbf{k}_{(h)}) \cdot \mathbf{k}, \\ V_2 &= i \frac{2l^2 r^2}{3r_0} h \left(\frac{rr_0}{l^2} \right) k_i k_j k_{(h)i} \delta u_j(\omega_{(h)}, \mathbf{k}_{(h)}).\end{aligned}\quad (3.49)$$

Above, h gives the hydrodynamic correction to the background metric which is proportional to $k_{(h)i} \delta u_j + (i \leftrightarrow j)$ as in (3.38).

The behavior of the general solution of $\Phi^{(0)}(\omega, \mathbf{k}, r)$ near the horizon is well-known. It can be split into an incoming and outgoing wave as below :

$$\Phi^{(0)}(\omega, \mathbf{k}, r) \approx A^{in}(\omega, \mathbf{k}) \left(1 - \frac{rr_0}{l^2} \right)^{-i \frac{\omega}{4\pi T}} + A^{out}(\omega, \mathbf{k}) \left(1 - \frac{rr_0}{l^2} \right)^{i \frac{\omega}{4\pi T}} \quad (3.50)$$

near $r = \frac{l^2}{r_0}$.

In order to select the incoming wave, we should put

$$A^{out}(\omega, \mathbf{k}) = 0. \quad (3.51)$$

Chapter 3. The Holographic Spectral Function in Non-Equilibrium States

We can also normalize the overall solution by choosing

$$A^{in}(\omega, \mathbf{k}) = \mathcal{C}, \quad (3.52)$$

with \mathcal{C} being a numerical constant. This overall normalization will play no role in the Green's functions.

The behavior of the general non-equilibrium part of the solution near the horizon is :

$$\begin{aligned} \Phi^{(1)}(\omega, \omega_{(h)}, \mathbf{k}, \mathbf{k}_{(h)}, r) \approx & A^{in}(\omega, \omega_{(h)}, \mathbf{k}, \mathbf{k}_{(h)}) \left(1 - \frac{rr_0}{l^2}\right)^{-i\frac{\omega+\omega_{(h)}}{4\pi T}} \\ & + A^{out}(\omega, \omega_{(h)}, \mathbf{k}, \mathbf{k}_{(h)}) \left(1 - \frac{rr_0}{l^2}\right)^{i\frac{\omega+\omega_{(h)}}{4\pi T}} \\ & + i\mathcal{C} \left(\frac{4\pi T l^2}{r_0}\right)^2 \left(\frac{2}{9\left(1 - \frac{r_0^4}{r^4}\right)^2}\right) \frac{\omega \delta \mathbf{u}(\omega, \mathbf{k}_{(h)}) \cdot \mathbf{k}}{(2\omega + \omega_{(h)})\omega_{(h)}} \left(1 - \frac{rr_0}{l^2}\right)^{-i\frac{\omega}{4\pi T}}, \end{aligned} \quad (3.53)$$

near $r = \frac{l^2}{r_0}$.

The first two terms on the RHS above are the homogeneous incoming and outgoing solutions for frequency mode $\omega + \omega_{(h)}$. The third term is the particular solution which is determined completely by the equilibrium solution. The above behavior at the horizon is exact up to first order in $\mathbf{k}_{(h)}$. In fact the full general solution which reproduces the above can be given elegantly in an integral representation as in appendix B.

Obviously, we need to impose the incoming boundary condition again. Therefore,

$$A^{out}(\omega, \omega_{(h)}, \mathbf{k}, \mathbf{k}_{(h)}) = 0. \quad (3.54)$$

We will now show that in order to impose regularity at the horizon, we also need to dispose of the ingoing non-equilibrium homogeneous solution at the horizon. We recall that finally we need to integrate over $\omega_{(h)}$.

In order to be consistent with the derivative expansion, $A^{in}(\omega, \omega_{(h)}, \mathbf{k}, \mathbf{k}_{(h)})$ must take the form as follows. It is proportional to components of $\delta \mathbf{u}$ at the linear order as it should vanish in absence of the background perturbation. It's dependence on $\omega_{(h)}$ and $\mathbf{k}_{(h)}$ can be expanded systematically in terms of rotationally invariant scalars like $\delta \mathbf{u} \cdot \mathbf{k}$, $k_i k_j k_{(h)i} \delta u_j$,

Chapter 3. The Holographic Spectral Function in Non-Equilibrium States

$\omega_{(h)} k_i k_j k_{(h)i} \delta u_j$, etc. Up to first order in the derivative expansions only the first two scalars will appear. The coefficients of these scalars should be functions of ω and \mathbf{k} only, as the dependence on $\omega_{(h)}$ and $\mathbf{k}_{(h)}$ can be absorbed in coefficients of the scalars appearing at higher orders in the derivative expansion. Thus, up to first order in derivative expansion, we should have :

$$A^{in}(\omega, \omega_{(h)}, \mathbf{k}, \mathbf{k}_{(h)}) = A_1^{in}(\omega, \mathbf{k}) \delta \mathbf{u}(\omega_{(h)}, \mathbf{k}_{(h)}) \cdot \mathbf{k} + A_2^{in}(\omega, \mathbf{k}) k_i k_j k_{(h)i} \delta u_j(\omega_{(h)}, \mathbf{k}_{(h)}). \quad (3.55)$$

We recall for the hydrodynamic shear mode $\delta \mathbf{u} \cdot \mathbf{k}_{(h)} = 0$, so there is no more possible terms up to first order in $\mathbf{k}_{(h)}$. When we integrate over $\omega_{(h)}$, the Fourier transform of $\delta \mathbf{u}$ as given by (3.44) will give a pole contribution. Taking this into account the behavior of the ingoing non-equilibrium mode at the horizon will be :

$$\left(1 - \frac{rr_0}{l^2}\right)^{-i\frac{\omega}{4\pi T} - \frac{\mathbf{k}_{(h)}^2}{16\pi^2 T^2}}. \quad (3.56)$$

Therefore, we find the ingoing homogeneous non-equilibrium mode diverges at the horizon as $\mathbf{k}_{(h)}^2/(16\pi^2 T^2)$ is strictly positive. This divergence is not an artifact of the coordinate system because we are studying the behavior of a scalar field. The only way this divergence can be removed is by putting

$$A^{in}(\omega, \omega_{(h)}, \mathbf{k}, \mathbf{k}_{(h)}) = 0, \text{ i.e. } A_1^{in}(\omega, \mathbf{k}) = A_2^{in}(\omega, \mathbf{k}) = 0. \quad (3.57)$$

The particular solution at the horizon as defined as the third term in (3.53) produces no divergence after we do the integral over $\omega_{(h)}$. It is regular at and outside the horizon.

Summing up, the full solution with the non-equilibrium correction is the following :

$$\begin{aligned} \Phi(\mathbf{x}, t, r) \approx & \mathcal{C} \left(\left(1 - \frac{rr_0}{l^2}\right)^{-i\frac{\omega}{4\pi T}} e^{-i(\omega t - \mathbf{k} \cdot \mathbf{x})} + i \left(\frac{4\pi T l^2}{r_0}\right)^2 \left(\frac{2}{9 \left(1 - \frac{r_*^4}{r_0^4}\right)^2}\right) \right. \\ & \left. \frac{\omega \delta \mathbf{u}(\omega, \mathbf{k}_{(h)}) \cdot \mathbf{k}}{(2\omega + \omega_{(h)})\omega_{(h)}} \left(1 - \frac{rr_0}{l^2}\right)^{-i\frac{\omega}{4\pi T}} e^{-i((\omega + \omega_{(h)})t - (\mathbf{k} + \mathbf{k}_{(h)}) \cdot \mathbf{x})} \right), \end{aligned} \quad (3.58)$$

near $r = \frac{l^2}{r_0}$.

The above behavior when specified near the horizon uniquely fixes the full non-equilibrium

Chapter 3. The Holographic Spectral Function in Non-Equilibrium States

solution aside for an overall normalization \mathcal{C} .

We can numerically extrapolate the full solution all the way to the boundary $r = 0$. As the background is asymptotically AdS , we should have the following behavior :

$$\Phi(\mathbf{x}, t, r) \approx J(\mathbf{x}, t)r^{3-\Delta} + O(\mathbf{x}, t)r^\Delta \quad \text{near } r = 0. \quad (3.59)$$

By the holographic dictionary, J is indeed the source and O is the expectation value of the dual operator in the dual non-equilibrium state ⁷. Also, Δ is the scaling dimension of the dual operator given by the mass of the scalar field as below :

$$\Delta = \frac{3}{2} + \sqrt{\frac{9}{4} + m^2 l^2}. \quad (3.60)$$

The positivity of the Hamiltonian requires $m^2 l^2 > -9/4$ [38].

Furthermore, near $r = 0$, the equilibrium and non-equilibrium parts of the solution individually have the same behavior, so

$$\begin{aligned} \Phi^{(0)}(\omega, \mathbf{k}, r) &\approx J^{(0)}(\omega, \mathbf{k})r^{3-\Delta} + O^{(0)}(\omega, \mathbf{k})r^\Delta, \\ \Phi^{(1)}(\omega, \omega_{(h)}, \mathbf{k}, \mathbf{k}_{(h)}, r) &\approx J^{(1)}(\omega, \omega_{(h)}, \mathbf{k}, \mathbf{k}_{(h)})r^{3-\Delta} + O^{(1)}(\omega, \omega_{(h)}, \mathbf{k}, \mathbf{k}_{(h)})r^\Delta \end{aligned} \quad (3.61)$$

Therefore,

$$\begin{aligned} J(\mathbf{x}, t) &= J^{(0)}(\omega, \mathbf{k})e^{-i(\omega t - \mathbf{k} \cdot \mathbf{x})} + \int_{-\infty}^{\infty} d\omega_{(h)} J^{(1)}(\omega, \omega_{(h)}, \mathbf{k}, \mathbf{k}_{(h)})e^{-i((\omega + \omega_{(h)})t - (\mathbf{k} + \mathbf{k}_{(h)}) \cdot \mathbf{x})}, \\ O(\mathbf{x}, t) &= O^{(0)}(\omega, \mathbf{k})e^{-i(\omega t - \mathbf{k} \cdot \mathbf{x})} + \int_{-\infty}^{\infty} d\omega_{(h)} O^{(1)}(\omega, \omega_{(h)}, \mathbf{k}, \mathbf{k}_{(h)})e^{-i((\omega + \omega_{(h)})t - (\mathbf{k} + \mathbf{k}_{(h)}) \cdot \mathbf{x})} \end{aligned} \quad (3.62)$$

The unique solution of $\Phi^{(1)}$ with our prescribed behavior near the horizon (3.58) gives us the precise non-equilibrium contributions to both the operator and the source in the

⁷When $-9/4 < m^2 l^2 < -5/4$, we can do an alternate quantization where J can be interpreted as the expectation value and O as the source [37]. This requires the scaling dimension of the operator to be $\Delta = 3/2 - \sqrt{9/4 + m^2 l^2}$. The partition functions of the two theories are related by a Legendre transform.

Chapter 3. The Holographic Spectral Function in Non-Equilibrium States

following form :

$$\begin{aligned} O^{(1)}(\omega, \omega_{(h)}, \mathbf{k}, \mathbf{k}_{(h)}) &= O_A^{(1)}(\omega, \mathbf{k}) \delta \mathbf{u}(\omega_{(h)}, \mathbf{k}_{(h)}) \cdot \mathbf{k} + O_B^{(1)}(\omega, \mathbf{k}) k_i k_j k_{(h)i} \delta u_j(\omega_{(h)}, \mathbf{k}_{(h)}), \\ J^{(1)}(\omega, \omega_{(h)}, \mathbf{k}, \mathbf{k}_{(h)}) &= J_A^{(1)}(\omega, \mathbf{k}) \delta \mathbf{u}(\omega_{(h)}, \mathbf{k}_{(h)}) \cdot \mathbf{k} + J_B^{(1)}(\omega, \mathbf{k}) k_i k_j k_{(h)i} \delta u_j(\omega_{(h)}, \mathbf{k}_{(h)}). \end{aligned} \quad (3.63)$$

The explicit forms of $O_A^{(1)}$, $O_B^{(1)}$, $J_A^{(1)}$ and $J_B^{(1)}$ can be obtained as in appendix B. The integration over $\omega_{(h)}$ then will be given by the contribution from the pole in δu .

The non-equilibrium retarded correlator is ⁸:

$$\begin{aligned} G_R(\mathbf{x}_1, t_1, \mathbf{x}_2, t_2) &= \frac{O(\mathbf{x}_1, t_1)}{J(\mathbf{x}_2, t_2)} = e^{-i\omega(t_1-t_2)} e^{i\mathbf{k} \cdot (\mathbf{x}_1 - \mathbf{x}_2)} \\ &\quad \frac{O^{(0)}(\omega, \mathbf{k}) + O^{(1)}(\omega, \mathbf{k}, \mathbf{k}_{(h)}) e^{i\mathbf{k}_{(h)} \cdot \mathbf{x}_1} e^{-\frac{\mathbf{k}_{(h)}^2}{4\pi T} t_1}}{J^{(0)}(\omega, \mathbf{k}) + J^{(1)}(\omega, \mathbf{k}, \mathbf{k}_{(h)}) e^{i\mathbf{k}_{(h)} \cdot \mathbf{x}_2} e^{-\frac{\mathbf{k}_{(h)}^2}{4\pi T} t_2}} \\ &\approx e^{-i\omega(t_1-t_2)} e^{i\mathbf{k} \cdot (\mathbf{x}_1 - \mathbf{x}_2)} \frac{O^{(0)}(\omega, \mathbf{k})}{J^{(0)}(\omega, \mathbf{k})} \\ &\quad \left(1 + \left(\frac{O^{(1)}(\omega, \mathbf{k}, \mathbf{k}_{(h)})}{O^{(0)}(\omega, \mathbf{k})} e^{i\mathbf{k}_{(h)} \cdot \mathbf{x}_1} e^{-\frac{\mathbf{k}_{(h)}^2}{4\pi T} t_1} \right. \right. \\ &\quad \left. \left. - \frac{J^{(1)}(\omega, \mathbf{k}, \mathbf{k}_{(h)})}{J^{(0)}(\omega, \mathbf{k})} e^{i\mathbf{k}_{(h)} \cdot \mathbf{x}_2} e^{-\frac{\mathbf{k}_{(h)}^2}{4\pi T} t_2} \right) \right), \end{aligned} \quad (3.64)$$

where

$$\begin{aligned} O^{(1)}(\omega, \mathbf{k}, \mathbf{k}_{(h)}) &= O_A^{(1)}(\omega, \mathbf{k}) \delta \mathbf{u}(\mathbf{k}_{(h)}) \cdot \mathbf{k} + O_B^{(1)}(\omega, \mathbf{k}) k_i k_j k_{(h)i} \delta u_j(\mathbf{k}_{(h)}), \\ J^{(1)}(\omega, \mathbf{k}, \mathbf{k}_{(h)}) &= J_A^{(1)}(\omega, \mathbf{k}) \delta \mathbf{u}(\mathbf{k}_{(h)}) \cdot \mathbf{k} + J_B^{(1)}(\omega, \mathbf{k}) k_i k_j k_{(h)i} \delta u_j(\mathbf{k}_{(h)}). \end{aligned} \quad (3.65)$$

The difference of the above from (3.63) is that in $\delta \mathbf{u}$ which has no dependence in $\omega_{(h)}$. The latter has been integrated over. This integration produces the contribution from the diffusion pole and the residue has been obtained from (3.44).

Clearly, the choice of overall normalization of the solution given by \mathcal{C} in (3.58) does not matter as mentioned before. It cancels between the numerator and denominator in the

⁸At equilibrium, this prescription has been proposed in [22]. As noted in the Introduction, we can apply this prescription also at non-equilibrium using the validity of linear response theory.

retarded correlator. To readily compare with experimental data, we have to do the Wigner transform of the retarded correlator, as discussed before. We find

$$\begin{aligned}
 G_R(\omega, \mathbf{k}, \mathbf{x}, t) = & \int d\omega_0 \int d^2 k_0 \left[\frac{O^{(0)}(\omega_0, \mathbf{k}_0)}{J^{(0)}(\omega_0, \mathbf{k}_0)} \delta(\omega - \omega_0) \delta^2(\mathbf{k} - \mathbf{k}_0) \right. \\
 & - \frac{O^{(0)}(\omega_0, \mathbf{k}_0)}{J^{(0)}(\omega_0, \mathbf{k}_0)} \frac{1}{2\pi i} \left(\frac{O^{(1)}(\omega_0, \mathbf{k}_0, \mathbf{k}_{(h)})}{O^{(0)}(\omega_0, \mathbf{k}_0)} \delta^2\left(\mathbf{k} - \mathbf{k}_0 - \frac{\mathbf{k}_{(h)}}{2}\right) \frac{1}{\left(\omega - \omega_0 + i\frac{\mathbf{k}_{(h)}^2}{8\pi T}\right)} \right. \\
 & \left. \left. - \frac{J^{(1)}(\omega_0, \mathbf{k}_0, \mathbf{k}_{(h)})}{J^{(0)}(\omega_0, \mathbf{k}_0)} \delta^2\left(\mathbf{k} - \mathbf{k}_0 + \frac{\mathbf{k}_{(h)}}{2}\right) \frac{1}{\left(\omega - \omega_0 - i\frac{\mathbf{k}_{(h)}^2}{8\pi T}\right)} \right) \right. \\
 & \left. e^{i\mathbf{k}_{(h)} \cdot \mathbf{x}} e^{-\frac{\mathbf{k}_{(h)}^2}{4\pi T} t} \right].
 \end{aligned} \tag{3.66}$$

The first term above is just the equilibrium retarded propagator. The second and third terms are the non-equilibrium contributions. The non-equilibrium contributions have an explicit space-time dependence *which is co-moving with the velocity perturbation in the background*.

The spectral function can be obtained from the imaginary part of the retarded propagator by using $\mathcal{A}(\omega, \mathbf{k}, \mathbf{x}, t) = -2\text{Im}G_R(\omega, \mathbf{k}, \mathbf{x}, t)$.

3.2.2 Fermionic field equations and the non-equilibrium spectral function

We will now extend the prescription to obtain the non-equilibrium fermionic spectral function. We begin by constructing the equation of motion for a Dirac spinor explicitly in the same non-equilibrium background, which is AdS_4 Reissner-Nordstrom black hole with a hydrodynamic shear-mode perturbation.

We recall that the Dirac equation for a Dirac spinor of mass m and charge q in curved space is :

$$\left(e_A^M \Gamma^A \left(\partial_M + \frac{1}{8} \omega_M^{BC} [\Gamma_B, \Gamma_C] + iqA_M \right) + m \right) \Psi = 0, \tag{3.67}$$

where M are the space-time indices, and A, B and C are the tangent space indices collectively. We will denote tangent space indices with underlines as in $(\underline{r}, \underline{t}, \underline{x}, \underline{y})$ or more

Chapter 3. The Holographic Spectral Function in Non-Equilibrium States

compactly as $(\underline{r}, \underline{\mu})$ to distinguish from the space-time indices which will not be underlined as in (r, t, x, y) or (r, μ) .

In order to work with the holographic dictionary, it is convenient to choose the following representation for Gamma matrices [23]:

$$\Gamma^r = \begin{pmatrix} \mathbf{1} & 0 \\ 0 & -\mathbf{1} \end{pmatrix}, \quad \Gamma^\mu = \begin{pmatrix} 0 & \gamma^\mu \\ \gamma^\mu & 0 \end{pmatrix}, \quad (3.68)$$

where γ^μ s are the 2 + 1 dimensional Gamma matrices in a chosen representation. We will choose the latter in the following representation :

$$\gamma^t = i\sigma^3, \quad \gamma^x = \sigma^1, \quad \gamma^y = \sigma^2. \quad (3.69)$$

It is also useful to decompose the 3+1 space-time dimensional Dirac spinor as eigenvectors of Γ_\pm defined as :

$$\Gamma_\pm = \frac{1}{2}(1 \pm \Gamma^r), \quad (3.70)$$

so that

$$\Psi = \Psi_+ + \Psi_-, \quad \Psi_\pm = \Gamma_\pm \Psi. \quad (3.71)$$

The advantage of this decomposition is that both Ψ_+ and Ψ_- transform as 3 space-time dimensional Dirac spinors when the Gamma matrices are in the representation above.

It might be puzzling as to how a Dirac spinor in the bulk maps to two Dirac spinors in the boundary, but we note unlike the scalar field equation, the Dirac equation is first order. Therefore, as in the case of the scalar field we have two independent boundary data, corresponding to Ψ_+ and Ψ_- each. Eventually, we will see how these two boundary data maps to source and expectation value of the dual operator, and further how they get related to each other by regularity in the bulk giving us the dual fermionic retarded propagator.

Just as in the case of the scalar field, the space-time profile of the Dirac spinor also has an equilibrium and non-equilibrium part. We can first assume that the equilibrium part is in a specific (ω, \mathbf{k}) mode and determine the non-equilibrium correction to this. Later, we can obtain the most general solution by superimposing the full solutions corresponding to various equilibrium modes. The space-time profile of the Dirac spinor thus takes the

Chapter 3. The Holographic Spectral Function in Non-Equilibrium States

following form :

$$\Psi(\mathbf{x}, t, r) = \Psi^{(0)}(\omega, \mathbf{k}, r) e^{-i(\omega t - \mathbf{k} \cdot \mathbf{x})} + \Psi^{(1)}(\omega, \mathbf{k}, \omega_{(h)}, \mathbf{k}_{(h)}, r) e^{-i((\omega + \omega_{(h)})t - (\mathbf{k} + \mathbf{k}_{(h)}) \cdot \mathbf{x})}, \quad (3.72)$$

where $\Psi^{(0)}$ is the equilibrium part, $\Psi^{(1)}$ is the non-equilibrium part, and $(\omega_{(h)}, \mathbf{k}_{(h)})$ correspond to the frequency and momenta of the velocity field perturbation in the background. From now on, we will denote (ω, \mathbf{k}) collectively as k , and $(\omega_{(h)}, \mathbf{k}_{(h)})$ collectively as $k_{(h)}$.

The equations of motion for Ψ can be written as two coupled first order PDEs for Ψ_{\pm} . It will be convenient for us to decouple these PDEs and write a second order PDE for Ψ_{+} . It will turn out that Ψ_{-} will be then algebraically determined by Ψ_{+} . For the equilibrium AdS_4 Reissner-Nordstrom black brane background, this has been done in [14]. Following this, we write the equations of motion for $\Psi_{\pm}^{(0)}$ as below :

$$\begin{aligned} \left(\frac{\partial^2}{\partial r^2} + P(k, r) \frac{\partial}{\partial r} + Q(k, r) \right) \Psi_{+}^{(0)}(k, r) &= 0, \\ \Psi_{-}^{(0)}(k, r) &= -\frac{T_k}{T_k^2} \left(\frac{\partial}{\partial r} + \mathcal{A}^{+} \right) \Psi_{+}^{(0)}(k, r), \end{aligned} \quad (3.73)$$

where

$$\begin{aligned} P(k, r) &= \mathcal{A}^{+} + \mathcal{A}^{-} - \frac{r_0}{l^2} T'_k \frac{T_k}{T_k^2}, \\ Q(k, r) &= \mathcal{A}^{+} \mathcal{A}^{-} + \frac{r_0}{l^2} \mathcal{A}^{+'} - \frac{r_0}{l^2} T'_k \frac{T_k}{T_k^2} \mathcal{A}^{+} + T_k^2, \end{aligned} \quad (3.74)$$

and

$$\begin{aligned} \mathcal{A}^{\pm} &= -\frac{1}{2r} \left[3 - \frac{r f' \left(\frac{r r_0}{l^2} \right)}{2 f \left(\frac{r r_0}{l^2} \right)} \frac{r_0}{l^2} \right] \pm \frac{l}{r \sqrt{f \left(\frac{r r_0}{l^2} \right)}} m, \\ T_k &= \frac{i}{f \left(\frac{r r_0}{l^2} \right)} \left[(-\omega + q A_t^{(0)}) \gamma^{\pm} + \sqrt{f \left(\frac{r r_0}{l^2} \right)} k_i \gamma^{\pm} \right], \end{aligned} \quad (3.75)$$

with $'$ denoting differentiation w.r.t. $r r_0 / l^2$, $A_t^{(0)}$ representing the equilibrium configuration

Chapter 3. The Holographic Spectral Function in Non-Equilibrium States

of the gauge field and \mathcal{T}_k^2 is $\mathcal{T}_k \mathcal{T}_k$.

In order to obtain the equations of motion for $\Psi_{\pm}^{(1)}$ we need to obtain the non-equilibrium first order corrections to the vielbeins and spin connections in the derivative expansion. These are given in details in appendix C with the metric being (3.37) corresponding to the black brane perturbed by the hydrodynamic shear mode.

In order to simplify calculations, we will choose (without losing any generality) the momentum of the velocity field perturbation $\mathbf{k}_{(h)}$ in the background to be in the x direction; therefore the velocity perturbation $\delta \mathbf{u}$ being transverse should then be in the y direction. Later, we can make the results manifestly rotationally covariant by rotating, and also Lorentz covariant by boosting to an arbitrary frame. The momentum of the equilibrium part of Ψ of course can have arbitrary components in both x and y directions if we have to retain full generality.

The equations of motion of $\Psi^{(1)}$ are as follows :

$$\begin{aligned}
 \left(\frac{\partial^2}{\partial r^2} + P(k', r) \frac{\partial}{\partial r} + Q(k', r) \right) \delta^3(\bar{k}) \Psi_+^{(1)}(k, k_{(h)}, r) &= \left(\frac{\partial}{\partial r} + \mathcal{A}^- - \frac{r_0}{l^2} \mathcal{T}'_{k+k_{(h)}} \frac{\mathcal{T}_{k+k_{(h)}}}{T_{k+k_{(h)}}^2} \right) \\
 &\quad \mathcal{S}_+(k, k_{(h)}, r) \\
 &\quad - \mathcal{T}_{k+k_{(h)}} \mathcal{S}_-(k, k_{(h)}, r), \\
 \delta^3(\bar{k}) \Psi_-^{(1)}(k, k_{(h)}, r) &= - \frac{\mathcal{T}_{k'}}{T_{k'}^2} \left(\frac{\partial}{\partial r} + \mathcal{A}^+ \right) \delta^3(\bar{k}) \\
 &\quad \Psi_+^{(1)}(k, k_{(h)}, r) \\
 &\quad + \frac{\mathcal{T}_{k+k_{(h)}}}{T_{k+k_{(h)}}^2} \mathcal{S}_+(k, k_{(h)}, r), \quad (3.76)
 \end{aligned}$$

where $\bar{k} = k' - k - k_{(h)}$ and

$$\begin{aligned}
 \mathcal{S}_+(k, k_{(h)}, r) &= -\mathcal{X}_+(k_{(h)}, r) \Psi_+^{(0)}(k, r) - \mathcal{Y}(k_{(h)}, r) \Psi_-^{(0)}(k, r) \\
 \mathcal{S}_-(k, k_{(h)}, r) &= -\mathcal{X}_-(k_{(h)}, r) \Psi_-^{(0)}(k, r) - \mathcal{Y}(k_{(h)}, r) \Psi_+^{(0)}(k, r) \quad (3.77)
 \end{aligned}$$

with

$$\begin{aligned}
 \mathcal{X}_{\pm}(k_{(h)}, r) &= \mp \frac{1}{2} \left(\mathcal{E}(k_{(h)}, r) \gamma^{\underline{t}} \gamma^{\underline{y}} - \mathcal{F}(k_{(h)}, r) \gamma^{\underline{x}} \gamma^{\underline{y}} \right), \\
 \mathcal{Y}(k_{(h)}, r) &= \frac{1}{2} \left(\mathcal{B}(k_{(h)}, r) \gamma^{\underline{y}} - \mathcal{C}(k_{(h)}, r) \gamma^{\underline{t}} \gamma^{\underline{x}} \gamma^{\underline{y}} \right) + \mathcal{G}(k_{(h)}, r) \gamma^{\underline{t}} + \mathcal{H}(k_{(h)}, r) \gamma^{\underline{x}}. \quad (3.78)
 \end{aligned}$$

$\mathcal{B}, \mathcal{C}, \mathcal{E}, \mathcal{F}, \mathcal{G}, \mathcal{H}$ are given in terms of the inverse vielbeins and the spin connections as

$$\begin{aligned}
 \mathcal{B}(k_{(h)}, r) &= \frac{l}{r \sqrt{f\left(\frac{rr_0}{l^2}\right)}} \left(2i q e_{\underline{y}}^y A_y + 2i q e_{\underline{y}}^t A_t + e_{\underline{t}}^t \omega_{\underline{t}}^{\underline{ty}} + 2i \omega e_{\underline{y}}^t - 2i k_x e_{\underline{y}}^x \right)^{(1)} \\
 \mathcal{C}(k_{(h)}, r) &= \frac{l}{r \sqrt{f\left(\frac{rr_0}{l^2}\right)}} \left(-e_{\underline{t}}^t \omega_{\underline{t}}^{\underline{xy}} - e_{\underline{x}}^x \omega_{\underline{x}}^{\underline{ty}} + e_{\underline{y}}^y \omega_{\underline{y}}^{\underline{tx}} \right)^{(1)} \\
 \mathcal{E}(k_{(h)}, r) &= \frac{l}{r \sqrt{f\left(\frac{rr_0}{l^2}\right)}} \left(-e_{\underline{t}}^t \omega_{\underline{t}}^{\underline{yr}} - e_{\underline{y}}^y \omega_{\underline{y}}^{\underline{tr}} + e_{\underline{x}}^x \omega_{\underline{x}}^{\underline{ty}} - e_{\underline{y}}^t \omega_{\underline{t}}^{\underline{tr}} - e_{\underline{t}}^y \omega_{\underline{y}}^{\underline{yr}} \right)^{(1)} \\
 \mathcal{F}(k_{(h)}, r) &= \frac{l}{r \sqrt{f\left(\frac{rr_0}{l^2}\right)}} \left(e_{\underline{x}}^x \omega_{\underline{x}}^{\underline{yr}} - e_{\underline{y}}^y \omega_{\underline{y}}^{\underline{xr}} - e_{\underline{y}}^x \omega_{\underline{x}}^{\underline{rr}} + e_{\underline{x}}^y \omega_{\underline{y}}^{\underline{yr}} \right)^{(1)} \\
 \mathcal{G}(k_{(h)}, r) &= \frac{l}{r \sqrt{f\left(\frac{rr_0}{l^2}\right)}} \left(-i k_y e_{\underline{t}}^y \right)^{(1)} \\
 \mathcal{H}(k_{(h)}, r) &= \frac{l}{r \sqrt{f\left(\frac{rr_0}{l^2}\right)}} \left(-i k_y e_{\underline{x}}^y \right)^{(1)} \tag{3.79}
 \end{aligned}$$

Here $(\dots)^{(1)}$ means that we are extracting only those parts of the full expression which is first order (i.e. linear) in $\mathbf{k}_{(h)}$. Once again we mention that the exact expressions of the inverse vielbeins (or einbeins) and spin connections appearing above are given in appendix C exactly up to first order in $\mathbf{k}_{(h)}$.

The most important observation regarding the equation of motion for $\Psi^{(1)}$ is that just as in the case of $\Psi^{(0)}$, as evident from (3.76), $\Psi_+^{(1)}$ can be determined first by solving a second order ODE and $\Psi_-^{(1)}$ can be determined algebraically in terms of the solution for Ψ_+ . Therefore to uniquely specify $\Psi^{(1)}$ it is sufficient to uniquely specify $\Psi_+^{(1)}$. Moreover, the differential operator on the LHS of the equation of motion (3.76) for $\Psi_+^{(1)}$ is the same as that for $\Psi_+^{(0)}$ in (3.73) with k replaced by $k + k_{(h)}$. Therefore, the homogeneous solutions of $\Psi_+^{(1)}$ will be the same as those of $\Psi_+^{(0)}$ with k replaced by $k + k_{(h)}$.

The general behavior of the equilibrium part of the solution $\Psi_+^{(0)}$ at the horizon $r =$

Chapter 3. The Holographic Spectral Function in Non-Equilibrium States

l^2/r_0 is

$$\Psi_+^{(0)}(\omega, \mathbf{k}, r) \approx A_+^{in}(\omega, \mathbf{k}) \left(1 - \frac{rr_0}{l^2}\right)^{-i\frac{\omega}{4\pi T} - \frac{1}{4}} + A_+^{out}(\omega, \mathbf{k}) \left(1 - \frac{rr_0}{l^2}\right)^{i\frac{\omega}{4\pi T} - \frac{1}{4}} \quad (3.80)$$

Both A_+^{in} and A_+^{out} are arbitrary linear combinations of

$$\begin{pmatrix} 1 \\ 0 \end{pmatrix} \text{ and } \begin{pmatrix} 0 \\ 1 \end{pmatrix}.$$

The incoming wave boundary condition requires us to impose

$$A_+^{out}(\omega, \mathbf{k}) = 0. \quad (3.81)$$

Furthermore, the choice of $A_+^{in}(\omega, \mathbf{k})$ will not matter in the final answer for the retarded propagator, so we will choose

$$A_+^{in}(\omega, \mathbf{k}) = \begin{pmatrix} \mathcal{K} \\ 0 \end{pmatrix} \quad (3.82)$$

with \mathcal{K} being a constant. The behavior of $\Psi_-^{(0)}$ near the horizon can be obtained via the second algebraic equation of (3.73) as below :

$$\Psi_-^{(0)}(\omega, \mathbf{k}, r) \approx -\gamma^{\frac{1}{2}} \left(1 - \frac{rr_0}{l^2}\right)^{-i\frac{\omega}{4\pi T} - \frac{1}{4}} \begin{pmatrix} \mathcal{K} \\ 0 \end{pmatrix}. \quad (3.83)$$

Thus $\Psi_-^{(0)}$ is also incoming at the horizon and is $\Psi_+^{(0)}$ times a specific function of the frequency and momenta.

It is to be noted that the incoming wave solution of the fermion diverges at the horizon as well. That this divergence is not an artifact of choice of coordinates can be seen by computing the scalar $\bar{\Psi}\Psi$ at the horizon. In fact, it is believed that the fermion backreaction at the horizon is strong enough to change the near horizon geometry of the black brane [39]. As mentioned in the beginning of this section, we will assume here that the backreaction is suppressed by a factor of $O(1/N^2)$ ⁹.

We now turn our attention to the non-equilibrium part of the solution. From, the first

⁹At order $O(1/N^2)$ we cannot ignore the backreaction even in the linearized limit. This is because the scalar and fermionic fields have non-trivial profiles even in the background due to Hawking radiation. Particularly, the Hawking radiated fermions forms a Fermi-sea in the near-horizon region of the *AdS* Reissner-Nordstrom black hole.

Chapter 3. The Holographic Spectral Function in Non-Equilibrium States

equation in (3.76) we obtain that near the horizon, $\Psi_+^{(1)}$ behaves as :

$$\begin{aligned}
\Psi_+^{(1)}(\omega, \mathbf{k}, \omega_{(h)}, \mathbf{k}_{(h)}, r) &\approx A_+^{in}(\omega, \mathbf{k}, \omega_{(h)}, \mathbf{k}_{(h)}) \left(1 - \frac{rr_0}{l^2}\right)^{-i\frac{\omega+\omega_{(h)}}{4\pi T} - \frac{1}{4}} \\
&+ A_+^{out}(\omega, \mathbf{k}, \omega_{(h)}, \mathbf{k}_{(h)}) \left(1 - \frac{rr_0}{l^2}\right)^{i\frac{\omega+\omega_{(h)}}{4\pi T} - \frac{1}{4}} \\
&+ \alpha(\omega, \mathbf{k}, \omega_{(h)}, \mathbf{k}_{(h)}) \left(1 - \frac{rr_0}{l^2}\right)^{-i\frac{\omega}{4\pi T} - \frac{3}{4}} \begin{pmatrix} \mathcal{K} \\ 0 \end{pmatrix}, \\
\alpha(\omega, \mathbf{k}, \omega_{(h)}, \mathbf{k}_{(h)}) &= \sqrt{\frac{r_0}{\pi T}} \\
&\frac{(\omega_{(h)}(3i\pi T - \omega + \omega_{(h)}) - 2(\pi^2 T^2 + \omega^2))}{8(3\pi T + i\omega)(7\pi T + i\omega)} \delta u_y(k_{(h)}) \gamma^{\underline{t}} \gamma^{\underline{y}}.
\end{aligned} \tag{3.84}$$

when we have chosen the incoming wave boundary condition and our normalization for $\Psi_+^{(0)}$. Thus we have again two arbitrary coefficients for the incoming and outgoing homogeneous solutions at $2+1$ momenta $k + k_{(h)}$, and then we have a particular solution completely determined by the source term.

We now apply a similar logic as in the case of the scalar field. We put A^{out} in (3.84) to be zero again to satisfy the incoming boundary condition. In order to be consistent with the derivative expansion, A^{in} has to linear combinations of $\delta \mathbf{u}(\omega_{(h)}, \mathbf{k}_{(h)}) \cdot \mathbf{k}$ and $k_i k_j k_{(h)i} \delta u_j(\omega_{(h)}, \mathbf{k}_{(h)})$ with coefficients which are functions of ω and \mathbf{k} only. The integration over $\omega_{(h)}$ in presence of $\delta \mathbf{u}$ will give contribution from the diffusion pole which will cause a further singularity in the behavior of the fermionic field. This singularity involves an extra factor of

$$\left(1 - \frac{rr_0}{l^2}\right)^{-\frac{k_{(h)}^2}{16\pi^2 T^2}}.$$

So we put A^{in} to be zero too. There is however, a difference in the behavior of the particular solution near the horizon from the scalar case, as evident from (3.84). It diverges at the horizon with an extra factor of

$$\left(1 - \frac{rr_0}{l^2}\right)^{-\frac{1}{2}}.$$

The situation, therefore admittedly is confusing as both the incoming homogeneous solution and the particular solution are divergent by an extra power. Moreover, for sufficiently

small hydrodynamic momenta $k_{(h)}$, the divergence of the particular solution leads over that of the incoming homogeneous solution.

Nevertheless, we can argue as follows. When we take the backreaction into account, the part of the non-equilibrium solution completely determined by the source can be expected to be regular, as the source involving the regular equilibrium solution in the modified background will be regular in the next order in perturbation. This feature is observed in the case of fluid/gravity correspondence or for more general time-dependent solutions in gravity - if we make the solution regular up to n -th order in perturbation theory, the source terms in the equations for $n + 1$ -th order perturbations are also regular, and the divergences at the $n + 1$ -th order can be removed by adjusting the homogeneous solutions only [5, 29].

In the present case, we will argue that the divergence of the incoming homogeneous piece coming from the integration over $\omega_{(h)}$ is there as long as the backreacted background has a horizon at the zeroth order. If indeed there is a horizon, we can define an incoming wave also through geometrical optics approximation. We can certainly construct an appropriate function of r which we denote as $r_*(r)$ such that the incoming radial null geodesic at the (modified) horizon is :

$$v = t - r_*(r).$$

Clearly $r_*(r)$ has to increase indefinitely as r moves towards the horizon because of blue-shifting. The incoming wave at the horizon will always behave like :

$$\approx e^{-i(\omega + \omega_{(h)})v}$$

as the geometrical optics approximation is always good at the horizon due to the blue-shifting. Therefore, as long as the backreacted geometry still has a horizon, the integration over $\omega_{(h)}$ will produce a divergent factor :

$$(r_*(r))^{\frac{k_{(h)}^2}{16\pi^2 T^2}}.$$

Above we have used the result that the hydrodynamic dispersion relation up to the leading order remains the same in the presence of backreaction as η/s is universally $1/4\pi$ in Einstein's gravity minimally coupled to any form of matter [40]. Therefore, this divergence is not removable by backreaction as long as we do not get rid of the horizon completely.

Getting rid of the horizon is generically impossible if we demand that the solution in gravity is well behaved, as that would expose the singularity unless the latter is also

Chapter 3. The Holographic Spectral Function in Non-Equilibrium States

removed by the backreaction. The removal of singularity by back-reaction is impossible in Einstein's gravity minimally coupled to well-behaved matter. It is also hard to argue that solutions in gravity with naked singularities could be dual to states in thermal and chemical equilibrium in the dual theory.

We conclude that the sensible thing to do is to proceed as in the case of the scalar field and put *both* A^{in} and A^{out} to zero in the non-equilibrium part of the solution. This determines $\Psi_+^{(1)}$ completely and its behavior near the horizon is :

$$\begin{aligned} \Psi_+^{(1)}(\omega, \mathbf{k}, \omega_{(h)}, \mathbf{k}_{(h)}, r) &= \sqrt{\frac{r_0}{\pi T}} \frac{(\omega_{(h)}(3i\pi T - \omega + \omega_{(h)}) - 2(\pi^2 T^2 + \omega^2))}{8(3\pi T + i\omega)(7\pi T + i\omega)} \delta u_y(k_{(h)}) \gamma^t \gamma^y \\ &\quad \left(1 - \frac{rr_0}{l^2}\right)^{-i\frac{\omega}{4\pi T} - \frac{3}{4}} \begin{pmatrix} \mathcal{K} \\ 0 \end{pmatrix} + \text{sub-leading terms.} \end{aligned} \quad (3.85)$$

Once $\Psi_+^{(1)}$ is completely specified as above, we can determine $\Psi_-^{(1)}$ readily from the second equation in (3.76) as it is algebraic. The behavior near the horizon is given by :

$$\begin{aligned} \Psi_-^{(1)}(\omega, \mathbf{k}, \omega_{(h)}, \mathbf{k}_{(h)}, r) &= \sqrt{\frac{r_0}{\pi T}} \\ &\quad \frac{(2\pi iT - 2\omega + \omega_{(h)})(19\pi^2 T^2 + 11i\pi T\omega - 2\omega^2 + \omega_{(h)}(2i\pi T - \omega))}{8(3\pi T + i\omega)(7\pi T + i\omega)(\omega + \omega_{(h)})} \\ &\quad \delta u_y(k_{(h)}) \gamma^t \left(1 - \frac{rr_0}{l^2}\right)^{-i\frac{\omega}{4\pi T} - \frac{3}{4}} \begin{pmatrix} \mathcal{K} \\ 0 \end{pmatrix} + \text{sub-leading terms.} \end{aligned} \quad (3.86)$$

We can integrate numerically from the horizon and find the full profile of Ψ_{\pm} (both equilibrium and non-equilibrium parts included) all the way up to the boundary.

At the boundary, the behavior of Ψ_{\pm} is specified completely by the AdS_4 asymptotic nature of the background. When $m \geq 0$, the behavior of Ψ_+ at the boundary is :

$$\Psi_+(k, k_{(h)}, r) \approx \left(J^{(0)}(k) + J^{(1)}(k, k_{(h)})\right) r^{3-\Delta} + \left(\mathcal{M}^{(0)}(k) + \mathcal{M}^{(1)}(k, k_{(h)})\right) r^{\Delta+1}, \quad (3.87)$$

with Δ being the scaling dimension of the dual operator and is related to the mass of the fermionic field by :

$$\Delta = \frac{3}{2} + ml. \quad (3.88)$$

Clearly $J^{(0)}$ and $\mathcal{M}^{(0)}$ are determined by $\Psi_+^{(0)}$, and $J^{(1)}$ and $\mathcal{M}^{(1)}$ are determined by $\Psi_+^{(1)}$.

Chapter 3. The Holographic Spectral Function in Non-Equilibrium States

Similarly, the behavior of Ψ_- at the boundary for $m \geq 0$ and $m \neq 1/2l$ is :

$$\Psi_-(k, k_{(h)}, r) \approx \left(\mathcal{N}^{(0)}(k) + \mathcal{N}^{(1)}(k, k_{(h)}) \right) r^{4-\Delta} + \left(O^{(0)}(k) + O^{(1)}(k, k_{(h)}) \right) r^\Delta. \quad (3.89)$$

When $m = 1/2l$, the leading powers of the homogeneous solutions above become the same. The behavior of Ψ_- at the boundary is then given by :

$$\Psi_-(k, k_{(h)}, r) \approx \left(\mathcal{N}^{(0)}(k) + \mathcal{N}^{(1)}(k, k_{(h)}) \right) r^2 \ln r + \left(O^{(0)}(k) + O^{(1)}(k, k_{(h)}) \right) r^2. \quad (3.90)$$

As Ψ_- is determined by Ψ_+ algebraically, we get

$$\begin{aligned} O(k, k_{(h)}) &= -\frac{i\gamma \cdot k}{k^2} (2m+1) \mathcal{M}(k, k_{(h)}), \quad \mathcal{N}(k, k_{(h)}) = \frac{i\gamma \cdot k}{(2m-1)} J(k, k_{(h)}), \\ \gamma \cdot k &= \gamma^\mu k_\mu, \quad k^2 = k^\mu k_\mu, \end{aligned} \quad (3.91)$$

where $O = O^{(0)} + O^{(1)}$, etc. Thus we have just two independent boundary data corresponding to the fermionic source and expectation value of the fermionic operator dual to the field. The holographic dictionary indeed identifies J as the source and O as the expectation value of the operator when $m \geq 0$ [23]. Both these are fixed up to an overall normalization constant by the incoming boundary condition at the horizon and our regularity argument.

Changing the sign of m is equivalent to interchanging Ψ_+ with Ψ_- [23]. Consequently J gets interchanged with O , and \mathcal{M} gets interchanged with \mathcal{N} ¹⁰. When $m < 0$, the scaling dimension of the dual operator is given by :

$$\Delta = \frac{3}{2} - ml. \quad (3.92)$$

Once the solution in the bulk is determined, the source and the expectation value of the fermionic operator get related by a matrix \mathcal{D} :

$$J(\omega, \mathbf{k}, \omega_{(h)}, \mathbf{k}_{(h)}) = \mathcal{D}(\omega, \mathbf{k}, \omega_{(h)}, \mathbf{k}_{(h)}) O(\omega, \mathbf{k}, \omega_{(h)}, \mathbf{k}_{(h)}). \quad (3.93)$$

Clearly \mathcal{D} is independent of the choice of A_+^{in} for the equilibrium solution as we have

¹⁰When $0 \leq |m| < 1/2l$ we can also do an alternate quantization in which O is interpreted as the source and J as the expectation value. This requires the scaling dimension of the dual fermionic operator to be $\Delta = 3/2 - |m|l$. The partition functions of the two theories are related by a Legendre transform.

Chapter 3. The Holographic Spectral Function in Non-Equilibrium States

claimed earlier. The retarded propagator is given by [23]:

$$G_R(\omega, \mathbf{k}, \omega_{(h)}, \mathbf{k}_{(h)}) = i\mathcal{D}(\omega, \mathbf{k}, \omega_{(h)}, \mathbf{k}_{(h)})\gamma^{\frac{t}{2}}. \quad (3.94)$$

Furthermore, as the non-equilibrium part of the solution is completely determined by the equilibrium part of the solution, we can compute the relations :

$$\begin{aligned} O^{(1)}(\omega, \mathbf{k}, \omega_{(h)}, \mathbf{k}_{(h)}) &= \mathcal{R}_A(\omega, \omega_{(h)}, \mathbf{k}, \mathbf{k}_{(h)}) O^{(0)}(\omega, k), \\ J^{(1)}(\omega, \mathbf{k}, \omega_{(h)}, \mathbf{k}_{(h)}) &= \mathcal{R}_B(\omega, \omega_{(h)}, \mathbf{k}, \mathbf{k}_{(h)}) J^{(0)}(\omega, \mathbf{k}). \end{aligned} \quad (3.95)$$

Above \mathcal{R}_A and \mathcal{R}_B are fully determined by our boundary conditions on $\Psi_+^{(1)}$ at the horizon. They take the form :

$$\begin{aligned} \mathcal{R}_A(\omega, \omega_{(h)}, \mathbf{k}, \mathbf{k}_{(h)}) &= \mathcal{R}_{AA}(\omega, \mathbf{k}) \delta \mathbf{u}(\omega_{(h)}, \mathbf{k}_{(h)}) \cdot \mathbf{k} + \mathcal{R}_{AB}(\omega, \mathbf{k}) k_i k_j k_{(h)i} \delta u_j(\omega_{(h)}, \mathbf{k}_{(h)}), \\ \mathcal{R}_B(\omega, \omega_{(h)}, \mathbf{k}, \mathbf{k}_{(h)}) &= \mathcal{R}_{BA}(\omega, \mathbf{k}) \delta \mathbf{u}(\omega_{(h)}, \mathbf{k}_{(h)}) \cdot \mathbf{k} + \mathcal{R}_{BB}(\omega, \mathbf{k}) k_i k_j k_{(h)i} \delta u_j(\omega_{(h)}, \mathbf{k}_{(h)}). \end{aligned} \quad (3.96)$$

By going through the steps as in the case of the scalar field, we can easily see that the generalization of the form of the bosonic non-equilibrium retarded propagator (3.66) to the fermionic case is :

$$\begin{aligned} G_R(\omega, \mathbf{k}, \mathbf{x}, t) &= i \int d\omega_0 \int d^2 k_0 \left[\mathcal{D}^{(0)}(\omega_0, \mathbf{k}_0) \gamma^{\frac{t}{2}} \delta(\omega - \omega_0) \delta^2(\mathbf{k} - \mathbf{k}_0) \right. \\ &\quad - \frac{1}{2\pi} \left(\mathcal{D}^{(0)}(\omega_0, \mathbf{k}_0) \gamma^{\frac{t}{2}} \mathcal{R}_A(\omega_0, \mathbf{k}_0, \mathbf{k}_{(h)}) \delta^2\left(\mathbf{k} - \mathbf{k}_0 - \frac{\mathbf{k}_{(h)}}{2}\right) \frac{1}{\left(\omega - \omega_0 + i \frac{\mathbf{k}_{(h)}^2}{8\pi T}\right)} \right. \\ &\quad \left. \left. - \mathcal{R}_B(\omega_0, \mathbf{k}_0, \mathbf{k}_{(h)}) \mathcal{D}^{(0)}(\omega_0, \mathbf{k}_0) \gamma^{\frac{t}{2}} \delta^2\left(\mathbf{k} - \mathbf{k}_0 + \frac{\mathbf{k}_{(h)}}{2}\right) \frac{1}{\left(\omega - \omega_0 - i \frac{\mathbf{k}_{(h)}^2}{8\pi T}\right)} \right) \right. \\ &\quad \left. e^{i\mathbf{k}_{(h)} \cdot \mathbf{x}} e^{-\frac{\mathbf{k}_{(h)}^2}{4\pi T} t} \right] \end{aligned} \quad (3.97)$$

where

$$\begin{aligned}\mathcal{R}_A(\omega, \mathbf{k}, \mathbf{k}_{(h)}) &= \mathcal{R}_{AA}(\omega, \mathbf{k}) \delta \mathbf{u}(\mathbf{k}_h) \cdot \mathbf{k} + \mathcal{R}_{AB}(\omega, \mathbf{k}) k_i k_j k_{(h)i} \delta u_j(\mathbf{k}_{(h)}), \\ \mathcal{R}_B(\omega, \mathbf{k}, \mathbf{k}_{(h)}) &= \mathcal{R}_{BA}(\omega, \mathbf{k}) \delta \mathbf{u}(\mathbf{k}_h) \cdot \mathbf{k} + \mathcal{R}_{BB}(\omega, \mathbf{k}) k_i k_j k_{(h)i} \delta u_j(\mathbf{k}_{(h)}).\end{aligned}\quad (3.98)$$

The first line in (3.97) denotes the equilibrium correlator and the lines below are the non-equilibrium contributions co-moving with the background velocity perturbation. The difference between (3.98) and (3.96) is that the integration over $\omega_{(h)}$ has kept only the residue of the diffusion pole in the Fourier transform of $\delta \mathbf{u}$ given by (3.44).

Once again the spectral function can be obtained by computing the imaginary part of the retarded propagator above and using $A(\omega, \mathbf{k}, \mathbf{x}, t) = -2\text{Im}\left(\text{Tr}(\gamma^\pm G_R(\omega, \mathbf{k}, \mathbf{x}, t))\right)$.

3.2.3 Generalization to backgrounds with other quasinormal modes

The prescription we have presented so far is for the non-equilibrium retarded propagator in the hydrodynamic shear-wave background. We will now show that this prescription with its underlying logic can be readily generalized to any background which is a quasinormal mode fluctuation of the black brane geometry.

The key observations are as follows :

1. Even if the horizon fluctuates in presence of the non-equilibrium energy-momentum and charge current fluctuations in the dual state, i.e. the metric and gauge field quasinormal modes in the background, in the perturbation expansion, we need to apply the incoming boundary condition and regularity only at the radial location of the horizon at late time, which in our coordinates is always at $r = l^2/r_0$.
2. The quasinormal modes always have a negative imaginary part in their dispersion relation, so the pole in the complex frequency plane of the background perturbation will always be in the lower half plane.

The first point above makes sure that we can always write the non-equilibrium part of the solution as the incoming and outgoing homogeneous solutions plus a particular solution completely specified by the source at the horizon exactly as in the case of the hydrodynamic shear mode. The second point will imply that integration over the background frequency will produce a divergence at the horizon unless we put the coefficients of both the incoming and outgoing parts of the non-equilibrium part of the solution to zero. Therefore, the

Chapter 3. The Holographic Spectral Function in Non-Equilibrium States

non-equilibrium part of the solution is completely determined by the equilibrium part of the solution for any background quasinormal mode. We can thus simply repeat the exercise as we have done for the hydrodynamic shear-mode perturbation to obtain the retarded propagator for any background quasinormal perturbation.

One may wonder if our prescribed solution at the horizon involving the specific particular solution is itself regular at the horizon. We have checked this is always so for the scalar field. In case of the fermionic field, we can repeat the arguments we have made in case of the hydrodynamic shear-mode.

For instance, let us consider a quasinormal mode for metric perturbation in the tensor channel with momentum $\mathbf{k}_{(b)} = 0$. The frequency will be complex with a negative imaginary part as in (3.28). The explicit metric and gauge field for such a spatially homogeneous perturbation is as in (3.41). We can check that our prescribed non-equilibrium solution for the scalar field dies down at the horizon due to the factors :

$$\left(1 - \frac{rr_0}{l^2}\right)^n \left(\ln\left(1 - \frac{rr_0}{l^2}\right)\right)^m$$

multiplying the equilibrium incoming wave solution with n and m being positive integers¹¹.

The general dispersion relation for a quasi-normal mode may be written as :

$$\omega_{(b)}(\mathbf{k}_{(b)}) = \omega_{R(b)}(\mathbf{k}_{(b)}) - i\omega_{I(b)}(\mathbf{k}_{(b)}), \quad \text{with} \quad \omega_{I(b)}(\mathbf{k}_{(b)}) > 0. \quad (3.99)$$

Also both $\omega_{R(b)}$ and $\omega_{I(b)}$ admit Taylor expansion in $\mathbf{k}_{(b)}$ (and do not vanish when $\mathbf{k}_{(b)} = 0$).

¹¹This can be checked by expanding $\tilde{h}(s, \omega_{(n)})$ in (3.41) in $\omega_{(n)}$. Though this expansion as noted before is dangerous for seeing manifest regularity of the metric, it does good job for analyzing the behavior of the scalar field in the perturbed background.

Chapter 3. The Holographic Spectral Function in Non-Equilibrium States

The bosonic retarded propagator will take the following form in such a background :

$$\begin{aligned}
 G_R(\omega, \mathbf{k}, \mathbf{x}, t) = & \int d\omega_0 \int d^d k_0 \left[\frac{O^{(0)}(\omega_0, \mathbf{k}_0)}{J^{(0)}(\omega_0, \mathbf{k}_0)} \delta(\omega - \omega_0) \delta^2(\mathbf{k} - \mathbf{k}_0) \right. \\
 & - \frac{O^{(0)}(\omega_0, \mathbf{k}_0)}{J^{(0)}(\omega_0, \mathbf{k}_0)} \frac{1}{2\pi i} \left(\frac{O^{(1)}(\omega_0, \mathbf{k}_0, \mathbf{k}_{(b)})}{O^{(0)}(\omega_0, \mathbf{k}_0)} \delta^2\left(\mathbf{k} - \mathbf{k}_0 - \frac{\mathbf{k}_{(b)}}{2}\right) \right. \\
 & \left. \frac{1}{\left(\omega - \omega_0 - \frac{1}{2}\left(\omega_{R(b)}(\mathbf{k}_{(b)}) - i\omega_{I(b)}(\mathbf{k}_{(b)})\right)\right)} \right. \\
 & \left. - \frac{J^{(1)}(\omega_0, \mathbf{k}_0, \mathbf{k}_{(b)})}{J^{(0)}(\omega_0, \mathbf{k}_0)} \delta^2\left(\mathbf{k} - \mathbf{k}_0 + \frac{\mathbf{k}_{(b)}}{2}\right) \right. \\
 & \left. \frac{1}{\left(\omega - \omega_0 + \frac{1}{2}\left(\omega_{R(b)}(\mathbf{k}_{(b)}) - i\omega_{I(b)}(\mathbf{k}_{(b)})\right)\right)} \right) \\
 & \left. e^{i\mathbf{k}_{(b)} \cdot \mathbf{x}} e^{-i\left(\omega_{R(b)}(\mathbf{k}_{(b)}) - i\omega_{I(b)}(\mathbf{k}_{(b)})\right)t} \right]. \quad (3.100)
 \end{aligned}$$

The non-equilibrium part of the source and expectation values of the dual operators, $J^{(1)}(\omega, \omega_{(b)}, \mathbf{k}, \mathbf{k}_{(b)})$ and $O^{(1)}(\omega, \omega_{(b)}, \mathbf{k}, \mathbf{k}_{(b)})$ can be determined from the non-equilibrium part of the solution. $J^{(1)}(\omega, \mathbf{k}, \mathbf{k}_{(b)})$ and $O^{(1)}(\omega, \mathbf{k}, \mathbf{k}_{(b)})$ appearing in the retarded propagator above are the residues of $J^{(1)}(\omega, \omega_{(b)}, \mathbf{k}, \mathbf{k}_{(b)})$ and $O^{(1)}(\omega, \omega_{(b)}, \mathbf{k}, \mathbf{k}_{(b)})$ respectively in $\omega_{(b)}$ at $\omega_{R(b)}(\mathbf{k}_{(b)}) - i\omega_{I(b)}(\mathbf{k}_{(b)})$. These will be linear in the hydrodynamic fluctuations $\delta \mathbf{u}_i$, δT , $\delta \rho$ and the non-hydrodynamic fluctuations $\delta \pi_{ij}^{(nh)}$, ν_0 and $\nu_i^{(nh)}$, and will have a systematic expansion in $\mathbf{k}_{(b)}$ ¹².

¹²The Taylor expansion in $\mathbf{k}_{(b)}$ always make sense near equilibrium as the perturbations are slowly varying in space. However, all time derivatives need to be summed up for non-hydrodynamic perturbations at each order in the amplitude and $\mathbf{k}_{(b)}$ as the variation of these modes in time is not small even near equilibrium.

Chapter 3. The Holographic Spectral Function in Non-Equilibrium States

Similarly, the fermionic non-equilibrium retarded propagator will take the general form:

$$\begin{aligned}
 G_R(\omega, \mathbf{k}, \mathbf{x}, t) = & i \int d\omega_0 \int d^d k_0 \left[\mathcal{D}^{(0)}(\omega_0, \mathbf{k}_0) \gamma^t \delta(\omega - \omega_0) \delta^2(\mathbf{k} - \mathbf{k}_0) \right. \\
 & - \frac{1}{2\pi} \left(\mathcal{D}^{(0)}(\omega_0, \mathbf{k}_0) \gamma^t \mathcal{R}_A \left(\omega_0, \mathbf{k}_0, \mathbf{k}_{(b)} \right) \delta^2 \left(\mathbf{k} - \mathbf{k}_0 - \frac{\mathbf{k}_{(b)}}{2} \right) \right. \\
 & \quad \frac{1}{\left(\omega - \omega_0 - \frac{1}{2} \left(\omega_{R(b)}(\mathbf{k}_{(b)}) - i\omega_{I(b)}(\mathbf{k}_{(b)}) \right) \right)} \\
 & \quad - \mathcal{R}_B \left(\omega_0, \mathbf{k}_0, \mathbf{k}_{(b)} \right) \mathcal{D}^{(0)}(\omega_0, \mathbf{k}_0) \gamma^t \delta^2 \left(\mathbf{k} - \mathbf{k}_0 + \frac{\mathbf{k}_{(b)}}{2} \right) \\
 & \quad \left. \frac{1}{\left(\omega - \omega_0 + \frac{1}{2} \left(\omega_{R(b)}(\mathbf{k}_{(b)}) - i\omega_{I(b)}(\mathbf{k}_{(b)}) \right) \right)} \right) \\
 & \left. e^{i\mathbf{k}_{(b)} \cdot \mathbf{x}} e^{-i \left(\omega_{R(b)}(\mathbf{k}_{(b)}) - i\omega_{I(b)}(\mathbf{k}_{(b)}) \right) t} \right]. \tag{3.101}
 \end{aligned}$$

\mathcal{R}_A and \mathcal{R}_B can be determined from the non-equilibrium part of the solution via the defining relations :

$$\begin{aligned}
 O^{(1)}(\omega, \mathbf{k}, \omega_{(b)}, \mathbf{k}_{(b)}) &= \mathcal{R}_A(\omega, \omega_{(b)}, \mathbf{k}, \mathbf{k}_{(b)}) O^{(0)}(\omega, \mathbf{k}), \\
 J^{(1)}(\omega, \mathbf{k}, \omega_{(b)}, \mathbf{k}_{(b)}) &= \mathcal{R}_B(\omega, \omega_{(b)}, \mathbf{k}, \mathbf{k}_{(b)}) J^{(0)}(\omega, \mathbf{k}). \tag{3.102}
 \end{aligned}$$

$\mathcal{R}_A(\omega, \mathbf{k}, \mathbf{k}_{(b)})$ and $\mathcal{R}_B(\omega, \mathbf{k}, \mathbf{k}_{(b)})$ appearing in the retarded propagator above are the residues of $\mathcal{R}_A(\omega, \omega_{(b)}, \mathbf{k}, \mathbf{k}_{(b)})$ and $\mathcal{R}_B(\omega, \omega_{(b)}, \mathbf{k}, \mathbf{k}_{(b)})$ respectively in $\omega_{(b)}$ at $\omega_{R(b)}(\mathbf{k}_{(b)}) - i\omega_{I(b)}(\mathbf{k}_{(b)})$. Both $\mathcal{R}_A(\omega, \mathbf{k}, \mathbf{k}_{(b)})$ and $\mathcal{R}_B(\omega, \mathbf{k}, \mathbf{k}_{(b)})$ will be linear in the hydrodynamic fluctuations $\delta \mathbf{u}_i$, δT , $\delta \rho$ and the non-hydrodynamic fluctuations $\delta \pi_{ij}^{(nh)}$, ν_0 and $\nu_i^{(nh)}$, and will have a systematic expansion in $\mathbf{k}_{(b)}$.

Thus we indeed obtain an universal form of the holographic non-equilibrium retarded propagator (and hence the spectral function) in linearized non-equilibrium backgrounds at sufficiently late time.

3.3 Non-equilibrium Fermi surface and dispersion relations

We will show here that our prescription for obtaining the non-equilibrium retarded correlator gets a lot of support from field theoretic comparisons. We will begin with a brief review of how we obtain non-equilibrium correlation functions in field theory. Then we will show how our prescription reproduces the strongly coupled version of non-equilibrium dynamics at the Fermi surface in Landau's Fermi-liquid theory, and the non-equilibrium modifications of quasi-particle dispersion relations expected in field theory.

3.3.1 Comparison with field-theoretic approach

In field theory, there is no partition function which can play the role of a generating functional of non-equilibrium correlation functions. The way we obtain these is to construct a generalized effective action $\Gamma(O_l(x), G_{ll'}(x, y))$ whose arguments are not only the expectation value of the operator but also the two-point correlation functions of the operators. Extremizing this leads us to obtain non-equilibrium correlation functions as functionals of the expectation values of the operators in equilibrium and non-equilibrium states. The crucial point is that the generalized effective action has no dependence on temperature or other equilibrium/non-equilibrium parameters¹³. It is defined as a double Legendre transform of a vacuum observable constructed over the Schwinger/Keldysh closed real time contour as briefly reviewed in appendix D. Both equilibrium (temperature and chemical potential dependent) and non-equilibrium dynamics of expectation values of operators and their correlation functions can be derived by extremizing this generalized effective action. At equilibrium, we can take an alternative route by constructing a generating functional of thermal correlation functions as in vacuum, but in order to obtain non-equilibrium correlation functions the use of the generalized effective action is indispensable.

We would like to mention here that the generalized effective action not only allows us to obtain the non-equilibrium two-point correlation functions, but it is also sufficient to obtain the three, four and higher point correlation functions [18]. This is possible because through the effective action, we know the two point correlation function as a functional

¹³This is also true for kinetic equations, like the Boltzmann equation. These equations do not depend on temperature or non-equilibrium parameters, the latter parametrize equilibrium and non-equilibrium solutions of these equations.

Chapter 3. The Holographic Spectral Function in Non-Equilibrium States

of expectation values of operators, i.e. we know them not in one but in a manifold of states. Furthermore, the effective action technique readily ensures that we satisfy Ward identities. In practice, we need to make an uncontrolled but educated approximation of the effective action which allows us to obtain non-equilibrium dynamics of expectation values of operators and their correlation functions. This has been successful for instance in the case of dilute cold non-relativistic Bose gases in optical traps [41], and in constructing a quantum kinetic theory of hadrons for modeling their evolution after their chemical and thermal freeze-out in the RHIC fireball [11].

The important point to note is that we can obtain the non-equilibrium correlation function by extremizing the effective action with respect to the correlation function first as below :

$$\frac{\delta \Gamma (O_l, G_{ll'}^0(O_l))}{\delta G_{ll'}^0(x, y)} = 0. \quad (3.103)$$

Thus we obtain the two point correlation functions as functionals of expectation values of the operators. Here the time contour is the Schwinger-Keldysh closed real time contour, so this determines both the statistical function and the retarded propagator (or the spectral function). Further when we substitute the extremal forms of the two-point correlation functions in the generalized effective action, we obtain the ordinary effective action, i.e.

$$\Gamma (O_l, G_{ll'}^0(O_l)) = \Gamma(O_l). \quad (3.104)$$

Extremizing this further we obtain non-equilibrium dynamics of expectation values of operators.

It is certainly interesting to see if we can construct a generalized effective action to obtain non-equilibrium correlation functions in holography too. This will allow us to determine the statistical function also and not the retarded propagator alone as we have done here. However, we note two crucial points of our holographic prescription for obtaining the retarded correlator (equivalently the spectral function).

1. Our prescription obtains the non-equilibrium retarded propagator as a functional of the expectation value of the energy-momentum tensor and the charged current parametrized by $T, \rho, \delta T, \delta \mathbf{u}, \delta \rho, \nu_i^{(nh)}, \nu_0$ and $\pi_{ij}^{(nh)}$.
2. The non-equilibrium part of the correlation function is determined completely by the equilibrium part through universal rules at the horizon which do not depend on the non-equilibrium state concerned. The rule simply involves putting the homogeneous

pieces of the non-equilibrium part of the solution of the bulk bosonic/fermionic field to zero at the horizon.

Putting these together, we can see a parallel with field theory. In both approaches, we do not need a specific rule for each non-equilibrium state, there is a universal rule which allows us to extract the non-equilibrium correlation functions from observables defined at equilibrium. In field theory the equilibrium temperature arises as the boundary condition appearing in the far future. The generalized effective action as mentioned before is just the double Legendre transform of an equilibrium observable, therefore non-equilibrium dynamics can be obtained from equilibrium observables in field theory as well. Furthermore, our holographic prescription has the same measure of universality as the generalized effective action to bring all non-equilibrium spectral functions under one fold at least in perturbation theory.

The advantage of the holographic approach is that the late time behavior of the non-equilibrium spectral function is reproduced automatically without any need for resummation. Thus we can do conventional perturbation theory.

3.3.2 Non-equilibrium dynamics at the Fermi-surface

It might have been a bit surprising that the logic of regularity required that we put the extra boundary condition needed to determine the non-equilibrium part of the solution completely, at the horizon instead of at the boundary. It might seem that it would have been more natural to suppose that the source does not fluctuate from its equilibrium value, so a Dirichlet condition at the boundary would have been more justified. As we have already argued, this is not the case - the source gets screened or dressed by the collective excitations present in the non-equilibrium state also. From the holographic perspective, the horizon determines the screening/dressing of the source.

We will here give another holographic interpretation of the non-equilibrium modification of the source. This will further vindicate that we need to put the extra universal boundary condition at the horizon and not at the boundary. That we have allowed the source to fluctuate from its equilibrium value, is what will bring out the non-equilibrium oscillation of the energy per particle at the Fermi surface and non-equilibrium shifts in the quasi-particle dispersion relations.

A hallmark of Landau Fermi-liquid theory is that the collective modes as captured by the Boltzmann equation leads to non-equilibrium dynamics at the Fermi surface. This

Chapter 3. The Holographic Spectral Function in Non-Equilibrium States

dynamics is characterized by *shifts in energy per quasi-particle at the Fermi surface* $\delta\epsilon$ at a given direction $\hat{\mathbf{n}}$ and at a given point in space and time in response to a local fluctuation in occupation numbers of quasi-particles at the Fermi surface δn . Landau postulated the following phenomenological relation [42]:

$$\delta\epsilon(k_F\hat{\mathbf{n}}, \mathbf{x}, t) = \epsilon(k_F\hat{\mathbf{n}}, \mathbf{x}, t) - \epsilon_0(k_F\hat{\mathbf{n}}) = \sum_{\hat{\mathbf{n}}'} f(\hat{\mathbf{n}}, \hat{\mathbf{n}}') \delta n(k_F\hat{\mathbf{n}}', \mathbf{x}, t), \quad (3.105)$$

where $\epsilon_0(k_F\hat{\mathbf{n}})$ is the equilibrium energy of a quasi-particle at the Fermi surface which is just $k_F^2/2m^*(T, \mu)$ with $m^*(T, \mu)$ being the effective mass at the Fermi surface dependent on temperature and chemical potential. The parameters $f(\hat{\mathbf{n}}, \hat{\mathbf{n}}')$ are phenomenological inputs of the Landau model which can be obtained from field-theoretic two-point density correlation functions. These phenomenological parameters determine all thermodynamic and many non-equilibrium properties of Fermi liquids.

To obtain non-equilibrium properties one has to assume validity of Boltzmann equation for δn . The equilibrium distribution $n^{(0)}$ is the Fermi-Dirac distribution at a fixed temperature and chemical potential and is a trivial solution of the Boltzmann equation. Using (3.105) and the Boltzmann equation, it can be shown that the fluctuations δn follows :

$$\begin{aligned} \frac{\partial \delta n(k_F\hat{\mathbf{n}}, \mathbf{x}, t)}{\partial t} &+ \frac{k_F\hat{\mathbf{n}}}{m^*(T, \mu)} \cdot \frac{\partial \delta n(k_F\hat{\mathbf{n}}, \mathbf{x}, t)}{\partial \mathbf{x}} \\ &+ \frac{\partial n^{(0)}(k_F\hat{\mathbf{n}}, T, \mu)}{\partial \mathbf{k}} \cdot \sum_{\hat{\mathbf{n}}'} f(\hat{\mathbf{n}}, \hat{\mathbf{n}}') \frac{\partial \delta n(k_F\hat{\mathbf{n}}', \mathbf{x}, t)}{\partial \mathbf{x}} \\ &= I\left(n^{(0)}(T, \mu), \delta n(k_F\hat{\mathbf{n}}, \mathbf{x}, t)\right) \end{aligned} \quad (3.106)$$

in the linearized limit. Above I captures the so-called quasi-particle collision kernel. Studying this equation we can extract all collective excitations including the zero sound, hydrodynamic shear-mode and non-hydrodynamic relaxation modes. In order to obtain the zero sound velocity, the collision kernel is not necessary but it is so in order to obtain the viscosity and relaxation modes. Substituting a solution for δn in (3.105) we can obtain the oscillation of the energy per particle at the Fermi surface.

The crucial point is that the oscillation is related locally to the fluctuation in the occupation number of the quasi-particles in (3.105). So, the oscillation in energy per particle at the Fermi surface is in sync with the propagating collective excitation.

We note that in non-equilibrium, we cannot obtain the change in energy at the Fermi-

Chapter 3. The Holographic Spectral Function in Non-Equilibrium States

surface by looking at the spectral function alone. This is because the non-equilibrium change in the spectral function comes from both (i) the shift of the residue, and (ii) the shift in the pole itself. We need to identify which part of the non-equilibrium contribution comes from the shift in the residue and which part comes from the shift in the pole. Moreover, the situation could be worse, as there can be non-equilibrium contributions which are simply analytic near the location of the equilibrium Fermi surface and be neither the shift in the residue nor shift of the pole.

In the holographic set-up, the Fermi surface(s) is related to the existence of normalizable mode(s) of the bulk fermion field at zero frequency on a fixed momentum shell [13]. As the black brane retains rotational symmetry, the Fermi surface is spherical (circular for a $2 + 1$ dimensional system). We will be working in $2 + 1$ dimensional system (i.e. in a $3 + 1$ dimensional bulk) for the sake of concreteness.

It will be worthwhile for us to first define the Fermi surface holographically in a more general background which may not preserve rotational symmetry. This will help us to readily understand non-equilibrium dynamics at the Fermi surface.

A Fermi surface picks up an internal direction in spin space. Therefore, let us represent first an arbitrary normalized complex 2-vector which picks up a direction in spin space by two real angles θ and ϕ as below :

$$\begin{pmatrix} \cos \theta e^{i\phi} \\ \sin \theta e^{-i\phi} \end{pmatrix} \quad (3.107)$$

The vector above may still be multiplied by an overall phase, but this will be unimportant for us. We then note that the hermitian matrix P defined as

$$P(\theta, \phi) = \begin{pmatrix} \cos^2 \theta & \cos \theta \sin \theta e^{i2\phi} \\ \cos \theta \sin \theta e^{-i2\phi} & \sin^2 \theta \end{pmatrix} \quad (3.108)$$

is a matrix such that

$$P^2 = P, \quad P \begin{pmatrix} \cos \theta e^{i\phi} \\ \sin \theta e^{-i\phi} \end{pmatrix} = \begin{pmatrix} \cos \theta e^{i\phi} \\ \sin \theta e^{-i\phi} \end{pmatrix}, \quad P \begin{pmatrix} \sin \theta e^{i\phi} \\ -\cos \theta e^{-i\phi} \end{pmatrix} = 0. \quad (3.109)$$

Therefore P is a projection operator, and it projects in the direction (3.107) and in the orthogonal direction it has eigenvalue zero.

The holographic definition of Fermi surface at equilibrium is as follows. Let us choose

Chapter 3. The Holographic Spectral Function in Non-Equilibrium States

a direction $\hat{\mathbf{n}}$ in momentum space. Then there exists θ, ϕ specifying a vector in *spin space* and k_F for every $\hat{\mathbf{n}}$ such that :

$$\begin{aligned} \left[P(\theta, \phi), G_R(\omega = 0, \mathbf{k} = k_F \hat{\mathbf{n}}) \right] &= 0, \\ P(\theta, \phi) J(\omega = 0, \mathbf{k} = k_F \hat{\mathbf{n}}) &= 0. \end{aligned} \quad (3.110)$$

where P is as defined in (3.108) and J is the source obtained from the bulk solution. The first equation above says that G_R is diagonal in spin space in the following basis :

$$\begin{pmatrix} \cos \theta e^{i\phi} \\ \sin \theta e^{-i\phi} \end{pmatrix}, \quad \begin{pmatrix} \sin \theta e^{i\phi} \\ -\cos \theta e^{-i\phi} \end{pmatrix} \quad (3.111)$$

which is the same basis in which P is diagonal. Thus this defines θ and ϕ . We note if we replace θ by $\theta + \pi/2$, we merely exchange the eigenbasis. Therefore, if θ is a solution, so is $\theta + \pi/2$. The second equation is equivalent to :

$$J(\omega = 0, \mathbf{k} \equiv k_F \hat{\mathbf{n}}) \equiv \begin{pmatrix} \chi_1 \\ \chi_2 \end{pmatrix}, \quad \cos \theta e^{-i\phi} \chi_1 = \sin \theta e^{i\phi} \chi_2. \quad (3.112)$$

Thus we have one linear complex equation to define k_F . Therefore k_F is complex (at finite temperature) and associated with a specific direction in spin space. To get the Fermi surface associated with the orthogonal direction in spin space which is also an eigenvector of P and G_R we need to solve above with θ replaced by $\theta + \pi/2$, i.e.

$$J(\omega = 0, \mathbf{k} \equiv k_F \hat{\mathbf{n}}) \equiv \begin{pmatrix} \chi_1 \\ \chi_2 \end{pmatrix}, \quad \sin \theta e^{-i\phi} \chi_1 = -\cos \theta e^{i\phi} \chi_2. \quad (3.113)$$

As the AdS_4 Reissner-Nordstrom black brane background preserves rotational invariance, θ, ϕ and k_F will be independent of \mathbf{n} .

More generally, the holographic Fermi surface is $k_F(\mathbf{n})$ which solves (3.110) and is associated with a specific direction in spin space in which the retarded propagator can be diagonalized. The general definition stated here should be useful in analyzing cases where we have spontaneous symmetry breaking in the boundary, particularly when these order parameters break rotational invariance [43]. We note that at zero temperature k_F is strictly real and corresponds to the pole at $\omega = 0$, but for non-zero temperatures the pole at $\omega = 0$ is complex. The imaginary part of the pole is negative and represents smearing of the Fermi

Chapter 3. The Holographic Spectral Function in Non-Equilibrium States

surface at finite temperature, and vanishes as the temperature is reduced to zero. Thus we can think of k_F as a complex parameter whose imaginary part vanishes at zero temperature and has a small T expansion. The real part of k_F also has a small T expansion and is the Fermi surface. There is no dependence on ω as to find the Fermi surface ω is set to zero. In the Reissner-Nordstorm black brane, the dependence of the negative imaginary part of this complex parameter k_F on the temperature is given by a power law for small temperatures [44]. This power is controlled by the near horizon $AdS_2 \times R^2$ geometry.

It can also be shown that the retarded propagator and the spectral function also have a pole precisely when the source vanishes. Therefore, the holographic definition of the Fermi surface matches with the conventional definition which is that it is the location of pole of the spectral function in momentum space at vanishing frequency. In holographic systems we typically get a family of nested Fermi surfaces.

As an aside let us mention that the pole structure of the holographic spectral function at equilibrium is different at small frequencies from that of a conventional Fermi liquid and the scaling exponents are controlled by the near-horizon $AdS_2 \times R^2$ geometry [15]. This means that holographic systems have generically non-Fermi liquid behavior.

The full non-equilibrium source is :

$$J(\mathbf{x}, t) = \int d^3x \left(J^{(0)}(\omega, \mathbf{k}) + J^{(1)}(\omega, \mathbf{k}, \mathbf{k}_{(b)}) e^{i\mathbf{k}_{(b)} \cdot \mathbf{x}} e^{-i(\omega_{R(b)}(\mathbf{k}_{(b)}) - i\omega_{I(b)}(\mathbf{k}_{(b)}))t} \right) e^{-i(\omega t - \mathbf{k} \cdot \mathbf{x})}, \quad (3.114)$$

We recall that the full source J can be determined from the boundary behavior of our prescribed solution for Ψ_+ through (3.87). In fact we can explicitly write in case of the hydrodynamic shear-mode up to first order in the hydrodynamic momentum $\mathbf{k}_{(h)}$:

$$\begin{aligned} J^{(1)}(\omega, \mathbf{k}, \mathbf{k}_{(h)}) &= J_A^{(1)}(\omega, \mathbf{k}) \delta \mathbf{u}(\mathbf{k}_{(h)}) \cdot \mathbf{k} \\ &+ J_B^{(1)}(\omega, \mathbf{k}) k_i k_j k_{(h)i} \delta u_j(\mathbf{k}_{(h)}), \end{aligned} \quad (3.115)$$

where $J_A^{(1)}$ and $J_B^{(1)}$ can be determined from the solution.

We will be interested in obtaining the energy oscillation $\delta\omega(\hat{\mathbf{n}}, \mathbf{x}, t)$ at the Fermi surface by calculating shift of the frequency pole for a fixed Fermi momentum. We have to solve this perturbatively in the momentum of the collective background mode $\mathbf{k}_{(b)}$.

Perturbatively, the energy shift on the Fermi surface $\delta\omega$ in the direction $\hat{\mathbf{n}}$ at a given

Chapter 3. The Holographic Spectral Function in Non-Equilibrium States

point in space-time is thus obtained by solving :

$$\begin{aligned}
 \delta\omega(\hat{\mathbf{n}}, \mathbf{x}, t) & \left(P(\theta^{(0)}, \phi^{(0)}) \partial_\omega J^{(0)}(\omega = 0, \mathbf{k} = k_F \hat{\mathbf{n}}) \right) + \delta\theta(k_F \hat{\mathbf{n}}, \mathbf{x}, t) \left(\partial_\theta P(\theta^{(0)}, \phi^{(0)}) \right. \\
 & \left. J^{(0)}(\omega = 0, \mathbf{k} = k_F \hat{\mathbf{n}}) \right) \\
 + \delta\phi(\hat{\mathbf{n}}, \mathbf{x}, t) & \left(\partial_\phi P(\theta^{(0)}, \phi^{(0)}) J^{(0)}(\omega = 0, \mathbf{k} = k_F \hat{\mathbf{n}}) \right) = - \left(P(\theta^{(0)}, \phi^{(0)}) \right. \\
 & \left. J^{(1)}(\omega = 0, \mathbf{k} = k_F \hat{\mathbf{n}}, \mathbf{k}_{(b)}) \right) \\
 & e^{i\mathbf{k}_{(b)} \cdot \mathbf{x}} e^{-i \left(\omega_{R(b)}(\mathbf{k}_{(b)}) - i\omega_{I(b)}(\mathbf{k}_{(b)}) \right) t},
 \end{aligned} \tag{3.116}$$

where $\theta^{(0)}$ and $\phi^{(0)}$ label the spin orientation of the equilibrium Fermi surface as discussed before and P is as defined in (3.108). The above amounts to two complex equations and we have four unknowns, namely real $\delta\theta$ and $\delta\phi$ giving change in the orientation in spin space and complex $\delta\omega$. As we have mentioned earlier, the change in orientation in spin space cannot be directly read off from the change in retarded correlator due to the ambiguity in identifying which change is due to shift in the pole and which change is due to shift in the residue. We can obtain the non-equilibrium shift in spin space at the Fermi surface from the non-equilibrium source directly.

The shift in the energy of the equilibrium Fermi surface with orthogonal spin orientation can be obtained by solving the above equation with $\theta^{(0)}$ replaced by $\theta^{(0)} + \pi/2$.

Clearly in the hydrodynamic shear wave background, $\delta\omega$ takes the form :

$$\delta\omega(\hat{\mathbf{n}}, \mathbf{x}, t) = \left(\delta\omega_A(\hat{\mathbf{n}}, k_F) \delta\mathbf{u}(\mathbf{k}_{(h)}) \cdot \hat{\mathbf{n}} + \delta\omega_B(\hat{\mathbf{n}}, k_F) \hat{n}_i \hat{n}_j k_{(h)i} \delta u_j(\mathbf{k}_{(h)}) \right) e^{i\mathbf{k}_{(h)} \cdot \mathbf{x}} e^{-i \frac{\mathbf{k}_{(h)}^2}{4\pi T} t}. \tag{3.117}$$

Therefore, we find that the holographic Fermi surface indeed oscillates in space and time in sync with the background collective excitation. Nevertheless in order to obtain the analogue of (3.105) in holography linking the spectral shift at the Fermi surface to the statistical shift (i.e. shift in occupation number) we need to obtain the statistical function holographically also. We leave this for the future.

3.3.3 Non-equilibrium shifts in energy and spin of quasi-particles

Not only the energy per particle at the Fermi surface but other normalizable modes with non-zero frequencies also receive space-time dependent shifts in energy at a given momentum in sync with the background collective excitation. This can be interpreted as the space-time dependent shifts of the dispersion relations of the quasi-particles in the non-equilibrium medium. This is certainly expected as quasi-particles receive a thermal mass and if the temperature oscillates for instance, the dispersion relations indeed become space-time dependent. This is usually a hard calculation in non-equilibrium quantum field theory, but we can readily generalize the holographic strategy discussed above to obtain non-equilibrium shifts in quasi-particle dispersion relations.

A particular quasi-particle branch can be identified via the following steps at equilibrium.

1. Consider the equilibrium Green's function $G_R^{(0)}(\omega, \mathbf{k})$. This can be diagonalized at a given ω and \mathbf{k} and the eigenvectors can be labelled as in (3.111) by $\theta^{(0)}(\omega, \mathbf{k})$ and $\phi^{(0)}(\omega, \mathbf{k})$. Furthermore, if $\theta^{(0)}$ is a solution, so is the $\theta^{(0)} + \pi/2$ as this merely exchanges the eigenbasis.
2. The quasiparticle pole $\omega^{(0)}(\mathbf{k})$ can be identified with a definite orientation in spin space by solving :

$$P(\theta^{(0)}, \phi^{(0)}) J^{(0)}(\omega^{(0)}(\mathbf{k}), \mathbf{k}) = 0. \quad (3.118)$$

The above amounts to one complex equation which determines $\omega^{(0)}(\mathbf{k})$ with $\theta^{(0)}$ and $\phi^{(0)}$ determined in the previous step. The imaginary part of $\omega^{(0)}(\mathbf{k})$ is negative. To obtain the quasi-particle branch with opposite spin orientation, we need to solve the above with $\theta^{(0)}$ replaced by $\theta^{(0)} + \pi/2$.

Once again, if there is rotational symmetry in the background, i.e. if there are no order parameters of spontaneous symmetry breaking which breaks rotational invariance, $\theta^{(0)}$, $\phi^{(0)}$ and $\omega^{(0)}(\mathbf{k})$ can depend only on the modulus of \mathbf{k} .

The space-time dependent shift in dispersion relation is characterized by :

$$\omega = \omega^{(0)}(\mathbf{k}) + \delta\omega(\mathbf{k}, \mathbf{k}_{(b)}, \mathbf{x}, t). \quad (3.119)$$

Chapter 3. The Holographic Spectral Function in Non-Equilibrium States

The shift $\delta\omega$ can be obtained by solving :

$$\begin{aligned}
 \delta\omega(\mathbf{k}, \mathbf{x}, t) \left(P(\theta^{(0)}, \phi^{(0)}) \partial_\omega J^{(0)}(\omega = \omega^{(0)}(\mathbf{k}), \mathbf{k}) \right) &+ \delta\theta(\mathbf{k}, \mathbf{x}, t) \left(\partial_\theta P(\theta^{(0)}, \phi^{(0)}) \right. \\
 &\quad \left. J^{(0)}(\omega = \omega^{(0)}(\mathbf{k}), \mathbf{k}) \right) \\
 + \delta\phi(\mathbf{k}, \mathbf{x}, t) \left(\partial_\phi P(\theta^{(0)}, \phi^{(0)}) J^{(0)}(\omega = \omega^{(0)}(\mathbf{k}), \mathbf{k}) \right) &= - \left(P(\theta^{(0)}, \phi^{(0)}) \right. \\
 &\quad \left. J^{(1)}(\omega = \omega^{(0)}(\mathbf{k}), \mathbf{k}, \mathbf{k}_{(b)}) \right) \\
 &\quad e^{i\mathbf{k}_{(b)} \cdot \mathbf{x}} e^{-i \left(\omega_{R(b)}(\mathbf{k}_{(b)}) - i\omega_{I(b)}(\mathbf{k}_{(b)}) \right) t}.
 \end{aligned} \tag{3.120}$$

The above equation amounts to two complex equations which allows us to solve the real unknowns $\delta\theta$ and $\delta\phi$ giving shifts in spin space and the complex unknown $\delta\omega$. To obtain the non-equilibrium shift in the dispersion relation for the other equilibrium branch with orthogonal spin orientation, we need to solve the above with $\theta^{(0)}$ replaced by $\theta^{(0)} + \pi/2$.

The solution of $\delta\omega$ will take the form in a hydrodynamic shear-wave background, for instance, clearly takes the form :

$$\delta\omega(\mathbf{k}, \mathbf{x}, t) = \left(\delta\omega_A(\mathbf{k}) \delta\mathbf{u}(\mathbf{k}_{(h)}) \cdot \mathbf{k} + \delta\omega_B(\mathbf{k}) k_i k_j k_{(h)i} \delta u_j(\mathbf{k}_{(h)}) \right) e^{i\mathbf{k}_{(h)} \cdot \mathbf{x}} e^{-i \frac{\mathbf{k}_{(h)}^2}{4\pi T} t}. \tag{3.121}$$

Therefore, we see that the shift in the dispersion relation of the quasi-particle pole is also in sync with the propagating collective mode. Furthermore, though we have discussed the fermionic case explicitly here, clearly the same strategy can be applied to the bosonic field also. In fact, the source being a complex number instead of a complex 2-vector in the bosonic case, the equations will be much simpler.

The shift $\delta\omega$ in the quasi-particle pole is generically complex. Interestingly the sign of the imaginary part of $\delta\omega$ can be both positive and negative. Thus we can get both non-equilibrium suppression or enhancement of quasi-particle decays as indeed observed in the RHIC fireball for various resonances (short-lived quasi-particles) [10].

3.4 Taking into account non-linearities in the dynamics of the non-equilibrium variables

It is known that solutions of gravity which have regular future horizons reproduce non-linear phenomenological equations for irreversible processes in the dual field theory. The best studied examples are related to fluid/gravity correspondence. The full non-linear Navier-Stokes' equation with higher derivative corrections can be reproduced from gravity and this success has also been extended to the case of charged hydrodynamics [5]. As we have discussed before, gravity is expected to reproduce the general phenomenological equations which describe the full evolution of energy-momentum tensor and conserved currents which generalize hydrodynamics [6]. This has been shown explicitly for the case of spatially homogeneous relaxation [7]. In all cases, the regularity of the future horizon determines the phenomenological coefficients.

We would like to show that the prescriptions described so far can be readily generalized to include non-linearities in the dynamics of the energy-momentum tensor and conserved currents characterizing the non-equilibrium states. We can systematically include these non-linearities into the retarded correlator, the shifts in the dispersion relations of quasi-particles, etc.

The key is to see how the solutions for the bosonic and fermionic fields get determined in the perturbed background. Let us focus on the case of the hydrodynamic background. If we take into account non-linearities in $\delta \mathbf{u}(\mathbf{k}_{(h)})$ in the background, clearly these non-linearities will also appear in the Laplacian of the bosonic field. Let us consider quadratic dependence on two distinct velocity perturbations $\delta \mathbf{u}(k_{(h)})$ and $\delta \mathbf{u}(k'_{(h)})$ for instance, at a given order in the derivative expansion m (i.e. at the m th order in the hydrodynamic momentum). The solution for Φ will receive a correction quadratic in the amplitude of velocity perturbation and at m th order in the derivative expansion which can be represented as:

$$\Phi^{(2,m)}\left(r, k, k_{(h)}, k'_{(h)}\right) e^{i(k+k_{(h)}+k'_{(h)})\cdot x}. \quad (3.122)$$

The radial dependence above can be determined from the equation of motion :

$$\square_k^{ARN} \delta^3(k - k') \Phi^{(2,m)}(r, k', k_{(h)}, k'_{(h)}) = S^{(2,m)}(r, k, k_{(h)}, k'_{(h)}), \quad (3.123)$$

where \square_k^{ARN} is the Laplacian for a scalar with 3-momentum k in the unperturbed AdS_4

Chapter 3. The Holographic Spectral Function in Non-Equilibrium States

Reissner-Nordstrom background and $S^{(2,m)}$ is a generic source term. For $m = 1$ the source $S^{(2,1)}$ can contain terms like $(\mathbf{k} \cdot \delta \mathbf{u}(k_{(h)}))(\mathbf{k}_{(h)} \cdot \delta \mathbf{u}(k'_{(h)}))$, etc. It also contains the solutions at the lower order in the perturbation expansion for instance $\Phi^{(1,1)}\Phi^{(1,0)}$.

Clearly the general solution of Φ near the horizon can again be separated into two homogeneous pieces, the incoming and the outgoing modes, and a particular piece which has no arbitrary integration constant and is completely determined by the source term $S^{(2,m)}$. In order to satisfy the incoming boundary condition, we should put the coefficient of the outgoing mode to zero. Also as discussed before, the integration over the hydrodynamic frequencies $\omega_{(h)}$ and $\omega'_{(h)}$ will produce a divergence at the horizon for the incoming mode, as for instance in the case above with dependence on two hydrodynamic shear wave background modes like :

$$\left(1 - \frac{rr_0}{l^2}\right)^{-i\frac{\omega}{4\pi T} - \frac{\mathbf{k}_{(h)}^2}{16\pi^2 T^2} - \frac{\mathbf{k}'_{(h)}^2}{16\pi^2 T^2} - \dots} \quad (3.124)$$

Obviously the coefficient of the incoming mode has to depend on $\delta \mathbf{u}$ and the hydrodynamic momenta required by the order in the perturbation expansion. The contribution from the frequency pole in $\delta \mathbf{u}(\omega_{(h)}, \mathbf{k}_{(h)})$ given by the hydrodynamic shear dispersion relation produces the above divergent behavior. In general the divergence will always be there for any quasinormal wave background as it's dispersion relation $\omega_{(h)}(\mathbf{k}_{(h)})$ will have a negative imaginary part. Therefore, we should put the coefficients of the incoming mode at the horizon to zero too. We are just left with the particular piece which is completely determined by the source term containing the solutions at the lower orders in the perturbation expansion. Therefore, applying induction, *at each order in the perturbation expansion, the non-equilibrium solution is uniquely determined by the equilibrium solution, i.e. the solution at the zeroth order in the unperturbed black brane background.* The consistency of holographic duality requires the solution at each order in the perturbation to be regular at the horizon.

As the solution is uniquely fixed at each order in the perturbation expansion, we can obtain the non-equilibrium contributions to the source and the expectation value of the dual operator by studying the asymptotic behavior of the solution at each order. This procedure can also be applied for fermionic fields.

Once the source is obtained at a given order in the perturbation expansion, it is straightforward to obtain the shift in the dispersion relation of quasi-particles. For example, $\delta \omega^{(2,m)}(\mathbf{k}, \mathbf{x}, t)$ along with the non-equilibrium shift in the spin orientation given by $\delta \theta^{(2,m)}(\mathbf{k}, \mathbf{x}, t)$

and $\delta\phi^{(2,m)}(\mathbf{k}, \mathbf{x}, t)$ can be obtained from $J^{(2,m)}$ by solving :

$$\begin{aligned}
 \delta\omega^{(2,m)} \left(P(\theta^{(0)}, \phi^{(0)}) \partial_\omega J^{(0)} \left(\omega = \omega^{(0)}(\mathbf{k}), \mathbf{k} \right) \right) &+ \delta\theta^{(2,m)}(\mathbf{k}, \mathbf{x}, t) \left(\partial_\theta P(\theta^{(0)}, \phi^{(0)}) \right. \\
 &\quad \left. J^{(0)} \left(\omega = \omega^{(0)}(\mathbf{k}), \mathbf{k} \right) \right) \\
 + \delta\phi^{(2,m)} \left(\partial_\phi P(\theta^{(0)}, \phi^{(0)}) J^{(0)} \left(\omega = \omega^{(0)}(\mathbf{k}), \mathbf{k} \right) \right) &= - \left(P(\theta^{(0)}, \phi^{(0)}) \right. \\
 &\quad \left. J^{(2,m)} \left(\omega = \omega^{(0)}(\mathbf{k}), \mathbf{k}, \mathbf{k}_{(b)} \right) \right) \\
 &\quad e^{i(\mathbf{k}_{(b)} + \mathbf{k}'_{(b)}) \cdot \mathbf{x}} \\
 &\quad e^{-i(\omega_{R(b)}(\mathbf{k}_{(b)}) + \omega_{R(b)}(\mathbf{k}'_{(b)}))t} \\
 &\quad e^{-(\omega_{I(b)}(\mathbf{k}_{(b)}) + \omega_{I(b)}(\mathbf{k}'_{(b)}))t}.
 \end{aligned} \tag{3.125}$$

A consistent perturbation theory for the solution in the non-equilibrium background thus suffices to take into account non-linearities in $\delta\mathbf{u}_i$, δT , $\delta\pi_{ij}^{(nh)}$ etc. in the retarded correlation function, spectral function, non-equilibrium shift in the dispersion relations, etc.

3.5 Summary and future directions

In this chapter we have discussed how to develop a general holographic formalism for determining non-equilibrium retarded correlator, spectral function, shifts in dispersion relations, etc. Needless to say, we would like to use this formalism to numerically calculate these space-time dependent quantities in the specific set up of charged bosonic and fermionic fields minimally coupled to Einstein-Maxwell gravity in AdS_4 discussed here. In particular, the following questions require attention.

1. It is known that at equilibrium the temperature modifies the spectral function only in the infrared, while in the ultraviolet the spectral function remains as in the vacuum. It can be expected that we have a similar feature even in non-equilibrium - the ultraviolet behavior of the spectral function, quasi-particle dispersion relations should be independent of the state. It will be interesting to see if this is reproduced in our case.

Chapter 3. The Holographic Spectral Function in Non-Equilibrium States

Some of the background quasi-normal modes indeed can have very high frequencies, while high frequency dependent corrections can also be generated by non-linearities. Therefore, numerical studies can help us understand how the effect of high frequency dependent background modes gets suppressed in the ultraviolet, if this is indeed the case.

2. The non-equilibrium shifts in the dispersion relations can have both positive and negative imaginary parts. If positive it leads to suppression and if negative it leads to enhancement of the decay. It will be interesting to see if one can use non-linearities to design a background in which a specific quasi-particle can be stabilized against decay to a large extent in a certain range of energies. This can allow us to observe otherwise short-lived quasi-particles. In particular, it will be interesting to see if some bound states of heavy quarks can indeed exist in the quark-gluon plasma at temperature 175 MeV.
3. The quasi-particle dispersion relations can change non-analytically with the temperature particularly if there is level crossing. It will be interesting to design a non-equilibrium background where the temperature varies in space and time over the range in which this non-analyticity can occur and study exactly how the quasi-particles behave in such backgrounds. It will be interesting to learn from such holographic examples how to describe such non-equilibrium states in field theory.

Work is in progress to tackle such issues numerically [45]. Our prescription here gives an algorithm to tackle such questions in specific holographic models.

Another direction we want to pursue in the future is to study non-equilibrium spectral functions in states corresponding to a plasma undergoing boost-invariant hydrodynamic expansion as in the RHIC fireball. This will give us insights into how hadrons are produced and transported in the medium, and finally get frozen chemically and thermally.

Appendices

A. Eddington-Finkelstein vs Schwarzschild coordinates

In order to see regularity at the horizon manifestly in the metric (3.37) corresponding to hydrodynamic shear-mode perturbation of the AdS_4 Reissner-Nordstrom black brane, we

Chapter 3. The Holographic Spectral Function in Non-Equilibrium States

can consider the following change of coordinates following [29] :

$$\begin{aligned} t &= v + \frac{l^2}{r_0} k\left(\frac{rr_0}{l^2}\right) + O(\epsilon^2), \\ x^i &= \tilde{x}^i + \frac{l^2}{r_0} k\left(\frac{rr_0}{l^2}\right) \delta u^i(k_{(h)}) e^{i(\mathbf{k}_{(h)} \cdot \tilde{\mathbf{x}} - \omega_{(h)} v)} \\ &\quad - i\omega_{(h)} \frac{l^4}{r_0^2} k_1\left(\frac{rr_0}{l^2}\right) \delta u^i(k_{(h)}) e^{i(\mathbf{k}_{(h)} \cdot \tilde{\mathbf{x}} - \omega_{(h)} v)} + O(\epsilon^2), \end{aligned} \quad (126)$$

where

$$k(a) = \int_0^a db \frac{1}{f(b)}, \quad (127)$$

and

$$k_1(a) = \int_0^a db \left(\frac{1 - f(b)}{f(b)} \right) k(b). \quad (128)$$

These new coordinates r, v and \tilde{x}^i are ingoing Eddington-Finkelstein coordinates.

In these coordinates, the metric assumes the form :

$$\begin{aligned} ds^2 &= -\frac{2l^2}{r^2} \left(dv - \delta u_i(k_{(h)}) e^{i(\mathbf{k}_{(h)} \cdot \tilde{\mathbf{x}} - \omega_{(h)} v)} d\tilde{x}^i \right) dr + \frac{l^2}{r^2} \left(-f\left(\frac{rr_0}{l^2}\right) dv^2 + d\tilde{x}^2 + d\tilde{y}^2 \right) \\ &\quad - 2\delta u_i(k_{(h)}) e^{i(\mathbf{k}_{(h)} \cdot \tilde{\mathbf{x}} - \omega_{(h)} v)} \left(1 - f\left(\frac{rr_0}{l^2}\right) + i\frac{\omega_{(h)} l^2}{r_0} f\left(\frac{rr_0}{l^2}\right) k\left(\frac{rr_0}{l^2}\right) \right) dv d\tilde{x}^i \\ &\quad - i2\frac{l^2}{r_0} k_{(h)i} \delta u_j(k_{(h)}) e^{i(\mathbf{k}_{(h)} \cdot \tilde{\mathbf{x}} - \omega_{(h)} v)} \left(\frac{1}{3} h\left(\frac{rr_0}{l^2}\right) - k\left(\frac{rr_0}{l^2}\right) \right) d\tilde{x}^i d\tilde{x}^j \\ &\quad + O(\epsilon^2). \end{aligned} \quad (129)$$

The bulk gauge field however no longer remains in the radial gauge and takes the form

:

$$\begin{aligned} A_r &= -i \frac{1}{f\left(\frac{rr_0}{l^2}\right)} \frac{\sqrt{3}g_F r_0}{l^2} \left(1 - \frac{rr_0}{l^2} \right) + O(\epsilon^2), \\ A_v &= \frac{\sqrt{3}g_F r_0}{l^2} \left(1 - \frac{rr_0}{l^2} \right) + O(\epsilon^2), \\ A_i &= -\frac{\sqrt{3}g_F r_0}{l^2} \left(1 - \frac{rr_0}{l^2} \right) \delta u_i(k_{(h)}) e^{i(\mathbf{k}_{(h)} \cdot \tilde{\mathbf{x}} - \omega_{(h)} v)} \left(1 - i\frac{\omega_{(h)} l^2}{r_0} k\left(\frac{rr_0}{l^2}\right) \right) + O(\epsilon^2). \end{aligned} \quad (130)$$

It can be checked that the gauge field is also regular at the horizon. A_v, A_i vanish while A_r is a constant at the horizon. We can bring the gauge field back to radial gauge by a regular gauge transformation.

Most importantly, the ij components of the metric is regular as

$$\frac{1}{3}h(a) - k(a) = \text{terms which are regular at the horizon (i.e. at } a = 1\text{)}. \quad (131)$$

So, the metric is manifestly regular up to the first order in the derivative expansion in these coordinates.

We can implement this change of coordinates order by order in the derivative expansion. Even beyond the fluid/gravity correspondence, such coordinate transformations can be implemented perturbatively to see manifest regularity [7].

B. The general solution for the non-equilibrium profile of the scalar field

At the zeroth order, the equilibrium solution for a given mode can be written as an arbitrary linear superposition of two linearly independent homogeneous solutions $\Phi^A(k, r)$ and $\Phi^B(k, r)$. Here k denotes (ω, \mathbf{k}) collectively. Thus

$$\Phi^{(0)}(k, r) = A^{(0)}(k)\Phi^A(k, r) + B^{(0)}(k)\Phi^B(k, r), \quad (132)$$

where $A^{(0)}(k)$ and $B^{(0)}(k)$ are arbitrary.

Using the method of variation of parameters, we can write the general solution for the equation of motion (3.48) for the non-equilibrium part can be found and is as below :

$$\begin{aligned} \Phi(k, k_{(h)}, r) = & -\Phi^A(k + k_{(h)}, r) \int_{l_1}^r dr' \frac{\Phi^B(k + k_{(h)}, r') (V_1 + V_2)(k, k_{(h)}, r') \Phi^{(0)}(k, r)}{W[\Phi^A(k + k_{(h)}, r'), \Phi^B(k + k_{(h)}, r')] r'^2 f\left(\frac{r' r_0}{l^2}\right)} \\ & + \Phi^B(k + k_{(h)}, r) \int_{l_2}^r dr' \frac{\Phi^A(k + k_{(h)}, r') (V_1 + V_2)(k, k_{(h)}, r') \Phi^{(0)}(k, r)}{W[\Phi^A(k + k_{(h)}, r'), \Phi^B(k + k_{(h)}, r')] r'^2 f\left(\frac{r' r_0}{l^2}\right)}. \end{aligned} \quad (133)$$

Above $k_{(h)}$ denotes $(\omega_{(h)}, \mathbf{k}_{(h)})$ collectively, W denotes the Wronskian of the two homoge-

neous solutions, and l_1 and l_2 are arbitrary setting the range of the two integrals.

One can readily verify that the above is independent of the choice of Φ^A and Φ^B for fixed l_1 and l_2 . To see the general behavior at the horizon given by (3.53) one can set Φ^A to be Φ^{in} and Φ^B to be Φ^{out} .

Furthermore, one notes that the above is consistent with the derivative expansion for any l_1 and l_2 as the dependence on δu_i and $k_{(h)}$ comes from V_1 and V_2 directly. Comparing (3.63) with (3.49) one gets that the explicit contribution to $O_A^{(1)}$ and $J_A^{(1)}$ comes from V_1 , and the contribution to $O_B^{(1)}$ and $J_B^{(1)}$ comes from V_2 .

C. Vielbeins and spin connections in the hydrodynamically perturbed black-brane metric

We calculate here vielbeins, their inverses (or einbeins) and spin connections for the metric (3.37) which corresponds to a black brane perturbed by a hydrodynamic shear mode. The notation we use here is the same as defined in subsection 3.2.2. As noted there, to ease computations we will choose, without loss of generality that $\delta \mathbf{u}$ is in the y direction. As $\delta \mathbf{u}$ is transverse in the shear-mode, $\mathbf{k}_{(h)}$ will be then in the x direction. On the other hand \mathbf{k} can have arbitrary x and y components in order to retain full generality.

The non-zero vielbeins upto first order of derivative expansion are :

$$\begin{aligned}
 e_t^t &= \frac{l}{r} \sqrt{f\left(\frac{rr_0}{l^2}\right)}, & e_y^t &= \frac{l}{2r} \frac{1 - f\left(\frac{rr_0}{l^2}\right)}{\sqrt{f\left(\frac{rr_0}{l^2}\right)}} \delta u_y(k_{(h)}) e^{i(k_{(h)}x - \omega_{(h)}t)}, \\
 e_x^x &= \frac{l}{r}, & e_y^x &= -i \frac{l}{r} \left(\frac{l^2}{6r_0^2}\right) k_{(h)x} \delta u_y(k_{(h)}) e^{i(k_{(h)}x - \omega_{(h)}t)} h\left(\frac{rr_0}{l^2}\right), \\
 e_t^y &= -\frac{l}{2r} \left(1 - f\left(\frac{rr_0}{l^2}\right)\right) \delta u_y(k_{(h)}) e^{i(k_{(h)}x - \omega_{(h)}t)}, \\
 e_x^y &= -i \frac{l}{r} \left(\frac{l^2}{6r_0^2}\right) k_{(h)x} \delta u_y(k_{(h)}) e^{i(k_{(h)}x - \omega_{(h)}t)} h\left(\frac{rr_0}{l^2}\right), \\
 e_y^y &= \frac{l}{r}, & e_r^x &= \frac{l}{r} \frac{1}{\sqrt{f\left(\frac{rr_0}{l^2}\right)}}.
 \end{aligned} \tag{134}$$

From this, one can also construct inverse vielbeins (or einbeins) which are as follows :

Chapter 3. The Holographic Spectral Function in Non-Equilibrium States

$$\begin{aligned}
e_{\underline{t}}^t &= \frac{r}{l \sqrt{f\left(\frac{rr_0}{l^2}\right)}}, & e_{\underline{y}}^t &= -\frac{r}{2l} \frac{1 - f\left(\frac{rr_0}{l^2}\right)}{f\left(\frac{rr_0}{l^2}\right)} \delta u_y(k_{(h)}) e^{i(k_{(h)x}x - \omega_{(h)}t)}, \\
e_{\underline{x}}^x &= \frac{r}{l}, & e_{\underline{y}}^x &= i \frac{r}{l} \left(\frac{l^2}{6r_0^2}\right) k_{(h)x} \delta u_y(k_{(h)}) e^{i(k_{(h)x}x - \omega_{(h)}t)} h\left(\frac{rr_0}{l^2}\right), \\
e_{\underline{t}}^y &= \frac{r}{2l} \frac{1 - f\left(\frac{rr_0}{l^2}\right)}{\sqrt{f\left(\frac{rr_0}{l^2}\right)}} \delta u_y(k_{(h)}) e^{i(k_{(h)x}x - \omega_{(h)}t)}, \\
e_{\underline{x}}^y &= i \frac{r}{l} \left(\frac{l^2}{6r_0^2}\right) k_{(h)x} \delta u_y(k_{(h)}) e^{i(k_{(h)x}x - \omega_{(h)}t)} h\left(\frac{rr_0}{l^2}\right), \\
e_{\underline{y}}^y &= \frac{r}{l} & e_{\underline{r}}^r &= \frac{r \sqrt{f\left(\frac{rr_0}{l^2}\right)}}{l}.
\end{aligned} \tag{135}$$

In order to derive the equation of motion of the Fermions in the given background, we require the spin connections associated with the first order metric.

Chapter 3. The Holographic Spectral Function in Non-Equilibrium States

The non-zero components of the spin connection, ω_M^{AB} are as below :

$$\begin{aligned}
\omega_{\underline{y}}^{\underline{tx}} &= -\omega_{\underline{y}}^{\underline{xt}} = -\frac{i \delta u_y(k_{(h)}) e^{i(k_{(h)x}x - \omega_{(h)}t)} k_{(h)x} \left[3r_0^3 \left(-1 + f\left(\frac{rr_0}{l^2}\right) \right) - 4i l^4 \eta \kappa^2 h\left(\frac{rr_0}{l^2}\right) \omega_{(h)} \right]}{6r_0^3 \sqrt{f\left(\frac{rr_0}{l^2}\right)}}, \\
\omega_{\underline{t}}^{\underline{ty}} &= -\omega_{\underline{t}}^{\underline{yt}} = -\frac{i \delta u_y(k_{(h)}) e^{i(k_{(h)x}x - \omega_{(h)}t)} \left(-1 + f\left(\frac{rr_0}{l^2}\right) \right) \omega_{(h)}}{2 \sqrt{f\left(\frac{rr_0}{l^2}\right)}}, \\
\omega_{\underline{x}}^{\underline{tx}} &= -\omega_{\underline{x}}^{\underline{xt}} = -\frac{l^2 \delta u_y(k_{(h)}) e^{i(k_{(h)x}x - \omega_{(h)}t)} h\left(\frac{rr_0}{l^2}\right) k_{(h)x} \omega_{(h)}}{3 r_0^2 \sqrt{f\left(\frac{rr_0}{l^2}\right)}}, \\
\omega_{\underline{r}}^{\underline{ty}} &= -\omega_{\underline{r}}^{\underline{yt}} = -\frac{\delta u_y(k_{(h)}) e^{i(k_{(h)x}x - \omega_{(h)}t)} r_0 \left(-1 + f\left(\frac{rr_0}{l^2}\right) \right) f'\left(\frac{rr_0}{l^2}\right)}{4 l^2 f^{\frac{3}{2}}\left(\frac{rr_0}{l^2}\right)}, \\
\omega_{\underline{t}}^{\underline{tr}} &= -\omega_{\underline{t}}^{\underline{rt}} = \frac{-f\left(\frac{rr_0}{l^2}\right)}{r} + \frac{r_0 f'\left(\frac{rr_0}{l^2}\right)}{2 l^2}, \\
\omega_{\underline{y}}^{\underline{tr}} &= -\omega_{\underline{y}}^{\underline{rt}} = \frac{\delta u_y(k_{(h)}) e^{i(k_{(h)x}x - \omega_{(h)}t)} \left[l^2 \left(-1 + f\left(\frac{rr_0}{l^2}\right) \right) - r r_0 f'\left(\frac{rr_0}{l^2}\right) \right]}{2 l^2 r}, \\
\omega_{\underline{t}}^{\underline{xy}} &= -\omega_{\underline{t}}^{\underline{yx}} = -\frac{1}{2} i \delta u_y(k_{(h)}) e^{i(k_{(h)x}x - \omega_{(h)}t)} \left(-1 + f\left(\frac{rr_0}{l^2}\right) \right) k_{(h)x}, \\
\omega_{\underline{x}}^{\underline{xr}} &= -\omega_{\underline{x}}^{\underline{rx}} = -\frac{\sqrt{f\left(\frac{rr_0}{l^2}\right)}}{r}, \\
\omega_{\underline{y}}^{\underline{xr}} &= -\omega_{\underline{y}}^{\underline{rx}} = \frac{i \delta u_y(k_{(h)}) e^{i(k_{(h)x}x - \omega_{(h)}t)} \sqrt{f\left(\frac{rr_0}{l^2}\right)} k_{(h)x} \left(3 l^2 h\left(\frac{rr_0}{l^2}\right) - 2 r r_0 h'\left(\frac{rr_0}{l^2}\right) \right)}{6 r r_0^2},
\end{aligned}$$

Chapter 3. The Holographic Spectral Function in Non-Equilibrium States

$$\begin{aligned}
\omega_{\frac{yr}{t}} &= -\omega_{\frac{ry}{t}} = -\frac{\delta u_y(k_{(h)}) e^{i(k_{(h)x}x - \omega_{(h)}t)} \left[2l^2 \left(-1 + f\left(\frac{rr_0}{l^2}\right) \right) f\left(\frac{rr_0}{l^2}\right) - r r_0 \left(1 + f\left(\frac{rr_0}{l^2}\right) \right) f'\left(\frac{rr_0}{l^2}\right) \right]}{4l^2 r \sqrt{f\left(\frac{rr_0}{l^2}\right)}}, \\
\omega_{\frac{yr}{x}} &= -\omega_{\frac{ry}{x}} = \frac{i \delta u_y(k_{(h)}) e^{i(k_{(h)x}x - \omega_{(h)}t)} \sqrt{f\left(\frac{rr_0}{l^2}\right)} k_{(h)x} \left(3l^2 h\left(\frac{rr_0}{l^2}\right) - 2r r_0 h'\left(\frac{rr_0}{l^2}\right) \right)}{6r r_0^2}, \\
\omega_{\frac{yr}{y}} &= -\omega_{\frac{ry}{y}} = -\frac{\sqrt{f\left(\frac{rr_0}{l^2}\right)}}{r}.
\end{aligned} \tag{136}$$

Here prime denotes derivative with respect to $\frac{rr_0}{l^2}$.

It can be checked that the above spin connections satisfy Cartan structure equations up to first order in the derivative expansion.

D. The generalized effective action

We will review the formalism for bosonic operators here. The generalization to fermionic operators is straightforward.

The starting point of the construction of the generalized effective action is to generalize the partition function which is a generating functional of the vacuum correlation functions. Here on top of a source $J_l(x)$ for a single operator $\mathcal{O}_l(x)$, we add a non-local source $K_{ll'}(x, y)$ for a pair of operators $\mathcal{O}_l(x)$ and $\mathcal{O}_{l'}(y)$, and define:

$$\begin{aligned}
Z(J_l, K_{ll'}) &= e^{iW(J_l, K_{ll'})} \\
&= \int \mathcal{D}\Phi_s \exp \left[i \left(S[\Phi_s] + \int d^D x J_l(x) \mathcal{O}_l(x) \right. \right. \\
&\quad \left. \left. + \frac{1}{2} \int d^D x d^D y \mathcal{O}_l(x) K_{ll'}(x, y) \mathcal{O}_{l'}(y) \right) \right].
\end{aligned} \tag{137}$$

Above D is the number of space-time dimensions in field theory.

We then define the expectation value of the operator $\mathcal{O}_l(x)$ and the Green's function

Chapter 3. The Holographic Spectral Function in Non-Equilibrium States

$G_{ll'}(x, y)$ through :

$$\begin{aligned}\frac{\delta W(J_l, K_{ll'})}{\delta J_l(x)} &= O_l(x), \\ \frac{\delta W(J_l, K_{ll'})}{\delta K_{ll'}(x, y)} &= \frac{1}{2} \left(O_l(x) O_{l'}(y) + G_{ll'}(x, y) \right).\end{aligned}\quad (138)$$

Eliminating J_l and $K_{ll'}$ in favor of O_l and $G_{ll'}$, we can now do a Legendre transform to define the generalized effective action :

$$\begin{aligned}\Gamma(O_l, G_{ll'}) &= W(J_l, K_{ll'}) - \int d^D x J_l(x) O_l(x) \\ &\quad - \frac{1}{2} \int d^D x d^D y K_{ll'}(x, y) \left(O_l(x) O_{l'}(y) + G_{ll'}(x, y) \right).\end{aligned}\quad (139)$$

Clearly,

$$\begin{aligned}\frac{\delta \Gamma(O_l, G_{ll'})}{\delta O_l(x)} &= -J_l(x) - \int d^D y K_{ll'}(x, y) O_{l'}(y), \\ \frac{\delta \Gamma(O_l, G_{ll'})}{\delta G_{ll'}(x, y)} &= -\frac{1}{2} K_{ll'}(x, y).\end{aligned}\quad (140)$$

Therefore, in absence of sources, extremizing the generalized effective action $\Gamma(O_l, G_{ll'})$ gives the dynamics of both the operators and their Green's functions.

Such an effective action is usually considered for the elementary fields and their Green's functions in the literature. However, as discussed above we can construct the same for the set of gauge-invariant single trace operators in a non-Abelian gauge theory.

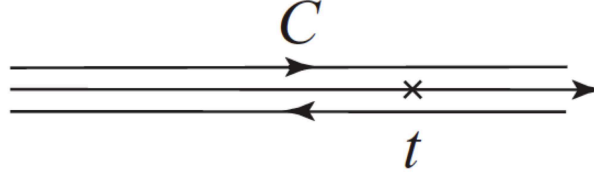
There is one important point in the above construction. The effective action is constructed over the so-called Schwinger-Keldysh real time contour shown in the figure below, which travels from $-\infty$ to ∞ infinitesimally above the real line and then back from ∞ to $-\infty$ infinitesimally below the real line. It is necessary to consider this "closed-time" contour because the usual time-ordered Green's function or the Feynmann propagator do not contain the full information about the operator in presence of sources in a non-equilibrium state as mentioned in the Introduction. The closed-time contour ensures we propagate the full information of the operator in presence of the sources. In fact, the full closed-time contour ordered Green's function can be written as a combination of the commutator and

Chapter 3. The Holographic Spectral Function in Non-Equilibrium States

the anti-commutator. For instance, if both operators are bosonic the

$$G_{CW}(x, y) = \frac{1}{2} \langle \{ \mathcal{O}_l(x), \mathcal{O}_l(y) \} \rangle - \frac{i}{2} \langle [\mathcal{O}_l(x), \mathcal{O}_l(y)] \rangle \text{sign}_C(x^0 - y^0). \quad (141)$$

Above C denotes the closed-time contour, and x^0 and y^0 are the time coordinates of the D-dimensional position vector x and y respectively.



The closed time Schwinger-Keldysh contour is as above. The forward and backward directed parts of the contour have been displaced slightly above and below the real axis just to distinguish them clearly.

In fact, as discussed in the beginning, the spectral function $\mathcal{A}_{ll'}(x, y)$ is related to the commutator and the statistical function (or Keldysh propagator) $G_{KL}(x, y)$ is related to the anti-commutator in the following way (for bosonic fields):

$$\begin{aligned} \mathcal{A}_{ll'}(x, y) &= i \langle [\mathcal{O}_l(x), \mathcal{O}_{l'}(y)] \rangle, \\ G_{KL}(x, y) &= \frac{1}{2} \langle \{ \mathcal{O}_l(x), \mathcal{O}_{l'}(y) \} \rangle. \end{aligned} \quad (142)$$

The coupled equation of motion of the spectral and statistical functions are obtained from the generalized effective action.

The generalized effective action has no dependence on temperature or non-equilibrium variables, it is defined as a Legendre transform of the vacuum persistence amplitude in the presence of single and double operator sources. However, thermal and non-equilibrium propagators also can be obtained as solutions which extremize this generalized effective action. In order to obtain thermal propagators, we need to impose translational invariance, so the Wigner transformed spectral and statistical functions $\mathcal{A}_{ll'}(\omega, \mathbf{p}, \mathbf{x}, t)$ and $G_{KL}(\omega, \mathbf{p}, \mathbf{x}, t)$ do not depend on the centre-of-mass coordinates \mathbf{x} and t . Furthermore, they should be related by a temperature dependent fluctuation-dissipation relation.

Bibliography

- [1] J. M. Maldacena, Int. J. Theor. Phys. **38**, 1113 (1999) [arXiv:hep-th/9711200]; S. S. Gubser, I. R. Klebanov and A. M. Polyakov, Phys. Lett. B **428**, 105 (1998) [arXiv:hep-th/9802109]; E. Witten, Adv. Theor. Math. Phys. **2**, 253 (1998) [arXiv:hep-th/9802150].
- [2] G. Policastro, D. T. Son, A. O. Starinets, JHEP **0209**, 043 (2002) [hep-th/0205052]; G. Policastro, D. T. Son, A. O. Starinets, JHEP **0212**, 054 (2002) [hep-th/0210220].
- [3] R. A. Janik and R. B. Peschanski, Phys. Rev. D **73**, 045013 (2006) [arXiv:hep-th/0512162]; R. A. Janik, Phys. Rev. Lett. **98**, 022302 (2007) [hep-th/0610144]; M. P. Heller and R. A. Janik, Phys. Rev. D **76**, 025027 (2007) [arXiv:hep-th/0703243].
- [4] R. Baier, P. Romatschke, D. T. Son, A. O. Starinets and M. A. Stephanov, JHEP **0804**, 100 (2008) [arXiv:0712.2451 [hep-th]]; M. Natsuume and T. Okamura, Phys. Rev. D **77**, 066014 (2008) [Erratum-ibid. D **78**, 089902 (2008)] [arXiv:0712.2916 [hep-th]].
- [5] S. Bhattacharyya, V. E. Hubeny, S. Minwalla and M. Rangamani, JHEP **0802**, 045 (2008) [arXiv:0712.2456 [hep-th]]; N. Banerjee, J. Bhattacharya, S. Bhattacharyya, S. Dutta, R. Loganayagam and P. Surowka, JHEP **1101**, 094 (2011) [arXiv:0809.2596 [hep-th]].
- [6] R. Iyer, and A. Mukhopadhyay, Phys. Rev. D **81**, 086005 (2010) [arXiv:0907.1156 [hep-th]].
- [7] R. Iyer and A. Mukhopadhyay, Phys. Rev. D **84**, 126013 (2011) [arXiv:1103.1814 [hep-th]].
- [8] R. Iyer and A. Mukhopadhyay, PoS **EPS-HEP2011**, 123 (2011) [arXiv:1111.4185 [hep-th]].
- [9] U. H. Danielsson, E. Keski-Vakkuri and M. Kruczenski, JHEP **0002**, 039 (2000) [hep-th/9912209]; S. B. Giddings and A. Nudelman, JHEP **0202**, 003 (2002) [hep-th/0112099]; V. Balasubramanian, A. Bernamonti, J. de Boer, N. Copland, B. Craps, E. Keski-Vakkuri, B. Muller and A. Schafer *et al.*, Phys. Rev. D **84**, 026010 (2011) [arXiv:1103.2683 [hep-th]]; J. Erdmenger, C. Hoyos and S. Lin, [arXiv:1112.1963 [hep-th]].

- [10] W. Florkowski, “*Phenomenology of Ultra-Relativistic Heavy-Ion Collisions*,” World Scientific, 2010
- [11] M. Bleicher, E. Zabrodin, C. Spieles, S. A. Bass, C. Ernst, S. Soff, L. Bravina and M. Belkacem *et al.*, J. Phys. G G **25**, 1859 (1999) [hep-ph/9909407].
- [12] S. S. Lee, Phys. Rev. D **79**, 086006 (2009) [arXiv:0809.3402 [hep-th]].
- [13] H. Liu, J. McGreevy, D. Vegh, Phys. Rev. **D83**, 065029 (2011) [arXiv:0903.2477 [hep-th]].
- [14] M. Cubrovic, J. Zaanen, K. Schalm, Science **325**, 439-444 (2009) [arXiv:0904.1993 [hep-th]].
- [15] T. Faulkner, H. Liu, J. McGreevy, D. Vegh, Phys. Rev. **D83**, 125002 (2011) [arXiv:0907.2694 [hep-th]].
- [16] S. A. Hartnoll and A. Tavanfar, Phys. Rev. D **83**, 046003 (2011) [arXiv:1008.2828 [hep-th]].
- [17] M. Cubrovic, J. Zaanen and K. Schalm, JHEP **1110**, 017 (2011) [arXiv:1012.5681 [hep-th]]; S. Sachdev, Phys. Rev. D **84**, 066009 (2011) [arXiv:1107.5321 [hep-th]].
- [18] T. Kita, Prog. Theor. Phys. Vol. 123 No. 4 (2010) pp.581-658 [arXiv:1005.0393[cond-mat]]; J. Berges, AIP Conf. Proc. **739**, 3 (2005) [arXiv:hep-ph/0409233].
- [19] L. Perfetti et. al. , Phys. Rev. Lett. **97**, 067402 (2006)
- [20] A. Mukhopadhyay, “Non-equilibrium fluctuation-dissipation relation from holography,” Phys. Rev. D **87**, 066004 (2013) [arXiv:1206.3311 [hep-th]].
- [21] C. P. Herzog and D. T. Son, JHEP **0303**, 046 (2003) [hep-th/0212072]; K. Skenderis and B. C. van Rees, Phys. Rev. Lett. **101**, 081601 (2008) [arXiv:0805.0150 [hep-th]]; G. C. Giecold, JHEP **0910**, 057 (2009) [arXiv:0904.4869 [hep-th]].
- [22] D. T. Son and A. O. Starinets, JHEP **0209**, 042 (2002) [hep-th/0205051].
- [23] N. Iqbal and H. Liu, Fortsch. Phys. **57**, 367 (2009) [arXiv:0903.2596 [hep-th]].
- [24] S. Banerjee, R. Iyer and A. Mukhopadhyay, Phys. Rev. D **85**, 106009 (2012) [arXiv:1202.1521 [hep-th]].

- [25] P. Arnold, G. D. Moore and L. G. Yaffe, JHEP **0011**, 001 (2000) [arXiv:hep-ph/0010177].
- [26] S. Chapman and T. Cowling, “*The Mathematical Theory of Non-Uniform Gases*”, Cambridge University Press, Cambridge, England, 1960, Chapters 7, 8, 10, 15 and 17; J. M. Stewart, *Ph. D. dissertation*, University of Cambridge, 1969.
- [27] H. Grad, Comm. Pure Appl. Math., **2** (1949), 331-407.
- [28] O. Aharony, S. S. Gubser, J. M. Maldacena, H. Ooguri and Y. Oz, Phys. Rept. **323**, 183 (2000) [hep-th/9905111].
- [29] R. K. Gupta and A. Mukhopadhyay, JHEP **0903**, 067 (2009) [arXiv:0810.4851 [hep-th]].
- [30] R. V. Gavai and S. Gupta, Phys. Rev. D **71**, 114014 (2005) [hep-lat/0412035].
- [31] I. R. Klebanov and A. M. Polyakov, Phys. Lett. B **550**, 213 (2002) [hep-th/0210114]; M. R. Gaberdiel and R. Gopakumar, Phys. Rev. D **83**, 066007 (2011) [arXiv:1011.2986 [hep-th]].
- [32] J. Erlich, E. Katz, D. T. Son and M. A. Stephanov, Phys. Rev. Lett. **95**, 261602 (2005) [hep-ph/0501128]; L. Da Rold and A. Pomarol, Nucl. Phys. B **721**, 79 (2005) [hep-ph/0501218].
- [33] A. O. Starinets, Phys. Rev. D **66**, 124013 (2002). [hep-th/0207133].
- [34] T. Faulkner and J. Polchinski, JHEP **1106**, 012 (2011) [arXiv:1001.5049 [hep-th]].
- [35] S. Bhattacharyya, V. E. Hubeny, R. Loganayagam, G. Mandal, S. Minwalla, T. Morita, M. Rangamani and H. S. Reall, JHEP **0806**, 055 (2008) [arXiv:0803.2526 [hep-th]].
- [36] G. T. Horowitz, V. E. Hubeny, Phys. Rev. D **62**, 024027 (2000). [hep-th/9909056].
- [37] V. Balasubramanian, P. Kraus and A. E. Lawrence, Phys. Rev. D **59**, 046003 (1999) [hep-th/9805171]; I. R. Klebanov and E. Witten, Nucl. Phys. B **556**, 89 (1999) [hep-th/9905104].
- [38] P. Breitenlohner and D.Z. Freedman, Ann. Phys. **144** (1982) 249.

- [39] S. A. Hartnoll, J. Polchinski, E. Silverstein and D. Tong, JHEP **1004**, 120 (2010) [arXiv:0912.1061 [hep-th]]; L. Y. Hung, D. P. Jatkar and A. Sinha, Class. Quant. Grav. **28**, 015013 (2011) [arXiv:1006.3762 [hep-th]].
- [40] N. Iqbal and H. Liu, Phys. Rev. D **79**, 025023 (2009) [arXiv:0809.3808 [hep-th]].
- [41] J. Rammer, "*Quantum field theory of non-equilibrium states*," Cambridge University Press, Cambridge, UK, 2007, Chapter 10.6.
- [42] J. W. Negele and H. Orland, "*Quantum many-particle systems (Advanced Book classics)*," Westview Press, USA 1998, Chapter 6.
- [43] P. Basu, J. He, A. Mukherjee and H. -H. Shieh, Phys. Lett. B **689**, 45 (2010) [arXiv:0911.4999 [hep-th]]; M. Ammon, J. Erdmenger, V. Grass, P. Kerner and A. O'Bannon, Phys. Lett. B **686**, 192 (2010) [arXiv:0912.3515 [hep-th]]; F. Benini, C. P. Herzog and A. Yarom, Phys. Lett. B **701**, 626 (2011) [arXiv:1006.0731 [hep-th]].
- [44] T. Faulkner, N. Iqbal, H. Liu, J. McGreevy and D. Vegh, arXiv:1101.0597 [hep-th].
- [45] S. Banerjee, A. Mukhopadhyay, in progress.

4

Cosmological Applications

Prelude

In recent years, understanding cosmology within the framework of string theory, has been an active and interesting field of study. Starting with [1], a substantial amount of research has been based on modeling the Universe by a 3-brane living in a higher-dimensional bulk space (brane world scenario). An incomplete list of references is [2–13]. The Hubble equation of cosmological evolution is thus reproduced by the trajectory of the brane. This chapter in the thesis, as mentioned in the introduction, is devoted to such cosmological studies.

This chapter is divided in two parts. Applying the gravity/gauge theory duality to a cosmological setting is not straightforward due to the fact that the metric on the boundary space in which the gauge theory lives must remain dynamical. This was long thought to be problematic due to the possibility of the fluctuations of the bulk metric corresponding to non-normalizable modes [14–20]. In the first part of this chapter we will discuss how one can get rid of this following the prescription given in [21] which shows that such problems can be avoided by introducing appropriate local boundary terms needed to cancel the infinities. Thus starting with a static bulk space-time we will end up in getting a dynamic cosmological boundary using this dynamic boundary condition. This possibility in cosmological set up was first shown in [22].

In applications of the gravity/gauge theory duality (holography) to cosmology and other settings, one generally places the boundary at a finite distance r and then takes the limit as the cutoff $r \rightarrow \infty$. The removal of the cutoff introduces infinities, which are canceled by the addition of a local action on the boundary with r -dependent coefficients (counterterms)

[23]. Unlike in quantum field theory, where counterterms are interpreted as renormalization of the (bare) parameters of the system, it is not clear if counterterms have a similar physical meaning in a holographic setting.

In this part we generalize the holographic approach to cosmology by placing the boundary hypersurface at a finite distance r and derive expressions for the various physical quantities (e.g., the stress-energy tensor) which are valid for arbitrary r . This leads to a generalized Hubble equation of cosmological evolution. We still need to introduce the standard counterterms to avoid infinities at large r . We show that these counterterms have the usual field theoretic interpretation of renormalizing the (bare) parameters of the system, namely Newton's constant and the cosmological constant. Moreover, we recover the brane-world scenario by fine-tuning Newton's constant. Thus we show that brane-world scenarios are a special case of our generalized holographic approach.

This part of the chapter is organized as follows. In section 4.1 we discuss the bulk space concentrating on a time-independent solution (general black hole) of the field equations, and define the boundary hypersurface. In section 4.2 we introduce the boundary conditions and the counterterms needed to cancel infinities. We calculate the stress-energy tensor and derive the Hubble equation of cosmological evolution. In section 4.3 we discuss the example of a bulk Reissner-Nordström black hole including thermodynamics. In section 4.4 we discuss various examples of cosmological evolution. In particular, we show that the brane-world scenarios are a special case of our holographic approach. Finally in section 4.5 we conclude.

The second part of this chapter deals with explicit construction of time-dependent supergravity solutions. The main motivation in this part is to understand the physics near cosmological singularity. As we know *AdS/CFT* relates a strongly coupled theory with a weakly coupled one. Consequently, it provides us with a way to tame the non-perturbative region of one by performing computations on its dual. Due to strong gravitational fluctuations, physics around cosmological singularities is dominated by non-perturbative effects and one hopes that the AdS/CFT correspondence would shed some light into it. Indeed, in recent years, we have witnessed several important investigations where attempts were made to find the signatures of these singularities in their gauge theory duals. Expectation is that the dual theory evolution might be able to provide a sensible quantum description of these singularities. Successes have been varied, please see the references [24] - [28].

Inspired by this line of developments, in this part, we search for D brane solutions in ten dimensional type IIB theory where the world volume metric expands anisotropically

and show instabilities within their supergravity descriptions. We find that appropriately tuning the five form field strength, it is possible to construct a D3 brane with four dimensional Kasner like world volume [44]. Along with a time-like singularity at $r = 0$, the metric shows an additional cosmological singularity at $t = 0$. Perturbation around $t = 0$ generates an analogue of Belinskii-Lifshitz-Khalatnikov (BKL) oscillations [39]. The near horizon geometry of this brane reduces to that of a Kasner-universe in AdS space plus a five sphere along with an appropriate five form field strength. In the next section we probe the geometry with a dynamical D3 brane whose world-volume inherits anisotropic expansion/contraction along with a BKL like oscillation. We show, in subsequent sections, that similar solutions can be constructed even within eleven dimensional supergravity. As an illustrative example, we discuss the case of M5 brane. The near horizon geometry is now a six dimensional Kasner space. A dynamical probe M5 brane in this space-time again acquires an anisotropic expansion in some directions and contraction along some. Amusingly, we find that it is possible to tune parameters in such a manner that three directions expand and the rest contract. Close to the cosmological singularities supergravity descriptions of all these solutions are expected to break down. We hope that the gauge theory description would shed some light on the physics near the singularities.

The first part of this chapter is based on our work, [29] while the second part follows our work, [30].

Part I : Static Bulk - Dynamic Boundary

4.1 The Bulk

We start with a non-extremal black hole in a $4 + 1$ dimensional bulk space in the presence of a negative cosmological constant

$$\Lambda_5 = -\frac{6}{L^2} . \quad (4.1)$$

We consider the metric *ansatz*

$$ds_5^2 = -A(r)dt^2 + B(r)dr^2 + r^2 d\Omega_k^2 , \quad (4.2)$$

r being the radial direction, and $k = +1, 0, -1$ depending on the geometry of the constant (t, r) hypersurfaces (spherical, flat, or hyperbolic, respectively). More general metrics are also possible, but will clutter the notation unnecessarily. In section 4.3, we shall concentrate on the special case of a Reissner-Nordström black hole for explicit calculations.

Asymptotically, we have AdS space of radius L , therefore as $r \rightarrow \infty$,

$$A(r) \approx \frac{1}{B(r)} \approx \frac{r^2}{L^2} . \quad (4.3)$$

We introduce a radial cutoff, $r = a$ and parametrise a and t as $a = a(\tau)$ and $t = t(\tau)$ so that $da = \dot{a}d\tau$. Then the metric on the cut-off surface (boundary) takes the form

$$ds_4^2 = \left[-A(a) \left(\frac{dt}{d\tau} \right)^2 + B(a) \dot{a}^2 \right] d\tau^2 + a^2(\tau) d\Omega_k^2 . \quad (4.4)$$

In order that the metric on the boundary take the FRW form,

$$ds_4^2 = -d\tau^2 + a^2(\tau) d\Omega_k^2 , \quad (4.5)$$

the metric components should satisfy the relation

$$\left(\frac{dt}{d\tau} \right)^2 = \frac{\mathcal{B}}{A} , \quad \mathcal{B} = B(a) \dot{a}^2 + 1 . \quad (4.6)$$

This in turn fixes our choice of the time parameter τ . Notice also that if T_H is the Hawking temperature, then the temperature on the boundary is redshifted,

$$T = \frac{T_H}{\sqrt{A\mathcal{B}}} . \quad (4.7)$$

This kind of parametrization has been used before, e.g., in [31–33]. Note that, while treating τ as a time parameter, we are effectively considering the radial motion of the cut-off surface in the $4 + 1$ dimensional bulk. By adopting appropriate boundary conditions, the cut-off surface can be thought of as the location of a brane, mimicking a moving brane scenario.

4.2 Boundary Conditions

The heart of the construction we are going to elaborate on is based on the observation that the afore-mentioned dynamics of the boundary hypersurface will be captured through the boundary conditions we impose on the system. This approach was first adopted in [22].

Let us consider a general five dimensional bulk action,

$$S_5 = \int_{\mathcal{M}} d^5x \sqrt{-g} \mathcal{L}_5, \quad (4.8)$$

where we keep the Lagrangian density \mathcal{L}_5 unspecified. In the simplest case, this consists of a five-dimensional Einstein-Hilbert action with a negative cosmological constant (4.1) plus the requisite Gibbons-Hawking surface term for a well-defined variational principle. If one varies this action with respect to the metric, one obtains a boundary term of the form

$$\delta S_5 = \frac{1}{2} \int_{\partial\mathcal{M}} d^4x \sqrt{-\gamma} T_{\mu\nu}^{(\text{CFT})} \delta\gamma^{\mu\nu}, \quad (4.9)$$

where $\gamma^{\mu\nu}$ is the induced boundary metric and γ is its determinant. $T_{\mu\nu}^{(\text{CFT})}$ denotes the (bare) stress-energy tensor of the dual conformal field theory that lives on the four-dimensional boundary hypersurface $r = a$. Generally in the context of the AdS/CFT correspondence, Dirichlet boundary conditions are employed, which fix the boundary metric and consequently eq. (4.9) vanishes. While this leads to a well-defined variational principle, it does not allow for a dynamical boundary metric. Since we are primarily interested in obtaining a cosmological evolution and hence a dynamical metric on the boundary, we seek different boundary conditions that can be imposed without fixing the metric on the boundary. It was noted in [22] that one could adopt appropriate *mixed* boundary conditions, which were shown to lead to valid dynamics in [21]. Their definition involves the addition of an appropriate local action, S_{local} , at the boundary. For cosmological evolution, this local action will be chosen as the four-dimensional Einstein-Hilbert action on the boundary with an arbitrary (positive, negative, or vanishing) four-dimensional cosmological constant Λ_4 ,

$$S_{\text{local}} = -\frac{1}{16\pi G_4} \int_{\partial\mathcal{M}} d^4x \sqrt{-\gamma} (\mathcal{R}[\gamma] - 2\Lambda_4), \quad (4.10)$$

where $\mathcal{R}[\gamma]$ is the Ricci scalar evaluated with the boundary metric which, in our case, is the FRW metric (4.5). Notice that the cosmological constant may be due, wholly or partly, to

a brane of finite tension at the boundary.

Additionally, to cancel divergences in the limit $a \rightarrow \infty$, it is necessary to introduce counterterms [23]. These are of the same form as the local action and renormalize the four-dimensional physical parameters G_4 and Λ_4 . We have

$$S_{\text{c.t.}} = -\frac{1}{2} \int_{\partial\mathcal{M}} d^4x \sqrt{-\gamma} (\kappa_1 \mathcal{R}[\gamma] + \kappa_2) , \quad (4.11)$$

which diverges as $a \rightarrow \infty$. The parameters κ_1 and κ_2 will be chosen so that physical quantities such as the energy density and pressure remain finite in this limit.

Putting these pieces together, we *define* our boundary condition as

$$T_{\mu\nu}^{(\text{CFT})} + T_{\mu\nu}^{(\text{local})} + T_{\mu\nu}^{(\text{c.t.})} = 0, \quad (4.12)$$

where $T_{\mu\nu}^{(\text{CFT})}$ is due to the variation δS_5 (eq. (4.9)), and the other two terms, $T_{\mu\nu}^{(\text{local})}$ and $T_{\mu\nu}^{(\text{c.t.})}$ come from the variations

$$\begin{aligned} \delta S_{\text{local}} &= \frac{1}{2} \int_{\partial\mathcal{M}} d^4x \sqrt{-\gamma} T_{\mu\nu}^{(\text{local})} \delta\gamma^{\mu\nu} , \\ \delta S_{\text{c.t.}} &= \frac{1}{2} \int_{\partial\mathcal{M}} d^4x \sqrt{-\gamma} T_{\mu\nu}^{(\text{c.t.})} \delta\gamma^{\mu\nu} , \end{aligned} \quad (4.13)$$

respectively, with respect to the boundary metric, $\gamma_{\mu\nu}$. Similarly to Dirichlet boundary conditions, the choice (4.12) leads to a well-defined variational principle with

$$\delta S_5 + \delta S_{\text{local}} + \delta S_{\text{c.t.}} = 0 . \quad (4.14)$$

To see the explicit physical content of our *mixed* boundary conditions (4.12), we shall derive explicit expressions for each of the three contributing terms. The bare stress-energy tensor on the boundary is given by

$$T_{\mu\nu}^{(\text{CFT})} = \frac{1}{8\pi G_5} (\mathcal{K}_{\mu\nu} - \mathcal{K} \gamma_{\mu\nu}) , \quad (4.15)$$

where $\mathcal{K}_{\mu\nu}$ is the extrinsic curvature, and \mathcal{K} is its trace. The components of this tensor can be evaluated by computing the velocity v^μ and unit normal n^ν vectors on the boundary

hypersurface, $r = a(\tau)$. For the metric (4.2), these vectors are given in component form as

$$v^\mu = \left(\sqrt{\frac{\mathcal{B}}{A}}, \dot{a}, 0, 0, 0 \right) ; \quad v_\mu = \left(-\sqrt{A\mathcal{B}}, B\dot{a}, 0, 0, 0 \right) . \quad (4.16)$$

and

$$n^\mu = \left(-\sqrt{\frac{\mathcal{B}}{A}}\dot{a}, -\sqrt{\frac{\mathcal{B}}{B}}, 0, 0, 0 \right) ; \quad n_\mu = \left(\sqrt{AB}\dot{a}, -\sqrt{B\mathcal{B}}, 0, 0, 0 \right) , \quad (4.17)$$

respectively. The direction of the unit normal vector is taken to be pointing inward, toward the bulk. The extrinsic curvature can be written in terms of the unit normal and velocity vectors as

$$\mathcal{K}_{ij} = \frac{1}{2} n^k \partial_k \gamma_{ij} \quad \mathcal{K}_{\tau\tau} = -\frac{\partial_\tau v_t}{n_t}. \quad (4.18)$$

Explicitly, they are

$$\mathcal{K}_{ij} = a\sqrt{\frac{\mathcal{B}}{B}}\gamma_{ij} , \quad \mathcal{K}_{\tau\tau} = -\frac{3}{2aAB} (2AB\ddot{a} + (AB)'\dot{a} + A') , \quad (4.19)$$

where i, j are indices for the spatial coordinates on the boundary (spanned by Ω_k).

We deduce the explicit expressions for the components of the bare stress-energy tensor (4.15),

$$T_{\tau\tau}^{(\text{CFT})} = -\frac{3}{8\pi G_5 a} \sqrt{\frac{\mathcal{B}}{B}} , \quad (4.20)$$

$$T_i^{(\text{CFT})} = \frac{1}{16\pi G_5} \frac{aA'\mathcal{B} + A[aB'\dot{a} + 2B(a\ddot{a} + 2\dot{a}^2) + 4]}{aA\sqrt{B\mathcal{B}}} , \quad (4.21)$$

where no summing over the index i is implied. Notice that the energy density $T_{\tau\tau}^{(\text{CFT})}$ obtained above is negative, however we should emphasize that this is only a *bare* quantity and therefore not physical. It will be corrected by the addition of counter terms resulting into a *positive* regularized (physical) quantity.

For the remaining two contributions in (4.12), we obtain the standard expressions one encounters in Einstein's four-dimensional equations,

$$T_{\mu\nu}^{(\text{local})} = -\frac{1}{8\pi G_4} \left(\mathcal{R}_{\mu\nu} - \frac{1}{2} \gamma_{\mu\nu} \mathcal{R} - \Lambda_4 \gamma_{\mu\nu} \right) , \quad T_{\mu\nu}^{(\text{c.t.})} = -\kappa_1 \left(\mathcal{R}_{\mu\nu} - \frac{1}{2} \gamma_{\mu\nu} \mathcal{R} \right) - \kappa_2 \gamma_{\mu\nu} , \quad (4.22)$$

where $\mathcal{R}_{\mu\nu}$ (\mathcal{R}) is the four-dimensional Ricci tensor (scalar) constructed from the four-dimensional boundary metric $\gamma_{\mu\nu}$. The counter terms diverge in the limit $a \rightarrow \infty$, and the parameters κ_1 and κ_2 will be chosen so that they cancel the divergences in the bare stress-energy tensor $T_{\mu\nu}^{(\text{CFT})}$. Notice that the counter terms are of the same form as the terms coming from the local action. Therefore, they admit the standard interpretation of inducing the renormalization of the physical four-dimensional constants G_4 (Newton's constant) and Λ_4 (cosmological constant).

The regularized (physical) stress-energy tensor is

$$T_{\mu\nu}^{(\text{reg})} = T_{\mu\nu}^{(\text{CFT})} + T_{\mu\nu}^{(\text{c.t.})} . \quad (4.23)$$

We deduce the energy density and pressure, respectively,

$$\begin{aligned} \epsilon = T_{\tau\tau}^{(\text{reg})} &= \kappa_2 + \kappa_1 \left(H^2 + \frac{k}{a^2} \right) - \frac{3}{8\pi G_5 a} \sqrt{\frac{\mathcal{B}}{B}} , \\ p = T_i^i{}^{(\text{reg})} &= -\kappa_2 - \kappa_1 \left\{ \left(H^2 + \frac{k}{a^2} + \frac{2\ddot{a}}{a} \right) \right\} \\ &\quad + \frac{1}{16\pi G_5} \frac{aA'\mathcal{B} + A[aB'\dot{a} + 2B(a\ddot{a} + 2\dot{a}^2) + 4]}{aA\sqrt{B\mathcal{B}}} . \end{aligned} \quad (4.24)$$

where $H = \dot{a}/a$ is the Hubble parameter. The choice

$$\kappa_1 = \frac{3L}{16\pi G_5} , \quad \kappa_2 = \frac{3}{8\pi G_5 L} \quad (4.25)$$

ensures finiteness in the limit $a \rightarrow \infty$. Unlike the bare energy density (4.20), the regularized energy density ϵ is positive.

The boundary conditions (4.12) now read

$$\mathcal{R}_{\mu\nu} - \frac{1}{2}\gamma_{\mu\nu}\mathcal{R} - \Lambda_4\gamma_{\mu\nu} = 8\pi G_4 T_{\mu\nu}^{(\text{reg})} , \quad (4.26)$$

which are the four-dimensional Einstein equations in the presence of a cosmological constant.

The cosmological evolution equation is the $\tau\tau$ component of the Einstein equations (4.26),

$$H^2 + \frac{k}{a^2} - \frac{\Lambda_4}{3} = \frac{8\pi G_4}{3} \epsilon , \quad (4.27)$$

where ϵ is the energy density given in (4.24) under the condition (4.25). This is deceptively similar to the standard equation of cosmological evolution. However, it differs in an essential way, because ϵ contains contributions that involve the Hubble parameter $H = \dot{a}/a$, leading to novel cosmological scenarios.

4.3 AdS Reissner-Nordström black hole

In this section we take up the example of an asymptotically AdS charged black hole, namely AdS Reissner-Nordström black hole for which the functions A and B of (4.2) are

$$A(r) = \frac{1}{B(r)} = \frac{r^2}{L^2} + k - \frac{M}{r^2} + \frac{Q^2}{r^4} . \quad (4.28)$$

The parameters M and Q are related to the mass and charge of the black hole, respectively. k can be $+1$, 0 , or -1 depending on whether the black hole horizon is spherical, flat, or hyperbolic, respectively.

The Hawking temperature is

$$T_H = \frac{2\frac{r_+^2}{L^2} + k}{2\pi r_+} , \quad (4.29)$$

where r_+ is the radius of the horizon satisfying

$$A(r_+) = \frac{r_+^2}{L^2} + k - \frac{M}{r_+^2} + \frac{Q^2}{r_+^4} = 0 . \quad (4.30)$$

The entropy is

$$S = \frac{r_+^3}{4G_5} V_3 , \quad (4.31)$$

where V_3 is the three-dimensional volume spanned by Ω_k . Notice that the entropy is independent of a , and therefore constant in time, leading to an adiabatic evolution.

According to (4.7), the redshifted temperature on the boundary is

$$T = \frac{T_H}{\sqrt{\dot{a}^2 + A(a)}} . \quad (4.32)$$

For large a , it is expanded as

$$T = \frac{T_H L}{a} - \frac{T_H L^3}{2a} \left(H^2 + \frac{k}{a^2} \right) + \dots \quad (4.33)$$

Similarly, we expand the regularized energy density and pressure (4.24), respectively,

$$\begin{aligned} \epsilon = & \frac{3L^3}{64\pi G_5} \left\{ \left(H^2 + \frac{k}{a^2} \right)^2 + \frac{4M}{L^2 a^4} \right\} \\ & - \frac{3L^5}{128\pi G_5} \left\{ \left(H^2 + \frac{k}{a^2} \right)^3 + \frac{4kM}{L^2 a^6} + \frac{8Q^2}{L^4 a^6} + \frac{4M}{L^2} \frac{H^2}{a^4} \right\} + \dots, \end{aligned} \quad (4.34)$$

$$\begin{aligned} p = & \frac{L^3}{64\pi G_5} \left\{ \left(H^2 + \frac{k}{a^2} \right)^2 + \frac{4M}{L^2 a^4} - 4 \left(H^2 + \frac{k}{a^2} \right) \frac{\ddot{a}}{a} \right\} \\ & - \frac{3L^5}{128\pi G_5} \left\{ \left(H^2 + \frac{k}{a^2} \right)^3 + \frac{4kM}{L^2 a^6} + \frac{8Q^2}{L^4 a^6} + \frac{4M}{L^2} \frac{H^2}{a^4} - 2 \left(H^2 + \frac{k}{a^2} \right)^2 \frac{\ddot{a}}{a} - \frac{8}{3L} \frac{M\ddot{a}}{a^5} \right\} \\ & + \dots \end{aligned} \quad (4.35)$$

We deduce the conformal anomaly which is given by the trace of the stress-energy tensor,

$$\begin{aligned} \text{Tr} T &= \epsilon - 3p \\ &= -\frac{3L^3}{16\pi G_5} \left(H^2 + \frac{1}{a^2} \right) \frac{\ddot{a}}{a} \\ &\quad - \frac{3L^5}{64\pi G_5} \left\{ \left(H^2 + \frac{k}{a^2} \right)^3 + \frac{4kM}{L^2 a^6} + \frac{8Q^2}{L^4 a^6} + \frac{4M}{L^2} \frac{H^2}{a^4} - 3 \left(H^2 + \frac{k}{a^2} \right)^2 \frac{\ddot{a}}{a} - \frac{4}{L} \frac{M\ddot{a}}{a^5} \right\} \\ &\quad + \dots \end{aligned} \quad (4.36)$$

The first term is the standard conformal anomaly one obtains in the large a limit [22].

As an example, consider the case of a flat static boundary of a Schwarzschild black hole. Then $k = 0$, $Q = 0$, and $H = 0$. The radius of the horizon is $r_+ = (ML^2)^{1/4}$. The

expressions for the energy density, pressure and temperature simplify to, respectively,

$$\begin{aligned}\epsilon &= T_{\tau\tau} = \frac{3}{8\pi G_5 L} \left(1 - \sqrt{1 - \frac{r_+^4}{a^4}} \right) , \\ p &= T_i^i = \frac{1}{8\pi G_5 L} \left(\frac{3 - \frac{r_+^4}{a^4}}{\sqrt{1 - \frac{r_+^4}{a^4}}} - 3 \right) , \\ T &= \frac{r_+}{\pi L a \sqrt{1 - \frac{r_+^4}{a^4}}} \end{aligned} \quad (4.37)$$

In the large a limit, we deduce the expansions

$$\begin{aligned}\epsilon &= \frac{3}{8\pi G_5 L} \left(\frac{(\pi L T)^4}{2} - \frac{7(\pi L T)^8}{8} + \dots \right) , \\ p &= \frac{1}{8\pi G_5 L} \left(\frac{(\pi L T)^4}{2} - \frac{3(\pi L T)^8}{8} + \dots \right) . \end{aligned} \quad (4.38)$$

Thus, at leading order, we have $\epsilon = 3p \propto T^4$, as expected for a conformal fluid. Including next-order corrections, we no longer have a traceless stress-energy tensor.

Returning to the general case, we obtain the law of thermodynamics

$$dE = TdS - pdV + \Phi dQ , \quad (4.39)$$

where $E = \epsilon V$, $V = a^3 V_3$ is the volume, and Φ is the potential

$$\Phi = \frac{Q}{G_5 a} . \quad (4.40)$$

This is easily verified, e.g., by differentiating with respect to τ , r_+ , and Q (after using (4.30) to express M in terms of the other two parameters, r_+ and Q).

4.4 Cosmological Evolution

Next, we discuss various explicit examples of cosmological evolution based on an AdS Reissner-Nordström black hole. For simplicity, in what follows we shall be working with units in which $L = 1$.

The Hubble equation (4.27) can be massaged into the form

$$\beta \left(H^2 + \frac{k}{a^2} \right) = \frac{1}{L'} - \sqrt{H^2 + \frac{A(a)}{a^2}}, \quad (4.41)$$

where we introduced the convenient combinations of parameters

$$\beta = \frac{G_5}{G_4} - \frac{1}{2}, \quad \frac{1}{L'} = 1 + \frac{(1 + 2\beta)\Lambda_4}{6}. \quad (4.42)$$

The Hubble equation can be expanded for large a as

$$\begin{aligned} H^2 + \frac{k}{a^2} - \frac{\Lambda_4}{3} &= \frac{G_4 L^3}{16G_5} \left\{ \left(H^2 + \frac{1}{a^2} \right)^2 + \frac{4M}{L^2 a^4} \right\} \\ &\quad - \frac{G_4 L^4}{16G_5} \left\{ \left(H^2 + \frac{1}{a^2} \right)^3 + \frac{4M}{L^2 a^6} + \frac{8Q^2}{L^4 a^6} + \frac{4M}{L^2 a^4} H^2 \right\} + \dots \end{aligned} \quad (4.43)$$

At leading order, it coincides with the result obtained in [22].

After squaring (4.41), we obtain a quadratic equation for H^2 . However, only one of the two roots is a solution of (4.41). Let us concentrate on the range of parameters with $\beta > 0$, $L' > 0$. We obtain

$$H^2 = \frac{\left(\frac{1}{L'} - \frac{k}{a^2} \beta \right)^2 - \frac{A(a)}{a^2}}{\frac{1}{2} + \frac{\beta}{L'} - \frac{k\beta^2}{a^2} + \sqrt{\frac{1}{4} + \frac{\beta}{L'} + (A(a) - k) \frac{\beta^2}{a^2}}}. \quad (4.44)$$

This can be solved for $a = a(\tau)$ to obtain the orbit of the boundary hypersurface. Once a solution of (4.44) is obtained, we still need to verify that it satisfies (4.41), because the solutions of (4.41) in general form a subset of the solutions of (4.44).

The fixed points of the orbits are found by setting $H = 0$ in (4.41). They are solutions of

$$V(a) \equiv \frac{1}{L'} - \frac{k}{a^2} \beta - \frac{1}{a} \sqrt{A(a)} = 0. \quad (4.45)$$

These fixed points are also fixed points of (4.44), but the converse is not always true.

With the choice of parameters such that $\beta = 0$ [34], eq. (4.44) simplifies to

$$H^2 = \left(1 + \frac{\Lambda_4}{6} \right)^2 - \frac{A(a)}{a^2}, \quad (4.46)$$

which coincides with the results from a brane world scenario. Thus we recover the evolution of a 3-brane in a five-dimensional bulk space if we fine tune the parameters of our system so that $\beta = 0$.

The fixed points are solutions of

$$V(a) \equiv 1 + \frac{\Lambda_4}{6} - \frac{1}{a} \sqrt{A(a)} = 0 . \quad (4.47)$$

Notice that no fixed points exist between the outer and inner horizons (with $A(a) < 0$), because of the square root in the potential $V(a)$. Notice also that $V(a) \approx \frac{\Lambda_4}{6}$ as $a \rightarrow \infty$, so the sign of the potential is determined by the sign of Λ_4 , and at the horizon, $V(r_+) = \frac{1}{L} > 0$. Up to two fixed points can be outside the horizon. However, our classical results likely receive significant quantum corrections as we approach the horizon. Therefore, our results are reliable for orbits away from the horizon, which typically end at infinite distance from the horizon.

For $\Lambda_4 = 0$, we recover from (4.46) the brane world scenario of [35]. This scenario is depicted in figure 4.1a for $k = +1$, $M = 8$, $Q = 1$. We notice here that we have only one solution that is bouncing. Of the two turning points, one is inside the inner horizon and the other outside the outer horizon. There is no fixed point between the inner and outer horizons, as noted earlier, because of the presence of the square root in the potential $V(a)$ (4.45). This can be explicitly seen from figure 4.2a where we see clearly the position of the inner fixed point as the point where the solid line cuts the a -axis. After crossing the turning point outside the outer horizon, the square of the Hubble parameter becomes negative and hence unphysical. The orbit of the bouncing solution is shown in figure 4.3. Although we reproduce the bouncing cosmology of [35], through this, as argued in [36] this kind of solution suffers from an instability. Indeed, the inner horizon is the Cauchy horizon for this charged AdS black hole and is unstable under linear fluctuations about the equilibrium black hole space-time. So when the orbit crosses the inner horizon of the black hole, it is not sufficient to consider only the unperturbed background. The backreaction on the background metric due to the fluctuating modes has to be taken into account. This backreaction is significant and may produce a curvature singularity. It should be noted that this pathology occurs only for $\beta = 0$. For $\beta \neq 0$, no outward crossing of the horizon occurs. Thus, from our point of view, β acts as a regulator; keeping it small, but finite, is essential for the handling of quantum fluctuations.

If we now tune Λ_4 to non-zero values, we obtain qualitatively different solutions. In the

simplest case, when there is no chemical potential ($Q = 0$), for sufficiently small $\Lambda_4 > 0$, and $k = 1$ (spherical geometry) we recover the de Sitter brane scenario of ref. [37]. As an example, set $M = 1$, $\Lambda_4 = 0.5$. For $\beta = 0$, we obtain two fixed points $a = 1.13, 2.11$, outside the outer horizon ($r_+ = 1.03$). As we increase β (i.e., G_5 , or equivalently, decrease G_4), the larger fixed point increases and the smaller one decreases. After it hits the horizon, the smaller fixed point disappears and we only have one fixed point. No fixed points exist inside the horizon.

In the same set up and keeping all other parameters fixed to the afore-mentioned values, if we now turn on the chemical potential, we obtain one more fixed point away from the outer horizon. For $Q = 1$ this is shown in figure 4.1b. Similarly to the $\Lambda_4 = 0$ case, here we also obtain one bouncing solution with two fixed points, one inside the inner horizon (figure 4.2b) and the other outside the outer horizon. This solution for $a(\tau)$ is plotted in figure 4.4a. Additionally, at $a = 7.09$ there is another fixed point. We obtain an accelerating solution from this point (figure 4.4b). In the region between the first fixed point outside the outer horizon ($a = 3.06$) and second one at $a = 7.09$, the square of the Hubble parameter is negative, hence there is no physical solution in this region.

Comparing the brane world scenario (4.46) with the general case, $\beta \neq 0$, we observe that there are no qualitative differences in the flat case ($k = 0$). In the case of curved horizon (boundary), $k = \pm 1$, in general one obtains fixed points other than the ones obtained in the brane world scenario. As an example, consider the choice of parameters

$$k = +1, \quad M = 8, \quad Q = 1, \quad \Lambda_4 = 0.05, \quad \beta = 6. \quad (4.48)$$

We have only one fixed point in this case, at $a = 7.705$ (figure 4.1d). The solution is accelerating as shown in figure 4.5. There is no bouncing solution for any set of parameters once we go away from the special case $\beta = 0$.

For $\beta \neq 0$, if we set $\Lambda_4 = 0$, we do not obtain any physical solution. One such situation is depicted in figure 4.1c. As we see, the square of the Hubble parameter is imaginary for all values of the cosmic scale a in this case.

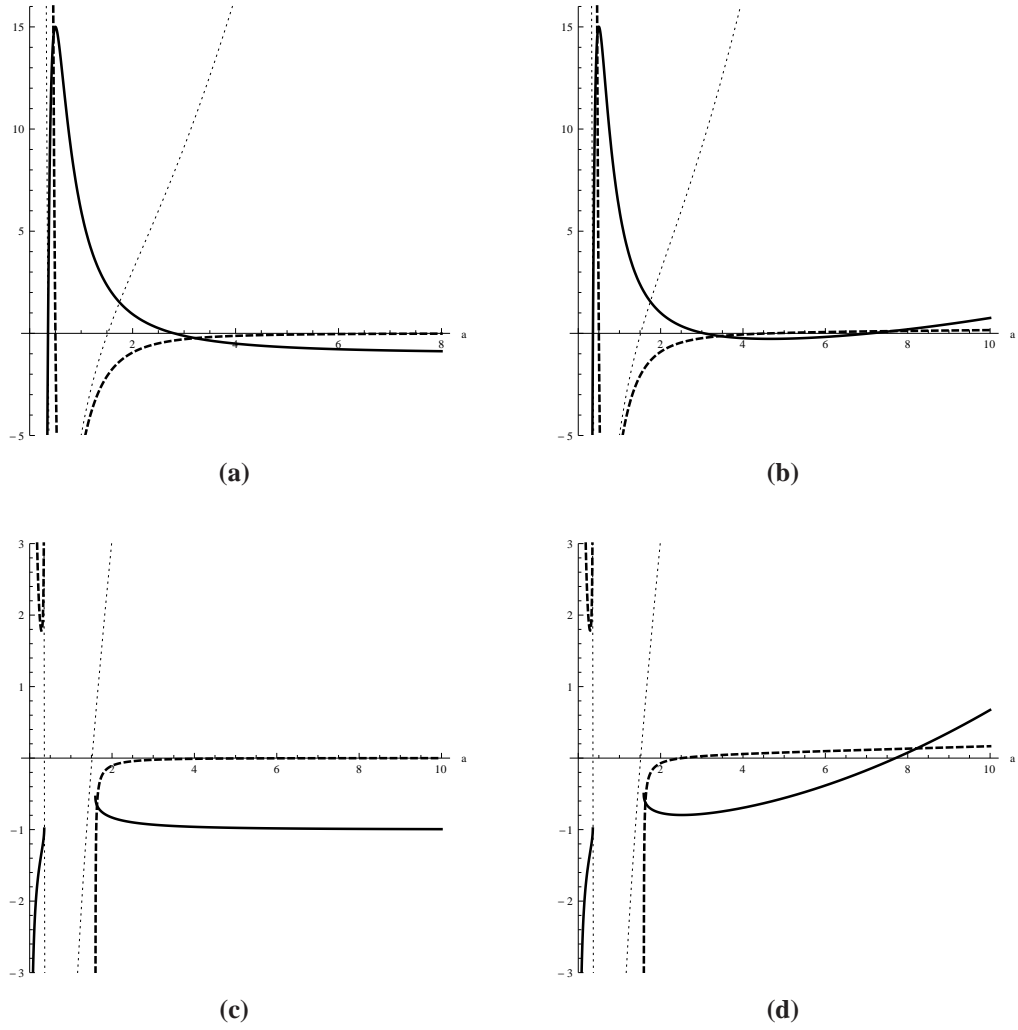


Figure 4.1: Cosmological evolution scenarios for various values of parameters. Solid and dashed lines are plots of \dot{a}^2 and \ddot{a} , respectively. Dotted lines denote the black hole potential with its zeros indicating the positions of the inner and outer horizons.

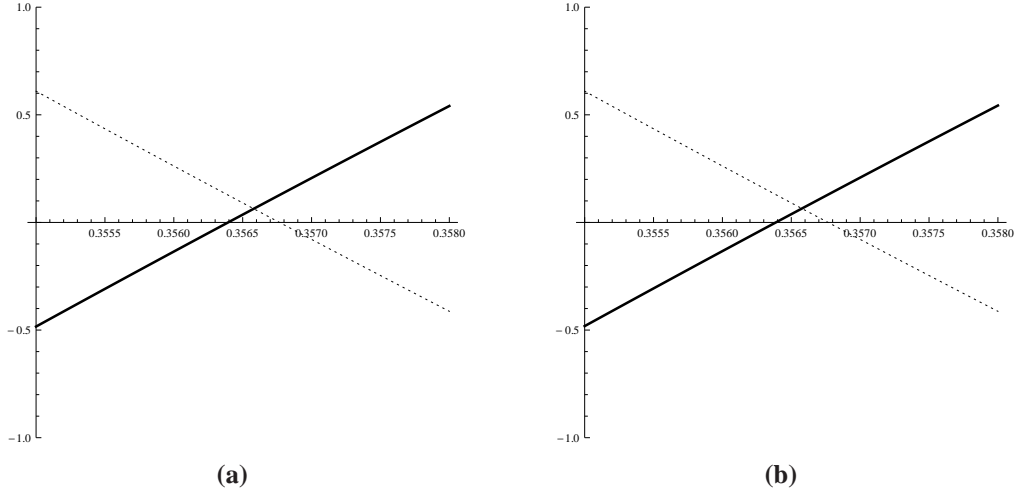


Figure 4.2: Solid lines are plots of \dot{a}^2 whereas dotted lines are plots of the black hole potential for $\beta = 0$ and (a) $\Lambda_4 = 0$, (b) $\Lambda_4 = 0.05$. The inner fixed points and the position of the inner horizon are shown.

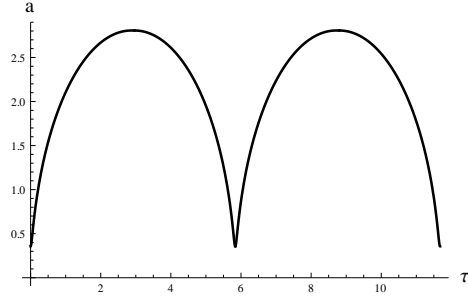


Figure 4.3: Plot of a vs τ for $\beta = 0$, $\Lambda_4 = 0$.

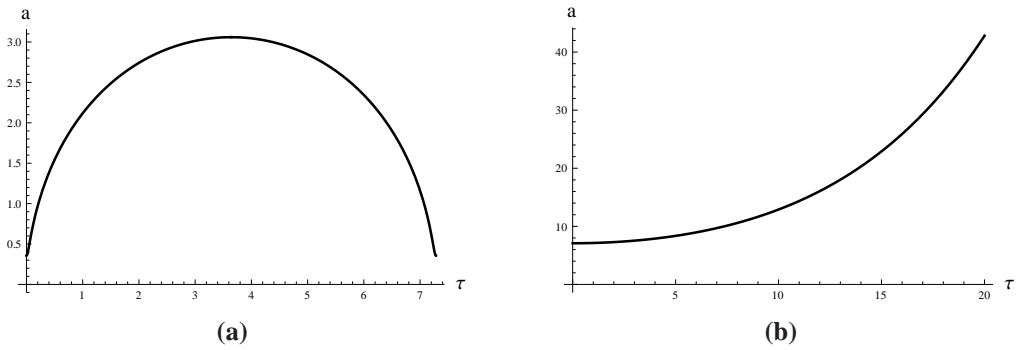


Figure 4.4: Plots of a vs τ for $\beta = 0$, $\Lambda_4 = 0.05$. In (a) we have a bounce. Initial conditions are chosen as $a(0) = 0.356$. At $\tau = 3.642$, a reaches the second fixed point, $a = 3.059$. In (b) we have an accelerating solution, with initial condition chosen as $a(0) = 7.090$.

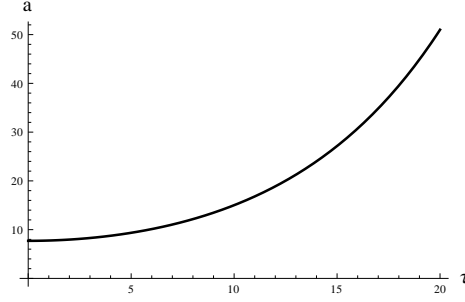


Figure 4.5: Plot of a vs τ for $\beta = 6$, $\Lambda_4 = 0.05$. The initial condition is chosen as $a(0) = 7.705$.

4.5 Summary and future directions : Part I

Let us pause here for a while and summarize this part before going into the next part of this chapter. We discussed here the cosmological evolution derived from a static bulk solution of the field equations with appropriately defined *mixed* boundary conditions using the gravity/gauge theory duality (holography). Such an approach was first discussed in [22]. We extended the results of [22] by considering a boundary hypersurface at arbitrary distance. We calculated the general form of the stress-energy tensor and arrived at a generalized form of the Hubble equation of cosmological evolution. We considered various explicit examples in detail based on an AdS Reissner-Nordström bulk black hole solution. Interestingly, we obtained the brane-world scenario as a special case, by fine-tuning the parameters of the system, setting $\beta = 0$ (eq. (4.42)). However, keeping β small but finite is important in order to avoid scenarios in which the boundary crosses the event horizon from within [35]. Thus, β acts as a regulator for such problematic solutions for which quantum fluctuations introduce instabilities [36]. Moreover, the counterterms one normally introduces to cancel the infinities were shown to have the usual field theoretic interpretation of renormalizing the bare parameters of the system (Newton's constant and the cosmological constant).

It would be interesting to explore the parameter space of the cosmological system further to obtain scenarios of cosmological evolution of interest, such as understanding inflation, and phase transitions in general, in a holographic setting. Various extensions are also possible, such as addition of matter fields on the boundary (without gravity duals). Also, anisotropic cosmologies are possible from a static bulk background, if the boundary hypersurface is chosen with a different geometry than the horizon (e.g., flat boundary ($k = 0$) in a bulk black hole background of spherical horizon ($k = +1$)). Work in this direction is in

progress [38].

Part II : Dynamic Bulk - Dynamic Boundary

As mentioned in the prelude, in this part of the chapter we will deal with time-dependent brane solutions in supergravity and their cosmological implications.

4.6 D3 brane with anisotropic time-dependent world volume

Besides the static D branes of odd space dimensions, the IIB string theory admits *time dependent* branes. Consider, for example, the case of D3 brane. The equations of motion following from the relevant part of standard IIB supergravity action

$$S_{IIB} = -\frac{1}{16\pi G_{10}} \int d^{10}x \sqrt{-g} \left(R - \frac{1}{2} \partial^\mu \phi \partial_\mu \phi - \frac{1}{2 \times 5!} F_5^2 \right). \quad (4.49)$$

has the following forms:

$$\begin{aligned} R_\nu^\mu &= \frac{1}{2} \partial^\mu \phi \partial_\nu \phi + \frac{1}{2 \times 5!} (5 F^{\mu \xi_2 \dots \xi_5} F_{\nu \xi_2 \dots \xi_5} - \frac{1}{2} \delta_\nu^\mu F_5^2), \\ \partial_\mu (\sqrt{g} F^{\mu \xi_2 \dots \xi_5}) &= 0, \\ \nabla^2 \phi &= 0. \end{aligned} \quad (4.50)$$

These equations are solved by

$$\begin{aligned} ds^2 &= \left(1 + \frac{l^4}{r^4}\right)^{-\frac{1}{2}} \left[-dt^2 + t^{2\alpha} dx^2 + t^{2\beta} dy^2 + t^{2\gamma} dz^2 \right] + \left(1 + \frac{l^4}{r^4}\right)^{\frac{1}{2}} \left[dr^2 + r^2 d\Omega_5^2 \right], \\ F_{txyzr} &= \frac{4l^4 t^{\alpha+\beta+\gamma} r^3}{(l^4 + r^4)^2}, \\ \phi &= 0, \end{aligned} \quad (4.51)$$

provided

$$\alpha + \beta + \gamma = 1 \quad \text{and} \quad \alpha^2 + \beta^2 + \gamma^2 = 1. \quad (4.52)$$

The numbers α, β, γ can be organized in an increasing order $\alpha < \beta < \gamma$ and they vary in the range

$$-\frac{1}{3} \leq \alpha \leq 0, \quad 0 \leq \beta \leq \frac{2}{3}, \quad \text{and} \quad \frac{2}{3} \leq \gamma \leq 1. \quad (4.53)$$

These numbers can also be parametrized as

$$\alpha(u) = \frac{-u}{1+u+u^2}, \quad \beta(u) = \frac{1+u}{1+u+u^2}, \quad \gamma(u) = \frac{u+u^2}{1+u+u^2}, \quad (4.54)$$

where the Lifshitz-Khalatnikov parameter $u \geq 1$. Further, values $u < 1$ lead to the same range as

$$\alpha\left(\frac{1}{u}\right) = \alpha(u), \quad \beta\left(\frac{1}{u}\right) = \beta(u), \quad \gamma\left(\frac{1}{u}\right) = \gamma(u). \quad (4.55)$$

The five form charge can be calculated by integrating $*F_5$ over the transverse space and it turns out to be time independent.

In our convention, the extremal D3 brane is represented by $\alpha = \beta = \gamma = 0$ and is not continuously connected to the above solution. Unlike extremal D3 brane, this solution breaks all the supersymmetries of IIB theory due to its explicit time dependence. The Kretschmann scalar for the metric is given by

$$R_{\mu\nu\rho\sigma}R^{\mu\nu\rho\sigma} = \frac{16(-\alpha^2(l^4 + r^4)^6 + \alpha^3(l^4 + r^4)^6 - 5l^8r^4(l^8 + 12r^8)t^4)}{r^4(l^4 + r^4)^5t^4}. \quad (4.56)$$

In writing the above equation, we have used the condition (4.52). It has a time-like singularity at $r = 0$ at any finite time. It, further, has a cosmological singularity at $t = 0$.

In the large r limit, equations in (4.51) reduce to a four dimensional Kasner solution plus a flat six-dimensional part. Within the Bianchi classification of homogeneous spaces, the Kasner metric corresponds to choosing all three of the structure constants to be zero. A generic perturbation near the singularity breaks these constraints generating Belinskii-Lifshitz-Khalatnikov (BKL) oscillations [39]. To briefly illustrate the BKL oscillation, appropriately generalized to our context, we replace the world volume metric on the brane by type IX homogeneous space.

To this end, let us consider the brane configuration of the form

$$ds^2 = \left(1 + \frac{l^4}{r^4}\right)^{-\frac{1}{2}} \left[-dt^2 + (a(t)^2 l_i l_j + b(t)^2 m_i m_j + c(t)^2 n_i n_j) dx^i dx^j \right] \\ + \left(1 + \frac{l^4}{r^4}\right)^{\frac{1}{2}} \left[dr^2 + r^2 d\Omega_5^2 \right]. \quad (4.57)$$

with the anti-symmetric five form field and the scalar

$$F_{txyzr} = \frac{4r^3 l^4 a(t)b(t)c(t) \sin(x)}{(r^4 + l^4)^2}, \quad (4.58)$$

$$\phi = 0. \quad (4.59)$$

Here l_i, m_i, n_i are frame vectors. For IX metric, all the three structure constants are 1 and the simplest choice for the frame vectors is

$$l_i = (\sin x, -\cos z \sin x, 0), \quad m_i = (\cos x, \sin z \sin x, 0), \quad n_i = (0, \cos x, 1). \quad (4.60)$$

The coordinates run through values in the ranges $0 \leq x \leq \pi, 0 \leq y \leq 2\pi, 0 \leq z \leq 4\pi^1$. The above configuration (4.57 - 4.59) is a solution provided they satisfy IIB equations of motion (4.50). This requirement leads to the following differential equations for a, b and c .

$$\begin{aligned} \frac{(a_t b c)_t}{abc} &= \frac{1}{2a^2 b^2 c^2} [(b^2 - c^2)^2 - a^4], \\ \frac{(a b_t c)_t}{abc} &= \frac{1}{2a^2 b^2 c^2} [(c^2 - a^2)^2 - b^4], \\ \frac{(a b c_t)_t}{abc} &= \frac{1}{2a^2 b^2 c^2} [(a^2 - b^2)^2 - c^4], \\ \frac{a_{tt}}{a} + \frac{b_{tt}}{b} + \frac{c_{tt}}{c} &= 0, \end{aligned} \quad (4.61)$$

where the subscript indicates derivative with respect to t .² These are exactly the equations responsible for generating standard BKL oscillations. Consequently, the brane world-volume metric will oscillate with negative powers of t oscillating from one direction to another. In the next paragraph, for the sake of completeness, we give a brief analysis of this oscillation.

To proceed, first we notice that if all the expressions on the right hand side of (4.61) are small in some region, the system will have a Kasner-like regime with

$$a \sim t^\alpha, b \sim t^\beta, c \sim t^\gamma, \quad (4.62)$$

where α, β, γ satisfy constraint as in (4.52). However, now since α is negative, close to

¹In all our discussion, we will closely follow [40]. [42] also has a lucid review of BKL oscillations for types VIII and IX spaces.

²For type I spaces, in which Kasner metric belongs, the right hand sides of all the equations in (4.61) would have been zero. This is due to the fact that all the structure constants are zero for type I spaces.

$t = 0$, a^4 term in the right hand sides of (4.61) will start dominating. It is useful to write these equation in terms of new variables defined as

$$a = e^p, \quad b = e^q, \quad c = e^s, \quad e^{p+q+s} d\tau = dt. \quad (4.63)$$

In the vicinity of $t = 0$, (4.61) reduces to

$$p_{\tau\tau} = -\frac{1}{4}e^{4p}, \quad q_{\tau\tau} = s_{\tau\tau} = \frac{1}{2}e^{4p}, \quad (4.64)$$

where the subscripts τ indicates derivative with respect to τ . The solution of these equations should describe the evolution of world-volume metric from the initial state of Kasner metric. In terms of the new variables, this is equivalent to

$$p_\tau = \alpha, \quad q_\tau = \beta, \quad s_\tau = \gamma. \quad (4.65)$$

Note that the first equation in (4.64) can be interpreted as a particle moving in the presence of an exponential wall-like potential. Due to the reflection from this barrier, particle will move with $p_\tau = -\alpha$. However we see from (4.64) that $p_\tau + q_\tau$ and $p_\tau + s_\tau$ are constants. So we get

$$q_\tau = \beta + 2\alpha, \quad s_\tau = \gamma + 2\alpha. \quad (4.66)$$

These lead to

$$e^p = e^{-\alpha\tau}, \quad e^q = e^{(\beta+2\alpha)\tau}, \quad e^s = e^{(\gamma+2\alpha)\tau} \quad \text{and} \quad t \sim e^{(1+2\alpha)\tau}. \quad (4.67)$$

In terms of the original variables, we can re-write the above as

$$a = t^{\frac{|\alpha|}{1-2|\alpha|}}, \quad b = t^{\frac{\beta-2|\alpha|}{1-2|\alpha|}}, \quad c = t^{\frac{\gamma-2|\alpha|}{1-2|\alpha|}}. \quad (4.68)$$

Therefore the action of the perturbation results oscillations between one Kasner regime to another with negative power shifting from a to b to c , inducing BKL oscillations on the world-volume of the D3 brane. We should however note that near the curvature singularity, string action receives higher derivative gravitational corrections. Consequently, the nature of the singularity and behaviour of its perturbation may get substantially modified. Solutions may also get modified when one introduces other matter fields into the theory. If they are represented by a perfect fluids on the world-volume, with pressure and energy density

related as $p = \omega\rho$, it can be argued that for $\omega < 1$, BKL oscillations still persist. However, situation changes drastically for $\omega = 1$, namely for the stiff-matter (a massless scalar field for example). A general discussion on these issues can be found in [41, 43]. Indeed it is easy to check that in our previous solution, one can introduce a dilaton with a profile

$$\phi = \lambda \log t. \quad (4.69)$$

The metric and the form field remains same as before. However, the exponents now satisfy new constraint relations : $\alpha + \beta + \gamma = 1$, $\alpha^2 + \beta^2 + \gamma^2 = 1 - \lambda^2$. The changes in these relations allow BKL oscillation for a finite time and the system finally reaches an attractor.

We now proceed to study the metric in the near horizon limit $r \rightarrow 0$. In this limit, the metric reduces to

$$ds^2 = -\frac{r^2}{l^2}dt^2 + \frac{l^2}{r^2}dr^2 + r^2(t^{2\alpha}dx^2 + t^{2\beta}dy^2 + t^{2\gamma}dz^2) + l^2d\Omega_5^2, \quad (4.70)$$

with

$$F_{txyzr} = \frac{4tr^3}{l^4}, \text{ giving potential } C_{txyz} = \frac{tr^4}{l^4}. \quad (4.71)$$

The Kretschmann scalar is,

$$R_{\mu\nu\rho\sigma}R^{\mu\nu\rho\sigma} = \frac{16\alpha^2(\alpha-1)l^4}{r^4t^4} - \frac{80}{l^4}. \quad (4.72)$$

We call it a Kasner-AdS space. This Kasner-AdS solution separately satisfies five dimensional Einstein equation in the presence of a negative cosmological constant and was found in [44] in the context of brane-cosmology.

4.7 Probing with a D3 brane

In this section, we will probe the geometry (4.51) with a D3 brane. Distance of the probe brane from the source now behaves as a scalar whose explicit time dependence can be determined via a dynamical equation. We take the world-volume directions of the D3 brane as $\xi = (t, x, y, z)$. The world-volume action of the D3 brane in background geometry, (4.51) takes the form :

$$S = T \int d^4\xi \sqrt{-\det G_{\alpha\beta}} + T \int d^4\xi \hat{C}_4, \quad (4.73)$$

Here $G_{\alpha\beta}$ is the induced metric on the world-volume and \hat{C}_4 is the pull-back of the background 4-form potential. T is the brane tension. We turn off all other fields on the brane. The Lagrangian can be cast in the form :

$$L = \sqrt{A(t, r) - B(t, r) \dot{r}^2} - C(r), \quad (4.74)$$

where,

$$\begin{aligned} A(t, r) &= t^2 \left(1 + \frac{l^4}{r^4} \right)^{-2} \\ B(t, r) &= t^2 \left(1 + \frac{l^4}{r^4} \right)^{-1} \\ C(r) &= -\frac{t l^4}{l^4 + r^4} \end{aligned} \quad (4.75)$$

The equation of motion for $r(t)$ is the Euler-Lagrange equation derived from (4.75) :

$$\begin{aligned} r^4 (l^4 + r^4)^2 [t\ddot{r} + \dot{r}] - (l^4 + r^4)^3 \dot{r}^3 - 2tl^4 r^3 [3(l^4 + r^4)\dot{r}^2 - 2r^4] \\ - 4tl^4 r [r^4 - (l^4 + r^4) \dot{r}^2]^{\frac{3}{2}} = 0 \end{aligned} \quad (4.76)$$

Here dot represents derivative with respect to t . Once this equation is solved with appropriate boundary conditions, the metric on the probe brane is uniquely determined. We will carry out this computation in this section. However, owing to the explicit time dependence in the background geometry, we find that the dynamical equation can not be solved analytically. Fortunately, it is not hard to find numerical solution and a typical behaviour is shown in the figure 4.6.

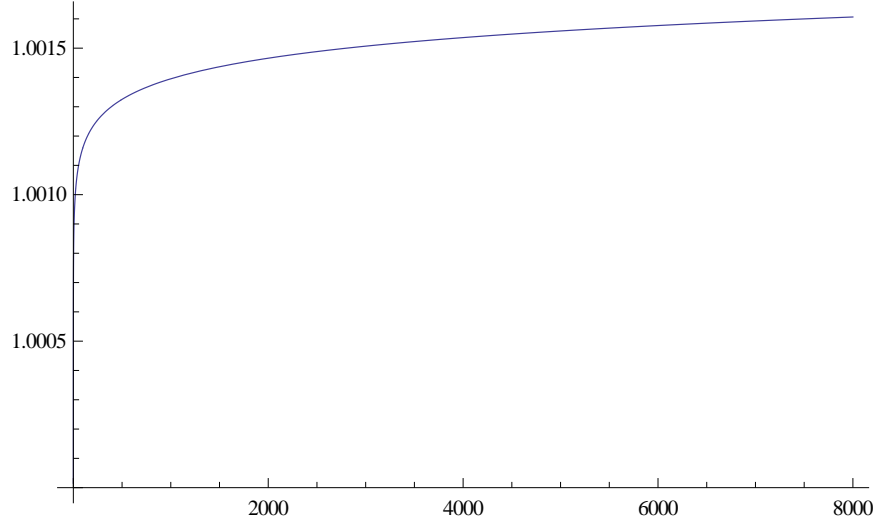


Figure 4.6: Plot of r as a function of time, t .

The functions that govern the anisotropic expansions in three spatial directions are $t^\alpha f(r)$, $t^\beta f(r)$, $t^\gamma f(r)$, where

$$f(r) = \left(1 + \frac{l^4}{r^4}\right)^{-\frac{1}{4}}. \quad (4.77)$$

In order that the near horizon geometry is an AdS , as mentioned earlier, α, β, γ must satisfy the constraint : $\alpha^2 + \beta^2 + \gamma^2 = \alpha + \beta + \gamma = 1$. This means, once we specify one of the three, say, α , the other two are automatically fixed :

$$\begin{aligned} \beta &= \frac{1}{2} \left(1 - \alpha + \sqrt{-3\alpha^2 + 2\alpha + 1}\right) \\ \gamma &= \frac{1}{2} \left(1 - \alpha - \sqrt{-3\alpha^2 + 2\alpha + 1}\right) \end{aligned} \quad (4.78)$$

Ideally, in cosmology, one defines cosmological time, η with which the metric on the probe brane takes the form :

$$dS_{brane}^2 = -d\eta^2 + \left(1 + \frac{l^4}{r^4(\eta)}\right)^{-\frac{1}{2}} (t^{2\alpha}(\eta)dx^2 + t^{2\beta}(\eta)dy^2 + t^{2\gamma}(\eta)dz^2). \quad (4.79)$$

with

$$\frac{d\eta}{dt} = \sqrt{\left(1 + \frac{l^4}{r^4}\right)^{-\frac{1}{2}} - \left(1 + \frac{l^4}{r^4}\right)^{\frac{1}{2}} \left(\frac{dr(t)}{dt}\right)^2}. \quad (4.80)$$

The behaviour of time, t as a function of η is depicted in figure 4.7.

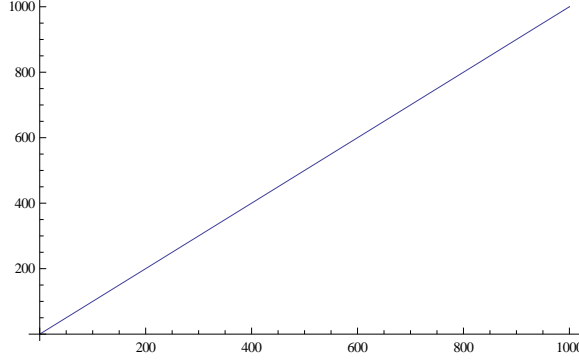


Figure 4.7: Plot of t as a function of η .

At this, we plot the functions $t^\alpha f(r)$, $t^\beta f(r)$, $t^\gamma f(r)$ as functions of η parametrically. Here $f(r)$ is defined through (4.77). One can tune the values of α , β , γ consistent with the Kasner constraints so that one of them goes down to zero (decelerating) while two of them go up (accelerating) with cosmic time and vice versa. One such plot is given in figure 4.8.

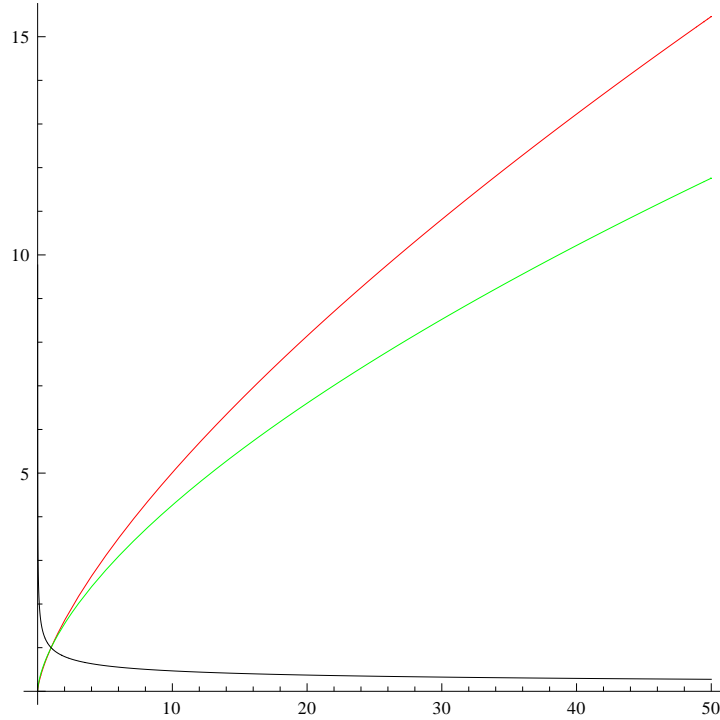


Figure 4.8: The functions, $f_1 = t^\alpha(\eta) f(r)$, $f_2 = t^\beta(\eta) f(r)$, $f_3 = t^\gamma(\eta) f(r)$, with $f(r)$ given in (4.77) are plotted as functions of η . α , β and γ are 0.7, .632, -0.332 respectively. The plot of f_1 is in red, and that of f_2 and f_3 are in green and black respectively.

4.8 The dynamic M5 Brane

Our previous discussion can easily be extended to eleven dimensions. Here we discuss the case of a M5 brane. We start with $d = 11$ supergravity action

$$S_{11d} = -\frac{1}{2 \kappa_{11}^2} \int d^{11}x \sqrt{-g} \left(R - \frac{1}{48} F_4^2 \right), \quad (4.81)$$

which is a generic action for the bosonic part of $d = 11$ supergravity so long as we concentrate on static, flat translationally invariant p-brane solutions.

The equations of motion arising from (4.81) admits a solution of the form :

$$\begin{aligned} ds^2 &= \left(1 + \frac{l^3}{r^3} \right)^{-\frac{1}{3}} \left[-dt^2 + t^{2\alpha_1} dx_1^2 + t^{2\alpha_2} dx_2^2 + t^{2\alpha_3} dx_3^2 + t^{2\alpha_4} dx_4^2 + t^{2\alpha_5} dx_5^2 \right] \\ &+ \left(1 + \frac{l^3}{r^3} \right)^{\frac{2}{3}} \left[dr^2 + r^2 d\Omega_4^2 \right], \end{aligned} \quad (4.82)$$

along with

$$F_{tx_1x_2x_3x_4x_5r} = \frac{3 l^3 t r^2}{(l^3 + r^3)^2} \quad (4.83)$$

provided $\alpha_1 + \alpha_2 + \alpha_3 + \alpha_4 + \alpha_5 = 1$ and $\alpha_1^2 + \alpha_2^2 + \alpha_3^2 + \alpha_4^2 + \alpha_5^2 = 1$.

In the near horizon limit, i.e. $r \rightarrow 0$, the metric and the non-zero component of the form field reduce to the forms :

$$\begin{aligned} ds^2 &= \frac{r}{l} \left[-dt^2 + t^{2\alpha_1} dx_1^2 + t^{2\alpha_2} dx_2^2 + t^{2\alpha_3} dx_3^2 + t^{2\alpha_4} dx_4^2 + t^{2\alpha_5} dx_5^2 \right] \\ &+ \frac{l^2}{r^2} \left[dr^2 + r^2 d\Omega_4^2 \right], \\ F_{tx_1x_2x_3x_4x_5r} &= \frac{3 t r^2}{l^3}, \end{aligned} \quad (4.84)$$

and hence the potential is given by $C_{tx_1x_2x_3x_4x_5} = \frac{t r^3}{l^3}$.

We now make the following change of coordinates :

$$w^2 = \frac{r}{l^3}. \quad (4.85)$$

With this, the metric in (4.84) takes the form :

$$ds^2 = \frac{w^2}{4l^2} \left(-d\bar{t}^2 + \bar{t}^{2\alpha_1^2} d\bar{x}_1^2 + \bar{t}^{2\alpha_2^2} d\bar{x}_2^2 + \bar{t}^{2\alpha_3^2} d\bar{x}_3^2 + \bar{t}^{2\alpha_4^2} d\bar{x}_4^2 + \bar{t}^{2\alpha_5^2} d\bar{x}_5^2 \right) + 4l^2 \frac{dw^2}{w^2} + l^2 d\Omega_4^2, \quad (4.86)$$

where \bar{x}_i and \bar{t} are suitably scaled versions of the coordinates, x_i and t respectively. It is worth mentioning in this regard that the scaling of the coordinates will not be the same because of the presence of different powers of t in front of dx_i^2 . This is a consequence of anisotropy.

Following our nomenclature, (4.86) is a metric of seven dimensional Kasner–AdS space plus a four sphere. For $\alpha_i = 0$ for $i = 1, \dots, 5$, this reduces to our known $AdS_7(2L) \times S^4(L)$ solution.

4.9 Probing with a M5 brane

In the same spirit as we considered the case of probe D3 brane, we now consider a probe M5 brane in the background (4.82) and (4.83).

In PST formalism [45], the world-volume action of M5 brane is given in terms of a gauge invariant 3-form field strength, $\mathcal{H}^{(3)} = d\mathcal{A}^{(2)} + \mathcal{C}^{(3)}$, where $\mathcal{A}^{(2)}$ is world-volume 2-form and $\mathcal{C}^{(3)}$, target space 3-form. The world volume action in this formalism is written as :

$$S_{M5} = T_{M5} \int d^6\xi [\mathcal{L}_{DBI} + \mathcal{L}_{KE} + \mathcal{L}_{WZ}], \quad (4.87)$$

where

$$\begin{aligned} \mathcal{L}_{DBI} &= \sqrt{-\det \left(G_{ij} + \tilde{\mathcal{H}}_{ij} \right)} \quad \text{is the Dirac-Born- Infeld Lagrangian,} \\ \mathcal{L}_{KE} &= \frac{1}{24 (\partial a)^2} \epsilon^{ijklmn} \mathcal{H}_{lmn} \mathcal{H}_{jkp} G^{pq} \partial_i a \partial_q a \quad \text{is the kinetic piece for the 3-form,} \\ \mathcal{L}_{WZ} &= \frac{1}{6!} \epsilon^{ijklmn} \left[\mathcal{C}_{ijklmn}^{(6)} + 10 \mathcal{H}_{ijk} \mathcal{C}_{lmn}^{(3)} \right] \quad \text{is the Wess-Zumino term.} \end{aligned} \quad (4.88)$$

Here $S_{\alpha\beta}$ is the induced metric on the world-volume, $\mathcal{C}^{(3)}$ and $\mathcal{C}^{(6)}$ are the pull-backs of the

3-form and 6-form background potentials respectively. $\tilde{\mathcal{H}}$ is defined as

$$\tilde{\mathcal{H}}^{ij} = \frac{1}{3! \sqrt{-\det G} \sqrt{-(\partial a)^2}} \epsilon^{ijklmn} \partial_k a \mathcal{H}_{lmn}. \quad (4.89)$$

“ a ” is an auxiliary scalar field introduced in PST formalism to maintain manifest covariance.

If we now take the world-volume directions of the M5 brane as $\xi = (t, x_1, x_2, x_3, x_4, x_5)$, it can be explicitly checked that, in this “static gauge”, there will be no component of $\mathcal{C}^{(3)}$ in world-volume directions. We further simplify the system by turning off the world-volume 2-form, $\mathcal{A}^{(2)}$. With all these taken into account, the full Lagrangian takes the simple form :

$$L = \sqrt{A(t, r) - B(t, r) \dot{r}^2} - C(r), \quad (4.90)$$

where,

$$\begin{aligned} A(t, r) &= t^2 \left(1 + \frac{l^3}{r^3} \right)^{-2} \\ B(t, r) &= t^2 \left(1 + \frac{l^3}{r^3} \right)^{-1} \\ C(r) &= -\frac{t l^3}{l^3 + r^3}. \end{aligned} \quad (4.91)$$

Here dot represents derivative with respect to t . The Euler Lagrange equation for $r(t)$ is :

$$\begin{aligned} 2r^4 (l^3 + r^3)^2 [t\ddot{r} + \dot{r}] - 2r (l^3 + r^3)^3 \dot{r}^3 - 3tl^3 r^3 [3(l^3 + r^3) \dot{r}^2 - 2r^3] \\ - 6tl^3 r^{\frac{3}{2}} [r^3 - (l^3 + r^3) \dot{r}^2]^{\frac{3}{2}} = 0. \end{aligned} \quad (4.92)$$

In order to draw a cosmological interpretation of the solutions we obtain from (4.92), as usual, we go to the “cosmic time” coordinate, η , in which the metric on the brane assumes a form :

$$ds_{brane}^2 = -d\eta(t)^2 + \left(1 + \frac{l^3}{r^3(\eta)} \right)^{-\frac{1}{3}} \left(\sum_{i=1}^5 t^{2\alpha_i(\eta)} dx_i^2 \right), \quad (4.93)$$

with

$$\frac{d\eta}{dt} = \sqrt{\left(1 + \frac{l^3}{r^3}\right)^{-\frac{1}{3}} - \left(1 + \frac{l^3}{r^3}\right)^{\frac{2}{3}} \left(\frac{dr(t)}{dt}\right)^2}. \quad (4.94)$$

The functions that govern the expansion of the universe in the spatial world-volume directions of the brane are in this case $t^{\alpha_i} f(r)$, where

$$f(r) = \left(1 + \frac{l^3}{r^3}\right)^{-\frac{1}{6}}. \quad (4.95)$$

We can choose α_i 's so that three of them are the same and mimics isotropic expansion in three directions. The other two are anisotropic. Such a situation can be parametrized as :

$$\begin{aligned} \alpha_1 &= \alpha_2 = \alpha_3 = p \\ \alpha_4 &= \frac{1}{2} \left(\sqrt{-15p^2 + 6p + 1} - 3p + 1 \right) \\ \alpha_5 &= \frac{1}{2} \left(-\sqrt{-15p^2 + 6p + 1} - 3p + 1 \right). \end{aligned} \quad (4.96)$$

Interestingly there exists a narrow window of parametric value for p , in which α_i for $i = 1, 2, 3$ are positive and α_4 and α_5 are negative. An illustrative plot is shown in figure 4.9 for a particular value of p .

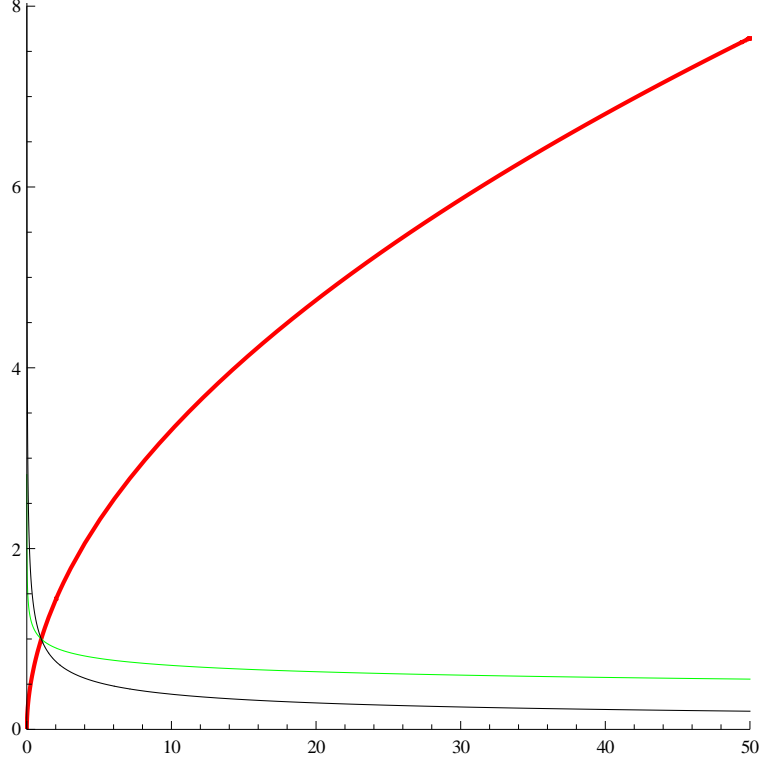


Figure 4.9: The functions, $t^{\alpha_i}(\eta) f(r)$, for $i = 1, 2, \dots, 5$ are plotted as functions of η for $p = 0.52$. The corresponding values for α_i 's are : $\alpha_1 = \alpha_2 = \alpha_3 = 0.52$, $\alpha_4 = -0.15$ and $\alpha_5 = -0.41$. The isotropic expansion corresponding to $\alpha_1, \alpha_2, \alpha_3$ is plotted in red. The contraction corresponding to α_4, α_5 are plotted in green and black respectively.

4.10 Summary and future directions : Part II

In this part we have presented a class of time-dependent brane configurations of 10 and 11 dimensional supergravity. In particular, we showed probing certain brane configurations with appropriate choice of parameters with another brane dynamically compactifies the extra dimensions on the brane world-volume and hence mimics the cosmological evolution of universe. Furthermore, near their cosmological singularities, this class of configurations shows BKL oscillation. It will be worthwhile to look for the signatures of these oscillations in their dual gauge theory descriptions as well.

Bibliography

- [1] L. Randall and R. Sundrum, “An alternative to compactification,” *Phys. Rev. Lett.* **83** (1999) 4690 [arXiv:hep-th/9906064].
- [2] P. Binetruy, C. Deffayet and D. Langlois, “Non-conventional cosmology from a brane-universe,” *Nucl. Phys. B* **565** (2000) 269 [arXiv:hep-th/9905012].
- [3] P. Binetruy, C. Deffayet, U. Ellwanger and D. Langlois, “Brane cosmological evolution in a bulk with cosmological constant,” *Phys. Lett. B* **477** (2000) 285 [arXiv:hep-th/9910219].
- [4] C. Csaki, M. Graesser, C. F. Kolda and J. Terning, “Cosmology of one extra dimension with localized gravity,” *Phys. Lett. B* **462** (1999) 34 [arXiv:hep-ph/9906513].
- [5] J. M. Cline, C. Grojean and G. Servant, “Cosmological expansion in the presence of extra dimensions,” *Phys. Rev. Lett.* **83** (1999) 4245 [arXiv:hep-ph/9906523].
- [6] P. Kraus, “Dynamics of anti-de Sitter domain walls,” *JHEP* **9912**, 011 (1999). [hep-th/9910149].
- [7] C. Barcelo and M. Visser, “Living on the edge: Cosmology on the boundary of anti-de Sitter space,” *Phys. Lett. B* **482** (2000) 183 [arXiv:hep-th/0004056].
- [8] H. Collins and B. Holdom, “Brane cosmologies without orbifolds,” *Phys. Rev. D* **62** (2000) 105009 [arXiv:hep-ph/0003173].
- [9] P. S. Apostolopoulos and N. Tetradis, “Brane cosmology with matter in the bulk,” *Class. Quant. Grav.* **21** (2004) 4781 [arXiv:hep-th/0404105]; “Brane cosmological evolution with a general bulk matter configuration,” *Phys. Rev. D* **71** (2005) 043506 [arXiv:hep-th/0412246]; “The generalized dark radiation and accelerated expansion in brane *Phys. Lett. B* **633** (2006) 409 [arXiv:hep-th/0509182].
- [10] C. van de Bruck, M. Dorca, C. J. A. Martins and M. Parry, “Cosmological consequences of the brane/bulk interaction,” *Phys. Lett. B* **495** (2000) 183 [arXiv:hep-th/0009056].
- [11] E. Kiritsis, G. Kofinas, N. Tetradis, T. N. Tomaras and V. Zarikas, “Cosmological evolution with brane-bulk energy exchange,” *JHEP* **0302** (2003) 035 [arXiv:hep-th/0207060].

- [12] N. Tetradis, “Cosmological acceleration from energy influx,” *Phys. Lett. B* **569** (2003) 1 [arXiv:hep-th/0211200].
- [13] E. Kiritsis, “Brane-bulk energy exchange and cosmological acceleration,” *Fortsch. Phys.* **52** (2004) 568 [arXiv:hep-th/0503189].
- [14] A. Ashtekar and A. Magnon, “Asymptotically anti-de Sitter space-times,” *Class. Quant. Grav.* **1** (1984) L39.
- [15] M. Henneaux and C. Teitelboim, “Asymptotically Anti-De Sitter Spaces,” *Commun. Math. Phys.* **98** (1985) 391.
- [16] M. Henneaux, in *Proceedings of the Fourth Marcel Grossmann Meeting on General Relativity, Rome 1985*, pp. 959–966, Elsevier, 1986.
- [17] J. D. Brown and M. Henneaux, “Central Charges in the Canonical Realization of Asymptotic Symmetries: An Example from Three-Dimensional Gravity,” *Commun. Math. Phys.* **104** (1986) 207.
- [18] V. Balasubramanian, P. Kraus and A. E. Lawrence, “Bulk vs. boundary dynamics in anti-de Sitter spacetime,” *Phys. Rev. D* **59** (1999) 046003 [arXiv:hep-th/9805171].
- [19] V. Balasubramanian, P. Kraus, A. E. Lawrence and S. P. Trivedi, “Holographic probes of anti-de Sitter space-times,” *Phys. Rev. D* **59** (1999) 104021 [arXiv:hep-th/9808017].
- [20] V. Balasubramanian, E. G. Gimon, D. Minic and J. Rahmfeld, “Four dimensional conformal supergravity from AdS space,” *Phys. Rev. D* **63** (2001) 104009 [arXiv:hep-th/0007211].
- [21] G. Compere and D. Marolf, “Setting the boundary free in AdS/CFT,” *Class. Quant. Grav.* **25** (2008) 195014 [arXiv:0805.1902 [hep-th]].
- [22] P. S. Apostolopoulos, G. Siopsis and N. Tetradis, “Cosmology from an AdS Schwarzschild black hole via holography,” *Phys. Rev. Lett.* **102** (2009) 151301 [arXiv:0809.3505 [hep-th]].
- [23] S. de Haro, S. N. Solodukhin and K. Skenderis, “Holographic reconstruction of spacetime and renormalization in the AdS/CFT correspondence,” *Commun. Math.*

- Phys. **217** (2001) 595 [arXiv:hep-th/0002230]; Class. Quant. Grav. **19** (2002) 5849 [arXiv:hep-th/0209067].
- [24] T. Hertog and G. T. Horowitz, “Holographic description of AdS cosmologies,” JHEP **0504**, 005 (2005) [hep-th/0503071].
- [25] B. Craps, T. Hertog and N. Turok, “On the Quantum Resolution of Cosmological Singularities using AdS/CFT,” Phys. Rev. D **86**, 043513 (2012) [arXiv:0712.4180 [hep-th]].
- [26] A. Awad, S. R. Das, S. Nampuri, K. Narayan and S. P. Trivedi, “Gauge Theories with Time Dependent Couplings and their Cosmological Duals,” Phys. Rev. D **79**, 046004 (2009) [arXiv:0807.1517 [hep-th]].
- [27] G. Horowitz, A. Lawrence and E. Silverstein, “Insightful D-branes,” JHEP **0907**, 057 (2009) [arXiv:0904.3922 [hep-th]].
- [28] A. Awad, S. R. Das, A. Ghosh, J. -H. Oh and S. P. Trivedi, “Slowly Varying Dilaton Cosmologies and their Field Theory Duals,” Phys. Rev. D **80**, 126011 (2009) [arXiv:0906.3275 [hep-th]].
- [29] S. Banerjee, S. Bhowmick, A. Sahay and G. Siopsis, “Generalized Holographic Cosmology,” Class. Quant. Grav. **30**, 075022 (2013) [arXiv:1207.2983 [hep-th]].
- [30] S. Banerjee, S. Bhowmick and S. Mukherji, “Anisotropic branes,” arXiv:1301.7194 [hep-th].
- [31] C. Barcelo and M. Visser, “Living on the edge: Cosmology on the boundary of Anti-de Sitter space,” Phys. Lett. B **482** (2000) 183 [hep-th/0004056].
- [32] I. Savonije and E. P. Verlinde, “CFT and entropy on the brane,” Phys. Lett. B **507** (2001) 305 [hep-th/0102042].
- [33] G. L. Cardoso and V. Grass, “On five-dimensional non-extremal charged black holes and FRW cosmology,” Nucl. Phys. B **803** (2008) 209 [arXiv:0803.2819 [hep-th]].
- [34] S. S. Gubser, “AdS / CFT and gravity,” Phys. Rev. D **63** (2001) 084017 [hep-th/9912001].

- [35] S. Mukherji and M. Peloso, “Bouncing and cyclic universes from brane models,” *Phys. Lett. B* **547** (2002) 297 [hep-th/0205180].
- [36] J. L. Hovdebo and R. C. Myers, “Bouncing brane worlds go crunch!,” *JCAP* **0311** (2003) 012 [hep-th/0308088].
- [37] A. C. Petkou and G. Siopsis, “dS / CFT correspondence on a brane,” *JHEP* **0202** (2002) 045 [hep-th/0111085].
- [38] S. Banerjee and G. Siopsis, in preparation.
- [39] E. Lifshitz, V. Belinsky and I. Khalatnikov, *Adv. Phys.* 19 525(1970).
- [40] L.D. Landau and E.M. Lifshitz, *Classical Theory of Fields*, Pergamon Press, 390 - 397, (1987).
- [41] V.A. Belinsky, I.M. Khalatnikov, *Sov. Phys. JETP* 36 591 (1973).
- [42] [http : //en.wikipedia.org/wiki/BKL_singularity](http://en.wikipedia.org/wiki/BKL_singularity).
- [43] I. M. Khalatnikov and A. Y. Kamenshchik, “Lev Landau and the problem of singularities in cosmology,” *Phys. Usp.* **51**, 609 (2008) [arXiv:0803.2684 [gr-qc]].
- [44] A. V. Frolov, “Kasner-AdS space-time and anisotropic brane world cosmology,” *Phys. Lett. B* **514**, 213 (2001) [gr-qc/0102064].
- [45] P. Pasti, D. P. Sorokin and M. Tonin, “On Lorentz invariant actions for chiral p forms,” *Phys. Rev. D* **55**, 6292 (1997) [hep-th/9611100].

5

In Lieu of a Conclusion

Physics out of equilibrium is a huge field of study in itself and governs most of the interesting real-life and real-time phenomena. Unfortunately, the field theory tools to understand non-equilibrium phenomena are not well-developed. This is primarily because of the lack of a reliable perturbation technique which in other branches of field theory has been proved to be immensely helpful a tool. In this thesis we have chosen a very few non-equilibrium phenomena, that too in a strongly coupled regime and have shown that machineries can be derived from the AdS/CFT conjecture to handle such situations. We discussed phenomena like temperature quench, non-Fermi liquid and early universe cosmologies and in each case we got some success. Successes are varied, however, leaving some still unanswered questions, here and there, but in conclusion, we can say, the successes, even if partial, in building up the problem-specific machineries that we have reported in the chapters of this thesis, definitely, hint at the point that AdS/CFT might be the very framework in which one can do further studies in non-perturbative phenomena, in particular, the otherwise intractable non-equilibrium scenarios.